TAMPEREEN TEKNILLINEN YLIOPISTO
TAMPERE UNIVERSITY OF TECHNOLOGY
Julkaisu 808 • Publication 808

Mikko Kohvakka

Medium Access Control and Hardware Prototype Designs for Low-Energy Wireless Sensor Networks

Tampere 2009

Tampereen teknillinen yliopisto. Julkaisu 808
Tampere University of Technology. Publication 808

Mikko Kohvakka

Medium Access Control and Hardware Prototype Designs for Low-Energy Wireless Sensor Networks

Thesis for the degree of Doctor of Technology to be presented with due permission for public examination and criticism in Tietotalo Building, Auditorium TB109, at Tampere University of Technology, on the 29th of May 2009, at 12 noon.

Tampereen teknillinen yliopisto - Tampere University of Technology
Tampere 2009

ISBN 978-952-15-2153-9 (printed)
ISBN 978-952-15-2189-8 (PDF)
ISSN 1459-2045

ABSTRACT

A Wireless Sensor Network (WSN) is an emerging technology consisting of small, cheap, and ultra-low energy sensor nodes, which cooperatively monitor physical quantities, actuate, and perform data processing tasks. A deployment may comprise thousands of randomly distributed autonomous nodes, which must self-configure and create a multi-hop network topology.

This Thesis focuses on low-energy WSNs targeting to long network lifetime. The main research problem is the combination of adaptive and scalable multi-hop networking with constrained energy budget, processing power, and communication bandwidth. The research problem is approached by energy-efficient protocols and low-power sensor node platforms.

The main contribution of this Thesis is an energy-efficient Medium Access Control (MAC) design for TUTWSN (Tampere University of Technology Wireless Sensor Network). The design comprises channel access and networking mechanisms, which specify data exchange, link synchronization, network self-configuration, and neighbor discovery operations. The second outcome are several low-power sensor node platforms, which have been designed and implemented to evaluate the performance of the MAC design and hardware components in real deployments. The third outcome are the performance models and analysis of several MAC designs including TUTWSN, IEEE 802.15.4, and the most essential research proposals.

The results and conclusion of this Thesis indicate that it is possible to implement multi-hop WSNs in harsh and dynamic operation conditions with years of lifetime using current low-cost components and batteries. Energy analysis results indicate that the lowest energy consumption is achieved by using simple and high data-rate transceivers. It is also critical to minimize sleep mode power consumption of all components and to use accurate wake-up timers. However, the selection of components constitutes only a minor part of the solution, and an energy-efficient MAC layer design being able to minimize radio duty cycle is required. A theoretically ideal MAC eliminates idle listening, overhearing, collisions, and control traffic overhead. The performance analysis shows that TUTWSN MAC achieves the highest energy-

efficiency in both router and leaf nodes compared to existing proposals and standards. Compared to the ideal MAC, the energy consumption of TUTWSN MAC is only 2.85% - 27.1% higher, depending on traffic load, radio, and node type. IEEE 802.15.4 performs the second best resulting in 2.92% to 229% energy overhead. Analysis and measurements indicate that TUTWSN can maintain high energy-efficiency also in dynamic networks. The MAC and platform designs are measured and validated in long-term deployments using full-scale WSN implementations.

The results of this Thesis can be used in the WSN research, development, and implementation in general. The designed mechanisms in the MAC layer are presented and analyzed separately on each other. Presented performance models can be easily adapted to other protocols. In addition, the developed sensor node platforms are applicable for experimenting other applications and protocol.

PREFACE

The research work for this Thesis was carried out in the Department of Computer Systems at Tampere University of Technology during the years 2002 - 2008.

I would like to express my sincere gratitude to my supervisor Professor Marko Hännikäinen for his guidance, support, and motivation during the research. I am also grateful to Professor Timo D. Hämäläinen for his farsighted guidance and for the opportunity to carry out the research in DACI research group. I would also like to thank the reviewers of my Thesis, Professor Jari Porras and Assistant Professor Evgeny Osipov for their valuable comments, and Professor Petri Mähönen for agreeing to serve as an opponent in the defense.

Many thanks to the members of the DACI research group for the inspiring and creative atmosphere. Special thanks to Dr. Mauri Kuorilehto, Mr. Jukka Suhonen, M.Sc., Mr. Ville Kaseva, M.Sc., Mr. Tero Arpinen, M.Sc., and all the members of TUTWSN team for their valuable work that have made this Thesis possible. Also, thanks to Dr. Panu Hämäläinen, Dr. Timo Vanhatupa, and Dr. Jari Heikkinen for valuable comments and discussions.

My Thesis was financially supported by Finnish Funding Agency for Technology and Innovation (TEKES), Academy of Finland, Nokia Foundation, Tekniikan edistämissäätiö (TES), and Ulla Tuomisen Säätiö.

Finally, I would like to express my gratitude to my family and friends for their support and encouragement. Especially, I am deeply grateful to my wife Salla for her love and understanding through these years.

Tampere, April 2009

Mikko Kohvakka

TABLE OF CONTENTS

Abstract i

Preface iii

Table of Contents v

List of Publications ix

List of Abbreviations xi

1. Introduction 1

1.1 WSN Technology Overview 2

1.2 Key WSN Design Requirements 5

1.3 Scope, Objectives and Methods of the Research 7

1.4 Research Outcomes 8

1.5 Thesis Outline 10

2. Applications and Standards 11

2.1 WSN Application Space 11

2.2 Deployments 13

2.3 Standards 15

2.3.1 Wireless Communication Standards 15

2.3.2 Standards Related to WSNs 17

3. Sensor Node Platforms 23

3.1 Platform Components 23

3.1.1 Communication subsystem 24

3.1.2 Computing subsystem 25

3.1.3 Sensing subsystem 27
3.1.4 Power subsystem 27
3.2 Existing Platforms 29
4. Medium Access Control for WSNs 35
4.1 Low-Energy MAC Design 35
4.2 Existing MAC Protocols 36
4.2.1 Unsynchronized Low Duty-Cycle MAC Protocols 37
4.2.2 Synchronized Low Duty-Cycle MAC Protocols 39
5. TUTWSN MAC Design 45
5.1 TUTWSN Networking Technology 45
5.2 TUTWSN Channel Access Mechanism 47
5.3 TUTWSN Networking Mechanisms 52
5.3.1 Self-Configuration 52
5.3.2 Neighbor Discovery 58
6. Performance Models 63
6.1 Utilized Parameters 64
6.2 Models 65
6.2.1 Ideal-MAC 66
6.2.2 B-MAC 66
6.2.3 SCP-MAC 68
6.2.4 X-MAC 70
6.2.5 T-MAC 71
6.2.6 IEEE 802.15.4 73
6.2.7 TUTWSN MAC 74
6.3 Results 75

7. TUTWSN Sensor Node Platforms and Deployments 79
7.1 TUTWSN Node Designs 79
7.1.1 Node Designs in 2004 80
7.1.2 Node Designs in 2005 83
7.1.3 Node Designs in 2006 88
7.1.4 Results 90
7.2 TUTWSN Deployments 93
7.2.1 Indoor Temperature Sensing Deployment 93
7.2.2 Environmental Monitoring Deployment 97
7.2.3 Building Monitoring Deployment 99
8. Summary of Publications 103
9. Conclusions 107
Publications 131

LIST OF PUBLICATIONS

This Thesis consists of an introductory part and the following publications. The publications are divided into three categories: protocol designs, performance analysis, and hardware platforms. The publications presenting new protocol designs are referred as [P1] - [P4]. The publications covering the performance analysis and optimizations of existing protocols are referred as [P5], [P6]. The publications discussing the implementation of hardware prototypes and real application deployments are referred as [P7] - [P10].

[P1] M. Kohvakka, "TUTWSN MAC Protocol," book chapter in *Ultra-low energy wireless sensor networks in practice: theory, realization and deployment*, M. Kuorilehto, M. Kohvakka, J. Suhonen, P. Hämäläinen, M. Hännikäinen, and T.D. Hämäläinen, Chichester: John Wiley, 2007, pp. 145-182.

[P2] M. Kohvakka, J. Suhonen, M. Hännikäinen, and T. D. Hämäläinen, "Transmission Power Based Path Loss Metering for Wireless Sensor Networks," in *Proceedings of the 17th Annual IEEE International Symposium on Personal, Indoor and Mobile Radio Communications (PIMRC 2006)*, Helsinki, Finland, Sep. 11–14, 2006, pp. 1–5.

[P3] M. Kohvakka, M. Kuorilehto, M. Hännikäinen, and T. D. Hämäläinen, "Network Signaling Channel for Improving ZigBee Performance in Dynamic Cluster-Tree Networks," *EURASIP Journal on Wireless Communications and Networking*, vol. 8, no. 3, pp. 1–15, January 2008.

[P4] M. Kohvakka, J. Suhonen, M. Kuorilehto, V. Kaseva, M. Hännikäinen, and T. D. Hämäläinen, "Energy-Efficient Neighbor Discovery Protocol for Mobile Wireless Sensor Networks," *Ad Hoc Networks*, vol. 7, no. 1, pp. 24–41, January 2009.

[P5] M. Kohvakka, M. Hännikäinen, and T. D. Hämäläinen, "Energy Optimized Beacon Transmission Rate in a Wireless Sensor Network," in *Proceedings*

of the 16th International Symposium on Personal Indoor and Mobile Radio Communications (PIMRC 2005), Berlin, Germany, Sep. 11–14, 2005, pp. 1269–1273.

[P6] M. Kohvakka, M. Kuorilehto, M. Hännikäinen, and T. D. Hämäläinen, "Performance Analysis of IEEE 802.15.4 and ZigBee for Large-Scale Wireless Sensor Network Applications," in *Proceedings of the 3rd ACM International Workshop on Performance Evaluation of Wireless Ad Hoc, Sensor, and Ubiquitous Networks (PE-WASUN 2006)*, Torremolinos, Spain, Oct. 6, 2006, pp. 48–57.

[P7] M. Kohvakka, M. Hännikäinen, and T. D. Hämäläinen, "Wireless Sensor Prototype Platform," in *Proceedings of the 29th Annual Conference of the IEEE Industrial Electronics Society (IECON 2003)*, Virginia, USA, Nov. 2–6, 2003, pp. 1499–1504.

[P8] M. Kohvakka, M. Hännikäinen, and T. D. Hämäläinen, "Ultra Low Energy Wireless Temperature Sensor Network Implementation," in *Proceedings of the 16th International Symposium on Personal Indoor and Mobile Radio Communications (PIMRC 2005)*, Berlin, Germany, Sep. 11–14, 2005, pp. 801–805.

[P9] M. Kohvakka, M. Hännikäinen, and T. D. Hämäläinen, "Wireless Sensor Network Implementation for Industrial Linear Position Metering," in *Proceedings of the 8th Euromicro Conference on Digital System Design – Architectures, Methods, and Tools (DSD 2005)*, Porto, Portugal, Aug. 30–Sept. 3, 2005, pp. 267–273.

[P10] M. Kohvakka, T. Arpinen, M. Hännikäinen, and T. D. Hämäläinen, "High-Performance Multi-Radio WSN Platform," in *Proceedings of the 2nd International Workshop on Multi-hop Ad Hoc Networks: from theory to reality (REALMAN 2006)*, Florence, Italy, May 26, 2006, Italy, pp. 95–97.

LIST OF ABBREVIATIONS

ACK	Acknowledgment
ADC	Analog-to-Digital Converter
AES	Advanced Encryption Standard
API	Application Programming Interface
ASIC	Application Specific Integrated Circuit
BER	Bit Error Rate
B-MAC	Berkeley Media Access Control
CAN	Controller Area Network
CAP	Contention Access Period
CCA	Clear Channel Assessment
CDMA	Code Division Multiple Access
CFP	Contention-Free Period
COTS	Commercial Off-The-Shelf
CSMA	Carrier Sense Multiple Access
CSMA/CA	Carrier Sense Multiple Access with Collision Avoidance
DSL	Digital Subscriber Line
DSSS	Direct Sequence Spread Spectrum
ENDP	Energy-efficient Neighbor Discovery Protocol
EEPROM	Electrically Erasable Programmable Read-Only Memory

FDMA	Frequency Division Multiple Access
FET	Field-Effect Transistor
FHSS	Frequency Hopping Spread Spectrum
FPGA	Field Programmable Gate-Array
GDI	Great Duck Island
GPS	Global Positioning System
GPRS	General Packet Radio Service
GSM	Global System for Mobile Communications
HR	High data Rate
HVAC	Heating, Ventilation & Air Conditioning
IC	Integrated Circuit
IEEE	Institute of Electrical and Electronics Engineers
IR	Infra-Red
ISM	Industrial, Scientific, Medicine
LAN	Local Area Network
LEACH	Low-Energy Adaptive Clustering Hierarchy
LED	Light Emitting Diode
LOS	Line-of-Sight
LPL	Low Power Listening
LR-WPAN	Low-Rate Wireless Personal Area Network
LR	Low data Rate
MAC	Medium Access Control
MACA	Multiple Access with Collision Avoidance
MCU	Micro-Controller Unit

MIPS	Million Instructions Per Second
NCAP	Network Capable Application Processor
NCB	Network Channel Beaconing
NFC	Near Field Communication
NiMH	Nickel-Metal Hydride
PACT	Power Aware Clustered TDMA
PAMAS	Power Aware Multi-Access protocol with Signaling
PCB	Printed Circuit Board
PDA	Personal Digital Assistant
PHY	Physical
PIR	Passive Infra-Red
QoS	Quality of Service
RF	Radio Frequency
RFID	Radio Frequency Identification
RSSI	Received Signal Strength Indicator
SCP-MAC	Scheduled Channel Polling Medium Access Control
SDU	Synchronization Data Unit
SIG	Special Interest Group
S-MAC	Sensor-MAC
SMACS	Self-Organizing Medium Access Control for Sensor Networks
SoC	System-on-Chip
SpeckMAC-B	Speck Medium Access Control Backoff
SpeckMAC-D	Speck Medium Access Control Data
SRAM	Static Random Access Memory

SRSA	Self-Organizing Slot Allocation
STEM	Sparse Topology and Energy Management
SYNC	Synchronization
TDMA	Time Division Multiple Access
TEDS	Transducer Electronic Data Sheet
TII	Transducer Independent Interface
TIM	Transducer Interface Module
T-MAC	Timeout-MAC
TRAMA	Traffic-Adaptive Medium Access
TUTWSN	Tampere University of Technology Wireless Sensor Network
TX	Transmit
UI	User Interface
UMTS	Universal Mobile Telecommunications System
USB	Universal Serial Bus
WiMAX	Wordwide Interoperability for Microwave Access
WiseMAC	Wireless Sensor MAC
WLAN	Wireless Local Area Network
WMAN	Wireless Metropolitan Area Network
WPAN	Wireless Personal Area Network
WSN	Wireless Sensor Network
WWAN	Wireless Wide Area Network
Z-MAC	Zebra MAC

1. INTRODUCTION

The most profound technologies are those that disappear.
They weave themselves into the fabric of everyday life
until they are indistinguishable from it.
– – Mark Weiser

Wireless network technologies have been under rapid development during the recent years [111]. Most people feel the strong impact of wireless technology mainly due to the astonishing growth of cell-phone markets [117]. In the future, the highest potential for growth will be in other types of networks [111]. One of the most potential technologies is wireless sensor networks [32].

Sensor networks gather information on entities of interest by multiple distributed sensor elements [32, 202]. Early sensor networks are found in the national power grid with its many sensors [43], in the radar networks used in air traffic control [32], and in factory floor, where fieldbusses interconnect various sensors, actuators, field controllers and man-machine interfaces [196, 214]. These sensor networks consist of large and expensive sensor elements interconnected by a wired network [32].

The rapid development and miniaturization of computing and communication circuits has created the vision of a Wireless Sensor Network (WSN), where thousands of tiny and cheap sensing nodes operate fully autonomously in interaction with their environment [4,5,40,124,207]. Nodes perform wireless communication by simple radios, while small processors provide sophisticated functionality [25, 28, 132]. By cooperation and in-network data fusion, nodes refine the measurement accuracy, detect and classify occurred events, and control actuators according to the events [31, 112]. Ultra-low energy consumption enables the network lifetime of years with small batteries, or supply energy scavenging solely from operation environment [150]. WSNs have a vast number of foreseen application fields including military, environmental and condition monitoring, building automation, object tracking, and interactive games [5, 32, 88, 124, 211]. They have also been seen as an enabling technology for ubiquitous networks, where computing power is embedded invisibly around us, and

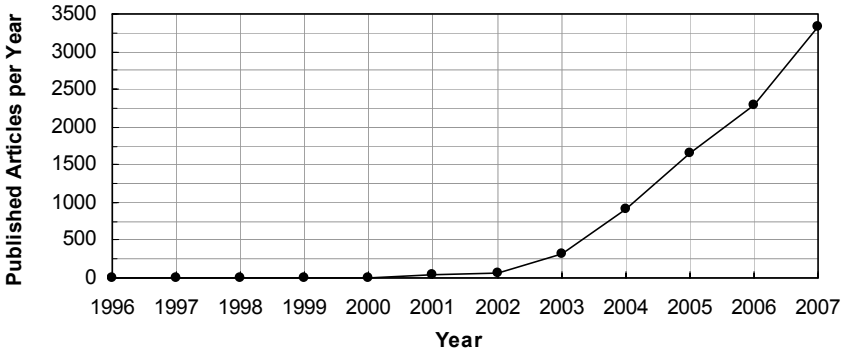

Fig. 1. *Annually published IEEE research articles containing a phrase "wireless sensor network".*

accessed through intelligent interfaces [65, 98, 206, 209].

WSNs have gained extensively growing academic and commercial interest during the recent years [207, 209, 210]. Fig. 1 illustrates the number of annually published articles in the conferences and journals of Institute of Electrical and Electronics Engineers (IEEE) containing a phrase "wireless sensor network" [78]. The first article [25] was published in 1996, and less than 50 articles were published until 2001. However, during a single year 2007, over 3300 WSN related articles were published. *Business Week* [208] predicted in September 1999 that WSNs will be one of the most important technologies of the 21st century.

1.1 WSN Technology Overview

So far, WSNs have been implemented mainly for research purposes [14, 16, 39, 69, 101, 123, 145, 155, 158, 168, 172, 179, 185, 199, 200, 219, 225], while only few commercial WSNs exist. Most of the commercial WSNs are development kits or radio modules necessitating engineering work in application development. Examples of development kit providers are Dust Networks, Inc. [48], Nanotron Technologies GmbH [116], Dynastream Innovations, Inc. [50], and Crossbow Technology, Inc. [36]. Sensicast [166] also provides some end-to-end solutions with sensor integrations and interfaces for external networks.

Since the application fields and their requirements for the network are diverse, WSN implementations are application specific. The energy consumption, communication bandwidth, and networking performance of nodes are optimized to execute a given application task. There are a number of limitations in the current WSN products, both

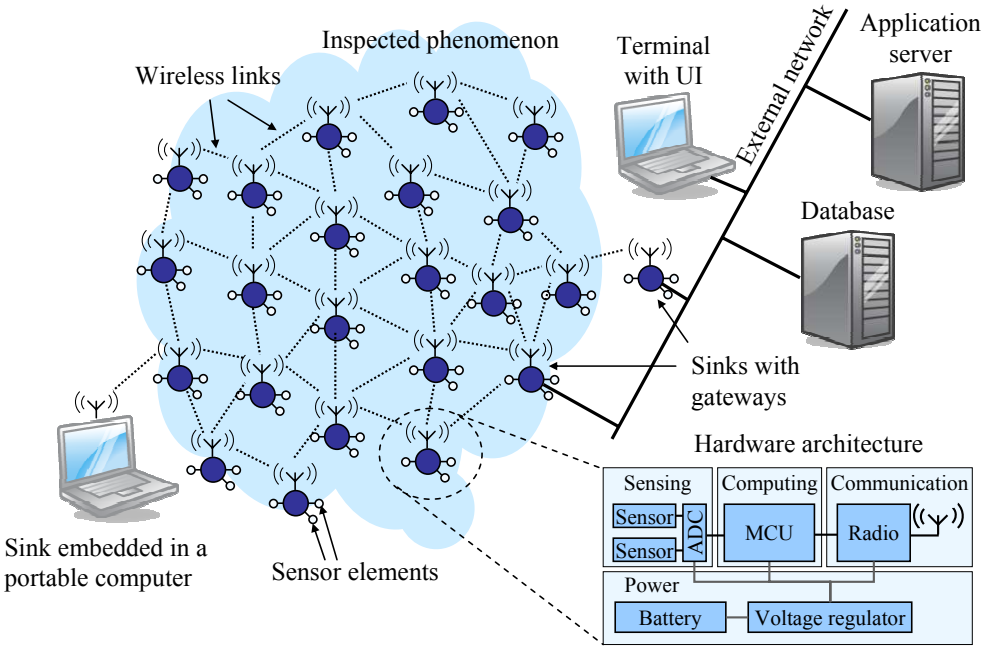

Fig. 2. *Example WSN application scenario.*

in software and hardware including power consumption, networking performance and physical size [224]. Due to the limitations, existing WSN realizations can implement only a subset of the envisioned features, and a trade-off has been made between energy consumption and data transfer performance.

For clarifying the characteristics of the WSN pursued in this Thesis, an example scenario is depicted in Fig. 2. An arbitrary number of nodes are randomly deployed in the area of an inspected phenomenon, where they self-configure network topology. In the figure, all nodes are similar (homogenous) in their hardware. It is possible that nodes are diverse (heterogenous) in their sensing, processing, and networking capabilities, when nodes can be specialized in different tasks. The network contains one or more sink nodes, which request other nodes to perform measurements, and then collect measured values for further use. Data is routed in the network by a chain of short and low-energy hops (multi-hop routing).

Sinks may operate in various locations in the network. Typically, a sink is integrated with a gateway connecting WSN to an external network. An external computer network may contain an application server that delivers applications for user terminals, performs data processing, and handles access to a database. The external network can also be another WSN operating e.g. at a different frequency band. A sink may also be

Table 1. *Component power consumptions and allowed activity levels.*

Component	Power consumption	Allowed activity
Radio (reception)	50 - 100 mW	0.1 - 1%
Radio (transmission)	25 - 50 mW	0.1 - 1%
MCU	1 - 5 mW	1 - 5%
Sensors	0.5 - 10 mW	0.01 - 1%
All components (sleep)	5 - 100 μW	100%

embedded in a portable computer providing a User Interface (UI). Moreover, nodes making actuating decisions according to received information from other nodes are sinks.

The focus of this Thesis is on low-energy WSNs, where long network lifetime is more important than throughput, latency, and data processing performance. Network lifetime can be increased by using low-power hardware components and high-capacity batteries. For clarifying the capability of current Commercial Off-The-Shelf (COTS) components, an example node assembly targeting to long lifetime and small size is presented [53, 152] . The node comprises a Micro-Controller Unit (MCU) having around 1 Million Instructions Per Second (MIPS) processing speed, tens of kilobytes program memory, few kilobytes data memory, and an Analog-to-Digital Converter (ADC). In addition, the node contains a short-range radio, and a set of sensors. Supply power is obtained from AA-size batteries.

Assuming a target lifetime of one year using AA-size batteries, the available power budget is around 1 mW. For reference, Table 1 presents the typical power consumptions of hardware components. For reaching the budget, allowed activity for transmissions, receptions, sensing and data processing is in the order of one percent, while the rest of time must be spent in a low power sleep mode. In a sleep mode, a node turns off the MCU and the radio such that only a low power wake up timer is active to be able to wake up according to a schedule. Thus, a low-energy WSN implementation necessitates the combination of low-power hardware components with energy-efficient protocols, which can eliminate the unnecessary activity of the hardware.

Wireless communication between nodes is enabled by network protocols. A protocol is a set of rules, which define what (semantics), how (syntax), and when (timing) to communicate for exchanging data between two entities [177]. Network protocols are typically divided into layers according to their responsibilities, and together they form a protocol stack. Each layer has precisely defined interfaces, which permits flexible updates and changes in the software and hardware implementations in a modular manner.

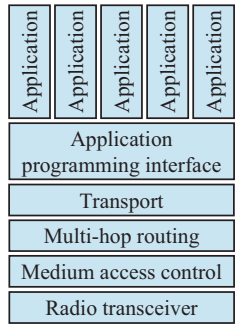

Fig. 3. *A WSN protocol stack used in this Thesis.*

An WSN protocol stack implementation used in this Thesis is presented in Fig. 3. A radio transceiver (radio) transmits and receives messages one bit or symbol at a time by making a conversion between digital data and analog symbols of the medium.

A Medium Access Control (MAC) protocol determines how and when to utilize radio functions for discovering network neighborhood, establishing wireless links, and exchanging different frame types. A routing protocol creates multi-hop routing paths between source and destination nodes, while the transport protocol implements end-to-end flow control, if necessary. An Application Programming Interface (API) abstracts the underlying communication and hardware for applications. Several applications may be executed in parallel, for example sensing, actuating, data fusion, and node diagnostics.

1.2 Key WSN Design Requirements

The key design requirements of low-energy WSNs differ in many ways from traditional wireless computer networks. As presented in Table 2, high throughput and low latency are the most critical requirements for wireless computer networks, e.g. IEEE 802.11 Wireless Local Area Network (WLAN) [79].

The most important design requirement for the low-energy WSN is *resource constrained implementation*. In this Thesis, WSN should be implementable in practice using current COTS components. Due to the size, cost, and lifetime requirements of applications, WSN nodes have scarce communication, computation, and energy resources.

Another important requirement is *networking performance*. WSN should be adaptive for ensuring network robustness in uncertain operation conditions, where network

Table 2. *Relation of requirements for wireless computer networks and low-energy WSNs.*

Requirement	Criticality for wireless computer networks	Criticality for low-energy WSNs
Resource constrained implementation	Low	Very high
Adaptivity	Low	High
Scalability	Moderate	High
Fairness	Moderate	Moderate
Latency	High	Low
Throughput	Very high	Low

size, node locations, and Radio Frequency (RF) propagation conditions vary dynamically. In order to enable mobile applications, network should tolerate node mobility at a pedestrian walking speed. In addition, scalability to support various network sizes up to tens of thousands of nodes, and node densities up to hundreds of active nodes in a radio range is required.

Due to the characteristics of WSN applications, *data transfer performance* has lower criticality than the above mentioned requirements. Fairness is desirable such that all nodes can transmit data to sinks equally, and that all sinks can receive data from nodes equally. A tolerable latency from nodes to a sink in a large network is even minutes, while a sufficient throughput is in the order of one kbits/s.

Existing standards for wireless communications, such as cellular telephone networks, WiMAX [215], IEEE 802.11 WLAN [79], and Bluetooth [20] are unsatisfactory for WSNs due to their limited energy-efficiency, scalability and adaptivity. IEEE 802.15.4 Low-Rate Wireless Personal Area Network (LR-WPAN) can be configured to a low-power operation mode and thus, it is a promising standard for enabling WSNs [64]. Still, it has problems of combining the energy-efficiency with adaptivity and scalability required by many potential applications [118].

Although many protocols have been proposed for traditional wireless ad hoc networks [126], these protocols aim to provide good throughput and delay characteristics. However, energy consumption takes up secondary importance, since batteries can be easily replaced or charged when needed. Hence, these protocols cannot provide adequate energy-efficiency for WSNs [5].

There are two wireless technologies, which can be categorized as low-end WSNs: Radio Frequency Identification (RFID) and Near Field Communication (NFC). RFID technology is typically seen as an intelligent version of the bar codes [75, 86]. In

general, RFID tags can communicate with a high-power reader device only [27]. NFC technology can be seen as a contactless smart card reader and writer, which is embedded in portable electronic devices, such as mobile phones. NFC devices can form a simple peer-to-peer network and exchange data in a range of about 10 cm [29]. The suitability of these technologies for WSNs is severely limited due to their short range, small network size, and limited networking capability.

1.3 Scope, Objectives and Methods of the Research

The scope of this research is on the MAC layer protocols and component-based sensor node hardware prototypes (platforms) for low-energy WSNs. Applications and upper protocol layers are covered only briefly for evaluating the requirements for the MAC and platform designs. Sensing, simulations, software design flow, and hardware design of Integrated Circuits (ICs) are outside the scope of this Thesis.

The main objective of this Thesis is to solve the problems of resource constrained WSN implementation and networking performance by a MAC layer design. An objective is to design feasible solutions for real deployments in harsh operation conditions. For obtaining realistic and feasible results, the MAC layer is designed according to the characteristics of current state-off-the-art low-power COTS components.

The methods for conducting the research results of this Thesis are presented in Fig. 4. In the first phase, a literature review is carried out and target applications are identified. At the same time, the capabilities and behavior of current state-of-the-art hardware components are analyzed and the requirements for MAC design are evaluated. According to this information, the initial version of a MAC design is formulated.

Next, the performance of the MAC design and other MAC approaches are evaluated by modeling them analytically. The performance of the approaches are analyzed and compared, while varying protocol, network, and application parameters. According to analysis results, the MAC design is refined.

As a potential MAC design is found, its feasibility is studied in real applications by experimental measurements. An objective is to identify the non-ideal characteristics of hardware components and radio environment. This information is used in the MAC design for improving and optimizing its performance. Thus, real sensor node platforms are designed and implemented using state-of-the-art commercial components. The power consumptions and operation mode switching times of the platforms are

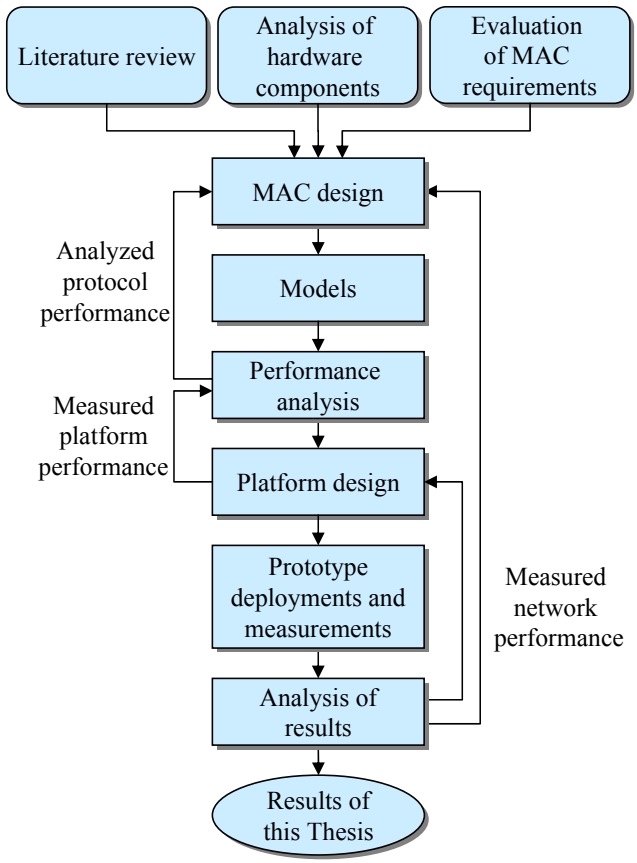

Fig. 4. *Methods for obtaining the results of this Thesis*

back-annotated to the performance analysis phase for improving analysis accuracy and for refining the MAC design.

Next, a prototype network is deployed and its performance is measured. The measured performance is used for improving and optimizing MAC and sensor node platform designs.

As results, this Thesis presents MAC protocol designs and sensor node platforms, which fulfill the presented requirements of low energy WSNs.

1.4 Research Outcomes

The results of this Thesis are summarized in Fig. 5. The main contribution is a MAC design for TUTWSN (Tampere University of Technology Wireless Sensor Network)

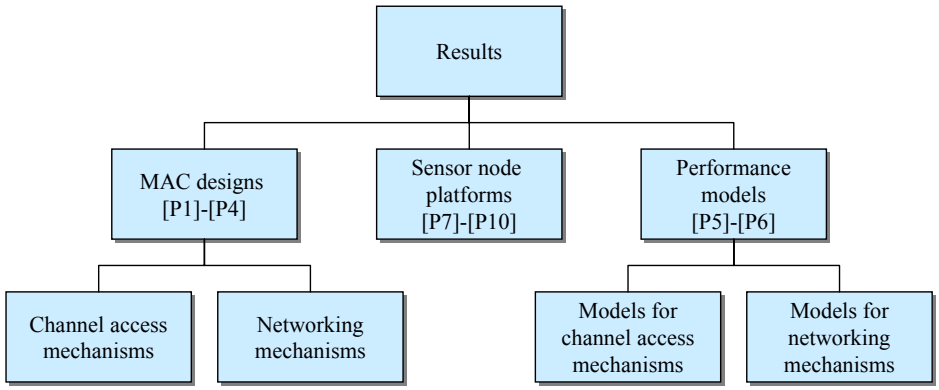

Fig. 5. *Results of this Thesis.*

([P1] - [P4]). The design comprises channel access and networking mechanisms. While channel access mechanism defines mainly frame exchanges and link synchronization, the networking mechanisms specify network self-configuration and neighbor discovery mechanisms.

The second research outcome are sensor node platforms ([P7] - [P10]). Several platforms have been designed and implemented to evaluate the performance of the MAC design and hardware components in real deployments.

The third main outcome of the research are performance models for various channel access and networking mechanisms ([P5], [P6]). MAC layer models are defined for TUTWSN, IEEE 802.15.4, and the most essential research proposals. Besides indicating the performance of the TUTWSN MAC design, the models are used for showing the energy-efficiency of the designed networking mechanisms for IEEE 802.15.4 [P3].

As a summary, the main contributions of the Thesis are:

- A survey of existing energy-efficient MAC protocols, standards, and low-power sensor node platforms for WSNs.
- Energy-efficient and scalable channel access mechanism for a resource constrained WSN called TUTWSN MAC.
- Networking mechanisms for improving network adaptivity in dynamic environments.
- Several low-power sensor node platforms for WSNs. The platforms enable real WSN deployments and experimental performance evaluation.

- Performance models and analysis of several MAC designs including TUTWSN, IEEE 802.15.4, and the most essential research proposals.
- Deployment cases that validate the analysis results and the feasibility of designed mechanisms and platforms.

1.5 Thesis Outline

The Thesis consists of an introductory part and 10 publications [P1-P10]. The introductory part motivates the work, presents technical background, and summarizes and analyzes the results. The main results are presented in the publications. Publication [P1] presents the overview of MAC layer, while the results in details are presented in publications [P2] - [P10]. The rest of the introductory part is organized as follows:

Chapter 2 presents the WSN application space and performed deployments. The chapter includes also an overview of existing standards related to WSNs.

Chapter 3 discusses the design principles of sensor node platforms, and presents existing platforms. The chapter presents the characteristics of low-power components and provides a basis for a MAC layer design.

Chapter 4 discusses the most essential MAC protocols for WSNs. The chapter provides a research background for TUTWSN MAC design.

Chapter 5 composes the research results of channel access and networking mechanism.

Chapter 6 presents the research results of performance models considering the most essential MAC layer designs for WSNs.

Chapter 7 presents the research results of sensor node platform designs and deployments cases.

Chapter 8 summarizes the publications included in the Thesis

Chapter 9 concludes the Thesis.

2. APPLICATIONS AND STANDARDS

This chapter presents the current state of WSN research in application development. First, the design space of WSN applications is presented including application tasks and usage classes. Then, the performed WSN deployments are discussed. As a reference, this chapter presents also existing standards for wireless communication. The state of the research in sensor node platforms and MAC protocols will be presented in the following chapters.

2.1 WSN Application Space

WSN application space is continuously emerging and extending together with the development of low-power circuits and communication protocols. Potential applications have been found in home automation, environmental and industrial monitoring, military, personal security, asset management, and traffic control [5, 32, 40, 88, 144, 146, 160]. WSN applications can execute one or more application tasks, which are build upon the sensing, actuating, communication, and computing capabilities of WSN nodes. The application tasks can be divided into five categories [5, 66, 93]:

Data logging: Determine periodically the value of a physical quantity in a given location, for example temperature, humidity and gas concentration.

Event detection: Detect the occurrence of an event of interest, for example motion or the exceeding of a predetermined physical quantity.

Object classification: Identify an object or an event according to measurements using different sensors.

Object tracking: Trace the movement, direction and speed of an object according to measurements at different locations.

Control: Control an actuator according to commands or measured sensor values within the network, for example a valve and an electrical switch.

Wireless data networks can be classified into six classes according to message latency and reliability requirements, as presented in Table 3 [83]. The classification is referred for clarifying the application space of WSNs.

The classes 5 - 4 are categorized as monitoring networks. The class 5 has the lightest message latency requirements, and it is suitable for data logging networks. Rather long delays are tolerated and some messages can be missed. The class 4 has slightly higher latency requirements and no messages should be missed. The class 4 is suitable for flagging networks performing event detection tasks.

The classes 3 - 1 are categorized as control networks. The class 3 contains open-loop control networks, where a human is in the loop. The class 2 contains closed loop supervisory control for non-critical control tasks. The class 1 networks perform closed loop regulatory control, where the criticality for latency and reliability is very high.

Class 0 contains safety networks having the highest requirements for message latency and reliability. These networks are used for emergency action.

The low-energy WSNs discussed in this Thesis are suitable for the classes 4 and 5, and the class 3 will be reached in the near future. The highest energy-efficiency and scalability are achieved at the class 5. As the requirements for latency and reliability raise, the need for a centralized network management also increases limiting the scalability and energy-efficiency.

Table 3. *Usage classes of wireless data networks.*

Class	Description	Criticality of latency and reliability	Suitability of current low-energy WSNs
0	Emergency action	Always critical	Very low
1	Closed loop regulatory control	Often critical	Very low
2	Closed loop supervisory control	Often non-critical	Low
3	Open loop control	Non-critical	Moderate
4	Flagging	Non-critical	High
5	Data logging	Non-critical	Very high

Table 4. *Examples of experimental WSN deployments.*

Deployment	Year	Scale	Duration (months)	Data period	Node platform	MAC protocol	Power (mW)
GDI [185]	2003	98	3.8	20 min	Mica2Dot	B-MAC	1.6
Vineyard [16]	2003	65	6	5 min	Mica2	CSMA	58
Macroscope [199]	2004	33	1.5	5 min	Mica2Dot	CSMA	1.5-6.3
ZebraNet [225]	2004	7	12	8 min	custom	Z-MAC	30-70
Heathland [200]	2005	24	0.5	1 hour	ESB	CSMA	30
SensorScope [13]	2007	17	1.5	2 min	Tiny node	S-MAC	N/A

2.2 Deployments

To illustrate potential application types in practice, few interesting WSN deployments are presented. The presented deployments have been selected according to the following requirements: networks should utilize multi-hop networking, and the deployment duration should be at least one week. The deployments are summarized in Table 4. The columns of the table give an overview and characteristics of the deployments. Focus is on the network size, duration of the deployment, utilized sensor node platform and MAC protocol, and average power consumption of nodes. The data period presents the activity of the network giving the frequency of data communication.

A deployment on Great Duck Island (GDI) [185] monitors the occupancy of small, underground nesting burrows and the role of micro-climatic factors in their habitat selection on an offshore breading colony. A 115 days long deployment in 2003 comprised 98 Mica2Dot [38] motes, which executed Berkeley Media Access Control (B-MAC) [129] protocol. Data was collected at 20 minutes intervals, and forwarded to a sink by multi-hop routing. The deployment indicated that most links are short lived: the median link is used to deliver only 13 packets. The packet loss was very significant, since nearly half of packets were lost during routing. Node lifetimes varied from 1 to 110 days causing connectivity problems for the network. The average power consumption was around 1.6 mW.

A temperature monitoring network deployed in a vineyard for 6 a months period in 2003 is presented in [16]. The deployment employed 65 Mica2 [37] motes, which executed TinyOS [58] protocol stack including a Carrier Sense Multiple Access (CSMA) type MAC layer. Their data was collected at 5 minutes intervals and multi-hop routed to a base station. Nodes utilized large 42 Ah battery packs. The reported lifetimes of routing nodes were about 3 months. According to the battery capacity, the calculated power consumption of routing nodes was 58 mW. The deployment demonstrated that

a WSN brings value to an agricultural setting and that the total cost of a WSN is lower than a wired data logger type network.

Macroscope [199] deployment recorded temperature, humidity, and solar radiation on the surface of a 70-meter tall redwood tree during 44 days period in the summer of 2004. The deployment consisted 33 Mica2Dot [38] motes, which collected data at 5 minutes intervals and multi-hop routed the data to a sink node. Nodes utilized TASK [26] protocol stack including a CSMA type MAC layer. The lifetime of the nodes using 560 mAh batteries were 11 to 44 days. Thus, the calculated power consumptions were between 1.5 mW and 6.4 mW. The experiment indicated that the network suffered from high packet loss, especially at nodes far from the sink. The packet loss was most probably caused by collisions.

ZebraNet [225] experiment tracked animal movements in Kenya on an area of 36 km^2. Seven nodes were attached on Zebras, and their locations were tracked during 12 months in 2004. Global Positioning System (GPS) was activated at 8 minutes periods at a time, and the data was multi-hop routed to a base station. Nodes comprised a low power MCU, a 900 MHz radio and a GPS receiver, and they executed Zebra MAC (Z-MAC) [143] protocol. The power consumptions of nodes were between 30 mW and 70 mW. Each node was powered by a rechargeable battery and a 200 grams solar panel. The experiment indicated that harsh operation conditions and the lack of a large ground plane reduced radio range significantly.

Heathland experiment [200] in Northern Germany analyzed wireless communication in an outdoor environment in March 2005. The deployment comprised 24 ESB [157] nodes, which formed a multi-hop network. The MAC protocol was based on a simple CSMA [91]. Data collection interval was 1 hour. As nodes were powered by three AA batteries, node lifetimes near the sink were 16 days. Thus, their power consumptions were around 30 mW. The experiment demonstrated that the quality of radio links varies considerably in the long run. The required adaptive protocols can be evaluated only in field trials.

SensorScope [13] measured the hydrological model of the Grand Saint Bernard pass during a 1.5 months period in 2007. The pass is 2400 m high and located in the Alps between Switzerland and Italy. In the deployment, 17 Tiny nodes [47] were located on a 900 m long line, and they measured humidity values at 120 s intervals. Nodes executed Sensor-MAC (S-MAC) [220] type channel access and multi-hop routed data to a sink having General Packet Radio Service (GPRS) connectivity. The network suffered from significant packet losses, which were mostly caused by hardware malfunctions.

Most of the performed deployments have been targeted for environmental monitoring, where data gathering interval has been several minutes. The scale of long-term WSN deployments has been tens of nodes. The average power consumption of nodes has ranged between 1.5 mW and 58 mW, and adequate network lifetime has been achieved by using large battery packs or solar panels [16, 225]. Common problems in the deployments have been unequal power consumption of nodes and weak tolerance against harsh operation conditions, network dynamics, and congestion [199, 200, 225].

Commercial networks are still rare and detailed information about their performance is not available. Most of them are development kits or radio modules necessitating engineering work in application development, for example Dust Networks, Inc. [48], Nanotron Technologies GmbH [116], Dynastream Innovations, Inc. [50], and Crossbow Technology, Inc. [36]. Sensicast [166] provides also various sensors and interfaces for external networks.

2.3 Standards

There exist numerous standards for wireless communication technologies for enabling inter-operability between products from different manufacturers. For end users the utilization of standards provides many benefits in technology support, product availability, and expandability. In this Thesis, the standards set a starting point and reference for the research. Next, the current status of standards is discussed in the WSN point of view, and the need for a proprietary solution is reasoned.

2.3.1 Wireless Communication Standards

The classification of standards originated by IEEE categorizes wireless communication technologies according to their range, data rate, and power consumption [75, 76, 170]. The categories of existing wireless technologies are presented in Table 5. The presented value ranges are not absolute but merely indicative [27, 64, 75, 111, 214]. Although WSN is not included in the conventional IEEE originated classification, it is presented for comparison.

Wireless Wide Area Networks (WWANs) provide the widest geographical coverage. The most well-known WWANs are digital cellular telephone networks, such as Global System for Mobile Communications (GSM), and their extensions for data

services, e.g. GPRS, and Universal Mobile Telecommunications System (UMTS). Also communication satellites belong to this category.

Wireless Metropolitan Area Networks (WMANs) are emerging technologies developed to specify broadband wireless access as an alternative to cable networks and Digital Subscriber Lines (DSLs). Thus, the provided data rates are much higher than in WWANs. WMAN is often called Wordwide Interoperability for Microwave Access (WiMAX) by an industry group called the WiMAX forum. Examples of WMANs are IEEE 802.16 and its mobile extensions.

WLANs were originally developed for extending or replacing wired computer Local Area Networks (LANs). Currently, WLAN is widely employed for providing network access with location freedom in homes, public buildings and enterprises, and for municipal public network implementations. The dominating WLAN technology is IEEE 802.11 [79] with its numerous extensions for higher communication speeds, Quality of Service (QoS) support, security, and mesh networking.

Wireless Personal Area Networks (WPANs) are generally targeted at data communications between personal devices, including Personal Digital Assistants (PDAs), mobile phones, headsets, and laptops. The most well-known and mature WPAN technology is Bluetooth [20], which is also known as IEEE 802.15.1 [80]. The WPAN category also includes two emerging standards: an IEEE 802.15.3 [81] standard for higher data rate multimedia content delivery, and an IEEE 802.15.4 [82] standard for low-rate and low-power communications. WPANs include very wide range of applications, and their characteristics are not clearly distinct from WLANs, sharing the same operational environments and application domains. The differences are in the non-functional requirements, such as cost, power, and networking range.

Table 5. *Categorization of wireless communication technologies.*

	Range	Data rate	Power consumption	Example technologies
WWAN	> 10 km	< 10 Mbits/s	medium/high	GSM, GPRS, UMTS, satellite
WMAN	< 10 km	< 100 Mbits/s	high	IEEE 802.16, HIPERMAN
WLAN	< 100 m	< 100 Mbits/s	medium	IEEE 802.11, HIPERLAN/2
WPAN	< 10 m	< 10 Mbits/s	low	Bluetooth, IEEE 802.15.4
WSN	< 1 km	< 100 kbits/s	ultra-low	Proprietary, IEEE 802.15.4

2.3.2 Standards Related to WSNs

In contrast to WLANs and WPANs, WSNs are envisioned to have much more network devices, which are application-oriented rather than measured by the coverage of a single radio cell or the nominal capacity of a link [5, 88]. WSNs nodes are stand-alone stations without the need or even possibility for human intervention. The network performance is measured as its capability to serve the implemented applications. Depending on the application, the data rate of a single node varies from few bits/s to hundreds of kilobits/s, and network coverage ranges from centimeters to several kilometers [94]. There is no pre-existing physical infrastructure that restricts the topology. Messages should not be sent to individual nodes but to geographical locations or regions defined by data content [178]. As resources are constrained, the feasibility of WSN lies on the joint effort of the nodes [178]. The most potential standardized technologies for realizing WSNs are ZigBee [64, 229], and emerging ISA-SP100.11a [83].

ZigBee AND IEEE 802.15.4

ZigBee [229] is an open specification for low data-rate wireless control and monitoring networks, where low-power consumption is a key requirement. The candidate applications are wireless sensors, lighting controls, and surveillance. The first version of the ZigBee specification was announced in December 2004. A refinement of the specification has been launched in December 2006 [55, 131].

ZigBee builds upon the MAC and Physical (PHY) layers defined by IEEE 802.15.4 LR-WPAN, as presented in Fig. 6 [70]. IEEE 802.15.4 is responsible for the channel access mechanism, acknowledged frame delivery, network association, and disassociation.

A Network (NWK) layer provides network self-organization and multi-hop routing capability. NWK performs route discovery and maintenance, and message relaying functions. NWK can initiate a new network and assign network addresses to new nodes associating with the network for the first time. A Security Service Provider (SSP) offers security functions including Advanced Encryption Standard (AES) encryption, key generation, key distribution, authentication and access control lists [227]. Overall node management is performed by a ZigBee Device Object (ZDO). Application endpoints may call ZDO in order to discover other ZigBee nodes on the network and services they offer, and to define security and network settings. An Application Support (APS) sub-layer connects NWK, SSP and endpoints, and routes

messages to different endpoints. An application layer at the top of the stack determines node relationships, and supervises network initiation and association functions. The application layer contains application profiles, which define the format of exchanged messages for a given applications. ZigBee defines a set of public profiles for common application scenarios. In addition, vendors may add additional features with private profiles [211].

IEEE 802.15.4 defines two Direct Sequence Spread Spectrum (DSSS) radio types operating in Industrial, Scientific, Medicine (ISM) frequency bands. A low-band PHY operates in the 868 MHz or 915 MHz frequency band and has a data-rate of 20 kbps or 40 kbps, respectively. A high-band PHY operating in the 2.4 GHz band specifies a data-rate of 250 kbps.

IEEE 802.15.4 defines three types of logical devices, a Personal Area Network (PAN) coordinator, a coordinator, and a device. PAN coordinator is the primary controller of PAN, which initiates the network and operates often as a gateway to other networks. Each PAN must have exactly one PAN coordinator. Coordinators collaborate with each other for executing data routing and network self-organization operations. Devices do not have data routing capability and they can communicate only with coordinators.

Besides star and peer-to-peer network topologies, ZigBee supports a cluster-tree topology. The network consists of clusters, each having a coordinator as a cluster head and multiple devices as leaf nodes. A PAN coordinator initiates the network and serves as the sink. The network is formed by parent-child relationships, where new nodes associate as children with the existing coordinators. This well-defined structure simplifies multi-hop routing and allows energy saving on the MAC layer. The applicability of ZigBee on WSN applications is limited by scalability, the energy consumption of coordinators, and the support for one sink only.

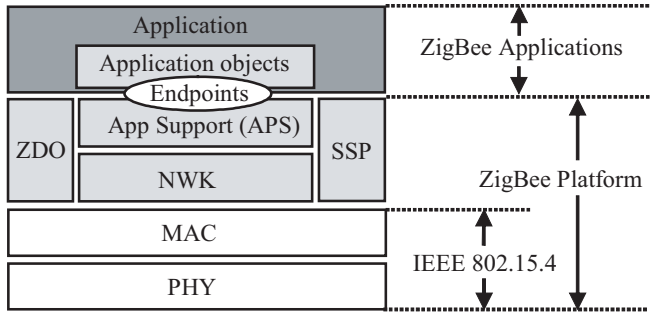

Fig. 6. *ZigBee protocol stack.*

MiWi

MiWi [57] developed by Microchip is a simpler version of ZigBee operating above a IEEE 802.15.4 compliant radio. MiWi is suitable for smaller networks having at most 1024 nodes. Supported network topologies are star and mesh. Simplifications for ZigBee stack reduces the cost of MCU even 40% - 60%. A disadvantage is that MiWi does not support the low duty-cycle mode of ZigBee. Thus, the energy consumption of MiWi is too high for most of WSN applications.

Z-Wave

Z-Wave [151] is another simpler version of ZigBee operating at 868 MHz and 915 MHz frequency bands. The maximum number of nodes in a network is 232. Supported network topologies are star and mesh. The suitability of Z-Wave for WSN applications is limited by scalability, and energy-efficiency, since the cluster-tree topology with power saving features is not supported.

Bluetooth

Bluetooth [20] is a wireless technology specified by the Bluetooth Special Interest Group (SIG). IEEE has standardized the MAC and PHY layers of Bluetooth as IEEE 802.15.1 [80]. Originally, it was only intended as a simple serial cable replacement for electronic devices. Presently, the technology supports various more advanced functionalities, such as ad hoc networking and access point operation for Internet connections.

Bluetooth operates in the 2.4 GHz unlicensed ISM band and utilizes the Frequency Hopping Spread Spectrum (FHSS) technique in the radio interface [20]. Current versions have up to 3 Mbps data rate, while the link range is from 10 cm to 100 m. A network composed of Bluetooth devices is called a *piconet*, which consists of a master and up to seven slave devices. Piconets can be linked together to form a larger network, known as *scatternet*. The applicability of Bluetooth in WSN applications is limited by scalability and energy consumption.

Ultra-Low-Power Bluetooth

Ultra-Low-Power Bluetooth (ULPB) [19,212] is a light-weight version of Bluetooth. It has been announced by Nokia Corp as Wibree at October 2006. ULPB is operating

at 2.4 GHz frequency band and it supports a star network topology with one master and seven slave nodes. For reducing the power consumption and expenses, ULPB utilizes lower transmission power and lower symbol rate. It is expected frequency hopping is not utilized, either. It is expected that the ULPB can reduce the power consumption of Bluetooth to one tenth.

ULPB may have a common RF part with Bluetooth making its integration into cellular phones and laptop computers cheaper. Yet, small devices, such as watches and sport sensors may utilize just a ULPB radio. Hence, ULPB can connect together two market segments: devices having Bluetooth and simple devices for which Bluetooth is too powerful and energy consuming. Yet, the applicability of ULPB in WSN applications is limited by scalability and network coverage.

ANT

ANT [49] developed by Dynastream Innovations is a simple low data-rate and low-latency technology specifying PHY, MAC and NWK layers. ANT operates at 2.4 GHz frequency band and has 1 Mbps radio data rate. ANT network is based on a star-topology, but more complex topologies can be achieved by using several channels: each node can be simultaneously a master and a slave on different channels. Master nodes always receive, while slaves transmit when new data is provided. A practical limit for network size is few thousands nodes. The disadvantages of ANT are high power consumption in master nodes and low scalability due to random access transmissions. These limit the usability of ANT in large multi-hop WSN applications.

WirelessHART

WirelessHART [67] is an open wireless communication standard ratified in 2007 by the HART Communication Foundation [67]. WirelessHART is specifically designed for process measurement and control applications having stringent requirements for end-to-end communication delay, reliability, and security [176]. WirelessHART utilizes a time-synchronized TDMA MAC on top of the IEEE 802.15.4 physical layer. MAC employs network wide time synchronization, channel hopping, channel blacklisting, and AES encryption. WirelessHART utilizes a self-organizing multi-hop mesh network with centralized control. For guaranteeing network performance, a central network manager is responsible for route updates and communication scheduling for entire network. The suitability of WirelessHART on WSN applications is limited. The centralized control of TDMA schedule and routes limits

network size and the tolerance against network dynamics. The centralized control causes a significant control frame overhead increasing network energy consumption.

ISA-SP100.11a

ISA-SP100.11a [83] is an emerging standard for non-critical process industry applications, where tolerable delays are in the order of 100 ms. Target applications include sensors, valves and actuators having low data rate requirements [197]. The standard is expected to be published during 2008 [213]. Later versions of the standard will also address factory automation and building automation [83]. Similarly with WirelessHART, ISA100.11a utilizes time synchronized TDMA and frequency hopping with channel blacklisting on top of the IEEE 802.15.4 physical layer. ISA-SP100.11a supports multi-hop routing in a mesh topology and battery powered routers. In contrast to WirelessHART, ISA-SP100.11a specifies utilization of multiple gateways and flexible TDMA slot length for improving data routing performance [22]. It is expected that ISA-SP100.11a will be a suitable technology for some WSN applications, too. The usability in WSN applications is possible limited by scalability, energy consumption, and tolerance against network dynamics.

IEEE 1451 Standard Family

IEEE 1451 is a suite of smart transducer interface standards, which describes communication interfaces for connecting sensors and actuators (transducers) to microprocessors, instrumentation systems, and networks.

IEEE 1451 defines two terms: Transducer Interface Module (TIM) and Network Capable Application Processor (NCAP). TIM is a device, which contains a set of transducers, signal conditioning and data conversion circuitry, and software modules. They consist of IEEE 1451 standard modules and a standardized wireless or wired network technology. NCAP is any kind of network-connected computing device, which receives data from a set of TIMs.

IEEE 1451.0 standard defines the functional specification of TIM, the discovery and management of TIMs, and a set of sensor API calls with message exchange protocols and commands required for interfacing with transducers. In addition, IEEE 1451.0 defines a Transducer Electronic Data Sheet (TEDS), which is used to describe the entire TIM including transducer, signal conditioner and data converter. Hence, TEDS eliminates error prone, manual entering of data and system configuration and allows transducers to be installed, upgraded, replaced or moved by plug-and-play principle.

IEEE 1451 supports numerous standardized technologies to establish wired and wireless connections between NCAP and TIMs by IEEE 1451.2 through IEEE 1451.6. IEEE 1451.2 defines wired point-to-point communication through UART or a Transducer Independent Interface (TII). IEEE 1451.3 defines distributed multi-drop system, where a large number of TIMs may be connected along a wired multi-drop bus. IEEE 1451.4 specifies mixed-mode communication protocols, which carry analog sensor values with digital TEDS data. IEEE 1451.6 defines a high-speed Controller Area Network (CAN) bus. IEEE 1451.5 standard [77] defines wireless sensors and thus, it is most closely related with WSNs. Supported communication technologies are IEEE 802.11a/b/g, IEEE 801.15.1 and IEEE 802.15.4.

Conclusion of Standards

Current standards for wireless communications are diverse, but none of these cover the entire WSN application space [93]. Currently, ZigBee and its variations are the most potential standardized technologies for WSNs. Their feasibility is mostly limited by the energy consumption of routers, scalability, and inadequate performance in dynamic networks. Yet, standards are improving and new standards are emerging continuously. One of the most interesting upcoming standards is the ISA-SP100.11a, which will most probably cover most of the application areas of ZigBee.

One of the most difficult challenges in WSN is to develop energy-efficient MAC layer protocols for very large and dynamically changing networks. This area is not covered by the current standards and the upcoming standards released in the near future. This area has been selected as the main focus in this Thesis.

3. SENSOR NODE PLATFORMS

Sensor node platforms implement the physical layer (hardware) of the protocol stack. In conventional wireless networks, such as WLANs, hardware affects very significantly on the achieved performance and the energy consumption of network terminals. In WSNs, the energy-efficiency is implemented mostly by the MAC layer, which at best can reduce the activity of a hardware to below 1% in low data-rate monitoring applications. Clearly, it is important to minimize hardware power consumption in active operation modes. Even more important is to minimize the power consumption in idle and sleep modes, which may dominate the power consumption and limit network lifetime in very low data-rate applications. Next, suitable low-power hardware components and existing sensor node platforms are discussed.

3.1 Platform Components

WSN applications typically necessitate small and cheap hardware realization having the battery lifetime in the order of years. The given requirements for are fulfilled best by Application Specific Integrated Circuits (ASICs), which perform computation powerfully and energy-efficiently by an application specific hardware [133]. Small physical size is achieved, since a single System-on-Chip (SoC) circuit contains all essential digital circuits. Due to high design and initial costs, and fixed hardware, ASIC suits best for implementing a mature and standardized technology having very high production volumes. For WSNs, COTS components are often the most feasible option. From now on, the focus will be on COTS based hardware components.

A general hardware architecture of a sensor node platform is presented in Fig. 7. The architecture can be divided into four subsystems:

Communication subsystem enabling wireless communication,

Computing subsystem allowing data processing and the management of node functionality,

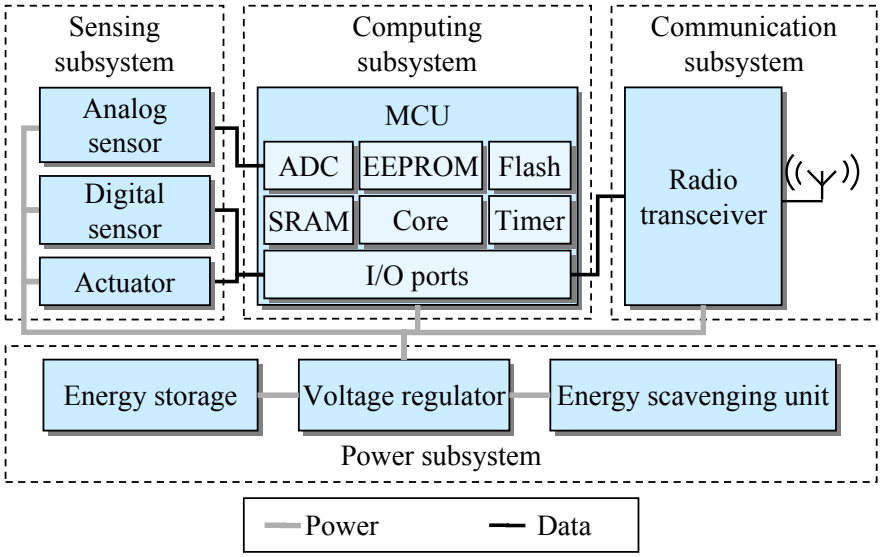

Fig. 7. *Sensor node hardware architecture.*

Sensing subsystem connecting the wireless sensor node to the outside world,

Power subsystem providing the system supply voltage.

The central component of the platform is MCU that forms the computing subsystem. In addition, the protocols of communication and sensing subsystems are executed on MCU.

3.1.1 Communication subsystem

The communication subsystem consists of a wireless transceiver and an antenna. A wireless transceiver can be based on acoustic, optical or RF waves. Acoustic communication is typically used for communication under water [92] or to measure distances based on time-of-flight measurements [15]. The disadvantages of acoustic communication are long and variable propagation delay, high path loss, noise, and very low data rate, which limit the achieved energy-efficiency. Also, a large external antenna is needed. In mobile networks, Doppler spread is significant reducing the data rate [92].

Optical communication [46, 216] has low energy consumption especially in reception mode, and it can utilize very small antenna. A transmitter can be implemented by a Light Emitting Diode (LED) or a laser, and a receiver by a photo diode. However, radiation is highly directional and a Line-of-Sight (LOS) condition is required.

Hence, the alignment of a transmitter to a receiver is difficult or even impossible in large-scale WSN applications [216].

RF communication combines the benefits of high data rate, long range and nearly omni-directional radiation, which make it the most suitable for WSNs. Disadvantages are large antenna size, and higher energy consumption compared to optical technology [46].

In general, an RF transceiver (radio) has four operation modes: transmit, receive, idle, and sleep. Radio is active in transmit and receive modes, when power consumption is also the highest. In idle mode, most of circuitry is shut down, but main oscillators remain active. Thus, the transition to the active mode is fast. The lowest power consumption is achieved in sleep mode, when all circuitry is switched off. Also, the transient time to the active mode is relatively long [P7].

Most short-range radios utilized with WSNs operate in the 433, 868, 915, and 2400 MHz license-free ISM frequency bands. The operating frequency affects RF wave propagation characteristics. In industry, the 2400 MHz band is beneficial, since the interferences emitted from the machinery are significant below few hundred megahertz and drops rapidly above 1 GHz frequency [136]. The 2400 MHz band is also the widest providing more channels and typically higher data rate than the lower ISM bands. Depending on the frequency band and antenna type, operating range with 1 mW Transmit (TX) power is from few meters to hundreds meters [P7]. The characteristics of the most potential commercial low power radios are summarized in Table 6 [P7]. Microchip, Nordic Semiconductor, and Texas Instruments utilize on-chip buffers for the adaptation of a high-speed radio with a low-speed MCU [P7]. Current consumptions are specified at the lowest band and 0 dBm transmission power. The table indicates that data rate and frequency band has only a low effect on current consumption. The last two paragraphs present the energy consumption of a received and transmitted bit of data, which are determined using 3.0 V supply voltage. The comparison indicates that radios operating at the 2.4 GHz frequency band are the most energy-efficient, which is mostly caused by their high data rates.

3.1.2 Computing subsystem

Computing subsystem consists of MCU, which integrates a processor core with program and data memories, timers, configurable I/O ports, ADC and other peripherals. Program memory is typically Flash, while data memory consists of Static Random Access Memory (SRAM) and Electrically Erasable Programmable Read-Only

Table 6. *Radio features, current consumptions, and energy efficiencies.*

Radio	Data rate ($kbps$)	Band (MHz)	Buffer (B)	Sleep (μA)	RX (mA)	TX (mA)	RX (nJ/b)	TX (nJ/b)
MC MRF24J40 [107]	250	2400	128	2	18	22	264	216
NS nRF2401A [120]	1000	2400	32	0.9	19.0	13.0	39	57
NS nRF24L01 [121]	2000	2400	32	0.9	12.3	11.3	17	18
NS nRF905 [122]	50	433-915	32	2.5	14.0	12.5	750	840
RFM TR1001 [141]	115.2	868	no	0.7	3.8	12	313	99
RFM TR3100 [142]	576	433	no	0.7	7.0	10	52	36
SE XE1201A [163]	64	433	no	0.2	6.0	11.0	516	281
SE XE1203F [165]	152.3	433-915	no	0.2	14.0	33.0	650	276
TI CC2400 [193]	1000	2400	32	1.5	24.0	19.0	57	72
TI CC2420 [194]	250	2400	128	1	18.8	17.4	209	226
TI CC2500 [189]	500	2400	64	0.4	17.0	21.2	127	102
TI CC1000 [192]	76.8	433-915	no	0.2	9.3	10.4	406	363
TI CC1020 [187]	153.6	433-915	no	0.2	19.9	16.2	316	389
TI CC1100 [188]	500	433-915	64	0.4	16.5	15.5	93	99

Abbreviations: Microchip (MC), Nordic Semiconductor (NS), RF Monolithics (RFM), Semtech (SE), Texas Instruments (TI)

Memory (EEPROM). The characteristics of potential MCU from different manufacturers are compared in Table 7. The energy-efficiencies of MCUs can be compared according to their current consumption at one MIPS processing speed. Since the instruction set affects the performance, only orders of magnitude are important [128]. The comparison indicates that Semtech XE8802 and TI MSP430F1611 MCUs have are the most energy-efficient [P7].

Table 7. *The comparison of the features of low power MCUs.*

MCU	FLASH (kB)	SRAM (kB)	EEPROM (B)	Sleep (μA)	1 MIPS (mA)
Atmel AT89C51RE2 (8051) [11]	128	8	0	75	7.4
Atmel ATmega103L (AVR) [9]	128	4	4096	1	1.38
Atmel AT91FR40162S (ARM) [10]	2048	256	0	400	0.96
Cypress CY8C29666 [41]	32	2	0	5	10
Freescale M68HC08 [59]	61	2	0	22	3.75
Microchip PIC18LF8722 [106]	128	3.9	1024	2.32	1.0
Microchip PIC24FJ128 [108]	128	8	0	21	1.6
Semtech XE8802 (CoolRisc) [164]	22	1	0	1.9	0.3
TI MSP430F1611 [190]	48	10	0	1.3	0.33

3.1.3 Sensing subsystem

Sensing subsystem consists of a set of sensors and actuators. The sensors observe phenomena such as thermal, optic, or acoustic event. They are equipped with an analog or digital interfacing for reading sensor values [3].

There exists a large variety of low power sensors suitable for WSNs. For example, sensors are available for acceleration, air pressure, humidity, illumination, infra-red, magnetic field, geographic position, and temperature. Important requirements for sensors are low power consumption and short sensing time, which determine the energy consumption of a single sensing. In addition, adequate accuracy is required within the entire temperature range. The features of some example sensors are presented in Table 8. Most of the sensors fulfill the requirements well. The suitability of a GPS position sensor for WSNs is questionable due to high energy consumption.

A WSN node can also operate as a decision unit, which takes sensor readings from the WSN as input and generates action commands as output. These action commands are then transformed into actions by actuators [3]. Besides an electric switch and a servo drive, an actuator can be a mobile robot. In order to improve the reliability of actions, the robot can be a WSN node and act based on its own sensor readings and the data of the other WSN nodes in the network [3, 45].

3.1.4 Power subsystem

The power subsystem stores supply energy and converts it to an appropriate supply voltage level. The subsystem consists of an energy storage, a voltage regulator, and possible an energy scavenging unit.

Table 8. *Features of typical sensors.*

Physical quantity	Example sensor	Accuracy	Active current	Sensing time	Energy cons.
Acceleration	VTI SCA3000 [204]	1%	120 μA	10 ms	3.6 μ J
Air pressure	VTI SCP1000 [205]	150 Pa	25 μA	110 ms	8.3 μ J
Humidity	Sensorion SHT15 [167]	2%	300 μA	210 ms	190 μ J
Illumination	Avago APDS-9002 [12]	50%	2.0 mA	1.0 ms	6.0 μ J
Infra-red	Fuji MS-320 [60]	-	35 μA	cont.	-
Magnetic field	Hitachi HM55B [74]	5%	9.0 mA	30 ms	810 μ J
Position	Fastrax iTRAX03 [56]	1.0 m	32 mA	4.0 s	380 mJ
Temperature	Dallas DS620U [42]	0.5°C	800 μA	200 ms	480 μ J

The energy storage can be a non-rechargeable (primary) battery, a rechargeable (secondary) battery, or a supercapacitor. Primary batteries are cheap and have the highest energy density. They are the most common power source for WSNs. Secondary batteries have lower energy density and are more expensive, but they can be recharged 500 - 1000 times. Secondary batteries are suitable, if batteries can be recharged occasionally. Generally, supercapacitors are capacitors having very high capacitance. Compared to secondary batteries, supercapacitors have lower energy density and they are more expensive. However, their lifetime is in the order of a million charging/discharging cycles. Supercapacitors are suitable to be used with an energy generator, since energy is typically generated in peaks during short periods of time, and the amount of stored energy can be relatively low.

The most potential sources for energy scavenging are photovoltaics and vibrations [149]. Solar cells are mature technology and they can provide up to 15 mW/cm^3 power at outdoor conditions. In indoor conditions, achieved power reduces to 10 μW/cm^3. A promising method for converting vibration to source power is a piezoelectric conversion. Commonly occurring vibrations can provide up to 200 μW / cm^3 power [150]. Other possible energy sources are temperature gradients (40 μW/cm^3 at 5 °C temperature differential) [127, 180] and air flow (380 μW/cm^3 at 5 m/s) [149].

A voltage regulator stabilizes system supply voltage to an appropriate and constant level. In order to minimizing static current consumptions, it is reasonable to use the minimum supply voltage specified by system components. The scarce energy budget sets strict requirements also for the voltage regulator. A typical current consumption waveform measured from two Tampere University of Technology Wireless Sensor Network (TUTWSN) nodes is presented in Fig. 8. The nodes are typically over 99% of time in a sleep mode. The regulator must be able to supply short peaks of relatively high, tens of milliamperes currents, while the quiescent current consumption must be very low.

Voltage regulators can be divided into linear and switched-mode regulators. Linear regulators control the output voltage by adjusting the voltage drop across a series power transistor, which is located between the unregulated input and the regulated output voltage. This transistor conducts continuously and the energy of voltage drop is converted to heat. Thus, linear regulators are simple, cheap, small and have very low electromagnetic interferences and quiescent current [115].

Switched-mode step-down type regulators convert and input voltage to a lower output voltage by a switching transistor that is opened and closed periodically. Then, the switching current is fed to a simple coil-capacitor (L-C) filter and a diode, which aver-

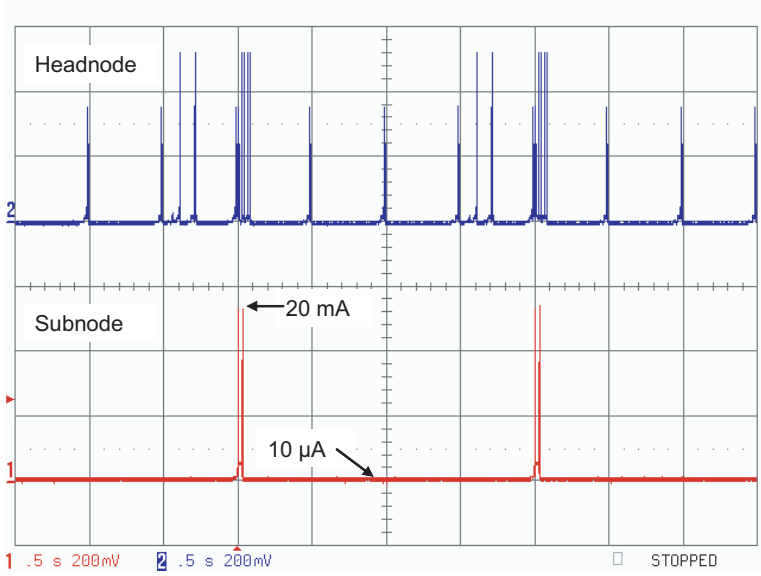

Fig. 8. *Measured current waveform from TUTWSN subnode and headnode.*

age the output voltage. Thus, the energy loss of the regulator is theoretically zero. In practice, some energy is consumed in the voltage drops, resistances and leakage currents of the switching transistor, diode, coil and capacitor, and for the supply power of a controller circuitry. Compared to linear regulators, switching mode regulators are more expensive and larger, and have significantly higher electromagnetic emissions and quiescent current [115].

Switched-mode regulators provide higher energy-efficiency, when the supply current and dropout voltage are high. Yet, in WSN applications linear regulators are more energy-efficient due to the low average supply current levels. For comparing the performance of linear (L) and switched-mode (S) regulators, Table 9 presents the features of some of the lowest power regulators available on the market.

3.2 Existing Platforms

Sensor node platforms have been improved significantly during the last decade along with the advances in low power processing and communication technology. Due to the strict energy constrains, and the visions of complex networking and data fusion, it is very challenging to fulfill all the requirements with the current level of technology. Thus, the platform research can be divided into two branches: high performance platforms, and low power platforms [72].

Table 9. *Features of low-power voltage regulators.*

Regulator	Type	Quiescent current (μA)	Max. load (mA)	Max. input (V)	Dropout (mV)
Maxim MAX1725 [102]	L	2.0	20	12.0	300
Maxim MAX8880 [103]	L	3.5	200	12.0	350
Microchip MCP1702 [110]	L	2.0	250	13.2	330
Minilogic ML62 [113]	L	2.8	150	10	800
SII S-1206 [162]	L	1.0	250	6.5	350
TI TPS71501 [195]	L	3.2	50	24	415
Analogic Tech AAT1112 [1]	S	42	1500	5.5	200
Microchip MCP1603 [109]	S	45	500	5.5	250
TI TPS62000 [191]	S	50	600	5.5	230

The high performance platforms have been developed for researching complex data processing and fusion in sensor nodes. The design target has been the reduction of transmitted data by efficient data processing. These platforms utilize high performance processors having at least tens of MIPSs processing performance and hundreds of kbytes program and data memories. For long-lived battery operation, their energy consumption is not adequate. However, these high power platforms can be used as a part of a WSN for data processing and data routing. Examples of the high performance platforms are Piconode [139], μAMPS [112], and Stargate [35].

Low power platforms are aiming to maximize the lifetime and minimizing the physical size of nodes. These are obtained by minimizing hardware complexity and energy consumption. These platforms are capable for performing low data rate communication and data processing required for networking and simple applications. Next, the most essential sensor node platforms are discussed.

The most well-known work among low power sensor node platforms has been conducted in the University of California, Berkeley. They have built a number of platforms called motes by a SmartDust project. The SmartDust [207] project was aiming to fabricate a cubic-millimeter sized WSN node containing sensing, computing and communication systems. An important goal of the project was to explore the limitations of microfabrication technology. Before that, Mote platforms were built to approximate the capabilities of an envisioned SmartDust node with COTS components.

In 2001, the first mote called Mica [73] was released. Mica is a general purpose platform for WSN research having Atmel ATmega103L MCU and RFM TR1000 radio that operates at 915 MHz frequency band and has up to 115.2 kbps data rate. The MCU contains 128 kbytes program memory and 4 kbytes data memory, and

has 4 MIPS processing speed. In addition, the platform contains a 4-Mbit external non-volatile memory and Atmel AT90LS2343 co-processor for handling wireless re-programming of the main processor. The most critical shortcoming of the platform is a switched-mode voltage regulator, which uses 200 - 300 μA quiescent current reducing significantly achieved node lifetime [130].

An improved version of Mica called Mica2 [37] was released in 2002. Sleep mode current consumption was reduced to about 17 μA by discarding the switched-mode regulator and utilizing Atmel ATmega128L MCU. The radio was changed to Chipcon CC1000 enabling tunable frequency channel from 300 MHz to 900 MHz. A smaller version of Mica2 called Mica2Dot [38] was also released in the same year. These two platforms became very popular in WSN research for many years.

MicaZ [34] replaces the CC1000 radio with an IEEE 802.15.4 compatible Chipcon CC2420 radio. This modification increased radio data rate from 76.8 kbps to 250 kbps. In addition, a wide-band DSSS modulation scheme provided better tolerance against noise and interferences.

Telos [130] is a new type of mote released in 2004. Telos combines the CC2420 radio with a very low power TI MSP430 MCU. A special feature is an Universal Serial Bus (USB) connector, which is used for programming the platform. Sleep mode current consumption is only 5.1 μA. An improved version of Telos is called Tmote Sky [114].

Also other research projects have been developing sensor node platforms intensively. Medusa MK-2 [156] is a versatile platform released in 2002 by University of California, Los Angeles. The platform combines ATmega128L MCU with TR1000 radio. Hence, it is quite similar to Mica and Mica2 motes. A special feature of Medusa MK-2 platform is a higher performance 16/32-bit Atmel AT91FR4081 ARM7TDMI co-processor, which is responsible for the processing of sensor data and localization algorithms. The platform is equipped with light, temperature, and acceleration sensors. The sleep mode current consumption is 27 μA, which is adequate for long-lived WSN applications.

ETH Zurich has developed a sensor node platform called BTnode in a Smart-Its project [174]. A BTnode combines Bluetooth radio with the ATmega128L MCU. A BTnode rev3 [18], released in 2004, is a dual-radio platform, which can employ simultaneously a Zeevo ZV4002 Bluetooth radio and the CC1000 radio. Hence, the BTnode rev3 platform can form a backbone network with Bluetooth technology, and exchange data with low power Mica2 and Mica2Dot platforms by the CC1000 radio [72]. A disadvantage is that typical sleep mode current consumption is 3 mA [23],

which limits the achievable node lifetime very significantly.

A ScatterWeb Embedded Sensor Board (ESB) [157] is a simple and low power platform developed by Freie Universität Berlin, Germany in 2003. The platform consists of the MSP430 MCU, RFM TR1001 radio and sensors for measuring light, acoustic noise, vibration, and movement by a Passive Infra-Red (PIR) sensor. In addition, a microphone, a speaker, and an Infra-Red (IR) transceiver are included. Long-lived WSN applications are possible, since the sleep mode current consumption is only 8 μA. Communication with external network is enabled by various gateway nodes having interfaces, for example, to Ethernet, GSM/GPRS, USB and RS-485. A very similar hardware architecture is employed also in nodes [140] developed by an European EYES research project.

A TinyNode [47] developed by Shockfish SA, Switzerland, is a very small and low power platform developed for research and industrial applications. The platform contains only the core components, while additional functionality and sensors are provided by extension boards. In addition, the platform contains a 512 kbytes external non-volatile memory for storing several firmware images and for logging data. Included main components are MSP430 MCU, Semtech XE1205 radio and a temperature sensor. The radio can operate in 433 MHz, 868 MHz and 915 MHz frequency bands having up to 152 kbps data rate. Long lifetime is possible, since the sleep mode current consumption is only 5.1 μA .

A ProSpeckz [8] is a very small and simple platform, which is equipped with a CY8C29666 Programmable System-on-Chip (PSoC) from Cypress Microsystems. PSoC combines a simple 8-bit MCU core having 16 kbytes of program memory and 256 bytes of data memory with versatile software reconfigurable analogue circuits to external interfaces and components. Employed radio is the TI CC2420. Although, the PSoC platform provides versatile processing capabilities for analog sensor values, high 330 μA current consumption in sleep mode reduces significantly the achievable lifetime.

Besides the COTS platforms presented above, a lot of research work has been conducted for developing SoC platforms targeting to even smaller size and higher energy-efficiency. For example, a WiseNET SoC sensor node [54] developed in Swiss Center for Electronics and Microtechnology integrates a low-power radio with CoolRISC MCU core, low-leakage memories, two ADCs and power management blocks. The reception mode current consumption is only 2 mA, which is nearly one order of magnitude less than in typical low power radios. Yet, a data rate is only 25 kbps. The transmission mode current consumption at 10 dBm output power is 24 mA. The sleep

mode current consumption of the radio block is 3.5 μA.

The characteristics of the presented sensor node platforms are summarized in Table 10. At best, low power platforms can perform various sensing tasks and they enable the extending of network lifetime to even years. This necessitates an energy-efficient MAC protocol, which maximizes the time node spends in the sleep mode. This will be discussed in details in the next Chapters.

In the future, data processing and sensing tasks within the network will be increased and they become more complex. In the component side, this necessitates the development of processors having high performance, energy-efficiency, and large memory resources. Also, the development of diverse low power sensor elements is important for enabling the application development.

This Thesis will present a series of sensor node platforms, which further improve the achieved network lifetime by focusing on the minimization of radio energy consumption. Also, various sensor integrations, interfaces to external networks, and application experiments will be presented.

Table 10. *Comparison of existing low-power sensor node platforms.*

Platform	MCU	Sensors	Radio	Data rate (kbps)	RF band (MHz)	Sleep (μA)	Size (mm^2)
Mica [73]	ATmega103L	no	TR1000	115.2	915	200-300	1856
Mica2 [37]	ATmega128L	no	CC1000	76.8	433-915	17	1856
Mica2dot [38]	ATmega128L	no	CC1000	76.8	433-915	17	492
MicaZ [34]	ATmega128L	no	CC2420	250	2400	30	1856
BTnode ver3 [23]	Atmega128L	no	ZV4002	1000	2400	3000	1890
			+ CC1000	+ 76.8	+ 433-915		
Medusa MK-2 [156]	ATmega128L	T, L, A	TR1000	115.2	915	27	ca. 4500
	+ ARM7						
EYES node [140]	MSP430	no	TR1001	115.2	868	5.1	ca. 2600
ScatterWeb ESB [157]	MSP430	L, AC, A, PIR	TR1001	115.2	868	8	ca. 3000
Tiny node [47]	MSP430	no	XE1205	152	433-915	5.1	1200
Tmote sky [114]	MSP430	H, T, L	CC2420	250	2400	5.1	2621
ProSpeckz [8]	CY8C29666	no	CC2420	250	2400	330	704

Abbreviations: Acceleration (A), Acoustic (AC), Humidity (H), Light (L), Passive Infra-Red (PIR), Temperature (T)

4. MEDIUM ACCESS CONTROL FOR WSNS

A MAC layer operates on top of the physical layer and manages radio transmissions and receptions on a shared wireless medium. Hence, it has a very high effect on the performance and energy consumption of a network. This chapter discusses MAC design requirements and existing MAC protocols for low-energy WSNs.

4.1 Low-Energy MAC Design

As WSNs are designed to operate in large geographic areas, the energy consumption of data transmissions is reduced by forwarding data in the network by several low energy hops (multi-hop routing). According to a distance-dependent path loss model [161], the mean path loss ($\overline{PL}$) increases exponentially with distance (d)

$$\overline{PL}(d) \propto \left(\frac{d}{d_0}\right)^n, \tag{1}$$

where n is the path loss exponent, d_0 is the reference distance, and d is the actual distance between the transmitter and the receiver. The value of the path loss exponent is typically between 2 and 3.5 depending on the operation environment [68, 137, 138, 161]. Thus, the reduction of a hop length to a half reduces the required transmission power to between 1/4 and 1/12. Yet, this model considers only the radiated transmission power and ignores the static power consumption of the transmitter and receiver circuitry, which dominate the power consumption at short hop distances. Thus, the advantage of multi-hop routing is limited [44, 226].

To be able to reach adequate energy-efficiency, a MAC protocol should be able to minimize all unnecessary activity of a radio. Most importantly, a MAC protocol should minimize [17, 88, 134, 207, 223]:

Idle listening: Idle listening occurs when a node is actively receiving a channel, but there is no meaningful activity on the channel resulting wasted energy.

Collisions: When two nodes transmit simultaneously at the same frequency channel their transmissions collide in the overlapping area of their transmission ranges. In this area the received data is most probably corrupted causing useless receive cost at the destination node and useless transmit cost at the source node.

Overhearing: An unicast transmission on a shared wireless broadcast medium may cause other nodes than the intended destination to receive a data packet, which is most probably useless to them and consumes unnecessarily energy.

Protocol overhead: The headers and trailers of data packets, and the control packet exchange may cause significant reception and transmission cost for all nodes consuming unnecessarily energy.

Start-up transients: The transient from sleep to active mode, and switching between active modes dissipate a lot of energy causing wasted energy.

As a principle, the radio should be activated only when transmitting or receiving a packet that is vital for the node operation. Moreover, a source and a destination node should be activated and tuned on a correct RF channel simultaneously, while other nodes remain in the sleep mode. This is very difficult in large networks, where operation conditions are uncertain and computing resources are constrained. Next, the operation principles of the most essential MAC protocols are discussed.

4.2 Existing MAC Protocols

MAC protocols can be categorized into contention and contention-free protocols. In contention protocols, nodes compete for a shared channel, while trying to avoid frame collisions.

ALOHA [147] is the simplest contention protocol, where nodes transmit data without coordination. Slotted ALOHA reduces collisions by dividing time into slots and transmitting data on the slot boundaries only. CSMA [91] further reduces collisions and improves achievable throughput by checking channel activity prior to transmissions and avoiding transmission during busy channel situations. Carrier Sense Multiple Access with Collision Avoidance (CSMA/CA) [33] is a modification of CSMA, which reduces the congestion on a channel by deferring a transmission for a random interval, if the channel is sensed to be busy (backoff). Still, collisions may occur due to a hidden node problem [198]: nodes separated by two hops may not detect

each other, and their transmissions may collide on the receivers of their intermediate nodes. Multiple Access with Collision Avoidance (MACA) [89] reduces hidden node collisions by performing a Request-To-Send (RTS) - Clear-To-Send (CTS) handshaking prior to a data transmission. This handshaking is also defined as an option in CSMA/CA. While contention-based protocols work well under low traffic loads, their performance and reliability degrades drastically under higher loads because of collisions and retransmissions.

In contention-free protocols, nodes get unique time slots or frequency channels for transmissions. Ideally, collisions are eliminated. Time Division Multiple Access (TDMA) [228] divides time into numerous slots, where only one node is allowed to transmit on each slot. Other alternatives are Frequency Division Multiple Access (FDMA) [2] and Code Division Multiple Access (CDMA) [85], which provide contention-free operation by separate frequency channels and spreading codes, respectively.

Contention-free protocols achieve high performance and reliability regardless of the traffic load. Yet, the bandwidth should be reserved in advance, which increases control traffic overhead [30, 84, 100, 186, 228].

Due to the power consumption of current low-power radios especially in the reception mode, the energy-efficiency of the conventional MAC approaches is not adequate for the low energy WSN as such. Further energy saving is achieved by duty cycling: time is divided into a short active period and a long sleep period, which are repeated consecutively. These low duty-cycle protocols can also be divided into two categories: unsynchronized and synchronized protocols, according to the synchronization of data exchanges.

4.2.1 Unsynchronized Low Duty-Cycle MAC Protocols

Unsynchronized low duty-cycle MAC protocols are based on a Low Power Listening (LPL) mechanism, where nodes poll channel asynchronously to test for possible traffic, as presented in Fig. 9. Transmissions are preceded with a preamble ($T_{preample}$) that is longer than the channel-polling interval ($T_{interval}$). Hence, the preamble part acts like a wake up signal. If a busy channel is detected, nodes begin to listen to the channel until a data packet is received or a time-out occurs.

B-MAC [129] is a simple LPL protocol, which utilizes CSMA for collision avoidance. The energy-efficiency of B-MAC is significantly limited by the transmission and reception energy costs due to the long preamble. In addition, energy-efficiency

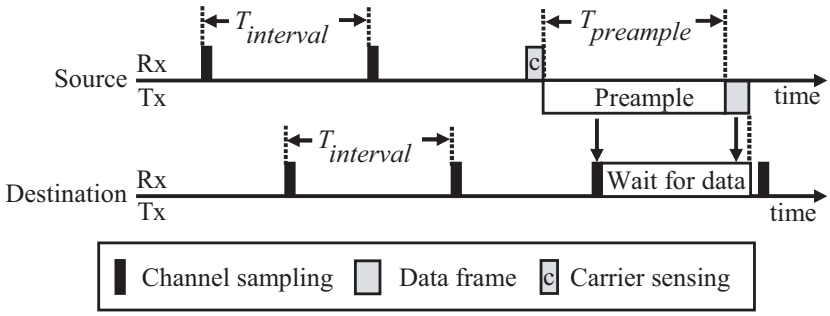

Fig. 9. *Operation of unsynchronized low duty-cycle protocols.*

is reduced by overhearing of frames intended to other nodes and idle listening caused by the frequent channel sampling.

Z-MAC [143] operates above B-MAC, but utilizes TDMA for managing congestion. As a principle, each node owns a slot during which a smaller contention window is used compared to other nodes. Thus, the slot owner always has the best possibility to access the channel. Under low contention, Z-MAC behaves like CSMA, and under high contention more like TDMA. The utilization of slots improves the fairness and throughput of B-MAC. Yet, the improvement on energy-efficiency is only limited.

There are numerous variations of B-MAC targeting at the reduction of the preample energy. Speck Medium Access Control Backoff (SpeckMAC-B) [217] replaces the long preamble with numerous short wake up packets containing a destination address and an exact time to the actual data transmission. Thus, nodes may return to sleep mode after receiving one wake up packet. Speck Medium Access Control Data (SpeckMAC-D) [217] replaces the long preamble with consecutive data packets reducing the required channel reception time. In X-MAC [24], a sender transmits multiple short preambles with the address of the intended receiver. Each preample is followed by a short reception period. Upon receiving a preamble, the desired destination node sends an Acknowledgment (ACK) between the preambles. Other nodes can enter early a sleep mode for reducing overhearing. After receiving the ACK, the source node begins the transmission of a data frame. Disadvantages of these protocols are the transmission cost of a preample and idle listening caused by CSMA mechanism, channel polling, overhearing and radio start-up transients.

There are two variations of B-MAC, which reduce preample energy by utilizing synchronization. Thus, they can also be categorized into the group of synchronized protocols. They are presented here, since their operation principle is very similar with B-MAC and other unsynchronized protocols. Wireless Sensor MAC (WiseMAC) [51]

utilizes ALOHA for transmissions. A network consists of an access point and numerous sensor nodes in a star-topology. The access point learns the sampling schedules of each sensor node and starts preamble transmission just prior to the channel sampling moment of a desired destination node. Major disadvantages of the protocol are very limited coverage and connectivity of the network due to the star-topology. Scheduled Channel Polling Medium Access Control (SCP-MAC) [221] is a synchronized variation of B-MAC, which operates in a mesh network by making the channel polling schedules of all nodes identical. Hence, only a short preamble is required to reach all neighbors. Synchronization is performed by transmitting periodically synchronization packets containing the schedule information, or piggybacking the information is data packets. SCP-MAC is currently the most energy-efficient unsynchronized low duty-cycle protocol. Still, the idle listening during a backoff mechanism and channel polling, collisions, frequent radio start-up transients, and overhearing reduces its energy-efficiency.

The preample can be eliminated by utilizing a wake-up radio [63]. The wake-up radio mechanism is based on the assumption that the listen mode of the wake-up radio is ultra low power and it can be active constantly. At the same time, the normal data radio is in the sleep mode as long as there is no packet transmission or reception required. Power Aware Multi-Access protocol with Signaling (PAMAS) [173] protocol enable collision avoidance mechanism by utilizing RTS-CTS handshaking in the wake-up radio channel. Sparse Topology and Energy Management (STEM) [159] protocol reduces the energy consumption of a wake-up radio by the LPL scheme. The wake-up radio protocols are successful in avoiding overhearing and idle listening in the data radio. Their major problems are the energy consumption and cost of the wake-up radio. In addition, the difference in the transmission ranges between data and wake-up radio may pose significant problems.

Unsynchronized protocols are relatively simple and robust, and require a small amount of memory compared to synchronized protocols. A general drawback is rather high overhearing, since each node must receive at least the beginning of each frame transmitted within radio range. Thus, they suit best for relatively simple WSNs utilizing very low data rates. Unsynchronized protocols tolerate dynamics in networks, but their energy-efficiency is limited by the channel sampling mechanism [223].

4.2.2 Synchronized Low Duty-Cycle MAC Protocols

Synchronized low duty-cycle MAC protocols utilize scheduling to ensure that listeners and transmitters have a regular, short active period (T_{active}) in which to exchange

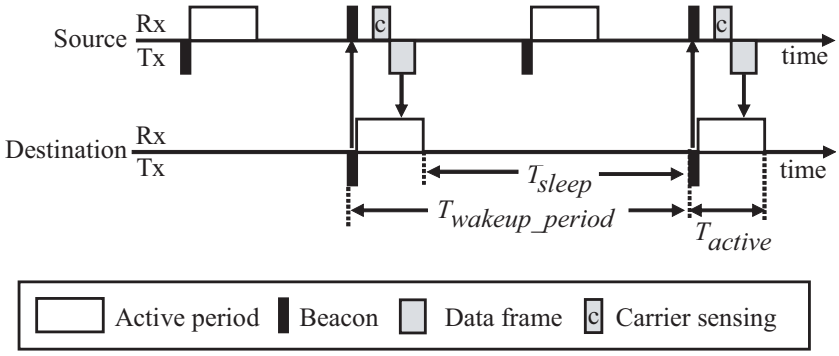

Fig. 10. *Operation of synchronized low duty-cycle protocols.*

one or more frames with neighbors. The active period is followed by a sleep period (T_{sleep}) for enabling energy saving. The active and sleep periods are repeated at T_{wakeup_period} intervals, as illustrated in Fig. 10. The active period is denoted as a superframe, when a node typically first broadcasts a control frame called beacon for signaling its schedule and status information, and then listen to the channel for possible incoming data until the end of the active period. Due to the synchronized operation, nodes know the exact moments of active periods in advance eliminating the need of long preambles. As a global synchronization is very difficult in large networks [99], synchronization is maintained locally by receiving periodically beacons from one or more neighboring nodes.

For establishing the synchronized operation, neighboring nodes are typically discovered by a network scan. The network scan means a long-term reception of frequency channels for receiving beacons from neighbors, since their schedules and frequency channels are unknown. Clearly, this is energy-hungry. However, the synchronized operation after the network scan is very energy-efficient [221, 223].

S-MAC [220] is one of the first synchronized low duty-cycle MAC protocols. The protocol utilizes a fixed active period length and an adjustable, network specific wake up period. Neighboring nodes may coordinate their active periods to occur simultaneously to form virtual clusters. At the beginning of an active period nodes wake up and exchange Synchronization (SYNC) frames for synchronizing their operation. Then, nodes having data to be send transmit RTS messages using CSMA/CA mechanism. According to received RTS messages, a destination node select a desired source node and sends a CTS message. Then, the source and destination nodes continue by exchanging data and ACK frames at most until the end of the active period. The energy-efficiency of S-MAC is reduced by long SYNC and RTS phases, and fixed active period length causing idle listening. In addition, the fixed duty cycle causes

poor adaptation to changing traffic conditions.

Timeout-MAC (T-MAC) [201] protocol is a variation of the S-MAC, which utilizes a short listening window after the CTS phase and each frame exchange. If no activity occurs during the listening window, node returns to sleep mode. Thus, the length of the active period is adjusted according to traffic. Still, the energy-efficiency is limited by the idle listening in SYNC and RTS phases.

DMAC [61] is a variation of S-MAC, which staggers the active/sleep schedules of the nodes in a tree topology. This allows continuous low latency packet forwarding flow from nodes to a sink. DMAC has mechanisms for notifying nodes of data delivery progress and duty-cycle adjustments.

Several variations of TDMA are also proposed for low-energy WSN. Low-Energy Adaptive Clustering Hierarchy (LEACH) [71] protocol uses TDMA with clustered network topology. LEACH utilizes a single base station, with which all cluster heads employ direct communications. Inter-cluster interferences are managed by CDMA. The problems of direct communication are limited network coverage and low energy-efficiency caused by high transmission power levels. However, cluster members operate quite energy-efficiently. For increasing network lifetime, LEACH proposes to compress data in cluster heads and to rotate the role of a cluster head among cluster members.

Self-Organizing Slot Allocation (SRSA) [218] protocol is a variation of LEACH, which manages inter-cluster interferences by a distributed time division algorithm. Time slot allocations for communication are adjusted according to observed collisions within a cluster. Reliance only on the local information ensures high scalability. Still, the problems with direct communication are not solved.

Power Aware Clustered TDMA (PACT) [125] protocol is a variation of LEACH, which performs multi-hop data routing between clusters by inter-cluster gateway nodes. Disadvantages of PACT are high control traffic overhead and idle listening in larger networks. Relatively complex data slot scheduling algorithm performs well in static networks, but lacks support for dynamic network.

Self-Organizing Medium Access Control for Sensor Networks (SMACS) [175] protocol assigns a locally unique contention-free slot for each link. Neighbor discovery is performed at semi-regular intervals by broadcasting invitation messages on a common signaling channel. Then, the channel is received for possible responses and other invitation messages. According to invitation messages, each pair of nodes mutually agrees a periodic time and frequency slot for data exchanges. A major disadvantage

is the energy consumption of a neighbor discovery requiring a long-term radio reception. This severely limits energy-efficiency and adaptivity in dynamic networks, where link lifetimes are short.

Traffic-Adaptive Medium Access (TRAMA) [135] is a scalable TDMA protocol designed for multi-hop networks. Time is divided into slots. A distributed algorithm selects only one sender for each slot per a two-hop neighborhood allowing collision-free operation. A sender can command a set of neighbors to receive a given data frame providing efficient unicast, multicast and broadcast transmissions. Nodes that are not selected as senders or receivers at a particular time slot go to a sleep mode. Neighbor information is updated during periodic random access periods. TRAMA can provide collision-free medium access in a static network. Energy-efficiency is reduced by signaling traffic overhead and the random access periods requiring a long-term radio reception. Hence, the energy-efficiency and performance decrease significantly in dynamic networks.

IEEE 802.15.4 [82] standard defines a MAC layer that can operate on beacon-enabled and non-beacon modes. In the non-beacon mode, a protocol is a simple CSMA/CA. Energy-efficient synchronized low duty-cycle operation is provided by the beacon-enabled mode, where all communications are performed in a superframe structure. The superframe is divided into three parts: the beacon, Contention Access Period (CAP) and Contention-Free Period (CFP). CAP is a mandatory part of a superframe during which channel is accessed using a slotted CSMA/CA scheme. CFP is an optional feature of IEEE 802.15.4 MAC, in which a channel access is performed in dedicated time slots. CFP can be utilized only for a direct communication with a PAN coordinator. Thus, its applicability and benefits are very limited in multi-hop networks.

IEEE 802.15.4 supports a *BatteryLifeExtension* option, which effectively reduces the coordinator energy consumption by minimizing the lengths of contention window and CAP. Due to the shortened CAP, this option significantly reduces available throughput. In addition, a collision probability is high due to shorter backoff time. Thus, this option is suitable only for small and very low data rate networks [P6].

The cluster-tree type IEEE 802.15.4 network can provide comparably good energy-efficiency in static and sparse networks. A major disadvantage is that coordinators must be active entire CAP causing significant idle listening. In addition, the hidden node problem reduces performance in dense networks, since any handshaking prior to transmissions are not used.

In current synchronized low duty-cycle protocols, the major advantage is that a sender

knows a receiver's wake up time in advance and thus can transmit efficiently. In dynamic networks, synchronized links are short-lived and new neighbors need to be searched frequently, which increases energy consumption rapidly. In contention protocols, a major disadvantage is the energy cost of receiving an entire active period [129]. Contention-free protocols have better energy-efficiency is stationary networks, but their performance reduces rapidly as network dynamics increases.

The features and major contributions of the presented MAC protocols are summarized in Table 11. The main problem of existing MAC protocols is the energy consumption of idle listening, which is mostly caused by channel polling, preample reception, contention mechanism, and neighbor discovery. Idle listening is further increased in WSN applications, where link quality varies and nodes are mobile. In addition, overhearing and frequent start-up transients limit the energy-efficiency of unsynchronized protocols. Hence, the energy-inefficiency of existing MAC protocols limits significantly network lifetime and disables many potential application areas. This Thesis presents a novel MAC protocol, which achieves higher energy-efficiency than the existing protocols. In addition, networking protocols for maintaining energy-efficient operation in dynamic networks are presented.

Table 11. *Comparison of low power WSN MAC protocols.*

Protocol	Network topology	# of channels	Channel access	Idle listening avoidance	Synchronization	Major contributions
Unsynchronized						
B-MAC	Mesh	1	CSMA	LPL	No	Combination of CSMA with preample sampling
PAMAS	Mesh	2	CSMA	Wake-up radio	No	Wake-up radio with RTS-CTS
SCP-MAC	Mesh	1	CSMA	Synchronized LPL	Yes	LPL with a synchronized sleep schedule
SpeckMAC	Mesh	1	CSMA	LPL	No	Reduction of frame reception time
STEM	Mesh	2	CSMA	Wake-up radio	No	Wake-up radio with LPL
WiseMAC	Star	1	Random access	LPL	No	Learning of LPL schedules
X-MAC	Mesh	1	CSMA	LPL	No	Multiple short preamples
Z-MAC	Mesh	1	TDMA/CSMA	LPL	Yes	Hybrid TDMA/CSMA above B-MAC
Synchronized						
DMAC	Mesh	1	CSMA	Periodic sleep	Yes	Staggered active/sleep schedules
LEACH	Clustered	1	TDMA	TDMA	Yes	Low energy clustering, rotation of cluster heads
PACT	Clustered	1	TDMA	TDMA with adaptive duty cycle	Yes	LEACH with multihop routing
S-MAC	Mesh	1	CSMA	Periodic sleep	Yes	Active/sleep schedules
SMACS	Mesh	Many	TDMA/FDMA	TDMA	Yes	Hybrid TDMA/FDMA
SRSA	Clustered	1	TDMA	TDMA	Inside clusters	Adaptive slot assignments for reducing interferences
T-MAC	Mesh	1	CSMA	Periodic sleep	Yes	Adaptive duty cycle
TRAMA	Mesh	1	TDMA	TDMA with adaptive duty cycle	Yes	Distributed algorithm for sender/receiver selection

5. TUTWSN MAC DESIGN

The results of this Thesis are summarized from now on. This chapter presents the MAC layer design for TUTWSN. The next chapter presents performance models for WSN MAC protocols. Then, TUTWSN sensor node platform designs and experimental deployments are presented. The details of the results are published in [P1]-[P10]. The performance of the designs is verified by performance analysis and experimental measurements. First, TUTWSN networking technology and the design requirements for the MAC layer are presented.

5.1 TUTWSN Networking Technology

TUTWSN networking technology has been developed for low data-rate monitoring applications, where a large number of nodes self-configure themselves, perform sensing and data processing tasks, and communicate with one or more sinks with very low energy consumption. Target applications fields are environmental monitoring, building monitoring, condition monitoring, object and human tracking, and access control. Target usage classes for message timeliness are 4 and 5 meaning non-critical flagging and data logging tasks [83].

The applications have strict requirements for network lifetime, scalability, and adaptivity for network dynamics. An important requirement has been that the designed protocols are feasible in practice in harsh operation environment using low-power hardware components. For these requirements, current networking technologies do not provide adequate energy-efficiency and performance. Thus, a completely new networking technology has been developed.

In this Thesis, the main focus is on an energy-efficient MAC layer, which consists of channel access and networking mechanisms. The main targets for the channel access mechanism have been maximized energy-efficiency and reliability. The networking mechanisms perform network self-configuration and neighbor discovery operations. The main objectives for them have been high energy-efficiency and adaptivity for

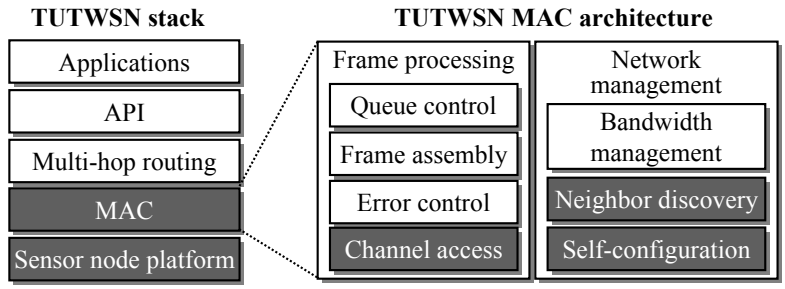

Fig. 11. *TUTWSN protocol stack and MAC layer architecture.*

tolerating unreliable radio links and node mobility. An important objective for the entire MAC layer has been compatibility with a simple and low-power hardware. This Thesis discusses also low-power and cost-effective sensor node platforms, which have been developed for various sensing applications. Thus, the requirement for long battery lifetime is solved by both MAC layer and sensor node platform designs.

The TUTWSN protocol stack is presented in Fig. 11. The focus of this Thesis is presented with boxes having a dark gray background. The MAC layer operates between the radio on a sensor node platform, and a multi-hop routing layer [184]. Above the routing layer are a transport layer and API [87]. API implements an abstraction layer between applications and network protocols. Application layer contain various sensing [181], data processing, and diagnostics [182] applications.

The architecture of the designed MAC layer is presented on the right side of the Fig. 11. Functions associated to frame processing are grouped to queue control, frame assembly, error control, and channel access. In operation, frames received from routing layer are queued, and then forwarded to a frame assembly according to frame priorities. Frame assembly builds headers, manages addressing, and performs piggybacking of control signaling in MAC frames. The error control performs error detection, acknowledgements, and retransmissions. The channel access controls frame transmissions and receptions on RF channels using contention based and contention-free mechanisms.

Network management contains mechanisms for bandwidth management, neighbor discovery, and network self-configuration. Bandwidth management controls slot allocations for the contention-free channel access mechanism. Neighbor discovery contains reactive and proactive mechanisms called Network Channel Beaconing (NCB) and Energy-efficient Neighbor Discovery Protocol (ENDP), which have been developed for maximizing network performance and energy-efficiency in dynamic radio environments. The self-configuration manages the formation of network topology,

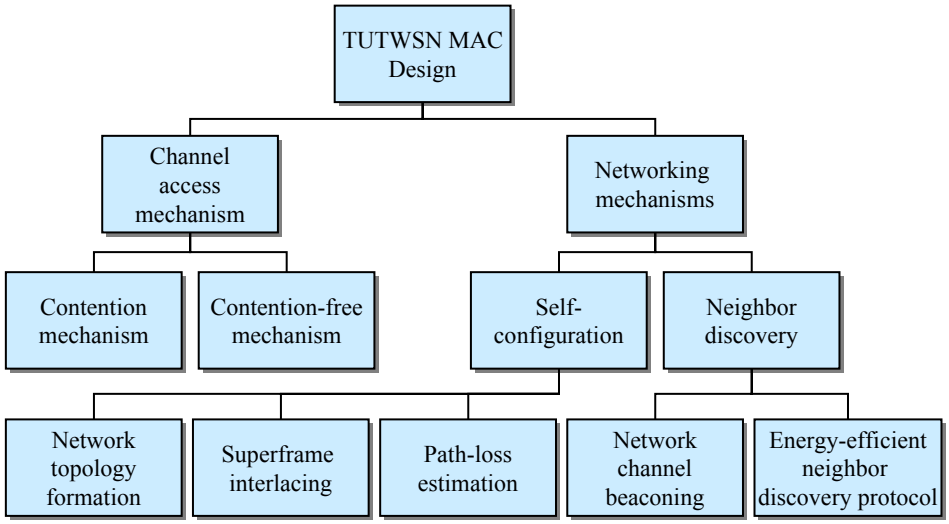

Fig. 12. *Designed MAC layer mechanisms.*

the interlacing of superframes for minimizing interferences, and the estimation of radio wave path-loss to neighboring nodes. In this Thesis, the self-configuration and neighbor discovery mechanisms are called networking mechanisms. The designed MAC layer mechanisms are summarized in Fig. 12.

5.2 TUTWSN Channel Access Mechanism

TUTWSN channel access mechanism pursues to minimize the duty cycle of communication. Until now, related proposals for channel access mechanism have reduced energy consumption by focusing on the minimization of long-term idle listening, overhearing, and the active period length, as discussed in the Section 4. Only a small research effort has been paid on the minimization of the energy overhead of a channel access as a whole.

For finding out the most essential causes of energy overhead, a simple energy analysis of a CSMA channel access is presented. CSMA can be considered a typical channel access mechanism in WSNs and it is used for example in IEEE 802.15.4, S-MAC, T-MAC, SCP-MAC, and X-MAC. The results of the analysis will clarify the guidelines for the designed TUTWSN channel access mechanism. To be able to focus purely on the data exchange between two nodes, an analyzed network contains only a source and a destination node. The actions of these nodes are presented in Fig. 13. At the beginning of a channel access period, a destination node activates its receiver lasting

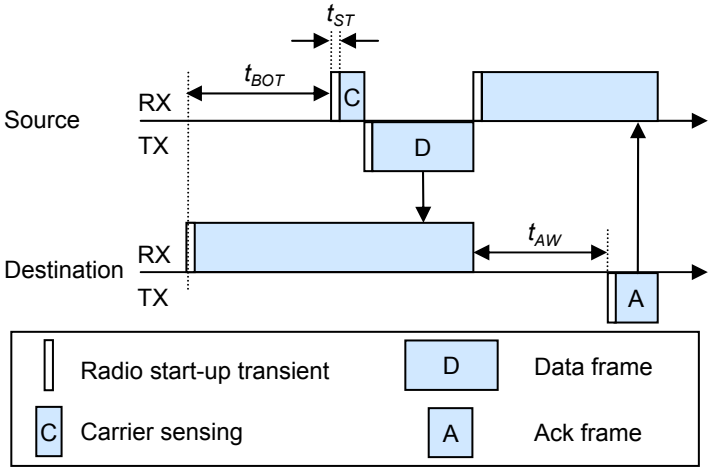

Fig. 13. *Analyzed frame exchange mechanism.*

t_{ST} and begins receiving the channel for possible incoming frames. Prior to a data frame transmission, the source node waits a random backoff time (t_{BOT}), activates its receiver, and performs a carrier sensing (t_{CCA}). For improving energy-efficiency, a blind backoff is assumed, where a source spends t_{BOT} in sleep mode. If the channel is idle, the source turns the receiver off, activates its transmitter, and transmits a data frame (t_{DATA}). The energy of inactivating the radio is negligible and it can be ignored. After receiving the data frame, the destination node turns off the receiver, checks the correctness of the data (t_{AW}), activates a transmitter and transmits ACK. Since the wait time (t_{AW}) prior to the reception of ACK is not pre-determined, and depends on the frame content and data processing performance, the source node needs to be in reception mode entire t_{AW}.

The consumed energy is divided into an effective energy comprising data and ACK exchange energies, and overhead energy consisting of radio start-up, backoff, and ACK wait energies. Next, models for these energies are determined.

The presented frame exchange procedure consists of two transmitter start-up and three receiver start-up transients (t_{ST}) during which power consumption equals to a transmitting power (P_{TX}) and a receiving power (P_{RX}), respectively. Hence, the total start-up energy (E_{ST}) of a frame exchange is

$$E_{ST} = t_{ST}\left(2P_{TX} + 3P_{RX}\right). \tag{2}$$

Although the source node may sleep during the backoff delay, the destination node

needs to be in the reception mode. An average idle listening time consists of a half of a contention window length (t_{CW}) and a carrier sensing time (t_{CCA}). Hence, the backoff energy consumption (E_{BO}) is

$$E_{BO} = \left(\frac{t_{CW}}{2} + t_{CCA}\right) P_{RX}. \tag{3}$$

The ACK wait energy consumption (E_{AW}) caused by an average ACK wait delay (t_{AW}) is

$$E_{AW} = t_{AW} P_{RX}. \tag{4}$$

The data exchange energy (E_{DATA}) consists purely of the transmission and reception energies of a data frame (L_{DATA}). As radio data rate is R, E_{DATA} is

$$E_{DATA} = \frac{L_{DATA}}{R} \left(P_{TX} + P_{RX}\right). \tag{5}$$

Similarly, the ACK exchange energy is

$$E_{ACK} = \frac{L_{ACK}}{R} \left(P_{TX} + P_{RX}\right). \tag{6}$$

Next, the energy consumptions are determined for a low power sensor node platform utilizing Microchip PIC18LF4620 MCU. Since the energy characteristics of low power radios are diverse, the energy consumptions are determined for two different types of generally used commercial off-the-shelf radios: a High data Rate (HR) Nordic Semiconductor nRF2401A [120] radio having 1 Mbps data rate, and a Low data Rate (LR) Chipcon CC1000 [192] radio having 76.8 kbps data rate. The utilized parameter values are presented in Table 12 in subsection 6.3., p. 76. The analysis focuses on short (<128 Bytes) frame lengths, since they results the highest energy-efficiency at high ($> 1x10^{-4}$) Bit Error Rate (BER) conditions [7, 154]. High BER is typical for WSNs due to difficult operation environment and narrow band radios [7].

The resulted energies as the function of data frame size are presented in Fig. 14. Generally, the HR radio has nearly one order of magnitude lower effective energy consumption compared to the LR radio. The energy overhead is nearly equal for both radio types. The energy overhead is caused mostly by the backoff mechanism and carrier sensing causing idle listening. The mechanism also necessitates frequent operation mode changes causing significant start-up transient energy consumption. The

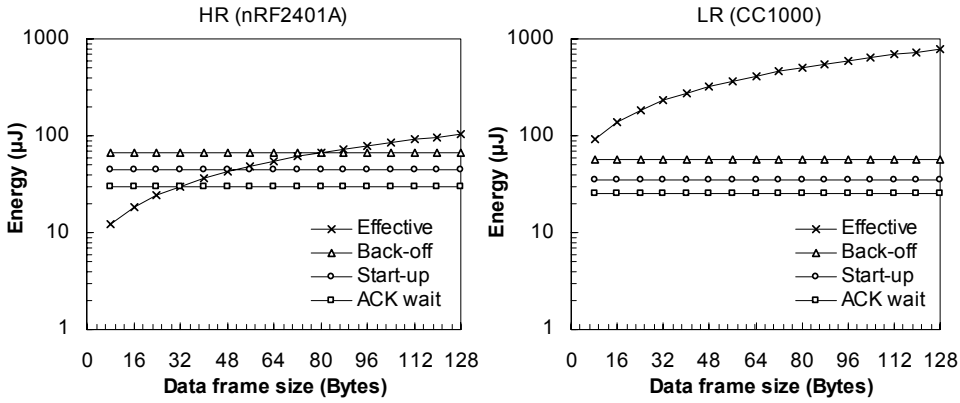

Fig. 14. *The effective and overhead energies of HR (nRF2401A) and LR (CC1000) platforms.*

results clearly indicate that energy overhead is dominating the energy consumption of the HR radio. For the LR radio, the energy overhead is also significant. In practice, busy channel situations and collisions make the energy overhead even higher [21].

The designed TUTWSN channel access mechanism pursues to maximize energy-efficiency by minimizing idle listening, unnecessary start-up transients, overhearing, control frame overhead, and collisions. These are minimized by two ways:

Predetermined frame exchange moments: Nodes maintain accurate local synchronization and exchange frames exactly at predetermined moments.

Reservation based channel access: Nodes avoid collisions and the energy overhead of contention mechanism by reserving their transmission moments in advance.

The designed channel access mechanism is illustrated in Fig. 15. For enabling frame exchanges, some or all nodes maintain a superframe structure (superframe manager). Superframes are repeated at regular intervals called an access cycle. A node can receive data and control frames from its neighbors in its own superframe, whilst frame transmissions to a neighbor is performed in the superframe of the desired neighbor. The rest of time, nodes can sleep and conserve energy. For eliminating collisions, superframes have locally unique schedules such that they do not overlap with each other.

At the beginning of each superframe, a superframe manager transmits a beacon. The beacon contains crucial information for the channel access, networking, and routing. For the channel access, two fields are the most essential: time to the next superframe,

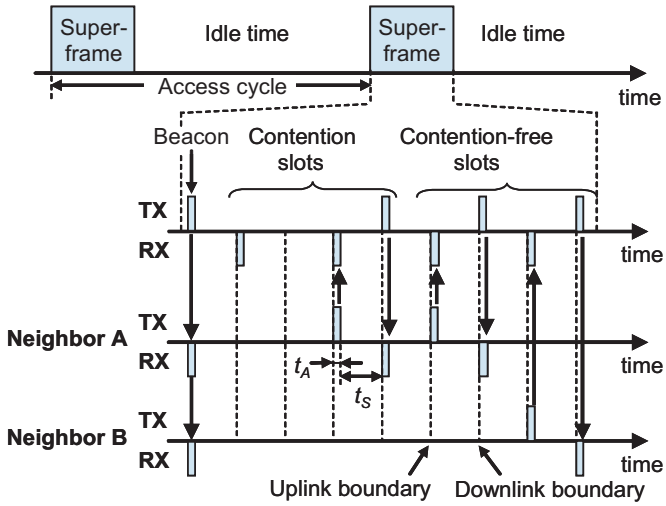

Fig. 15. *TUTWSN access cycle and superframe.*

which is used for maintaining synchronization, and reserved slot allocation table, which is used for granting transmission rights for associated neighbors.

The beacon is followed by time slots for data exchanges. Each superframe contains two types of time slots: contention slots and contention-free slots. Data frames utilize reservation based contention-free slots, while contention slots are used for control frames allowing network association and slot reservations. While the amount of the slots can vary depending on the application, the current TUTWSN implementation utilizes four contention slots and up to eight contention-free slots in each superframe.

Time slots are further divided into uplink and downlink subslots. Uplink subslots are used for transmitting data or control frames to the superframe manager. Downlink subslots are used by the superframe manager for transmitting ACKs. Each subslot contains an active part (t_A), which is used for transmitting a single frame, and a sleep part (t_S), which is used for data processing and preparing a next frame during which radio is in idle or sleep mode. Since the beacon at the beginning of each superframe performs synchronization, the clock drift is negligible at the slot boundaries. In the current implementation, t_A is slightly longer than the transmission time of a single frame, and length of each subslot is 10 ms.

To minimize the energy overhead, uplink frames are transmitted without any collision avoidance mechanism. Occasional collisions in contention slots are managed by re-transmissions. All downlink subslots are contention-free, since only the superframe manager can transmit in these slots. Collisions between superframes are avoided by the superframe interlacing mechanism presented in the next section. As carrier

sensing functionality is not needed, energy overhead is low and the designed channel access mechanism can be implemented with a simple and low cost hardware.

Since the superframe manager cannot predict which contention slots will be used, unnecessary reception of slots is unavoidable causing idle listening. This is common for all contention based mechanisms. The reduction of the number of contention slots reduces the idle listening of superframe managers, but increases the probability of collisions. This may reduce the energy-efficiency and performance of an entire network [153, 222].

In the designed contention mechanism, the energy consumption is minimized by three ways. First, the reception is always terminated as soon as an unused contention slot is detected, or at last when t_A has expired. Second, the utilization of contention slots is minimized by piggybacking bandwidth adjustment signaling in data frames. Third, the number of contention slots is dynamically adjusted according to their loading [P1].

The designed contention-free mechanism is inherently energy-efficient, since the utilized reserved slots in each superframe are determined in advance using bandwidth adjustment signaling and the slot allocation table. The idle listening is nearly eliminated, since only utilized subslots are received. A minor idle listening is caused by the inaccuracy of time synchronization and occasional link failures causing reception failures in the contention-free slots.

5.3 TUTWSN Networking Mechanisms

In this Thesis, networking mechanisms are included in the MAC layer. Networking mechanisms perform the creation and management of a scalable, reliable, and adaptive network topology for data routing. The networking mechanisms are divided into self-configuration and neighbor discovery mechanisms. The mechanisms are presented independently of each other to improve clarity and to facilitate the adaptation of individual mechanisms with other types of MAC layers.

5.3.1 Self-Configuration

The designed self-configuration mechanism performs three main functions: network topology formation, superframe interlacing, and path-loss estimation. The network topology formation determines the operation mode of each node and maintained radio links between nodes. The superframe interlacing ensures collision-free operation

for the channel access mechanism in large and dense networks by eliminating overlapping superframes. The path-loss estimation measures the attenuation of signal strength between nodes allowing the utilization of simple, low power and low cost radios without Received Signal Strength Indicator (RSSI) functionality. The path-loss estimation enables a dynamic transmission power control and the maintenance of robust routing paths. Self-configuration operations are decentralized, and each node makes its configuration according to observed information from neighborhood.

Network Topology Formation

To reduce the energy consumption of frame transmissions in large networks, multi-hop data routing between nodes is utilized [62, 96]. Frames are routed from a source to a destination along a chain of low-energy hops. Each node along the chain receives data from a neighbor (child) one hop closer to the source, maintains synchronization with a next-hop node (parent) by periodically receiving its beacons, and transmits data according to time slot assignments.

The selection of network topology between flat and clustered affects significantly on network energy consumption and bandwidth utilization [P1], [99, 203]. In the flat topology, all nodes participate in data routing and consume nearly equally power and network bandwidth. In the clustered topology, a network is formed as interconnected star networks. The master of each star is a cluster head, while other nodes are leaf nodes. Cluster heads utilize a majority of energy and bandwidth by managing superframes and exchanging data with other clusters. Leaf nodes synchronize themselves with a superframe schedule and transmit data on demand without the need of their own superframes, which reduces the bandwidth utilization of a network.

The designed network topology is based on the clustered topology. Each cluster consists of a cluster head (headnode), leaf nodes (subnodes), and associated headnodes (child headnodes) from neighboring clusters. The operation of a child headnode in a next hop cluster is similar with a subnode, which receives beacons and transmits data according to time slot assignments.

The utilization of a clustered topology is rationalized by a simple analysis, which considers the energy consumptions of clustered and flat topologies using the TUTWSN channel access mechanism. The analysis assumes that the energy consumptions of frame transmissions (E_{TX}) and receptions (E_{RX}) are equal for all frame types, which is realistic for the TUTWSN channel access utilizing a low power radio. Moreover, the density of cluster heads in the clustered topology is assumed to be adequate for

maintaining optimal hop lengths. Therefore, the number of required data and ACK frame exchanges for flat and clustered topologies is equal, as the entire network is considered.

A router node is defined as any node in the flat topology, and a cluster head in the clustered topology. The energy overhead of the router node (E_{OR}) consists of the transmissions and receptions of beacons, and the reception of S_A contention slots. For one access cycle, the energy overhead is

$$E_{OR} = E_{TX} + (S_A + 1) E_{RX}. \tag{7}$$

The energy overhead of a leaf node (E_{OL}) using TUTWSN channel access is caused by the reception of beacons. Hence, for one access cycle, E_{OL} equals to E_{RX}.

In the flat topology, all nodes have equal energy overhead, which equals to E_{OR}. In the clustered topology, where each cluster consists of n_S leaf nodes, the average energy overhead per a node (E_{OC}) is

$$E_{OC} = \frac{E_{TX} + (S_A + 1 + n_S) E_{RX}}{n_S + 1}. \tag{8}$$

If $n_S = 0$, then $E_{OC} = E_{OR}$. This is clear, since all nodes are cluster heads and the network is similar with the flat topology. As n_S increases, E_{OC} decreases, and when $n_S \to \infty$, then $E_{OC} \to E_{RX}$, which equals to E_{OL}. Hence, the clustered topology has always lower energy overhead than the flat topology, assuming that the network has at least one leaf node. The energy-efficiency of clustering is even more obvious, when cluster heads aggregate received data reducing the amount of forwarded data [203].

Network connectivity between clusters can be formed as a cluster-mesh or a cluster-tree topology. In the cluster-mesh topology, each cluster head maintains connectivity with all neighboring cluster heads resulting robust network, but higher energy consumption. In the cluster-tree topology, each cluster head maintains connectivity with one cluster head only, which is one hop closer to a sink locating at the root of the tree. This improves energy-efficiency, but reduces the tolerance against link failures due to low connectivity.

This Thesis presents a multi-cluster-tree topology [P1], which combines the strengths of cluster-tree and cluster-mesh topologies. The multi-cluster-tree topology consists of multiple super-positioned cluster-tree networks. An example multi-cluster-tree topology is illustrated in Fig. 16, where arrows indicate the directions of uplink

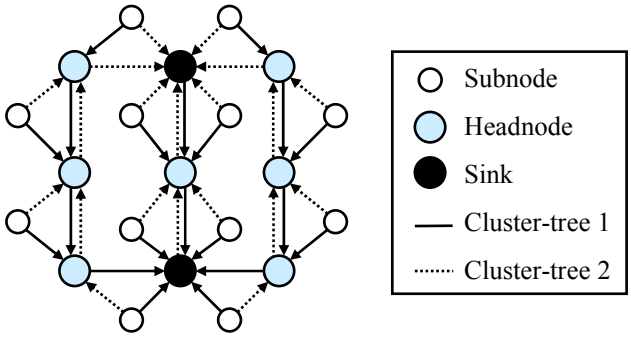

Fig. 16. *Multi-cluster-tree network topology (k = 2).*

routing paths. Each subnode and headnode maintains synchronization with k neighbors by receiving their beacons. This allows the adjustment of connectivity for both subnodes and headnodes allowing a trade-off between network robustness and energy consumption. Compared to the cluster-tree topology, which supports only one route to a single sink, the multi-cluster-tree allows the utilization of multiple sinks, multiple routes, and load balancing between headnodes. The value of k is uniform for entire network and it is selected before a deployment according to expected network dynamics. According to measurements with TUTWSN nodes, an optimal value for k is between 2 and 4 [P1].

Superframe interlacing

For guaranteeing contention-free channel access in a multi-hop network, the overlapping of superframes in two-hop neighborhood (interference range) is eliminated by interlacing. Typically, interlacing is implemented by time division, for example in IEEE 802.15.4 [82], DMAC [61], SRSA [218], and TRAMA. The time division limits network density especially when the superframe length is relatively long compared to the access cycle length. In the designed superframe interlacing mechanism, scalability is improved by time and frequency division. For reasoning this, a short analysis of the maximum scalability is presented. The maximum number (α) of nodes in an interference area can be determined by the access cycle length (T_{AC}), the superframe length, the average number of subnodes in each cluster, and the number of utilized non-interfering frequency channels (n_{CH}) as

$$\alpha = \frac{T_{AC} n_{CH} (1 + n_S)}{2 (1 + S_A + S_R) (t_A + t_S) + t_{guard}}, \tag{9}$$

where S_A and S_R are the maximum number of contention and contention-free slots, t_{guard} is a short guard time between consecutive superframes. α is maximized by maximizing T_{AC}, n_{CH}, and n_S, and by minimizing t_A and t_S. It can be clearly seen in the equation that by utilizing a high data-rate radio operating at a wide frequency band provides the highest scalability. In the current 2.4 GHz TUTWSN implementation, T_{AC} = 4 s, n_{CH} = 20, n_S = 8, S_A = 4, S_R = 8, $tA + tS$ = 10 ms, and t_{guard} = 100 ms. Thus, α equals to 2000 nodes per an interference area. If only one channel is used ($n_{CH} = 1$), α would be reduced to 10 nodes per an interference area. In TUTWSN sensor node platforms, the interference range in indoor conditions is around 100 m equaling to the area of 31400 m^2.

In the designed superframe interlacing mechanism, each headnode selects semi-randomly a time slot and a frequency channel (superslot) for its superframe among the free slots detected by a network scan. The simple randomization minimizes the energy overhead of signaling traffic. The superslot is selected at a node start-up and if interferences are detected by increased link error rate [P1].

Path-Loss Estimation Scheme

The measurement of path-loss to neighboring nodes is crucial for efficient network self-configuration; nodes should form and maintain robust routing paths with sufficient radio link quality and energy-efficient hop lengths [171]. Moreover, measured path-loss enables dynamic adjustment of transmission power levels for minimizing the energy consumption of the transmitter. Conventionally, the path-loss is measured by a RSSI functionality of a radio. A disadvantage of the RSSI functionality is increased radio hardware complexity. In general, the cheapest and lowest energy radios lack RSSI functionality, for example Nordic Semiconductor nRF2401A [120], and nRF24L01 [121].

The designed path-loss estimation scheme [P2] measures path-loss to a neighboring node according to the successfully and unsuccessfully received beacons, which the neighbor transmits at different transmission power levels. The operation principle of path loss metering is illustrated in Fig. 17, where Node 3 determines path losses to Node 1 and Node 2 by receiving their beacons. The transmission ranges of beacons transmitted at four power levels are illustrated by circles. As Node 1 is transmitting, Node 3 is within the range of the second lowest transmission power level resulting in low path loss. Only the highest transmission power reaches node 2 resulting in high path loss.

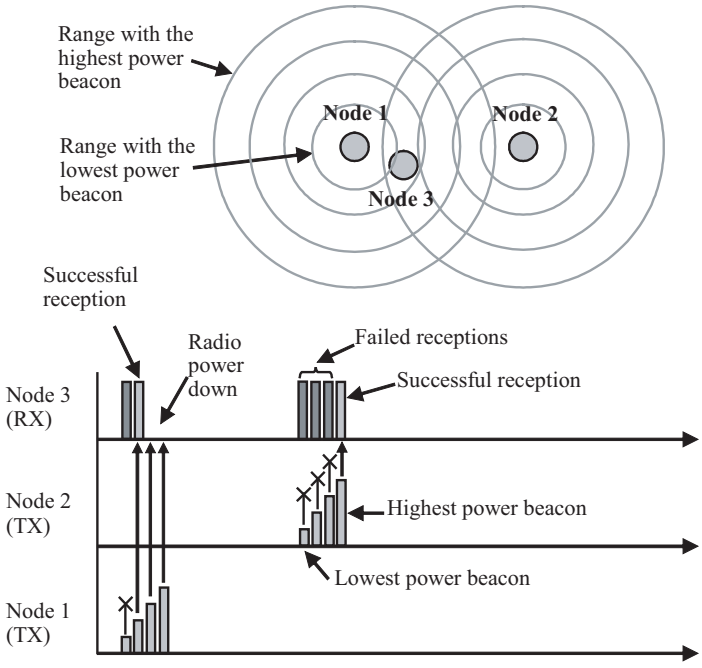

Fig. 17. *The operational principle of a path loss metering.*

In TUTWSN MAC implementation, all beacons are replaced by the train of beacons. Power consumption is further optimized by transmitting only two beacons in each train. Each train consists of the highest power beacon and an altering power beacon. The transmission power of the altering power beacon is alternately selected among all possible transmission power levels except the highest power, and it is signaled in the beacon header. Thus, the path loss estimation is gradually improved as multiple trains are received [P2].

Experimental performance measurements [P2] in indoor and outdoor environments indicate sufficient accuracy for managing robust network operation. Measurements presented in [90] show that the path loss metering scheme has adequate accuracy for node localization [169]. A performance analysis [P2] in a large scale ZigBee network indicate that the path loss metering consume less than 0.5% of the entire node power consumption. By utilizing a simple (Nordic semiconductor nRF24L01) radio with the path loss metering scheme results in over 51% power saving compared to a low power RSSI equipped radio (TI CC2400) [P2].

5.3.2 Neighbor Discovery

Low transmission power levels, harsh and dynamically changing operation environment, and mobile applications cause unreliability for wireless links. After a link failure, a new synchronized link is established by a neighbor discovery operation. Typically, the neighbor discovery is performed by a network scan by listening a frequency channel until adequate number of beacons is received. To be able to detect all neighbors operating at different frequency channels, the network scan duration in each utilized channel must be at least one beacon transmission interval. This method is utilized, for example, in IEEE 802.15.4 [82].

An energy analysis [P5] with a typical low power radio indicates that each second of a network scan consumes the energy equaling to the transmission of nearly 2800 beacon frames. Clearly, the scanning increases significantly the energy consumption of a node, especially as network dynamics is high and the number of utilized frequency channels is high.

In this Thesis, two solutions for energy-efficient neighbor discovery are presented: a Network Channel Beaconing (NCB) scheme [P1], [P3], [P5], which can be complemented with an Energy-efficient Neighbor Discovery Protocol (ENDP) [P4] for further improving adaptivity. The objective of the both solutions is to maximize achieved energy efficiency and to minimize data routing breaks in dynamic networks.

Network channel beaconing

The designed NCB scheme dedicates one globally known channel for short network beacons, which are broadcast by all headnodes more frequently than ordinary beacons (cluster beacons). A network beacons contain the frequency channel and exact time to the next superframe. In addition, required information for selecting an appropriate headnode as a parent is included. The network beacons are received during a neighbor discovery only. As illustrated in Fig. 18, the neighbor discovery is performed by receiving the network channel for one network beacon interval [P3]. For clarity, the additional beacons of the path-loss estimation scheme are not presented in the figure. In normal operation, beacons are received only in the cluster channel.

A potential shortcoming of the network channel beaconing mechanism is unequal transmission range in different frequency channels due to antenna characteristics and different interference levels. To avoid this, the neighbor discovery is completed with the reception of cluster beacons from the most suitable parents in their cluster chan-

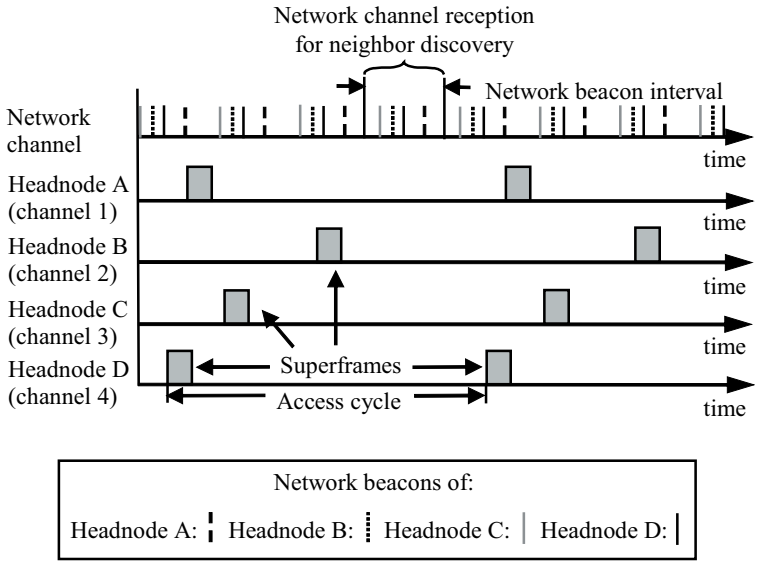

Fig. 18. *Neighbor discovery with network beacons.*

nels. This validates the link quality measurements and the set of new parents with which synchronized links can be established.

The performance of the network channel beaconing scheme has been analyzed in a general case with a network using the synchronized low duty-cycle channel access scheme [P5], and in a ZigBee network [P3].

To show the achieved energy saving, Fig. 19 presents the results of an energy analysis [P3] comparing network maintenance power consumptions with and without the NCB scheme. The network maintenance power is the sum of network scanning and beacon transmission powers. Cluster beacon interval and average network scan interval are set to 3.96 s and 2000 s, respectively. The analysis is performed using the hardware parameters of TI CC2420 [194] radio, and PIC18LF8722 [106] MCU. As the standard specified passive scans are used, the network maintenance power consumptions for networks using one and four channels are 132 μW and 468 μW. When NCB is utilized, the minimum of network maintenance power is 42 μW regardless of the number of channels. This power is achieved at 2.6 Hz network beacon rate. Thus, NCB achieves up to 96% energy saving compared to the standard ZigBee [P3].

An analysis in [P3] indicates that an energy optimal network beacon transmission rate f_b^* is a function network scanning interval (I_{NS}), beacon frame transmission energy (E_{TX}), radio power consumption in the reception mode (P_{RX}), and the average number of leaf nodes in each cluster (n_S), as

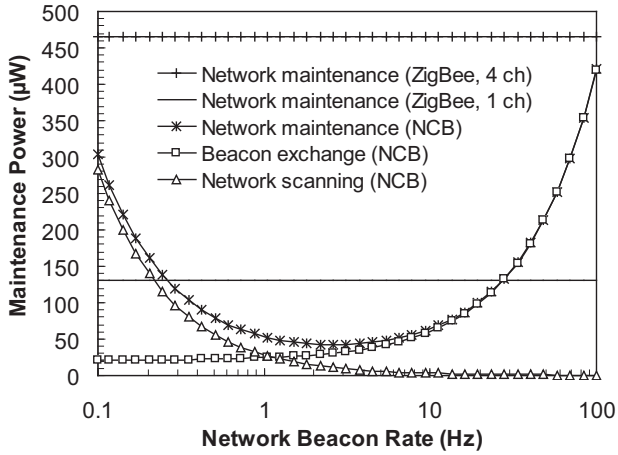

Fig. 19. *Beacon exchange, network scanning and network maintenance power consumptions and comparison with standard ZigBee neighbor discovery.*

$$f_b^* = \sqrt{\frac{P_{RX}(n_S+1)}{E_{TX}I_{NS}}}. \tag{10}$$

The function of f_b^* is similar for ZigBee, TUTWSN and other networks utilizing the synchronized low duty-cycle MAC scheme with regular beacon transmissions and network scans.

Energy-efficient neighbor discovery protocol

The designed ENDP reduces the need of network scans by a proactive distribution of synchronization information about potential parents in a two-hop neighborhood. Nodes transmit the synchronization information about their direct parents in beacons. A Synchronization Data Unit (SDU) referring to a node consists of two parts: the channel on which the node is operating, and the time base difference (offset) between the node and the sender of SDU. As NCB is used, SDUs are transmitted in network beacons [P4].

The operation of ENDP is illustrated in Fig. 20. In the figure, the number of maintained synchronized links (k) is two. Node M receives SDUs from its parents I and L. Node I composes SDUs from its parents A and B. Similarly, Node L composes SDUs from nodes H and G yielding that node M gathers synchronization information about nodes A, B, H, and G [P4].

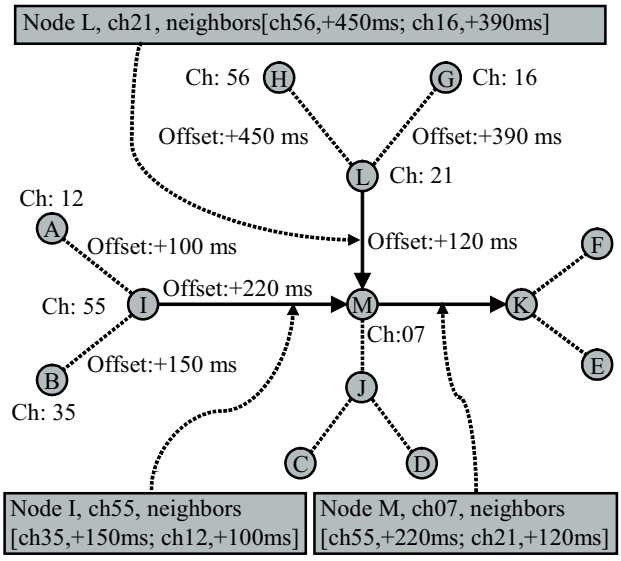

Fig. 20. *Connectivity and distributed neighbor information. Arrows indicate synchronization between nodes.*

If a link failure occurs or the link quality to a neighbor degrades significantly, a node first tries to receive beacons and form a new synchronized link according to the received SDUs. The energy consumption of these beacon receptions is negligible compared to the energy consumption of a network scan. A network scan is performed only if a suitable parent is not discovered by SDUs. The performance of ENDP can be adjusted according to the parameter k of the multi-cluster-tree topology.

The energy-efficiency of ENDP is analyzed in [P4]. The analysis utilizes the hardware parameters of a TUTWSN temperature sensing prototype consisting of Microchip PIC18LF8722 [106] MCU and Nordic Semiconductor nRF2401A [120] radio having 1 Mbps data rate. In the analysis, radio range is set to 10 m. Fig. 21 compares the network maintenance power consumptions as the function of network beacon rate at 0.1 m/s and 10 m/s node velocities. Curves are plotted using NCB with and without ENDP. When ENDP is used, k is varied from 1 to 4. When ENDP is not used, k is fixed to one resulting in the lowest power consumption. For comparison, the network maintenance power consumption using conventional network scans in one channel without NCB is plotted [P4].

The network maintenance power consumptions at 0.1 m/s and 10 m/s node velocities using conventional network scans are 1.23 mW and 60.17 mW, respectively. By adding the NCB scheme, network maintenance power consumption decreases at optimal network beacon rate to 95 μW and 742 μW. With ENDP, the minimum net-

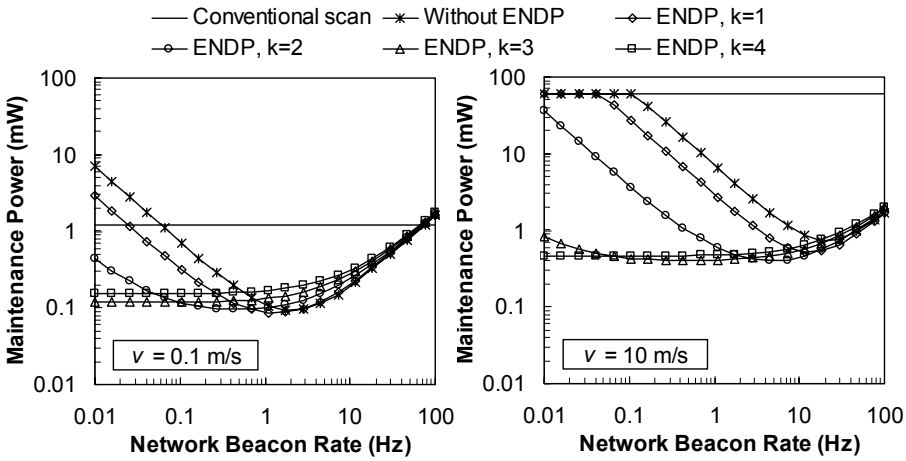

Fig. 21. *Network maintenance powers with and without ENDP and network beacons.*

work maintenance power further reduces to 87 μW (k = 1) and 397 μW (k = 2). The results show that ENDP reduces the network maintenance power consumption, as node mobility is higher than 1 m/s and the achieved energy saving increases with node mobility [P4]. Experimental measurements of ENDP are presented in Chapter 7 validating the results in practice.

6. PERFORMANCE MODELS

This chapter presents performance models for analyzing the power consumptions of the most essential low power channel access mechanisms and comparing them against the designed TUTWSN MAC. The focus is on data and ACK frame exchanges and on the maintenance of link synchronization by a beacon or SYNC frame exchange.

Performance models are determined for the following MAC protocols: T-MAC [201] and B-MAC [129], which are well known synchronized and unsynchronized low duty-cycle protocols, X-MAC [24] and SCP-MAC [221], which are two interesting proposals for unsynchronized protocols, and IEEE 802.15.4 [82], which is the most potential standardized technology for WSNs. For comparison, an ideal MAC protocol is defined and modeled.

The following performance models are based on the analysis of S. Yoon presented in [223]. For this Thesis, the set of models has been extended by IEEE 802.15.4 and TUTWSN MAC protocols. In addition, the effects of start-up transitions, contention windows and crystal tolerance have been modeled more accurately. In addition, the models and their presentation has been simplified and clarified.

The performance models are derived using the following assumptions:

- Each sensor node measures one sensor sample and forwards it to a next-hop node during one data generation interval;
- Each data frame is followed by an ACK for fair comparison;
- There are no transmission errors nor collisions;
- There is no contention, and carrier sense attempts produce an idle result;
- The power consumption of idle listening equals to the reception mode power;
- The active time of MCU equals to the active time of radio.

Therefore, the performance models can focus on the power consumption of the channel access mechanisms, while the effects of data processing, contention, and control frame exchanges are eliminated. For contention based protocols, obtained results are slightly better than in practice with contention. As TUTWSN MAC utilizes contention-free mechanism for data and ACK exchanges, the obtained results for TUTWSN are realistic.

6.1 Utilized Parameters

For determining the channel access models, all essential parameters describing the characteristics of a sensor node platform, application, and network topology are identified. The sensor node platform is defined by the following parameters:

ε	Crystal tolerance of a wake up timer
P_Y	The power consumed for Y, where $Y \in RX$ (receive), S (sleep), TX (transmit)
R	The data rate of a radio
t_{ST}	Radio start-up transient duration (crystal running)

Application and network topology are defined by the following parameters:

L_X	The length of frame X, where $X \in ACK$, B (beacon or SYNC), CTS, $DATA$, P (preample), RTS
n	The number of direct neighbors for a given node
n_{DL}	The number of descendent nodes of a given node in the routing tree, i.e. the number of data frames the node needs to forward during one data generation interval
T_{DATA}	Data generation interval in each node

In addition, there are protocol implementation specific parameters. Generally utilized parameters of that kind are:

t_{CCA}	The time for a clear channel assessment or carrier sensing
t_{CW}	Contention window length in CSMA
t_{sleep}	Sleep period length
T_{AC}	Access cycle length or channel polling interval
T_{SYNC}	SYNC or beacon frame transmission interval

6.2 Models

Energy consumptions are analyzed for a router node (**A**), and a leaf node (**B**) presented in Fig. 22. Both nodes have eight neighbors (n), which may cause overhearing and interferences for the channel access. Data generation interval (T_{DATA}) is equal for each node, and it varies from 1 s to 1000 s. Arrows in the figure indicate data routing directions. The traffic load is accumulated in routers, since they transmit their own data and the multi-hop routed data from n_{DL} nodes. For example, the router node **A** routes data from three nodes ($n_{DL} = \{\mathbf{B, D, E}\}$), while the router node **C** routes data from four nodes ($n_{DL} = \{\mathbf{A, B, D, E}\}$). This increases the power consumption of these routers, but also the overhearing and interferences among other nodes in their transmission range.

Average power consumptions (P) for each protocol are calculated by normalized transmission (t_{TX}) and reception (t_{RX}) activities and their power consumptions as

$$P = t_{TX}P_{TX} + t_{RX}P_{RX} + (1 - t_{TX} - t_{RX})P_S. \tag{11}$$

The normalized activity is determined by dividing the duration of an activity by the interval of the activity resulting in a percentage value of the activity. Data exchanges are normalized by T_{DATA} during which all nodes in the network generate exactly one data frame. Similarly, the transmission and reception activity for maintaining synchronization is normalized by T_{SYNC}.

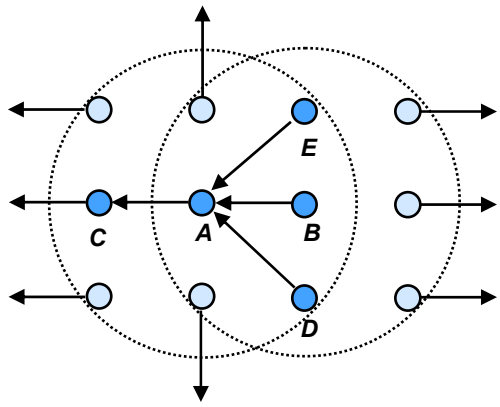

Fig. 22. *Network topology for channel access comparison.*

6.2.1 Ideal-MAC

First, an ideal MAC (Ideal-MAC) protocol [223] is defined. All nodes can exchange data and ACK frames without the need of any synchronization or contention mechanism. Nodes can sleep all the time between frame exchanges. Hence, the Ideal-MAC does not cause any idle listening or control frame overhead.

The required activity for exchanging one data frame is presented in Fig. 23. Although MAC is ideal and practically impossible to implement, a sensor node platform is realistic. Thus, each data transmission and reception is preceded by a radio start-up transient (t_{ST}). Thus, t_{TX} and t_{RX} for the leaf node are

$$t_{TX} = \left(t_{ST} + \frac{L_{DATA}}{R}\right)\frac{1}{T_{DATA}}, \tag{12}$$

$$t_{RX} = \left(t_{ST} + \frac{L_{ACK}}{R}\right)\frac{1}{T_{DATA}}. \tag{13}$$

The router node receives data frames from n_{DL} leaf nodes, transmit them ACKs, forwards the received and own data frames to a parent and receives ACKs. Thus, t_{TX} and t_{RX} for the router are

$$t_{TX} = \left(t_{ST} + \frac{L_{DATA}}{R}\right)\frac{n_{DL}+1}{T_{DATA}} + \left(t_{ST} + \frac{L_{ACK}}{R}\right)\frac{n_{DL}}{T_{DATA}}. \tag{14}$$

$$t_{RX} = \left(t_{ST} + \frac{L_{DATA}}{R}\right)\frac{n_{DL}}{T_{DATA}} + \left(t_{ST} + \frac{L_{ACK}}{R}\right)\frac{n_{DL}+1}{T_{DATA}}. \tag{15}$$

6.2.2 B-MAC

B-MAC [129] uses the LPL scheme, where nodes sleep (t_{sleep}), wake up (t_{ST}) and poll channel (t_{CCA}) periodically at T_{AC} intervals. The frame exchanges of B-MAC are

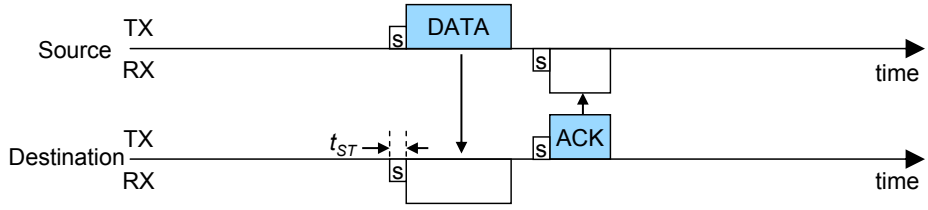

Fig. 23. *The activity of radio in Ideal-MAC.*

presented in Fig. 24.

The normalized channel polling time (t_{POLL}) is

$$t_{POLL} = \frac{t_{ST} + t_{CCA}}{T_{AC}}. \tag{16}$$

The leaf node transmits data frames at T_{DATA} intervals. Each transmission is preceded by a carrier sensing (t_{CCA}) and a preamble transmission lasting T_{AC}. Thus, t_{TX} for the leaf node is

$$t_{TX} = \left(t_{ST} + T_{AC} + \frac{L_{DATA}}{R} \right) \frac{1}{T_{DATA}}. \tag{17}$$

In B-MAC, all data in a radio range is received. As the leaf node has n neighbors, and the router in a range forwards n_{DL} data frames from leaf nodes, totally $n + n_{DL}$ data frames are received during T_{DATA}. Since channel is polled randomly, average preamble reception time is a half of T_{AC}. Thus, t_{RX} for the leaf node is

$$t_{RX} = t_{POLL} + \left(\frac{T_{AC}}{2} - t_{CCA} + \frac{L_{DATA}}{R} \right) \frac{n + n_{DL}}{T_{DATA}} + \left(t_{ST} + \frac{L_{ACK}}{R} \right) \frac{1}{T_{DATA}}. \tag{18}$$

The operation of the router node is similar to the leaf node, except the amount of exchanged data. The router node forwards data frames from n_{DL} nodes and transmits ACKs. The normalized transmission and reception times for the B-MAC router are

$$t_{TX} = \left(t_{ST} + T_{AC} + \frac{L_{DATA}}{R} \right) \frac{n_{DL} + 1}{T_{DATA}} + \left(t_{ST} + \frac{L_{ACK}}{R} \right) \frac{n_{DL}}{T_{DATA}}. \tag{19}$$

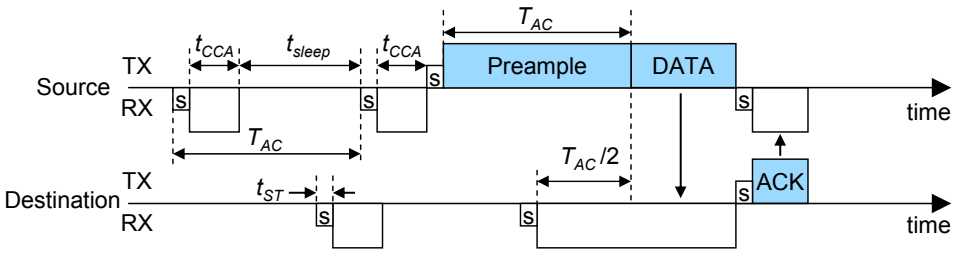

Fig. 24. *The activity of radio in B-MAC.*

$$t_{RX} = t_{POLL} + \left(\frac{T_{AC}}{2} - t_{CCA} + \frac{L_{DATA}}{R}\right)\frac{n+n_{DL}+1}{T_{DATA}} + \left(t_{ST} + \frac{L_{ACK}}{R}\right)\frac{n_{DL}+1}{T_{DATA}}. \quad (20)$$

The power consumption reaches its unique minimum at an optimal polling interval (T^*_{AC}) obtained by setting $\partial(t_{TX}P_{TX} + t_{RX}P_{RX})/\partial T_{AC} = 0$. Performance results are calculated using the optimal polling interval of the router, which is

$$T^*_{AC} = \sqrt{\frac{T_{DATA}(t_{ST}+t_{CCA})}{(n_{DL}+1)P_{TX}/P_{RX} + (n+n_{DL}+1)/2}}. \quad (21)$$

6.2.3 SCP-MAC

SCP-MAC [221] replaces the long preample with a short wake-up tone by waking up the senders and the receiver at the same time. The best-case situation is considered, where all synchronization signaling is piggybacked with data frames. Thus, the synchronization does not cause control frame exchanges. The frame exchanges of SCP-MAC are presented in Fig. 25.

SCP-MAC utilizes similar channel polling than B-MAC, and t_{POLL} equals to (16). The duration of the wake-up tone (t_{TONE}) is determined according to the clock drift (ε), the rate of frame receptions containing synchronization information, and the minimum tone duration (t_{CCA}) to detect a transmission. Thus, t_{TONE} is

$$t_{TONE} = \frac{4T_{DATA}\varepsilon}{n+n_{DL}} + t_{CCA}. \quad (22)$$

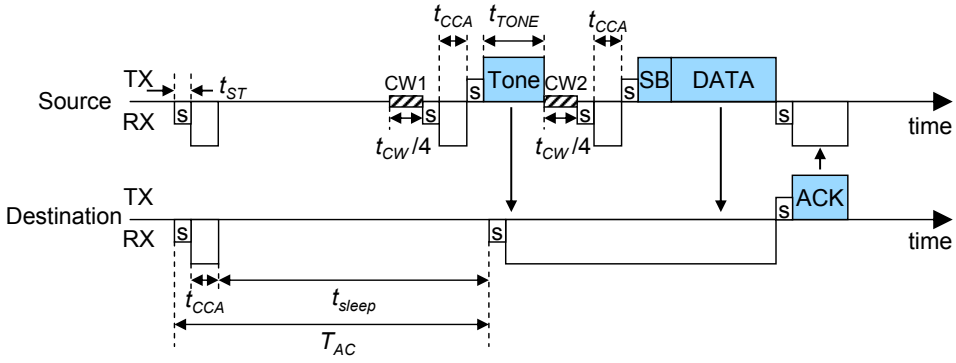

Fig. 25. *The activity of radio in SCP-MAC.*

A data frame transmission consists of the wake-up tone, and the frame transmission. SCP-MAC utilizes two contention windows (CW1 and CW2) being $t_{CW}/2$ long. Thus, an average backoff time in each contention window is $t_{CW}/4$ during which the source node is asleep. After a start-up transient, the destination node receives on average halves of the wake-up tone and the second contention window. Data frames are piggybacked with synchronization data (SB). Thus, t_{TX} and t_{RX} of the SCP-MAC leaf node are

$$t_{TX} = \left(2t_{ST} + t_{TONE} + \frac{L_{SB} + L_{DATA}}{R}\right) \frac{1}{T_{DATA}}. \tag{23}$$

$$\begin{aligned} t_{RX} = t_{POLL} &+ \left(3t_{ST} + 2t_{CCA} + \frac{L_{ACK}}{R}\right) \frac{1}{T_{DATA}} \\ &+ \left(3t_{ST} + \frac{t_{TONE}}{2} + \frac{t_{CW}}{4} + t_{CCA} + \frac{L_{SB} + L_{DATA}}{R}\right) \frac{n + n_{DL}}{T_{DATA}}. \end{aligned} \tag{24}$$

The SCP-MAC router transmits $n_{DL} + 1$ data frames to a next hop node, and ACKs to the leaf nodes. Thus, t_{TX} and t_{RX} of the SCP-MAC router node are

$$t_{TX} = \left(2t_{ST} + t_{TONE} + \frac{L_{SB} + L_{DATA}}{R}\right) \frac{n_{DL} + 1}{T_{DATA}} + \left(t_{ST} + \frac{L_{ACK}}{R}\right) \frac{n_{DL}}{T_{DATA}}. \tag{25}$$

$$\begin{aligned} t_{RX} = t_{POLL} &+ \left(3t_{ST} + 2t_{CCA} + \frac{L_{ACK}}{R}\right) \frac{n_{DL} + 1}{T_{DATA}} \\ &+ \left(3t_{ST} + \frac{t_{TONE}}{2} + \frac{t_{CW}}{4} + t_{CCA} + \frac{L_{SB} + L_{DATA}}{R}\right) \frac{n + n_{DL} + 1}{T_{DATA}}. \end{aligned} \tag{26}$$

For achieving the best energy-efficiency, a node should only poll the channel when there is a transmission from a neighbor. Performance results are calculated using the optimal polling interval of the router, which is

$$T_{AC}^{*} = \frac{T_{DATA}}{n_{DL} + 1}. \tag{27}$$

6.2.4 X-MAC

In X-MAC [24], each data frame transmission is preceded by the strobed preamble, as presented in Fig. 26. The minimum channel polling time to receive at least one entire preamble (P) equals to the lengths of two preamples (t_p) and one ACK (t_{al}). The normalized channel-polling time in X-MAC is

$$t_{POLL} = \frac{2t_p + t_{al}}{T_{AC}}, where \tag{28}$$

$$t_p = t_{ST} + \frac{L_P}{R}, \tag{29}$$

$$t_{al} = t_{ST} + \frac{L_{ACK}}{R}. \tag{30}$$

Assuming uniform distribution of wake-up moments, the average length of the strobed preamble is a half of the wake up period (T_{AC}), during which $T_{AC}/(2(t_p + t_{al}))$ preamples are transmitted. Overhearing is limited to the channel polling time. Hence, t_{TX} and t_{RX} the leaf node are

$$t_{TX} = \left(\frac{T_{AC}}{2(t_p + t_{al})} t_p + t_{ST} + \frac{L_{DATA}}{R} \right) \frac{1}{T_{DATA}}, \tag{31}$$

$$t_{RX} = t_{POLL} + \left(\frac{T_{AC}}{2(t_p + t_{al})} + 1 \right) \frac{t_{al}}{T_{DATA}}. \tag{32}$$

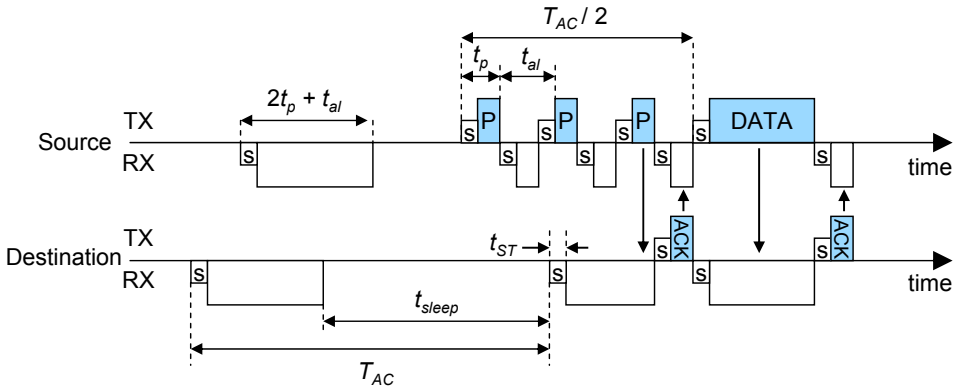

Fig. 26. *The activity of radio in X-MAC.*

As the router node receives and forwards data frames from n_{DL} nodes, the normalized transmission and reception times of the X-MAC router node are

$$t_{TX} = \left(\frac{T_{AC}}{2(t_p + t_{al})} t_p + \frac{L_{DATA}}{R} \right) \frac{n_{DL}+1}{T_{DATA}} + \frac{2t_{al} n_{DL}}{T_{DATA}}, \tag{33}$$

$$t_{RX} = t_{POLL} + \left(\frac{T_{AC}}{2(t_p + t_{al})} + 1 \right) \frac{t_{al}\,(n_{DL}+1)}{T_{DATA}} + \left(t_{ST} + \frac{L_{DATA}}{R} \right) \frac{n_{DL}}{T_{DATA}}. \tag{34}$$

The power consumption reaches its unique minimum at an optimal polling interval (T^*_{AC}) obtained by setting $\partial P / \partial T_{AC} = 0$. Performance results are calculated using the optimal polling interval of the router, which is

$$T^*_{AC} = \sqrt{\frac{2T_{DATA}(t_p + t_{al})(2t_p + t_{al})}{(t_p P_{TX}/P_{RX} + t_{al})\,(n_{DL}+1)}}. \tag{35}$$

6.2.5 T-MAC

Next, the synchronized low duty-cycle protocols are modeled. For comparability, T_{AC} is determined such that each active period in the router node contains n_F data frames

$$T_{AC} = \frac{n_F T_{DATA}}{n_{DL}+1}. \tag{36}$$

In T-MAC [201], each node polls channel for RTS messages at T_{AC} intervals, as presented in Fig. 27. If no traffic exists, radio is turned off after a period of T_A. Hence, the normalized channel polling time without traffic is

$$t_{POLL} = \frac{t_{ST} + T_A}{T_{AC}}, where \tag{37}$$

$$T_A = t_{ST} + t_{CW} + t_{RTS}. \tag{38}$$

A data frame transmission consists of a random delay within a Contention Window (CW) being followed by an RTS - CTS - DATA - ACK frame exchange. L_B bytes long SYNC frames are transmitted at T_{SYNC} intervals using a random delay within CW. For maximum energy-efficiency, adaptive listening and virtual clusters are assumed.

According to received RTS frames, nodes are in sleep mode during the transmissions intended to other nodes. Thus, t_{TX} and t_{RX} for the leaf node are

$$t_{TX} = \left(2t_{ST} + \frac{L_{RTS} + L_{DATA}}{R}\right)\frac{1}{T_{DATA}} + \left(t_{ST} + \frac{L_B}{R}\right)\frac{1}{T_{SYNC}}, \tag{39}$$

$$\begin{aligned} t_{RX} = t_{POLL} &+ \left(2t_{ST} + \frac{t_{CW}}{2} + \frac{L_{RTS}}{R}\right)\frac{n + n_{DL}}{T_{DATA}} \\ &+ \left(2t_{ST} + \frac{L_{CTS} + L_{ACK}}{R}\right)\frac{1}{T_{DATA}} + \left(t_{ST} + t_{CW} - \frac{L_B}{R}\right)\frac{1}{T_{SYNC}}. \end{aligned} \tag{40}$$

The router node receives data frames from n_{DL} nodes, transmits $n_{DL}+1$ frames to a next-hop node, and transmits and receives SYNC frames. Thus, t_{TX} and t_{RX} for the T-MAC router node are

$$\begin{aligned} t_{TX} = &\left(2t_{ST} + \frac{L_{RTS} + L_{DATA}}{R}\right)\frac{n_{DL} + 1}{T_{DATA}} \\ &+ \left(2t_{ST} + \frac{L_{CTS} + L_{ACK}}{R}\right)\frac{n_{DL}}{T_{DATA}} + \left(t_{ST} + \frac{L_B}{R}\right)\frac{1}{T_{SYNC}}, \end{aligned} \tag{41}$$

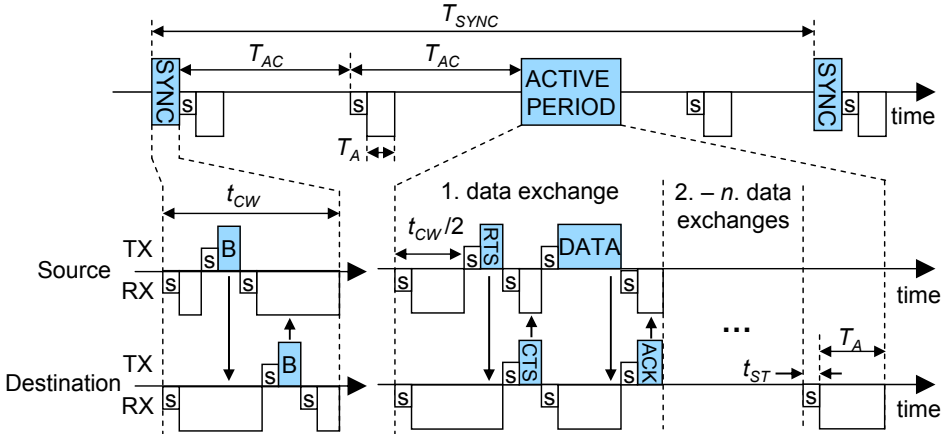

Fig. 27. *The activity of radio in T-MAC.*

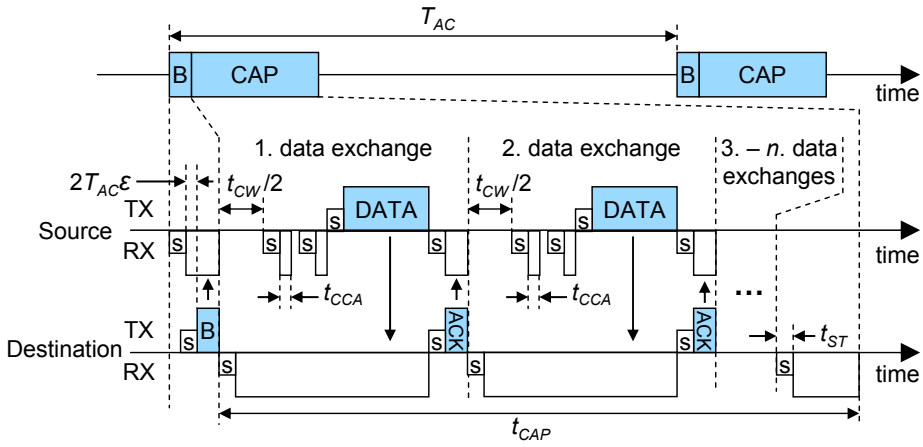

Fig. 28. *The activity of radio in IEEE 802.15.4.*

$$t_{RX} = t_{POLL} + \left(3t_{ST} + \frac{t_{CW}}{2} + \frac{L_{RTS}+L_{DATA}}{R}\right)\frac{n_{DL}}{T_{DATA}} + \left(t_{ST} + t_{CW} - \frac{L_B}{R}\right)\frac{1}{T_{SYNC}} + \left(t_{ST} + \frac{t_{CW}}{2} + \frac{L_{RTS}}{R}\right)\frac{n+n_{DL}+1}{T_{DATA}} + \left(2t_{ST} + \frac{L_{CTS}+L_{ACK}}{R}\right)\frac{n_{DL}+1}{T_{DATA}}. \quad (42)$$

6.2.6 IEEE 802.15.4

For obtaining the best energy-efficiency, IEEE 802.15.4 [82] is analyzed in the beacon-enabled mode, with inactive time, and employing a cluster-tree network topology. Nodes maintain synchronization by receiving beacon frames from a parent at the beginning of active periods. Beacons are transmitted by cluster heads only. The required activity of radio is presented in Fig. 28.

Beacons are transmitted at T_{AC} intervals. As a crystal tolerance is ε, the normalized beacon reception (polling) time is

$$t_{POLL} = \left(t_{ST} + 2T_{AC}\varepsilon + \frac{L_B}{R}\right)\frac{1}{T_{AC}}. \quad (43)$$

A data frame transmission is preceded by a random backoff delay and two Clear Channel Assessment (CCA) operations [82]. IEEE 802.15.4 utilizes blind backoffs, where nodes spend the backoff delay in the sleep mode. A data frame is followed by

an ACK, which is transmitted within a maximum waiting time of 864 μs. Assuming the best case situation, where the hardware processes the received frame instantly, ACK is transmitted without a delay. Thus, t_{TX} and t_{RX} for the IEEE 802.15.4 leaf node are

$$t_{TX} = \left(t_{ST} + \frac{L_{DATA}}{R}\right)\frac{1}{T_{DATA}}, \tag{44}$$

$$t_{RX} = t_{POLL} + \left(3t_{ST} + 2t_{CCA} + \frac{L_{ACK}}{R}\right)\frac{1}{T_{DATA}}. \tag{45}$$

The IEEE 802.15.4 router node (coordinator) transmit beacons, receives entire CAP except ACK transmissions, and forward data to a next hop node. Thus, t_{TX} and t_{RX} for the IEEE 802.15.4 router node are

$$t_{TX} = \left(t_{ST} + \frac{L_B}{R}\right)\frac{1}{T_{AC}} + \left(t_{ST} + \frac{L_{DATA}}{R}\right)\frac{n_{DL}+1}{T_{DATA}} + \left(t_{ST} + \frac{L_{ACK}}{R}\right)\frac{n_{DL}}{T_{DATA}}, \tag{46}$$

$$t_{RX} = t_{POLL} + \frac{t_{CAP}}{T_{AC}} - \left(t_{ST} + \frac{L_{ACK}}{R}\right)\frac{n_{DL}}{T_{DATA}} + \left(3t_{ST} + 2t_{CCA} + \frac{L_{ACK}}{R}\right)\frac{n_{DL}+1}{T_{DATA}}. \tag{47}$$

For achieving the maximum energy-efficiency, analysis results are determined using the minimum CAP length, where the required frame exchanges can be performed. The minimum CAP length is

$$t_{CAP} = \left(4t_{ST} + \frac{t_{CW}}{2} + 2t_{CCA} + \frac{L_{DATA} + L_{ACK}}{R}\right)n_F. \tag{48}$$

6.2.7 TUTWSN MAC

For comparison, the energy consumption of TUTWSN is modeled. Due to the stationary network, the following analysis considers the basic channel access mechanism without the networking mechanisms. Each node maintains synchronization with one parent. Superframe contains S_A contention slots and the required number of contention-free slots. The activity of radio in TUTWSN is presented in Fig. 29.

In TUTWSN, the normalized channel polling time t_{POLL} is similar with IEEE 802.15.4. The leaf node (subnode) receives the beacons and transmits data using a contention-free slot. Thus, t_{TX} is similar with IEEE 802.15.4 leaf node, and t_{RX} for the leaf node is

$$t_{RX} = t_{POLL} + \left(t_{ST} + \frac{L_{ACK}}{R}\right)\frac{1}{T_{DATA}}. \quad (49)$$

The TUTWSN router node (headnode) receives and transmits beacons, receives S_A/T_{AC} contention slots and n_{DL}/T_{DATA} contention-free slots, and transmits received and own generated data to a parent in contention-free slots. Thus, t_{TX} and t_{RX} for the TUTWSN router are

$$t_{TX} = \left(t_{ST} + \frac{L_B}{R}\right)\frac{1}{T_{AC}} + \left(t_{ST} + \frac{L_{ACK}}{R}\right)\frac{n_{DL}}{T_{DATA}} + \left(t_{ST} + \frac{L_{DATA}}{R}\right)\frac{n_{DL}+1}{T_{DATA}}, \quad (50)$$

$$t_{RX} = t_{POLL} + \left(t_{ST} + \frac{L_{DATA}}{R}\right)\left(\frac{S_A}{T_{AC}} + \frac{n_{DL}}{T_{DATA}}\right) + \left(t_{ST} + \frac{L_{ACK}}{R}\right)\frac{n_{DL}+1}{T_{DATA}}. \quad (51)$$

6.3 Results

By utilizing parameter values presented in Table 12, average power consumptions are determined for HR and LR platforms.

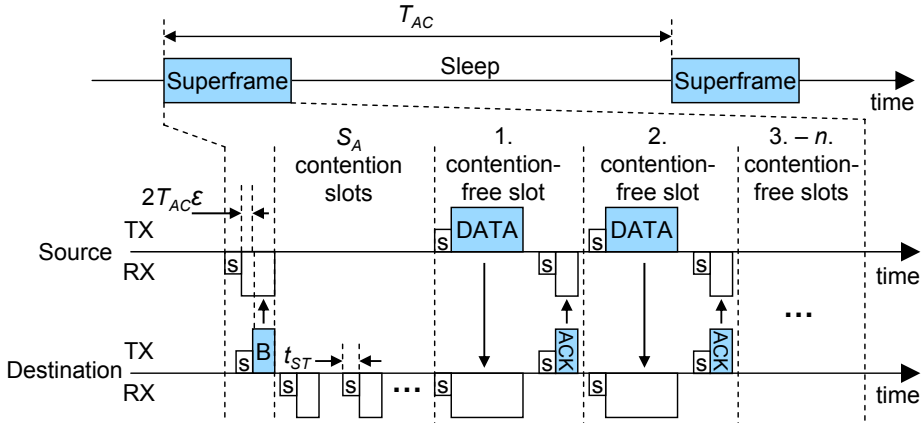

Fig. 29. *The activity of radio in TUTWSN MAC.*

The results for HR platform are presented in Fig. 30. According to the results, synchronized protocols outperform clearly unsynchronized proposals in the analyzed network. For both node types, the order of power consumptions is the same. B-MAC results in the highest power, while TUTWSN performs closest to the Ideal-MAC. As data generation interval increases from 1 s to 1000 s, the power consumptions of the Ideal-MAC leaf and router nodes are 68 μW to 37 μW, and 270 μW to 37 μW, respectively. The power consumption of TUTWSN leaf and router nodes are 23.4% to 6.54%, and 18.8% to 6.60% higher than the Ideal-MAC and the same data generation intervals. IEEE 802.15.4 performs the second best and results in 80.4% to 6.64 % and 229% to 8.14% higher power consumption than the Ideal-MAC.

The utilization of LR platform increases power consumptions, as presented in Fig. 31. However, TUTWSN MAC maintains its energy-efficiency resulting in the lowest power consumption. The power consumptions of the Ideal-MAC leaf and router nodes are 171 μW to 37 μW, and 945 μW to 38 μW, respectively. The power consumption of TUTWSN leaf and router nodes are 27.1% to 2.85%, and 20.2% to 3.18% higher than the Ideal-MAC and the same data generation intervals. IEEE 802.15.4 performs the second best and results in 42.1% to 2.92% and 66.3% to 4.33% higher power consumption than the Ideal-MAC.

The results indicate that the designed channel access mechanism achieves higher

Table 12. *Utilized parameter values.*

Parameter	Value (HR)	Value (LR)
ε	20 ppm	20 ppm
L_{ACK}, L_{CTS}, L_{RTS}, L_P	8B	8B
L_B, L_{DATA}	32B	32B
L_{SB} (SCP-MAC)	2B	2B
n	8	8
n_F	8	8
n_{DL}	3	3
P_{RX}	60.2 mW	25.4 mW
P_S	37 μW	37 μW
P_{TX}	34.7 mW	29.9 mW
R	1 Mbps	76.8 kbps
S_A (TUTWSN)	2	2
T_{SYNC} (T-MAC)	90 s	90 s
t_{CCA}	128 μs	256 μs
t_{CW}	2 ms	4 ms
t_{ST}	195 μs	250 μs

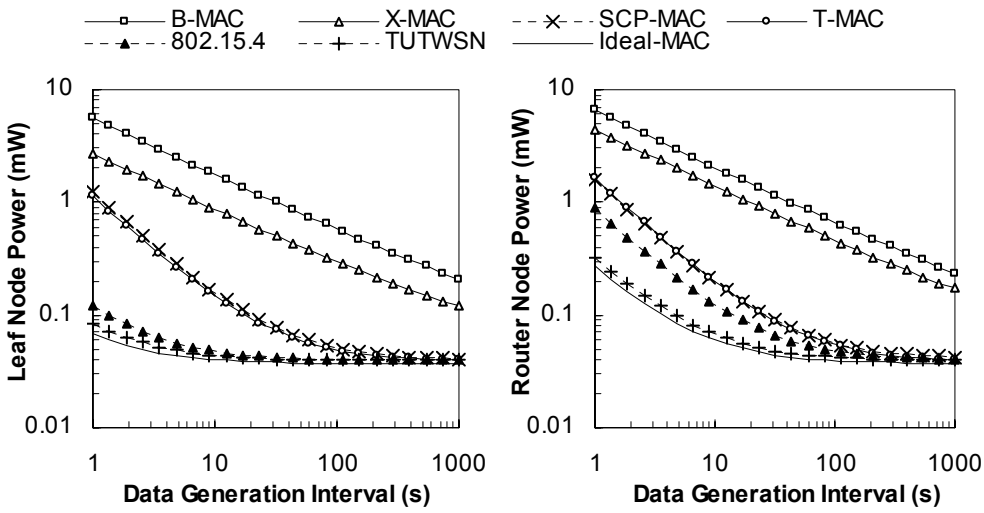

Fig. 30. *Power consumption comparison using HR (nRF2401A) radio.*

energy-efficiency than the most essential existing low-power MAC protocols. Depending on the traffic loading, radio type, and data routing capability, the energy overhead of TUTWSN nodes is only 2.85% to 27.1%. The high energy-efficiency is achieved in both leaf and router nodes. It should be noted that the TUTWSN channel access can operate without the designed networking mechanisms (NCB and ENDP). Then, the neighbor discovery operations are performed similarly with IEEE 802.15.4 passive scans.

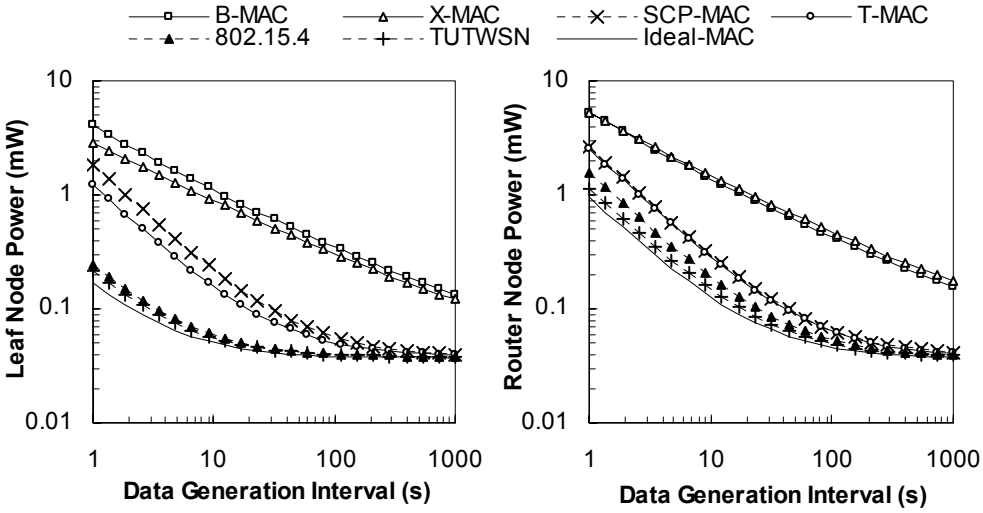

Fig. 31. *Power consumption comparison using LR (CC1000) radio.*

7. TUTWSN SENSOR NODE PLATFORMS AND DEPLOYMENTS

This chapter summarizes the research results of TUTWSN sensor node platforms and deployments. The sensor node platforms have been designed for three reasons. First, for measuring and understanding the behavior of low power components in real operation environment, which is critical for the design of a feasible MAC layer. Second, for measuring the performance of the TUTWSN MAC layer design in large scale networks, which is critical for validating and optimizing the design. Third, for developing and demonstrating new WSN applications and long-lived WSN nodes in practice. Important information obtained from the sensor node platforms have been the constraints and non-ideal characteristics of low-power hardware components and radio wave propagation, and their effect on protocol implementation, network performance, and power consumption.

The TUTWSN sensor node platforms have been designed in parallel with the MAC layer. The platforms have been tailored according to the memory, processing power and timing accuracy requirements of the TUTWSN protocol stack and the MAC layer. Existing platforms have not been used, since they have not been commercially available, or their energy consumption has been too high.

7.1 TUTWSN Node Designs

This Thesis presents twelve TUTWSN sensor node platforms, which have been designed in the years 2004 to 2006. Along the time, TUTWSN protocol stack has been developed and its memory requirements have been increased. One of the most critical design decisions has been the selection of a radio and MCU. Since the radio is a significant (in most nodes the largest) source of power consumption [P7], TUTWSN platforms have utilized simple and low energy radios. MCU has been selected according to sleep mode power consumption, the energy-efficiency in active mode, and memory resources for software. In addition, an accurate wake up timer has been required for ensuring link synchronization accuracy.

The platforms are presented chronologically and summarized at the end of this Section. Performance results obtained by the platforms are presented in the next Section.

7.1.1 Node Designs in 2004

The first embedded TUTWSN sensor node platforms were designed in 2004. At that time, TUTWSN protocol stack contained only the basic MAC functionality and very simple upper protocol layers.

According to an energy analysis [P7], Nordic Semiconductor nRF2401A [120] radio and Xemics (Semtech) XE88LC02 [163] MCU were selected as the basis of the designed platforms. The radio operates at 2.4 GHz frequency band and has 1 Mbps data rate resulting in high energy-efficiency and enabling the utilization of a very small ceramic antenna. The MCU utilizes an energy-efficient CoolRISC core and 16-bit ADC. Available 22kB program memory and 1 kB data memory were sufficient for the protocol stack of that time.

TUTWSN Node

First, a platform called TUTWSN node [P8] was build. The platform was targeted at indoor temperature sensing applications. It was equipped with a simple analog temperature sensor and a linear voltage regulator. External EEPROM was used for non-volatile data. The implemented TUTWSN node is presented in Fig. 32.

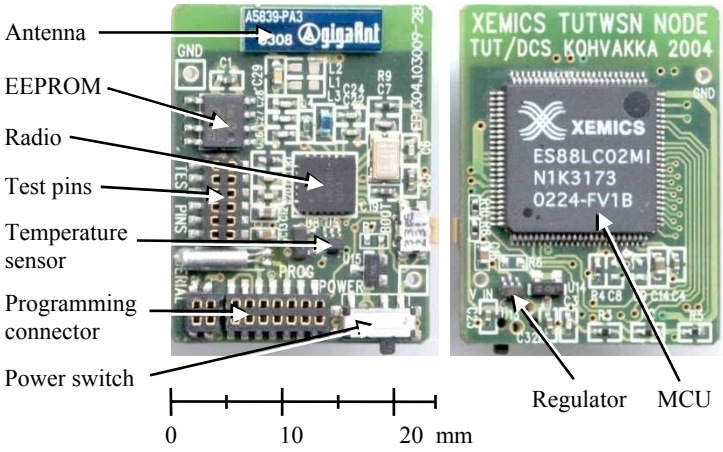

Fig. 32. *TUTWSN node.*

Although the platform was energy-efficient [P8], it had some problems in experimental networks. A small ceramic antenna limited the radio range to around 15 meters. In addition, tolerances in a low-cost temperature sensor and its voltage reference caused inaccuracy to measurements.

TUTWSN Position Sensor Node

For demonstrating the feasibility of TUTWSN in industrial applications, a platform called TUTWSN position sensor node [P9] was implemented. The platform was equipped with a linear position sensor, a small 150 mAh (3.6 V) rechargeable Nickel-Metal Hydride (NiMH) battery, and it was packed in a robust aluminum casing. The battery capacity was adequate, since the required battery lifetime was one month [P9]. The Printed Circuit Board (PCB) and the aluminum casing of the node is presented in Fig. 33.

According to measurements, the TUTWSN position sensor node obtained better radio

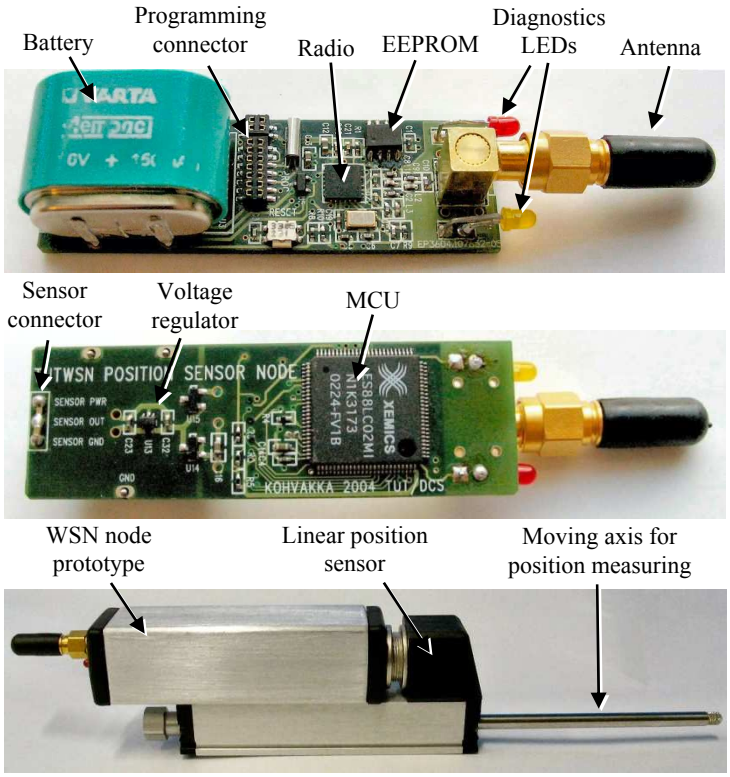

Fig. 33. *TUTWSN position sensor node.*

range than the TUTWSN node. The usability of the platform was also improved by the robust mechanical design and the on-board battery. In addition, the connector for the linear position sensor could be used for charging the battery. Measurements with the TUTWSN position sensor nodes indicated that TUTWSN technology has adequate performance for measuring low-speed movements by the sensor element. Observed problems of the platform were low battery capacity, and expensive antenna. In addition, strong fluctuation of a radio link quality caused frequent link failures and network scans, which increased power consumption at long hop lengths.

TUTWSN Gateway

For implementing a sink and a gateway to PC, a platform called TUTWSN gateway was designed [P9]. The platform was equipped with an RS-232 serial interface. For improving usability, the platform obtained its supply energy directly from the RS-232 port using a rectifier and large electrolytic filter capacitors. The TUTWSN gateway is presented in Fig. 34.

TUTWSN SoC Node

A platform called TUTWSN SoC node was implemented [P8] for experimenting and measuring the performance of commercial SoC components integrating radio and MCU. The platform was targeted at a subnode operation.

The platform utilized Nordic Semiconductor nRF24E1 [119] chip, which contains a nRF2401A radio, ADC and a 8051 MCU core having 4 kB program memory and 256 B data memory. External EEPROM was required for storing program memory. Because of a common radio interface, the platform was compatible with other

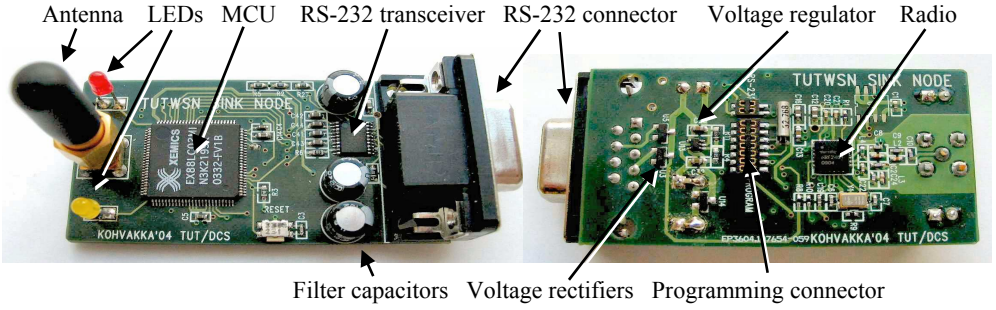

Fig. 34. *TUTWSN gateway.*

TUTWSN platforms. The platform was equipped with a simple temperature sensor and a linear voltage regulator. The TUTWSN SoC node on a 5 cent coin is presented in Fig. 35. The size of the platform was only 23 mm x 13 mm x 5 mm.

The utilization of the SoC component reduced node size and cost. Yet, an inaccurate wake up timer caused serious problems for link synchronization. Link synchronization was possible by either extending the frame reception periods, or keeping MCU always active. According to energy measurements, the latter resulted better energy-efficiency. Still, the measured average power consumption was over two orders of magnitude higher than the power consumption of other TUTWSN platforms.

7.1.2 Node Designs in 2005

As TUTWSN protocol stack was improved and extended, the memory resources of the Xemics MCU exceeded. In 2005, new family of sensor node platforms was designed and implemented. Microchip PIC18LF4620 [105] MCU was selected according to an analysis of the energy-efficiency, sleep mode power consumption, wake up timers, and memory resources of available MCUs. It should be noted that the energy-efficiency of PIC is around four times worse than in Xemics, which slightly increases the power consumption of these platforms.

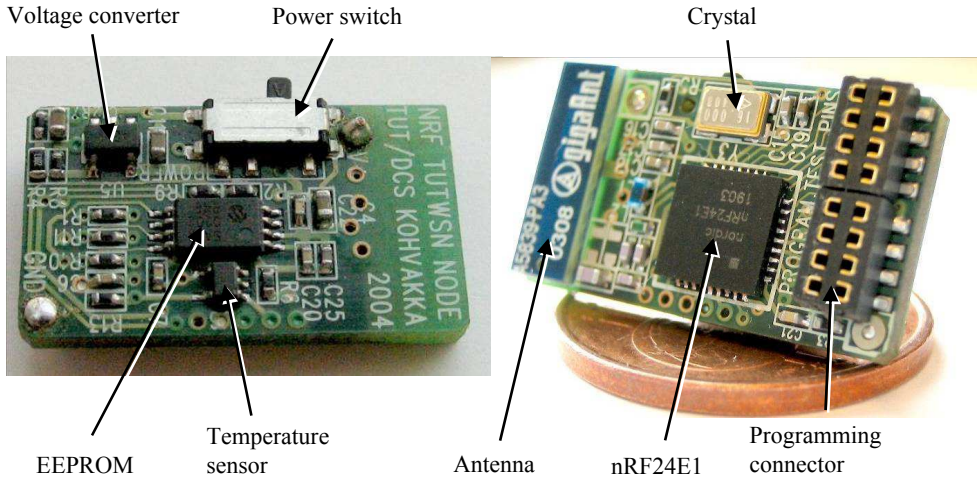

Fig. 35. *TUTWSN SoC node on a 5-euro-cent coin.*

TUTWSN Temperature Sensor Node

First, a platform called TUTWSN temperature sensor node was designed [P2]. The platform was designed to tolerate arctic conditions, and all utilized components were specified with an extended temperature range beginning from -40 °C. The range of the nRF2401A [120] radio was improved by a loop antenna, which was implemented as a PCB trace and experimentally tuned for the best performance. The accuracy of temperature measurements was improved by utilizing a Dallas DS620U [42] digital thermometer. The platform was powered by a lithium battery having high performance in low temperature conditions. Support for a solar panel as a power source was improved by an under voltage protection circuit in the power subsystem. The circuitry was required to eliminate the under voltage lockout condition of MCU and radio, since the supply voltage depends on the illumination.

The implemented TUTWSN temperature sensing node is presented in Fig. 36. The platform contained two attachable boards: a MCU board and an extension board, which was equipped with a battery holder. The utilization of detachable extension board allowed the change of a power source and easy implementation of application specific sensors and network interfaces.

According to experiments, the platform had good mechanical design for outdoor field tests. Operation in temperatures as low as -37.5 °C were experimentally verified. The digital thermometer improved highly the accuracy of temperature measurements. Measured transmission range of the loop antenna was up to 500 meters, which drastically reduced the required number of hops, and transmission power levels. Yet, high directivity of the antenna reduced the accuracy of node localization.

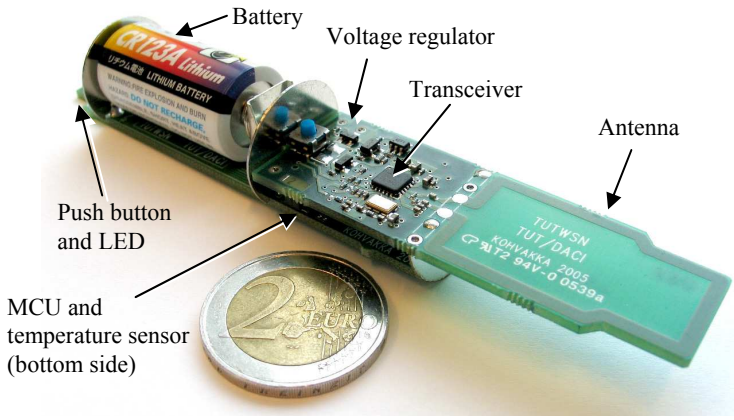

Fig. 36. *Implemented TUTWSN temperature sensor node.*

TUTWSN Long-Range Node

For improving the applicability of TUTWSN in environmental monitoring applications, a TUTWSN long-range node was implemented. The platform was targeting at over 1 km hop lengths enabling the coverage of large geographic areas by using a relatively small number of nodes. The platform utilized similar design with the TUTWSN temperature sensor node, except the radio. Due to the increased requirements for communication range, the platform utilized a Nordic Semiconductor nRF905 [122] radio operating at the 433 MHz frequency band. The radio has 50 kbps data rate and 10 mW maximum transmission power. Antenna was selected and fine-tuned according to experimental measurements. According to the results, a half-wave loop was the best tradeoff between size and performance, and had nearly omni-directional radiation pattern. The TUTWSN long-range node is presented in Fig. 37.

Experiments with the platform indicated up to 3 km radio range in a deployed network. Thus, very large and sparse networks were possible. Observed problems with the platform were lower energy-efficiency and scalability than with the 2.4 GHz radio. These were caused by the low data rate, and only few usable channels due to significant inter-channel interferences and the narrow 433 MHz frequency band.

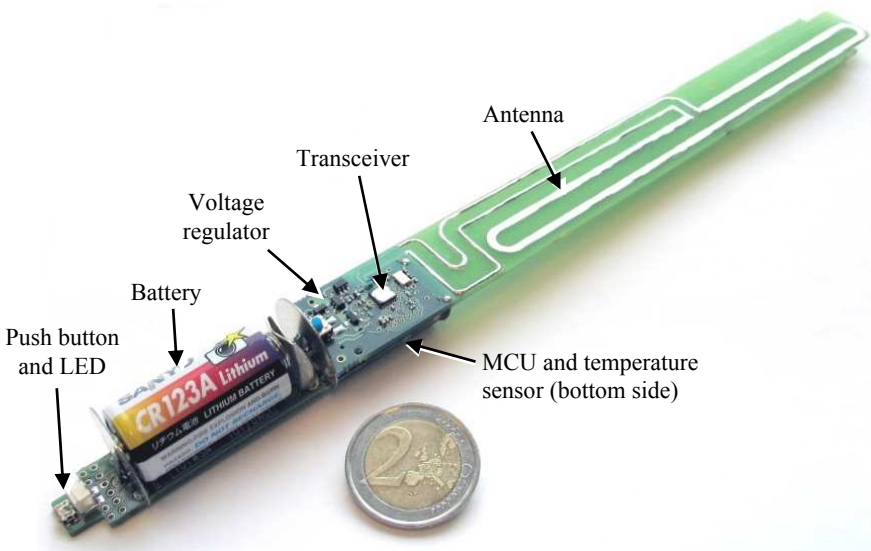

Fig. 37. *TUTWSN long-range node.*

TUTWSN Wrist Node

For indoor localization applications, a platform called TUTWSN wrist node was designed. Since the platform was intended for human localization and access control applications, the design targeted at significantly smaller size than the previous PIC-based platforms. Due to the size constrains, a small ceramic antenna was selected. Since only subnode operation was required, MCU was changed to a smaller PIC18LF2520 [104] model. The node obtained supply power from a CR2450 lithium coin cell battery. Since the coin cell battery can supply only around 100 μA current, a NiMH battery was used as a temporary energy storage supplying high current peaks.

The implemented TUTWSN wrist node is presented in Fig. 38. The PCB is circular shaped having a diameter of 30 mm. The PCB is enclosed in a plastic enclosure presented in the figure. The top side of the board contains the antenna, radio, sensor, push-button and LED. The bottom side contains MCU and a voltage regulator.

Observed problems with the platform were expensive power subsystem and short transmission range.

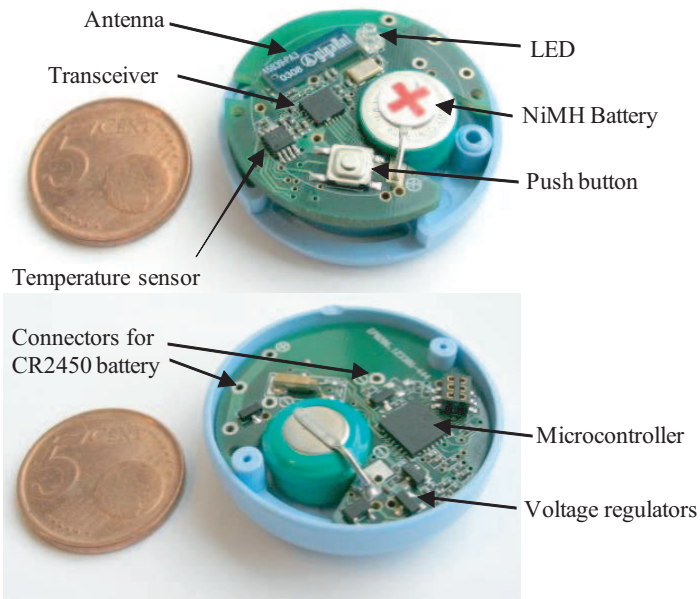

Fig. 38. *Implemented TUTWSN wrist node.*

TUTWSN Badge Node

For reducing the cost of the power subsystem and improving the battery capacity, a variation the TUTWSN watch node called TUTWSN badge node was designed. Larger physical size allowed the use of AAA-type batteries, accelerometer, and a larger PCB antenna having longer range and a nearly omni-directional radiation pattern improving the performance of node localization. The movement of the node could be measured by both signal strength and acceleration measurements. The implemented TUTWSN badge node with a plastic container is presented in Fig. 39.

Multi-Radio Platform

For minimizing routing latency in real-time control applications, a multi-radio platform was developed [P10]. The platform was targeted at a mains-powered backbone node operation, where absolute minimum latency was needed.

For compatibility with other TUTWSN nodes, the multi-radio platform was equipped with nRF2401A [120] radios. Efficient routing of multiple frames simultaneously was enabled by utilizing four parallel radios controlled by an Altera Cyclone EP1C20 [6] Field Programmable Gate-Array (FPGA) circuit. The FPGA has enough gates for four NIOS processor software cores and MAC layer frame forwarding functionality as a hardware accelerator implementation. The complete multi-radio platform is presented in Fig. 40. The platform size is 125 mm $\times$ 112 mm $\times$ 30 mm [P10].

The platform enabled the minimization of routing latency by receiving and transmitting frames simultaneously using different radios. The platform determined the next hop node as soon as the frame header was received after which the frame forwarding

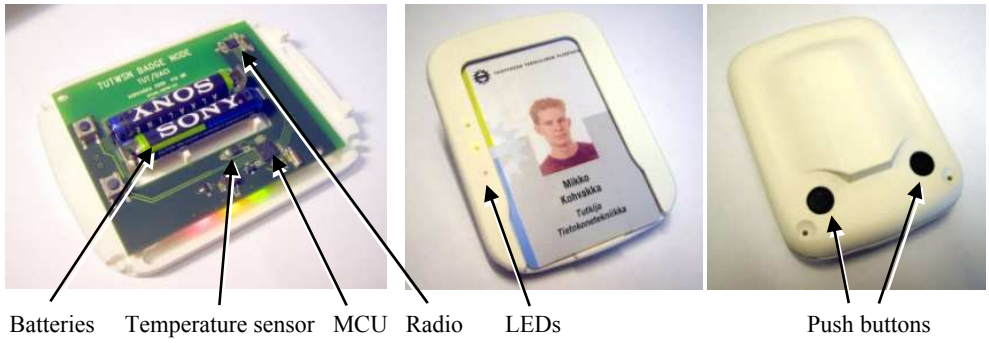

Fig. 39. *TUTWSN badge node for human positioning.*

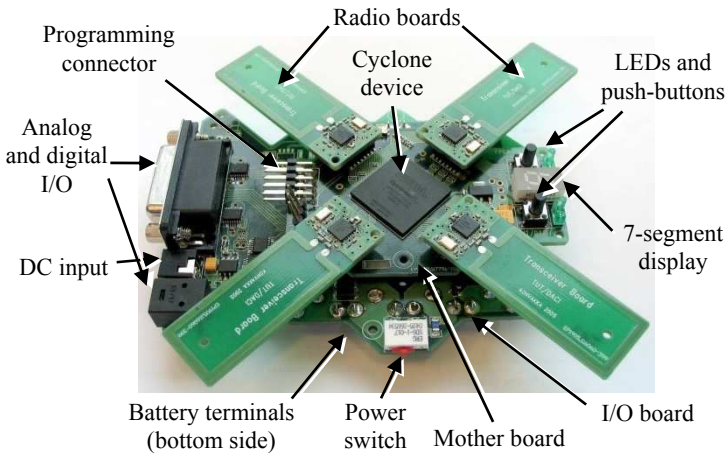

Fig. 40. *Multi-radio platform.*

began instantly. Theoretical minimum routing delay was as low as 106 μs per a hop [P10].

7.1.3 Node Designs in 2006

In 2006, the TUTWSN protocol stack was extended by several new protocols and sensor applications. The utilization of many new features was limited by the constrained memory resources. In addition, new monitoring applications necessitated the integration of new types of sensors in platforms. Thus, new versions of the TUTWSN sensor node platforms were designed. The design targets were cost-effectiveness, improved interfaces for external networks, improved mechanical design, and versatile sensors.

TUTWSN Universal Node

First, a TUTWSN universal node was developed. The previous MCU was replaced with a larger PIC18LF8722 [106] having 128 kB program memory and 4 kB data memory. For allowing larger data buffers and the development of SensorOS operating system on nodes, data memory was extended by an external 128 kB SRAM. Previously used nRF2401A radio was changed to nRF24L01 [121] having up to 2 Mbps data rate with lower active mode power consumption. Antenna was modified for achieving more omni-directional radiation. The node was equipped with acceleration, temperature and illumination sensors. User interface was implemented by push button and two LEDs. In addition, Lantronix XPort [97] was optionally assembled

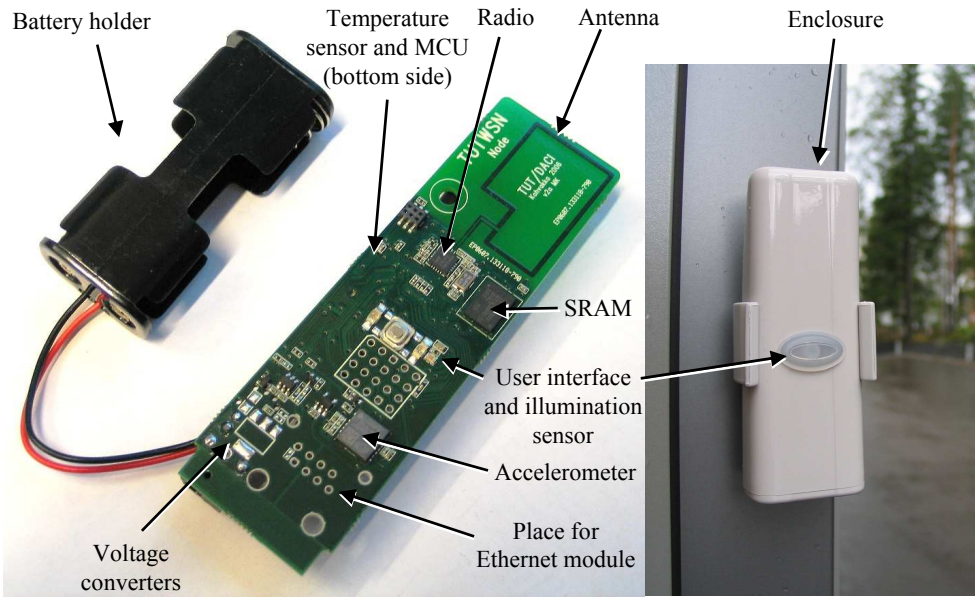

Fig. 41. *TUTWSN universal node and the plastic enclosure.*

for providing Ethernet connectivity. Hence, the node could also operate as a stand-alone sink having Ethernet gateway functionality. In normal operation, the node was powered by two AA-batteries. The utilization of Ethernet necessitates the use of a mains power adapter.

Power subsystem was improved by a two-step dynamic voltage scaling. A higher voltage setting allowed the utilization of a higher clock frequency, while lower voltage setting minimized the sleep mode power consumption. Moreover, the sleep mode power consumption was reduced by a Field-Effect Transistor (FET) circuitry, which switches off the supply voltage of sensors, when they are not used. The appearance and mechanical strength of the node was improved by a designed splash-proof plastic enclosure. The PCB and the plastic enclosure of the TUTWSN universal node are presented in Fig. 41.

TUTWSN Long-Range Universal Node

For improving the applicability of the TUTWSN universal node in environmental monitoring applications, a TUTWSN long-range universal node was designed. The node had similar hardware with the TUTWSN universal node, but the radio was replaced to nRF905 [122]. The radio is similar with the TUTWSN long-range node providing up to multiple kilometers range. The node is presented in Fig. 42.

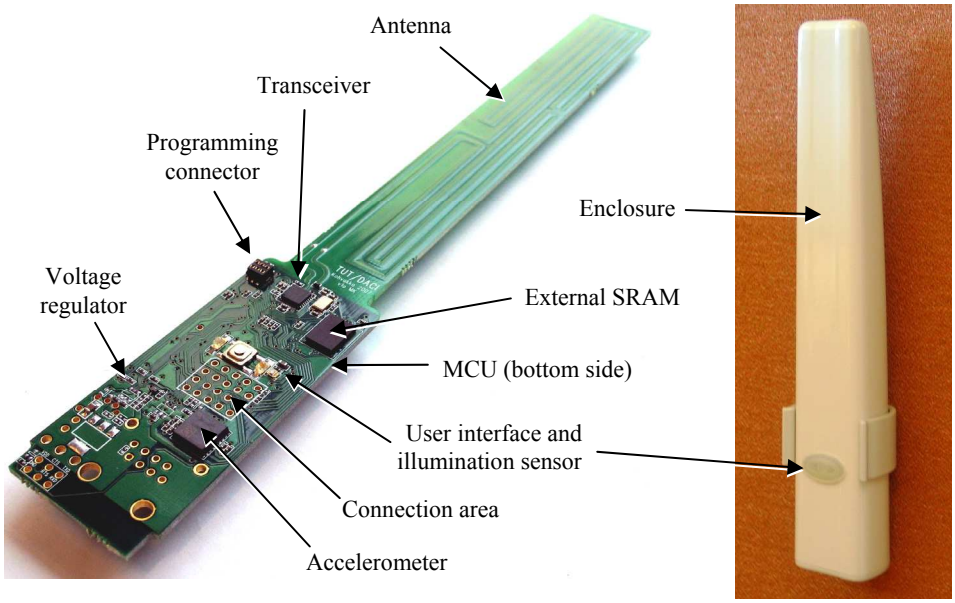

Fig. 42. *TUTWSN long-range universal node.*

Multi-Sensor Node

For extending the sensing capability of nodes, a TUTWSN multi-sensor node was developed. Computing, communication, and power subsystems were similar to the TUTWSN universal node. The sensing subsystem contained sensors for acceleration [204], temperature [42], humidity [167], illumination [12], acoustic (microphone), orientation and magnetic field (compass) [74], image (VGA camera) [148], motion (PIR) [60], and location (GPS) [56]. The TUTWSN multi-sensor node is presented in Fig. 43.

The designed TUTWSN platforms are summarized in Table 13.

7.1.4 Results

This Thesis has presented twelve TUTWSN sensor node platforms, which have been designed according to the requirements of TUTWSN protocols and applications. Along with the evolution of TUTWSN sensor node platforms, their sensing and data processing capabilities have improved, and lifetime increased.

Low power consumption necessitates high energy-efficiency in radio and MCU. Most of the designed TUTWSN platforms utilize low power and high data rate radios re-

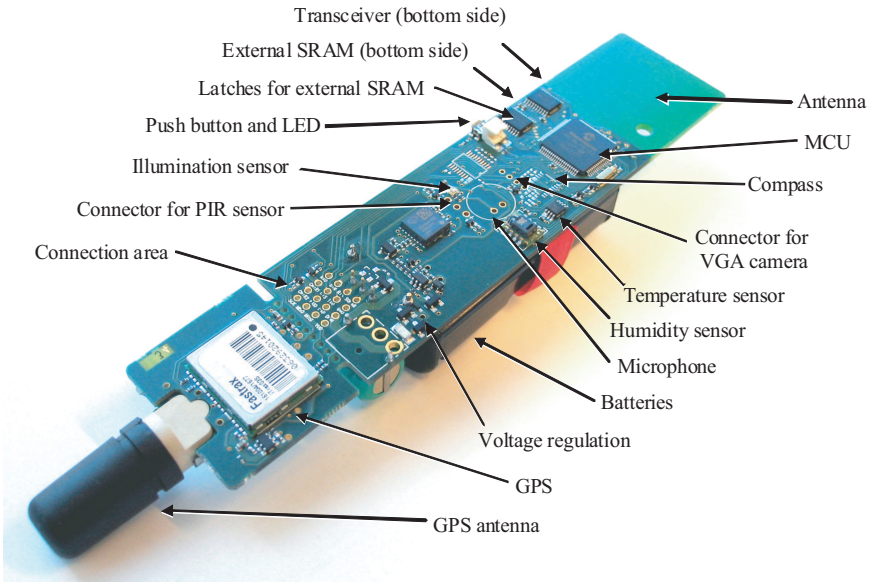

Fig. 43. *TUTWSN multi-sensor node.*

sulting the lowest energy per a transmitted and received bit of data [P7]. Experiments indicate that the energy efficiency of high data rate radios can be exploited only with an accurate (better than 20 ppm) wake-up timer enabling precise link synchronization. In addition, high data rate radios necessitate transmission and reception data buffers in the radio, due to the speed limitations of low power MCUs. The data buffer length determines the maximum frame size. TUTWSN sensor node platforms utilize radios from Nordic Semiconductor having 32 bytes data buffers, which are relatively short for WSN applications. In practice, the buffer size limits the data payload size and the number of reserved slots signaled in beacons. Thus, if a radio having larger data buffers with the same power consumption exists, even higher energy efficiency and data forwarding performance would be achieved.

Experiments also indicate that high scalability necessitates the utilization of radios having a large number of non-interfering channels. Thus, the platforms utilizing narrow band radios in the wide 2.4 GHz frequency band enable the highest scalability. Platforms operating in the narrow 433 MHz frequency band suffer from limited scalability and inter-channel interferences. These platforms are the most suitable for sparse environmental monitoring networks enabling even kilometers long hop lengths.

The platforms prove that it is feasible to perform versatile and low power sensing in small nodes. To maximize energy-efficiency, it is essential to minimize the duty

Table 13. *Summary of TUTWSN sensor node platforms.*

Platform	MCU	Radio	Sensors and Interfaces
TUTWSN node	XE88LC02	nRF2401A	T
TUTWSN position sensor node	XE88LC02	nRF2401A	L
TUTWSN gateway	XE88LC02	nRF2401A	T, RS-232
TUTWSN SoC node	8051	nRF2401A	T
TUTWSN temperature sensor node	PIC18LF4620	nRF2401A	T, RS-232
TUTWSN long-range node	PIC18LF4620	nRF905	T, RS-232
TUTWSN wrist node	PIC18LF2520	nRF2401A	T
TUTWSN badge node	PIC18LF2520	nRF2401A	A, T
Multi-radio platform	4*NIOS	4*nRF2401A	RS-232
TUTWSN universal node	PIC18LF8722	nRF24L01	A, I, T, Eth, RS-232
TUTWSN long-range universal node	PIC18LF8722	nRF905	A, I, T, Eth, RS-232
TUTWSN multi-sensor node	PIC18LF8722	nRF24L01	A, C, G, M, P, T, H, I, IM, RS-232

Abbreviations: acceleration (A), compass (C), GPS (G), humidity (H), illumination (I), image (IM), linear position (L), microphone (M), Passive infra-red (P), temperature (T), Ethernet (Eth)

cycle of sensing. Quantities changing slowly are easy to monitor, for example temperature and humidity. These sensors can be sampled infrequently at intervals of tens of seconds. A reliable and energy-efficient monitoring of rapidly changing quantities is more difficult. Generally, a high frequency sampling of a sensor increases significantly energy consumption. Higher energy-efficiency is achieved by utilizing a low power comparator circuit, which generates an interrupt to MCU, if a predetermined threshold is exceeded. These kind of sensors utilized with TUTWSN are the accelerometer [204] and PIR motion detection sensor [60].

In the newest platform designs, node lifetime has been increased by the two level dynamic voltage scaling. The sleep mode current consumption is minimized by using the lowest possible supply voltage, which is 2.0 V in TUTWSN nodes. Higher, 2.7 V supply voltage is used only on-demand, when the MCU clock frequency is temporarily increased, or when some sensor requires higher voltage, for example the accelerometer [204]. According to measurements, dynamic voltage scaling reduces the sleep mode power consumption around 30% compared to the utilization of a constant 2.7 V voltage. When battery voltage drops below 2.7 V, only the lower supply

voltage is used, and node functionalities requiring 2.7 V are disabled. Thus, batteries can be discharged to around 2.1 V voltage extending node lifetime at least tens of percents [52].

The measured performance of TUTWSN sensor node platforms and protocol stack in real deployments is presented in the next section.

7.2 TUTWSN Deployments

In this section, three TUTWSN deployments are presented. The main objective of the deployments is to prove and demonstrate that the MAC and platform designs, and WSN applications are feasible in practice in real operation conditions. Power consumption measurements during the deployments provide information about the energy consumptions of data processing, sensing, and random synchronization errors, which are difficult to estimate analytically.

The first deployment is a small indoor temperature sensing network, where nodes utilize a simple protocol stack and the basic MAC functionality. The deployment proves that the TUTWSN channel access mechanism and sensor node platforms are feasible, and they can achieve high energy-efficiency in practice.

The second deployment discusses a long-term outdoor environmental monitoring network. The deployment verifies the operation of the designed MAC mechanisms and the TUTWSN long-range nodes in harsh outdoor conditions.

The third deployment is an indoor building monitoring network, where nodes utilize the full TUTWSN protocol stack containing all designed channel access and networking mechanisms. The deployment proves that high energy-efficiency is achieved with the full MAC implementation, with mobile nodes, and with a larger and denser network size than the previous deployments.

The deployments are presented as follows. First, the application is presented shortly. Then, the power analysis of utilized platforms is presented, which is followed by the experimental results of the deployment.

7.2.1 Indoor Temperature Sensing Deployment

Temperature sensing is one of the most straightforward applications for WSNs, and it can be used for example for Heating, Ventilation & Air Conditioning (HVAC) control in building. Compared to wired sensors, the utilization of WSN technology

will reduce cabling and installation costs, and it makes the system easily extendable. The data rate and latency requirements are low, but the required node lifetime should be years [P8].

The indoor temperature sensing deployment [P8] was carried out in 2004. The target of the deployment was to prove that the TUTWSN channel access mechanism with accurate local time synchronization is feasible, and that the high energy-efficiency can be achieved in practice using the designed sensor node platforms. Due to practical reasons, the measured network is rather small containing five TUTWSN nodes, one TUTWSN SoC node, and a TUTWSN gateway. Nodes utilized a simple protocol stack, which consists of the channel access mechanism, path-loss estimation scheme, network channel beaconing mechanism, and simple upper protocol layers. The nodes acquired temperature values at 5 s intervals, and routed data to the TUTWSN gateway. Utilized network beacon interval was fixed to 500 ms [P8].

Power Analysis

The power analysis measures the power consumptions of the main components in different operation modes. In the all presented deployments, power analysis is performed as follows. MCU power consumption is measured in active and sleep modes. The sleep mode, only a wake up timer is active. The ADC and sensor power consumptions are measured in active and shut down (off) modes. The radio power consumption is measured in sleep, reception, and transmission modes with a minimum and maximum transmission power levels. Results are measured using 3 V battery voltage. The results are used in the performance analysis for specifying the power consumption characteristics of the hardware.

The power analysis results of the TUTWSN SoC node and the TUTWSN node are presented in Table 14 [P8]. The sleep mode power consumptions for the platforms are 15 μW and 24 μW. The maximum power consumptions are 66.03 mW and 59.55 mW, which are achieved when all components are in the active mode and the radio is in the receive mode. The radio clearly dominates the momentary power consumption in both platforms, especially in the reception mode. The node power consumption over doubles during reception compared to transmission using the lowest -20 dBm transmission power. The analysis also shows that the 8051 core of the TUTWSN SoC node has 6 times higher power consumption than the CoolRISC core of TUTWSN node [P8].

Table 14. *The power analysis of the TUTWSN node and TUTWSN SoC node.*

MCU mode	ADC mode	Sensor mode	Radio mode	TUTWSN node (mW)	TUTWSN SoC node (mW)
active	active	active	RX	59.55	66.03
active	active	active	TX ($0dBm$)	37.70	44.10
active	active	active	TX ($-20dBm$)	26.60	32.90
active	active	active	sleep	3.04	11.64
active	active	off	sleep	3.01	11.60
active	off	off	sleep	1.69	10.56
sleep	off	off	sleep	0.024	0.015

Experimental Results

First, the functionality and timing accuracy of the MAC design is verified by oscilloscope measurements. The current consumption waveforms of a subnode and a headnode during a superframe are presented in Fig. 44. Transmissions and receptions produce narrow and high current peaks indicating precise time synchronization and very low idle listening. MCU activity is shown after transmissions and receptions as wider and lower current peaks. In the figure, subnode receives network and cluster beacons, transmits a slot reservation request in a contention slot and a data frame in a contention-free slot. After each transmission, the subnode receives ACK. The headnode exchanges data with other nodes resulting activity in the fourth contention slot and second contention-free slot [P8].

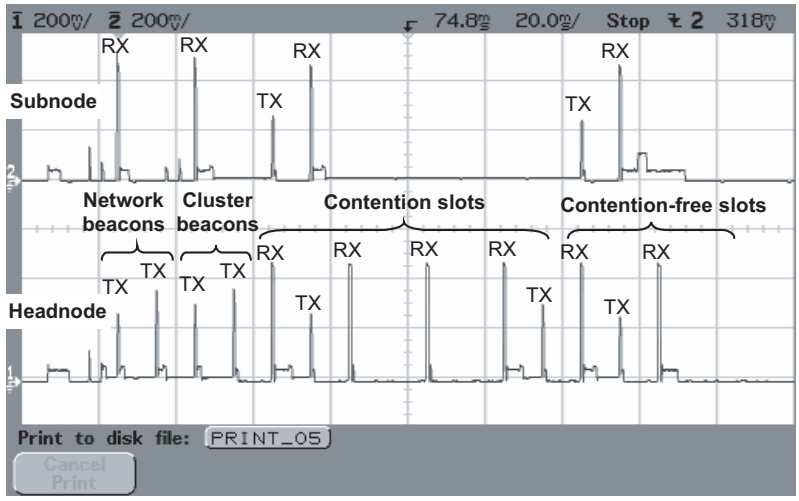

Fig. 44. *Measured current consumption waveforms of a subnode and a headnode during a superframe.*

Table 15. *Measured subnode power consumptions and estimated lifetimes.*

Platform	Average power	Lifetime with CR2450	Lifetime with 2 x AA
TUTWSN node	88.2 μW	879 days	10.1 years
TUTWSN SoC node	10.6 mW	6.6 days	30.5 days
TUTWSN SoC node with power saving (estimated)	80.7 μW	960 days	11.0 years

Then, the power consumptions of the platforms operating as subnodes are measured. The power results with 5 s MAC access cycle length are presented in Table 15 [P8]. The resulted power consumptions of TUTWSN node and TUTWSN SoC node are 88.2 μW and 10.6 mW. The significantly higher power consumption in the SoC node is caused by an inaccurate wake-up timer having inadequate accuracy for timing the channel access mechanism. The clock frequency of the timer varied between 1 kHz and 5 kHz depending on temperature and process variables. However, the calibration of the timer was possible, but a small program memory size prevented its implementation in practice. Thus, sleep mode was not utilized during the measurements. The estimated power consumption with the full power saving would be 80.7 μW [P8].

According to the power consumption results, node lifetimes are estimated with two battery types: a CR2450 lithium coin battery and two serially connected AA alkaline batteries. With the full power saving, the lifetimes of both platforms with the CR2450 are about 900 days, and with the two AA batteries over 10 years. This proves the energy-efficiency of TUTWSN subnodes in practice. The lifetime of the TUTWSN SoC node with the limited power saving is below a month. This clearly shows the importance of sleep mode power consumption and timing accuracy for the achieved power consumption [P8].

Next, the power consumption of a headnode is measured using the TUTWSN node platform. The MAC access cycle length is fixed to 5 s, and the number of associated subnodes is varied from 0 to 4. The results indicate that headnode power consumption increases from 390 μW to 560 μW, as presented in the left side of Fig. 45 [P8]. As the headnode operation is rotated among nodes, the average power consumption of the TUTWSN nodes reduce from 390 μW to 183 μW depending on the number of subnodes [P8].

The right side of Fig. 45 presents the resulted lifetimes using two AA batteries. The calculated lifetime of the headnode is between 2.3 and 1.6 years, depending on the number of subnodes. As the rotation of headnode operation between nodes is applied, the lifetime of nodes is up to 4.9 years, as the number of subnodes is four

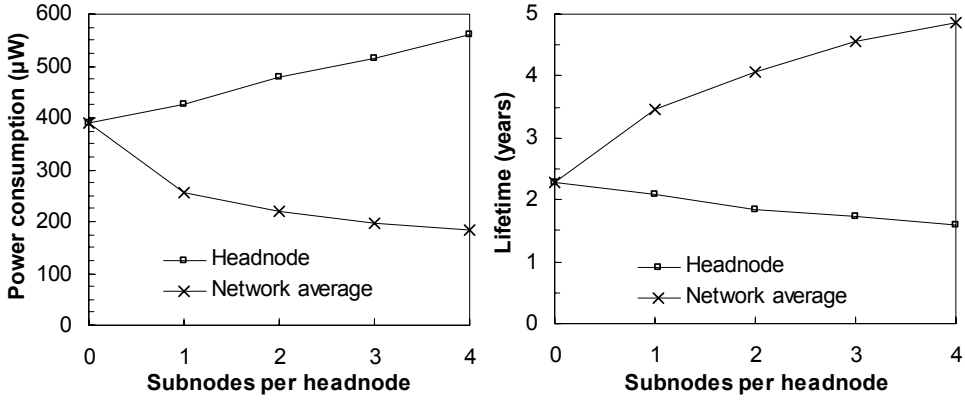

Fig. 45. *Measured power consumptions of TUTWSN nodes.*

times higher than the headnodes. This proves the energy efficiency of TUTWSN headnodes in practice.

The deployment proves that the designed channel access mechanism is functional and feasible in practical implementations. As the drift of a wake-up timer clock source is in the order of 20 parts-per-million (ppm) or less, the energy-efficiency of subnodes and headnodes is very high enabling long-lived WSN applications. Similar power consumption results are also obtained from a linear position sensing deployment performed in 2004 [P9].

7.2.2 Environmental Monitoring Deployment

Environmental monitoring is one of the most potential WSN applications. Such networks can be utilized in hostile environments and in large geographical areas to provide accurate and localized data. By conventional wireless technology, the implementation of such functionality is very expensive and difficult requiring large battery packs and manual network configuration.

The described deployment has been the first large-scale and long-term field test of TUTWSN network. The deployment has been active from autumn 2005 and is still running. A four months time period nearly at the beginning of the deployment has been published in [181]. The objective of the deployment has been to prove that the designed TUTWSN long-range nodes can survive and maintain high energy-efficiency in arctic operation conditions having high temperature variations and moisture levels. In addition, an objective was to prove that the designed path-loss estimation scheme is feasible in harsh outdoor conditions, and that nodes can maintain

adequate link reliability with long hop lengths.

The deployment utilized 20 TUTWSN long-range nodes, which formed a multi-hop network in an area of few square kilometers. One of the nodes was equipped with a RS-232 interface and operated as a sink and a gateway to a computer. The resulted network was very sparse and the distances between nodes were up to 3 km. Nodes utilized a MAC layer utilizing the designed channel access, NCB and path-loss metering mechanisms, and the multi-cluster-tree topology. ENDP was not used. MAC utilized 2 s access cycle length, 500 ms network beacon interval, 4 contention slots and at maximum 8 contention-free slots per a superframe. Upper protocol layers contained a simple multi-hop routing protocol, API, and applications for data gathering and node diagnostics [181].

Power Analysis

The results of a power analysis are presented in Table 16. The sleep mode power consumption is 31 μW. The maximum power consumption is 95.9 mW, which is achieved as all components are in active mode and the nRF905 radio is in transmission mode at 10 dBm transmission power. The power consumption is significantly higher than in nodes having the nRF2401A radio. Also, radio data rate is only 50 kbps, which further increases the energy consumption of exchanged frames. However, expected transmission range is nearly ten times longer than with the nRF2401A radio, which compensates well the higher energy consumption.

Table 16. *The static power consumption of the TUTWSN long-range node.*

MCU mode	ADC mode	Sensor mode	Radio mode	Power (mW)
active	active	active	TX ($10dBm$)	95.9
active	active	active	TX ($6dBm$)	65.9
active	active	active	TX ($-2dBm$)	47.9
active	active	active	TX ($-10dBm$)	32.9
active	active	active	RX	43.3
active	active	active	sleep	5.91
active	active	off	sleep	3.68
active	off	off	sleep	3.17
sleep	off	off	sleep	0.031

Experimental Results

The deployment provided experimental results about the network operation in forested, low temperature outdoor environment. According to the experiments, a forest attenuates radio wave propagation very significantly. Achieved radio range in a forest was below 100 meters, while the longest measured hop lengths were near to 3 km. Also, radio wave propagation was notably affected by snow fall, rain, humidity, temperature, and the frost and snow in trees, ground, and around the nodes. Hence, the quality of radio links altered continuously although the nodes were stationary [181].

The outdoor temperatures during the test period from November 2005 to March 2006 ranged from -31.5 °C to 12.0 °C. High temperature variation reduced significantly the accuracy of crystals and thus, the accuracy of time synchronization. Some nodes were inside buildings and other outdoors resulting in nearly 50 °C difference in the operation temperatures. According to the experiments, the implemented sensor node platforms performed well during the whole test period [181].

Network lifetime with 1600 mAh CR123 batteries was 6 - 8 months. As a comparison, the calculated lifetime using two AA-type batteries per node is around one year. It should be noted that the network traffic consisted not only of temperature measurements but also diagnostics information, which increased load. Lifetime was lower than in the deployments utilizing nRF2401A radios due to the higher power consumption and lower data rate of the radio [181].

7.2.3 Building Monitoring Deployment

The building monitoring deployment has been operating in indoor conditions at Tampere University of Technology premises from the year 2005. The network has been used for demonstrating the TUTWSN technology, for verifying the operation of designed protocols, and for measuring the network performance. The network has been measuring various quantities, for example temperature, humidity, CO_2, motion, acceleration, and illumination [95, 182, 184], [P4].

The presented deployment [95] was carried out in 2006. One of the main objectives of the deployment was to prove that the ENDP scheme and multi-cluster-tree topology are energy-efficient and feasible in practice. The deployment was also used for measuring the energy consumption of link failures and neighbor discovery operations, and to evaluate the effect of node mobility on them.

The deployment utilized up to 28 TUTWSN temperature sensor nodes, which mea-

sured temperature values at 30 s intervals. Ten of the nodes were equipped with a PIR motion detection sensor. The platforms are executing the TUTWSN protocol stack containing the full MAC layer design, an interest-based routing protocol, API, and applications for sensing and self-diagnostics [182]. Utilized access cycle length and network beacon interval were 2 s and 500 ms [95].

Power Analysis

The results of a power analysis are presented in Table 17. The sleep mode power consumption is 37 μW. The power consumption at transmission mode is between 29.57 mW and 42.17 mW, as the transmission power level ranges from -20 dBm to 0 dBm. The maximum power of 60.17 mW is consumed as MCU is active and radio is in the reception mode.

Experimental Measurements

The deployment provided two main results: the power consumption of a stationary network, and the performance of the ENDP scheme in a mobile network.

The power consumptions of various subnodes and headnodes were measured in a stationary network, where headnodes routed data to a sink using several parallel routes. The routes were changing dynamically for adapting to varying RF propagation conditions and for balancing energy consumptions between nodes. ENDP was not used and the number of maintained synchronized links (k) was fixed to 2. The average power consumptions of subnodes and headnodes were 257 μW and 693 μW [95].

The results are 134 μW and 300 μW higher than in the MAC layer performance analysis. The difference is mostly caused by the energy consumptions of data processing,

Table 17. *The static power consumption of the TUTWSN temperature sensor node.*

MCU mode	Radio mode	Power (mW)
active	RX	60.17
active	TX ($0dBm$)	42.17
active	TX ($-6dBm$)	34.67
active	TX ($-12dBm$)	31.37
active	TX ($-20dBm$)	29.57
active	idle	3.29
active	sleep	3.17
sleep	sleep	0.037

sensor sampling, and the frame exchanges caused by the routing layer, which are ignored in the analysis. In addition, the implementation is not fully optimized. Utilized time margins for reception are longer than the optimal margins utilized in the analysis. By noticing the non-ideal implementation, the obtained experimental measurements are analogous with the analytical results, and the energy-efficiency of the MAC layer design is verified.

The performance of ENDP was measured in a network containing eight stationary headnodes and one mobile subnode [P4]. During the measurements, k was varied from 2 to 4. The mobile node transmitted a 32 byte diagnostics data frame on a contention-free time slot at 8 s intervals. In addition, control frames for association and slot reservation were transmitted after communication link changes. Three mobility levels were utilized: 0 m/s, 1 m/s, and 3 m/s [P4].

The measured power consumption are presented in Fig. 46. Without ENDP, the power consumptions at 0 m/s, 1 m/s and 3 m/s mobility levels were 326 μW, 2.18 mW and 4.76 mW. As ENDP was utilized, the power consumptions with an optimal k value were 627 μW ($k = 2$), 933 μW ($k = 3$), and 968 μW ($k = 3$). Thus, the achieved energy saving is 57% - 80% compared to the situation without ENDP. At higher values of k, the energy consumption of maintained synchronized links increases, which reduces the achieved energy-efficiency. At lower values of k, the probability of finding a suitable neighbor using SDUs decreases increasing the energy consumption of network scans [P4].

The measured power consumption is higher than the analysis results presented in the Chapter 5. This is caused by the energy consumptions of data processing and the synchronization inaccuracy of a protocol implementation. In addition, the operation

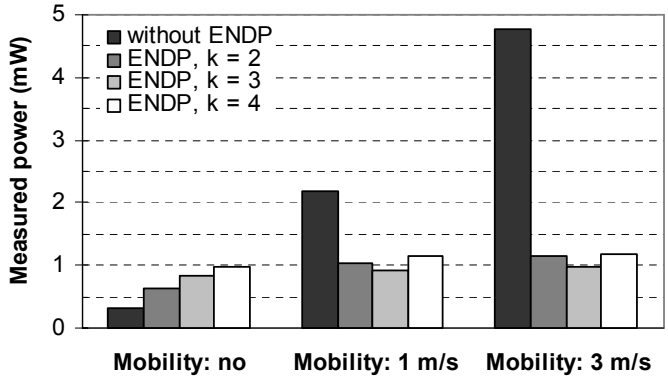

Fig. 46. *Measured power consumption with and without ENDP at three levels of mobility.*

environment had significant fluctuation in the radio link quality depending on node position due to shadowing and multi-path propagation. Thus, the actual link failure rate was much higher than in the analysis. However, the results prove that ENDP improves significantly the energy-efficiency of mobile nodes. ENDP can be used with IEEE 802.15.4, TUTWSN MAC and other synchronized low duty-cycle MAC protocols having regular beacon transmissions [P4].

8. SUMMARY OF PUBLICATIONS

The publications of this Thesis are based on the work of the author during years between 2003 and 2007. This chapter summarizes the contents of the publications and clarifies the contribution of the author. The co-authors have seen and agree with the descriptions. None of the publications have previously been used as a part of a doctoral thesis.

The publications can be divided into three main groups. The publications [P1] - [P4] propose protocols and energy-efficient mechanisms for WSNs. The publications [P5], [P6] cover the performance analysis and optimizations of existing protocols. The publications [P7] - [P10] discuss the implementation of hardware prototypes and real application deployments.

Publication [P1] is a book chapter presenting a summary of TUTWSN MAC layer design. Sections 13.1 - 13.3. present the channel access mechanism, network topology formation and superframe interlacing, which are previously unpublished material. Sections 13.4 - 13.8. present the energy-efficient neighbor discovery protocol, the path-loss estimation scheme and the measured power consumption of TUTWSN MAC, which have been reproduced from the publications [P2], [P4], [P5], [P9], and [183].

The author has been the main architect of the TUTWSM MAC layer, and he has specialized in energy-efficiency. The publication was mainly written by the author. Jukka Suhonen reproduced the section 13.5 from publication [183]. Mauri Kuorilehto gave important ideas for the MAC design and revised the draft version of the publication. Prof. Marko Hännikäinen and Prof. Timo D. Hämäläinen have supervised the work, outlined the functional requirements, and revised the draft version of the publication.

Publication [P2] presents the path-loss estimation scheme, which allows signal strength measurements using simple radios without RSSI functionality. The performance of the scheme is experimentally verified by indoor and outdoor measurements. In addition, performance analysis indicates very low energy-overhead of the scheme, and a

significant energy saving in ZigBee by replacing an IEEE 802.15.4 compliant radio by a simpler one.

The author designed the path-loss estimation scheme, as well as designed and implemented hardware platforms. In addition, the author developed the performance models, performed the performance analysis, and experimental performance measurements. The publication was written by the author. Jukka Suhonen implemented by scheme in software and gave ideas for optimizing the performance. Prof. Marko Hännikäinen and Prof. Timo D. Hämäläinen gave ideas for the mechanism and revised the draft version of the publication.

Publication [P3] proposes the use of the network channel beaconing scheme in ZigBee. The publication presents an introduction on ZigBee protocol stack and neighbor discovery operation, and implementation guidelines for the network channel beaconing scheme. The performance of the scheme is proven by a performance analysis and simulations. In addition, an optimal network beacon rate has been determined as the function of node mobility and cluster size.

The author designed the network channel beaconing scheme, as well as performed the performance analysis and optimizations. The publication was written by the author, except the Section 7. Jukka Suhonen performed the simulations by NS-2 and wrote the Section 7 presenting the simulation results. In addition, Mauri Kuorilehto, Prof. Marko Hännikäinen and Prof. Timo D. Hämäläinen gave ideas for the mechanism and revised the draft version of the publication.

Publication [P4] presents the energy-efficient neighbor discovery protocol for mobile WSNs. The publication presents the mechanism for proactive distribution of neighbor information and a neighbor discovery algorithm for using the distributed information for neighbor discovery. The performance of the protocol is proven by performance analysis and experimental measurements.

The author has been the main architect of the energy-efficient neighbor discovery protocol. He designed the mechanisms for distributing and utilizing neighbor information in network, performed performance analysis and optimizations, designed and implemented hardware prototypes, and performed experimental measurements. Jukka Suhonen improved the utilization of the neighbor information by designing a neighbor discovery algorithm, and wrote the software with the help of Ville Kaseva. The main parts of publication were written by the author. Jukka Suhonen wrote the Subsection 3.2 presenting the pseudocode of the algorithm. Mauri Kuorilehto, Prof. Marko Hännikäinen and Prof. Timo D. Hämäläinen gave ideas for the protocol and revised the draft version of the publication.

Publication [P5] presents the optimization of beacon transmission rate for reducing energy consumption in synchronized low-duty cycle MAC protocols. The publication divides the energy consumption of a WSN node in a node start-up, data exchange and network maintenance energies, and then focuses on minimizing the network maintenance energy. It has been shown that the network maintenance power is a sum of beacon exchange and network scanning powers, and an optimal network beacon rate is a function of average link failure interval, and radio power consumption.

The author determined the performance models and analysis for beacon rate optimization, as well as designed and implemented the reference hardware platform. The publication was written by the author. Prof. Marko Hännikäinen and Prof. Timo D. Hämäläinen gave ideas for the protocol and revised the draft version of the publication.

Publication [P6] presents a performance analysis of ZigBee in a large-scale wireless sensor network application. The analysis focuses on a cluster-tree network topology and beacon-enabled mode. Analysis includes models for a hardware platform, channel access mechanism, and contention. As results, average power consumptions, goodputs and energy-efficiencies are obtained with various MAC parameter values. Analysis results are validated by simulations.

The author determined the performance models and performed the performance analysis. The publication was written by the author, except Section 7. Mauri Kuorilehto performed simulations and wrote the Section 7 presenting the simulation results. Prof. Marko Hännikäinen and Prof. Timo D. Hämäläinen gave ideas for the analysis and revised the draft version of the publication.

Publication [P7] presents a study and analysis of energy-efficient components for WSN node platforms. In addition, photovoltaics and magnetic coupling based energy scavenging mechanisms are experimentally measured. According to the study, a WSN node prototype is implemented using partly evaluation boards of component manufacturers. In addition, a random access communication protocol and a simple sensing application has been implemented for demonstrating the performance of the prototype.

The author performed the study, analysis, and measurements. In addition, the author designed and implemented the WSN node prototype and the software. The publication was written by the author. Prof. Marko Hännikäinen and Prof. Timo D. Hämäläinen gave ideas for the publication and revised the draft version of the publication.

Publication [P8] presents the design and implementation of an ultra low energy WSN

for in-building temperature sensing. The publication contains the design, implementation and performance measurements of two prototypes: TUTWSN node, and TUTWSN SoC prototype. The presented WSN executes a simple TUTWSN protocol stack containing the MAC layer, a multi-hop routing with a fixed stationary routing tree, and a simple sensing application. Results indicate nearly 5 years network lifetime for TUTWSN nodes, when each node is powered by two AA-type batteries. Moreover, TUTWSN SoC prototype is around the size of a 5 cents coin, but inaccurate wake-up timer limits severely its energy-efficiency.

The author performed the design and implementation of the prototypes. In addition, the author designed the simple protocol stack utilized in the prototypes. Moreover, the author performed the performance measurements and analysis. The publication was written by the author. Prof. Marko Hännikäinen and Prof. Timo D. Hämäläinen gave ideas for the prototypes and revised the draft version of the publication.

Publication [P9] presents the design and implementation of a WSN for industrial linear position sensing application. The design and implementation of position sensing prototype and TUTWSN gateway having RS-232 interface are presented. The implemented network executes the same simple TUTWSN protocol stack than in [P8]. Results indicate very high energy-efficiency, but the small capacity of used rechargeable battery limits network lifetime to around 2 months.

The author designed and implemented the prototypes. In addition, the author designed the protocol stack utilized in the prototypes, and performed the performance measurements and analysis. The publication was written by the author. Prof. Marko Hännikäinen and Prof. Timo D. Hämäläinen gave ideas for the prototypes and revised the draft version of the publication.

Publication [P10] presents the design and implementation of a high-performance multi-radio platform. The publication focuses on hardware design covering electronics design and a multi-processor design in FPGA. For demonstrating the applicability of the platform, two reference applications are presented, which are targeting to minimize routing latency, and to maximize routing throughput.

The author designed and implemented the electronics of the prototype. In addition, the author designed and analyzed the reference applications. Tero Arpinen designed and implemented the multi-processor design in the FPGA. The main parts of the publication was written by the author. Tero Arpinen wrote the Section 3 presenting the multi-processor architecture. Prof. Marko Hännikäinen and Prof. Timo D. Hämäläinen gave ideas for the prototype design and revised the draft version of the publication.

9. CONCLUSIONS

The emerging of low-energy WSNs has been possible by the recent advances in low-power communication and computing circuits. Still, the power consumption of hardware is too high for long-lived WSN applications without energy-efficient communication protocols and applications. The main research problem is the combination of a scalable and adaptive multi-hop networking with constrained hardware resources and scarce energy budget.

This Thesis has presented a survey of existing energy-efficient MAC protocols and standards. It was shown that none of existing MAC protocols fulfilled adequately the energy-efficiency, scalability, and adaptivity requirements of low-energy WSNs. This motivated the design of a new MAC layer called TUTWSN MAC concentrating on channel access and networking mechanisms. The main focus has been on ultra-low duty cycle frame exchanges, scalable network self-configuration, and energy-efficient neighbor discovery mechanisms improving adaptivity against network dynamics.

The second outcome of this Thesis has been sensor node platforms. The development of low-power platforms has been vital for measuring, validating, and demonstrating the designed communication protocols in real operation conditions. A survey of low-power hardware components and sensor node platforms revealed the potential to design lower energy platforms than existing ones. This motivated the design of twelve TUTWSN sensor node platforms, which were emerged together with the TUTWSN protocol stack and applications. The performance measurements of the platforms were used for developing and optimizing MAC layer mechanisms.

The third outcome of this Thesis has been performance models and analysis. Performance models have been presented for the state-of-the-art channel access mechanisms and their energy-efficiencies have been compared against TUTWSN MAC.

The results of this Thesis enable the implementation of multi-hop WSNs in harsh and dynamic operation conditions with years of lifetime using current low-cost components. In the MAC layer, the results have been achieved by minimizing idle listening, overhearing, collisions, and control traffic overhead. In sensor node platforms, the

results have been achieved by using transceivers having high data-rate and several non-interfering channels, and hardware components having low sleep mode power consumption and accurate wake-up timers. The performance analysis and comparison to existing proposals and standards have shown that TUTWSN MAC achieves the highest energy-efficiency in both router and leaf nodes. Compared to the theoretically ideal MAC, the energy consumption of TUTWSN MAC is only 2.85% - 27.1% higher, depending on traffic load, radio, and node type. IEEE 802.15.4 performs the second best resulting in 2.92% to 229% energy overhead compared to the ideal MAC. It has been shown that TUTWSN can maintain high energy-efficiency also in dynamic networks. The long-term deployments with the platforms have validated the feasibility of the MAC layer and platform designs in real operation environment.

The presented MAC layer mechanisms are presented and analyzed clearly and separately on each other, and they can be utilized with other MAC layer designs, and sensor node platforms. The developed sensor node platforms present a good low-power hardware design and they are applicable for experimenting other applications and protocols. The performance models can determine the energy consumption of channel access mechanisms simply, clearly, and accurately, and they can be easily adapted to other hardware, protocols, and applications.

Although the absolute energy consumption of low-power components constantly reduces, it can be assumed that the operation principles will not change dramatically. Thus, the principles and results of this Thesis are valid also in future, while it is expected that the power consumption, physical size, and cost of implementations will reduce.

[1] Advanced Analogic Technologies, Inc., "Product datasheet AAT1112 - 1.5A, 1.4MHz step-down converter," Available: http://www.analogictech.com/products/digitalfiles/AAT1112.pdf, 2007.

[2] S. Agarwal, R. Katz, S. Krishnamurthy, and S. Dao, "Distributed power control in ad hoc wireless networks," in *Proc. 12th IEEE International Symposium on Personal, Indoor and Mobile Radio Communications (PIMRC'01)*, vol. 2, San Diego, CA, USA, September 30 - October 3 2001, pp. 59–66.

[3] I. F. Akyildiz and I. H. Kasimoglu, "Wireless sensor and actor networks: Research challenges," *Elsevier Ad Hoc Networks*, vol. 2, no. 4, pp. 351–367, October 2004.

[4] I. F. Akyildiz, W. Su, Y. Sankarasubramaniam, and E. Cayirci, "A survey on sensor networks," *IEEE Communications Magazine*, vol. 40, no. 8, pp. 102–114, August 2002.

[5] ——, "Wireless sensor networks: a survey," *Elsevier Computer Networks*, vol. 38, no. 4, pp. 393–422, March 2002.

[6] Altera, Corp., "Section I. cyclone FPGA family data sheet," Available: http://www.altera.com/literature/hb/cyc/cyc_c5v1_01.pdf, 2007.

[7] J. Ammer and J. Rabaey, "Low power synchronization for wireless sensor network modems," in *Proc. IEEE Wireless Communications and Networking Conference (WCNC'05)*, vol. 2, New Orleans, LA, USA, March 13-17 2005, pp. 670–675.

[8] D. K. Arvind and K. J. Wong, "Speckled computing: Disruptive technology for networked information appliances," in *Proc. IEEE Int'l Symposium on Consumer Electronics (ISCE'04)*, Reading, UK, September 2004, pp. 334–338.

[9] Atmel, Corp., "8-bit AVR microcontroller with 128K bytes in-system programmable flash," Available: http://www.atmel.com/dyn/resources/prod_documents/0945s.pdf, 2001.

[10] ——, "AT91 ARM Thumb microcontrollers AT91FR40162S," Available: http://www.atmel.com/dyn/resources/prod_documents/doc6174.pdf, 2005.

[11] ——, "8-bit flash microcontroller AT89C51RE2," Available: http://www.atmel.com/dyn/resources/prod_documents/doc7663.pdf, 2007.

[12] Avago Technologies, Ltd., "Data sheet - APDS-9002 miniature surface mount ambient light photo diode," Available: http://www.avagotech.com/, 2006.

[13] G. Barrenetxea, F. Ingelrest, G. Schaefer, and M. Vetterli, "Wireless sensor networks for environmental monitoring: the SensorScope experience," in *Proc. IEEE International Zurich Seminar on Communications*, Zurich, Switzerland, March 12-14 2007, pp. 98–101.

[14] M. A. Batalin, M. Rahimi, Y. Yu, D. Liu, A. Kansal, G. S. Sukhatme, W. J. Kaiser, M. Hansen, G. J. Pottie, M. Srivastava, and D. Estrin, "Call and response: experiments in sampling the environment," in *Proc. 2nd Int'l Conf. on Embedded Networked Sensor Systems (SenSys'04)*, Baltimore, MD, USA, November 3–5 2004, pp. 25–38.

[15] M. Baunach, R. Kolla, and C. Mühlberger, "Beyond theory: Development of a real world localization application as low power wsn," in *Proc. 32nd IEEE Conference on Local Computer Networks (LCN'07)*, Dublin, Ireland, October 15–18 2007, pp. 872–884.

[16] R. Beckwith, D. Teibel, and P. Bowen, "Report from the field: Results from an agricultural wireless sensor network," in *Proc. 29th Annual IEEE Int'l Conf. on Local Computer Networks (LCN'04)*, Tampa, FL, USA, November 16–18 2004, pp. 471–478.

[17] L. Benini, A. Bogliolo, and G. D. Micheli, "A survey of design techniques for system-level dynamic power management," *IEEE Transactions on Very Large Scale Integration Systems*, vol. 8, no. 3, pp. 299–316, June 2004.

[18] J. Beutel, M. Dyer, M. Hinz, L. Meier, and M. Ringwald, "Next-generation prototyping of sensor networks," in *Proc. 2nd Internation Conf. on Embedded Networked Sensor Systems (SenSys'04).* Baltimore, MD, USA: ACM Press, November 2004, pp. 291–292.

[19] I. Bluetooth SIG, "Bluetooth low energy technology," Available: http://www.bluetooth.com/Bluetooth/Products/Low_Energy.htm, 2008.

[20] *Specification of the Bluetooth System*, Bluetooth Special Interest Group (SIG) Std. 2.0 + EDR, 2004.

[21] B. Bougard, F. Catthoor, D. Daly, A. Chandrakasan, and W. Dehaene, "Energy efficiency of the IEEE 802.15.4 standard in dense wireless microsensor networks: modeling and improvement perspectives," in *Proc. Design, Automation*

and Test in Europe (DATE'05), vol. 1, Munich, Germany, March 7-11 2005, pp. 196–201.

[22] T. Bourke, "ISA100.11a completely obviates the need for WirelessHART," *Measurement and Testing*, vol. 1, no. 1, pp. 18–19, October 2007.

[23] BTnode project @ ETH Zurich, "BTnode rev3 hardware reference," Available: http://www.btnode.ethz.ch/Documentation/BTnodeRev3HardwareReference/, 2007.

[24] M. Buettner, G. Yee, E. Anderson, and R. Han, "X-MAC: A short preamble MAC protocol for duty-cycled wireless sensor networks," in *Proc. 4th ACM Conf. Embedded Networked Sensor Systems (SenSys'06)*, Boulder, Colorado, USA, October 31 – November 3 2006, pp. 307–320.

[25] K. Bult, A. Burstein, D. Chang, M. Dong, M. Fielding, E. Kruglick, J. Ho, F. Lin, T. Lin, W. Kaiser, H. Marcy, R. Mukai, P. Nelson, F. Newburg, K. Pister, G. Pottie, H. Sanchez, K. Sohrabi, O. S. amd K.B. Tan, G. Yung, S. Xue, and J. Yao, "Low power systems for wireless microsensors," in *Proc. International Symposium on Low Power Electronics and Design (ISLPED'96)*, Monterey, CA, USA, August 12–14 1996, pp. 17–21.

[26] P. Buonadonna, D. Gay, J. Hellerstein, W. Hong, and S. Madden, "TASK: Sensor network in a box," in *Proc. 2nd IEEE European Workshop on Wireless Sensor Networks (EWSN'05)*, Istanbul, Turkey, January 31 - February 2 2005, pp. 133–144.

[27] X. Carcelle, T. Dang, and C. Devic, "Industrial wireless technologies: applications for the electrical utilities," in *Proc. IEEE International Conference on Industrial Informatics (INDIN'06)*, Singapore, August 16-18 2007, pp. 108–113.

[28] A. Chandrakasan, R. Min, M. Bhardwaj, S.-H. Cho, and A. Wang, "Power-aware wireless microsensor systems," in *Proc. 28th European Solid-State Circuits Conference (ESSCIRC'02)*, Firenze, Italy, September 24-26 2002, pp. 47–54.

[29] G. Chavira, S. Nava, R. Hervas, J. Bravojose, and C. Sanchez, "Combining rfid and nfc technologies in an ami conference scenario," in *Proc. 8th Mexican International Conference on Current Trends in Computer Science (ENC'07)*, Morelia, Mexico, September 24-28 2007, pp. 165–172.

[30] I. Chlamtac, A. Farago, A. Myers, V. Syrotiuk, and G. Zaruba, "Adapt: A dynamically self-adjusting media access control protocol for ad hoc networks," in *Proc. IEEE Global Telecommunications Conference (GLOBECOM'99)*, vol. 1A, Rio de Janeiro, Brazil, December 5-9 1999, pp. 11–15.

[31] C. Y. Chong, S. Mori, and K. C. Chang, "Distributed multitarget multisensor tracking," in *Multitarget Multisensor Tracking: Advanced Applications*, Y. Bar-Shalom, Ed. Norwood, MA: Artech House, 1990, vol. 1, pp. 247–295.

[32] C.-Y. Chong and S. P. Kumar, "Sensor networks: Evolution, opportunities, and challenges," *Proceedings of the IEEE*, vol. 91, no. 8, pp. 1247–1256, August 2003.

[33] A. Colvin, "CSMA with collision avoidance," *Computer Communications*, vol. 6, no. 5, pp. 227–235, October 1983.

[34] Crossbow Technology, Inc., "MICAz wireless measurement system," Available: xbow.com/Products/Product_pdf_files/Wireless_pdf/6020-0060-01_A_MICAz.pdf, 2004.

[35] ——, "Stargate X-Scale processor platform," Available: http://www.xbow.com/Products/Product_pdf_files/Wireless_pdf/6020-0049-01_B_STARGATE.pdf, 2004.

[36] ——, "2007 wireless sensor networks product reference guide," Available: http://www.xbow.com/Products/Product_pdf_files/Wireless_pdf/Wireless_Catalog_2006.zip, 2007.

[37] ——, "MICA2 wireless measurement system," Available: http://www.xbow.com/Products/Product_pdf_files/Wireless_pdf/MICA2_Datasheet.pdf, 2007.

[38] ——, "MICA2DOT wireless microsensor mote," Available: www.xbow.com/Products/Product_pdf_files/Wireless_pdf/MICA2DOT_Datasheet.pdf, 2007.

[39] K. Crowley, J. Frisby, S. Murphy, M. Roantree, and D. Diamond, "Web-based real-time temperature monitoring of shellfish catches using a wireless sensor network," *Sensors and Actuators A: Physical*, vol. 122, no. 2, pp. 222–230, August 2005.

[40] D. Culler, D. Estrin, and M. Srivastava, "Guest editors' introduction: Overview of sensor networks," *Computer*, vol. 37, no. 8, pp. 41–49, August 2004.

[41] C. Cypress Semiconductor, "PSoC mixed-signal array final data sheet," Available: http://download.cypress.com.edgesuite.net/design_resources/datasheets/contents/cy8c29666_8.pdf, 2007.

[42] Dallas Semiconductor, Inc., "DS620 low-voltage ±0.5 °c accuracy digital thermometer and thermostat," Available: http://datasheets.maxim-ic.com/en/ds/DS620.pdf, 2008.

[43] E. J. Davison and N. K. Tripathi, "The optimal decentralized control of a large power system: Load and frequency control," *IEEE Trans. Automatic Control*, vol. 23, no. 2, pp. 312–325, April 1978.

[44] J. Deng, Y. S. Han, P.-N. Chen, and P. K. Varshney, "Optimal transmission range for wireless ad hoc networks based on energy efficiency," *IEEE Transactions on Communications*, vol. 55, no. 9, pp. 1772–1782, September 2007.

[45] A. Deshpande, C. Guestrin, and S. Madden, "Resource-aware wireless sensor-actuator networks," *Data Engineering Bulletin*, vol. 28, no. 1, pp. 40–47, March 2005.

[46] L. Doherty, B. Warneke, B. Boser, and K. Pister, "Energy and performance considerations for smart dust," *Int'l Journal of Parallel and Distributed Systems and Networks*, vol. 4, no. 3, pp. 121–133, December 2001.

[47] H. Dubois-Ferriere, R. Meier, L. Fabre, and P. Metrailler, "Tinynode: A comprehensive platform for wireless sensor network applications," in *Proc. 5th International Symposium on Information Processing in Sensor Networks (IPSN'06)*, Nashville, TN, USA, April 2006, pp. 358–365.

[48] Dust Networks, Inc., "SmartMesh-XR evaulation kit," Available: http://www.dustnetworks.com/docs/Evaluation_Kit.pdf, 2005.

[49] Dynastream Innovations, Inc., "ANT message protocol and usage," Available: http://www.nordicsemi.com/files/Product/data_sheet/User_guide_ANT.pdf, 2007.

[50] ——, "User manual development kit ANTDKT3," Available: http://www.thisisant.com/, 2008.

[51] A. El-Hoiydi, J.-D. Decotignie, and J. Hernandez, "Low power MAC protocols for infrastructure wireless sensor networks," in *Proc. 5th European Wireless Conf. (EW'04)*, Barcelona, Spain, February 2004.

[52] Energizer Holdings, Inc., "Energizer e91 product data sheet," Available: http://data.energizer.com/PDFs/E91.pdf, 2008.

[53] C. Enz, N. Scolari, and U. Yodprasit, "Ultra low-power radio design for wireless sensor networks," in *Proc. IEEE Int. Workshop on Radio-Frequency Integration Technology (RFIT'05)*, Singapore, November 30 - December 02 2005, pp. 1–17.

[54] C. C. Enz, A. El-Hoiydi, J.-D. Decotignie, and V. Peiris, "WiseNET: An ultralow-power wireless sensor network solution," *Computer*, vol. 37, no. 8, pp. 62–70, August 2004.

[55] C. Evans-Pughe, "Bzzzz zzz [zigbee wireless standard]," *IEE Review*, vol. 49, no. 3, pp. 28–31, March 2003.

[56] Fastrax Oy, "iTrax MP family - OEM GPS receiver modules," Available: http://www.fastraxgps.com/, 2007.

[57] D. Flowers and Y. Yang, "AN1066 - MiWi wireless networking protocol stack," Available: http://ww1.microchip.com/downloads/en/AppNotes/01066a.pdf, 2007.

[58] T. C. Forum, "An open-source OS for the networked sensor regime," Available: http://www.tinyos.net, 2004.

[59] Freescale Semiconductor, Inc., "Data sheet M68HC08 microcontrollers," Available: http://www.freescale.com/files/microcontrollers/doc/data_sheet/MC68HC908AP64.pdf, 2005.

[60] Fuji & CO. (Piezo Science), "MS300-series - PIR module with lens," Available: http://www.fuji-piezo.com/ms300.htm, 2006.

[61] Gang Lu, B. Krishnamachari, and C. S. Raghavendra, "An adaptive energy-efficient and low-latency MAC for data gathering in wireless sensor networks," in *Proc. Parallel and Distributed Processing Symposium (IPDPS'04)*, April 2004, pp. 224–231.

[62] Q. Gaoa, K. Blowa, D. Holdinga, I. Marshallb, and X. Penga, "Radio range adjustment for energy efficient wireless sensor networks," *Ad Hoc Networks*, vol. 4, no. 1, pp. 75–82, January 2006.

[63] C. Guo, L. Zhong, and J. Rabaey, "Low power distributed MAC for ad hoc sensor radio networks," in *Global Telecommunications Conf. (GLOBECOM'01)*, vol. 5, San Antonio, TX, USA, November 2001, pp. 2944–2948.

[64] J. A. Gutierrez, E. H. C. Jr, and R. L. Jr, *Low-Rate Wireless Personal Area Networks: Enabling Wireless Sensors with IEEE 802.15.4*. IEEE Press, 2004, vol. 1.

[65] M. Haenggi, *Handbook of Sensor Networks: Compact Wireless and Wired Sensing Systems*, 1st ed., M. Ilyas and I. Mahgoub, Eds. CRC Press, Florida, 2004.

[66] J. K. Hart and K. Martinez, "Environmental sensor networks: A revolution in the earth system science?" *Earth-Science Reviews*, vol. 78, no. 3-4, pp. 177–191, October 2006.

[67] HART Communication Foundation, "Main page," Available: http://www.hartcomm2.org/index.html, 2008.

[68] D. Hawbacker and T. Rappaport, "Indoor wideband radiowave propagation measurements at 1.3 GHz and 4.0 GHz," *Electronics Letters*, vol. 26, no. 21, pp. 1800–1802, October 1990.

[69] T. He, S. Krishnamurthy, L. Luo, T. Yan, L. Gu, R. Stoleru, G. Zhou, Q. Cao, P. Vicaire, J. A. Stankovic, T. F. Abdelzaher, J. Hui, and B. Krogh, "VigilNet: An integrated sensor network system for energy-efficient surveillance," *ACM Transactions on Sensor Networks*, vol. 2, no. 1, pp. 1–38, February 2006.

[70] B. Heile, "Wireless sensors and control networks: Enabling new opportunities with ZigBee," Available: http://www.zigbee.org, 2006.

[71] W. B. Heinzelman, A. P. Chandrakasan, and H. Balakrishnan, "An application-specific protocol architecture for wireless microsensor networks," *IEEE Wireless Communications*, vol. 1, no. 4, pp. 660–670, October 2002.

[72] J. Hill, M. Horton, R. Kling, and L. Krishnamurthy, "Wireless sensor networks: The platforms enabling wireless sensor networks," *Communications of the ACM*, vol. 6, no. 47, pp. 41–46, June 2004.

[73] J. Hill and D. Culler, "Mica: a wireless platform for deeply embedded networks," *IEEE Micro*, vol. 22, no. 6, pp. 12–24, November/December 2002.

[74] Hitachi Metals, Ltd., "Magnetic compass sensor HM55B data sheet," Available: http://www.hitachimetals.com/product/sensors/mems/files/h_dst_e.pdf, 2008.

[75] P. Hämäläinen, "Cryptographic security designs and hardware architectures for wireless local area networks," Tampere University of Technology, PhD Thesis, Tampere, Finland, December 2006.

[76] M. Hännikäinen, "Design of quality of service support for wireless local area networks," Tampere University of Technology, PhD Thesis, Tampere, Finland, November 2002.

[77] IEEE, "IEEE p1451.5 project," Available: http://grouper.ieee.org/groups/1451/5/, 2006.

[78] ——, "IEEE xplore release 2.4," Available: http://ieeexplore.ieee.org/, 2007.

[79] *IEEE Std 802.11-1997 Information Technology- telecommunications And Information exchange Between Systems-Local And Metropolitan Area Networks-specific Requirements-part 11: Wireless Lan Medium Access Control (MAC) And Physical Layer (PHY) Specifications*, IEEE 802.11, 1997.

[80] *IEEE Standard for Information Technology—Telecommunications and Information Exchange Between Systems—Local and Metropolitan Area Networks—Specific Requirements—Part 15.1: Wireless Medium Access Control (MAC) and Physical Layer (PHY) Specifications for Wireless Personal Area Networks (WPANs)*, IEEE 802.15.1, 2002.

[81] *IEEE Standard for Information Technology—Telecommunications and Information Exchange Between Systems—Local and Metropolitan Area Networks—Specific Requirements—Part 15.3: Wireless Medium Access Control (MAC) and Physical Layer (PHY) Specifications for High Rate Wireless Personal Area Networks (WPANs)*, IEEE 802.15.3, 2003.

[82] *IEEE Standard for Information Technology—Telecommunications and Information Exchange Between Systems—Local and Metropolitan Area Networks—Specific Requirements—Part 15.4: Wireless Medium Access Control (MAC) and Physical Layer (PHY) Specifications for Low-Rate Wireless Personal Area Networks (LR-WPAN)*, IEEE 802.15.4, 2003.

[83] ISA, "ISA100.11a release 1," Available: http://www.isa.org/source/ISA100.11a_Release1_Status.ppt, 2007.

[84] S. Jiang, J. Rao, D. He, X. Ling, and C. C. Ko, "A simple distributed PRMA for MANETs," *IEEE Transactions on Vehicular Technology*, vol. 51, no. 2, pp. 293–305, March 2002.

[85] K. Jin and D. Cho, "Multi-code MAC for multi-hop wireless ad hoc networks," in *Proc. 56th Vehicular Technology Conference (VTC'02 (fall))*, vol. 2, Vancouver, British Columbia, Canada, September 24-29 2002, pp. 1100–1104.

[86] A. Juels, "RFID security and privacy: a research survey," *IEEE Journal on Selected Areas in Communications*, vol. 24, no. 2, pp. 381 – 394, February 2006.

[87] J. K. Juntunen, M. Kuorilehto, M. Kohvakka, V. A. Kaseva, M. Hännikäinen, and T. D. Hämäläinen, "WSN API: Application programming interface for wireless sensor networks," in *Proc. The 17th Annual IEEE Int'l Symposium on Personal, Indoor and Mobile Radio Communications (PIMRC'06)*, Helsinki, Finland, September 11–14 2006.

[88] H. Karl and A. Willig, *Protocols and Architectures for Wireless Sensor Networks*. John Wiley & Sons Ltd, 2005.

[89] P. Karn, "MACA - a new channel access method for packet radio," in *Proc. ARRL/CRRL Amateur Radio 9th Computer Networking Conf.*, 1990, pp. 134–140.

[90] V. Kaseva, M. Kohvakka, M. Kuorilehto, M. Hännikäinen, and T. D. Hämäläinen, "A wireless sensor network for RF-based indoor localization," *EURASIP Journal on Advances in Signal Processing*, vol. 2008, no. doi:10.1155/2008/731835, pp. 1–27, 2008.

[91] L. Kleinrock and F. Tobagi, "Packet switching in radio channels: part i-the carrier sense multiple access modes and their throughput-delay characteristics," *IEEE Transactions on Communications*, vol. COM-23, no. 12, pp. 1400 – 1416, December 1975.

[92] J. Kong, J.-H. Cui, D. Wu, and M. Gerla, "Building underwater ad-hoc networks and sensor networks for large scale real-time aquatic applications," in *Proc. IEEE Military Communications Conference (MILCOM'05)*, vol. 3, Atlantic City, NJ, USA, October 17–20 2005, pp. 1535–1541.

[93] M. Kuorilehto, "System level design issues in low-power wireless sensor networks," Tampere University of Technology, PhD Thesis, Tampere, Finland, June 2008.

[94] M. Kuorilehto, M. Hännikäinen, and T. D. Hämäläinen, "A survey of application distribution in wireless sensor networks," *EURASIP Journal on Wireless Communications and Networking, Special Issue on Ad Hoc Networks: Cross-Layer Issues*, vol. 2005, no. 5, pp. 774–788, December 2005.

[95] M. Kuorilehto, J. Suhonen, M. Hännikäinen, and T. D. Hämäläinen, "Tool-aided design and implementation of indoor surveillance wireless sensor network," in *Lecture Notes in Computer Science*, S. Vassiliadis, S. Wong, and T. D. Hämäläinen, Eds. Springer, 2007, vol. 4599, pp. 396–407.

[96] J. Kuruvila, A. Nayak, and I. Stojmenovic, "Hop count optimal position-based packet routing algorithms for ad hoc wireless networks with a realistic physical layer," *IEEE Journal of Selected Areas in Communications*, vol. 23, no. 6, pp. 1267–1275, June 2005.

[97] Lantronix, Inc., "XPort data sheet," Available: http://www.lantronix.com/pdf/XPort_DS.pdf, 2005.

[98] D. Ley, "Emerging technologies for learning: Ubiquitous computing," Available: http://www.becta.org.uk/research, British Educational Communications and Technology Agency Becta, Tech. Rep. volume 2 (2007), 2007.

[99] C. Lin and M. Gerla, "Adaptive clustering for mobile wireless networks," *IEEE Journal of Selected Areas in Communications*, vol. 15, no. 7, pp. 1265–1275, September 1997.

[100] M. J. Markowski and A. Sethi, "Fully distributed wireless MAC transmission of real-time data," in *Proc. 4th IEEE Real-Time Technology and Applications Symposium (RTAS'98)*, Denver, Colorado, USA, June 3-5 1998.

[101] K. Martinez, P. Padhy, A. Riddoch, R. Ong, and J. Hart, "Glacial environment monitoring using sensor networks," in *Proc. Workshop on Real-World Wireless Sensor Networks (REALWSN'05)*, Stockholm, Sweden, June 20–21 2005.

[102] Maxim Integrated Products, "MAX1725/MAX1726 12V, Ultra-low-IQ, low-dropout linear regulators," Available: http://datasheets.maxim-ic.com/en/ds/MAX1725-MAX1726.pdf, 2003.

[103] ——, "MAX8880/MAX8881 12V, Ultra-low-IQ, low-dropout linear regulators with pok," Available: http://datasheets.maxim-ic.com/en/ds/MAX8880-MAX8881.pdf, 2007.

[104] Microchip Technology, Inc., "PIC18F2420/2520/4420/4520 data sheet," Available: http://ww1.microchip.com/downloads/en/DeviceDoc/39631a.pdf, 2004.

[105] ——, "PIC18F2525/2620/4525/4620 data sheet," Available: http://ww1.microchip.com/downloads/en/DeviceDoc/39626b.pdf, 2004.

[106] ——, "PIC18F8722 family data sheet," Available: http://ww1.microchip.com/downloads/en/DeviceDoc/39646b.pdf, 2004.

[107] ——, "MRF24J40 data sheet," Available: http://ww1.microchip.com/downloads/en/DeviceDoc/39776a.pdf, 2006.

[108] ——, "PIC24FJ128GA family data sheet," Available: http://ww1.microchip.com/downloads/en/DeviceDoc/39747C.pdf, 2006.

[109] ——, "MCP1603 2.0 MHz, 500 mA synchronous buck regulator," Available: http://ww1.microchip.com/downloads/en/DeviceDoc/22042a.pdf, 2007.

[110] ——, "MCP1702 250 mA low quiescent current LDO regulator," Available: http://ww1.microchip.com/downloads/en/DeviceDoc/22008b.pdf, 2007.

[111] A. Mihovska, F. Platbrood, G. Karetsos, S. Kyriazakos, R. Muijen, R. Guarneri, and J. Pereira, "Towards the wireless 2010 vision: A technology roadmap," *Wireless Personal Communications*, vol. 42, no. 3, pp. 303–336, August 2007.

[112] R. Min, M. Bhardwaj, S.-H. Cho, N. Ickes, E. Shih, A. Sinha, A. Wang, and A. Chandrakasan, "Energy-centric enabling technologies for wireless sensor networks," *IEEE Wireless Communications*, vol. 9, no. 4, pp. 28–39, August 2002.

[113] Minilogic Device, Corp., "ML62 series positive voltage regulator," Available: http://www.minilogic.com.hk/specification/ML62.pdf, 2005.

[114] Moteiv, Corp., "Tmote sky ultra low power IEEE 802.15.4 compliant wireless sensor module," Available: http://www.eecs.harvard.edu/~konrad/projects/shimmer/references/tmote-sky-datasheet.pdf, 2006.

[115] S. Mozar, "An evaluation of low cost power supply alternatives for high volume consumer products," in *Proc. 10th Int. Symposium on Consumer Electronics (ISCE'06)*, St. Petersburg, Russia, June 28- July 01 2006, pp. 1–4.

[116] Nanotron Technologies GmbH, "nanoNET development kit," Available: http://www.nanotron.com/EN/pdf/Factsheet_nanoNET-Dev-Kit.pdf, 2008.

[117] Y. Neuvo, "Future wireless technologies," in *Proc. IEEE 6th CAS Symposium on Emerging Technologies: Frontiers of Mobile and Wireless Communication*, vol. I, Shanghai, China, May 31 - June 2 2004, pp. 1–3.

[118] D. Niculescu, "Communication paradigms for sensor networks," *IEEE Communications Magazine*, vol. 43, no. 3, pp. 116–122, March 2005.

[119] Nordic Semiconductor ASA, "nRF24E1 product specification," Available: http://www.nordicsemi.com/files/Product/data_sheet/Product_Specification_nRF24E1_1_3.pdf, 2006.

[120] ——, "Single chip 2.4 GHz transceiver nRF2401A," Available: http://www.nordicsemi.no/files/Product/data_sheet/Product_Specification_nRF2401A_1_1.pdf, 2006.

[121] ——, "Single chip 2.4 GHz Transceiver nRF24L01," Available: http://www.nordicsemi.no/files/Product/data_sheet/Product_Specification_nRF24L01_1.0.pdf, 2006.

[122] ——, "Single chip 433/868/915 MHz transceiver nRF905," Available: http://www.nordicsemi.no/files/Product/data_sheet/nRF905_rev1_4.pdf, 2006.

[123] S. Oh, P. Chen, M. Manzo, and S. Sastry, "Instrumenting wireless sensor networks for real-time surveillance," in *Proc. 2006 IEEE Int'l Conf. on Robotics and Automation (ICRA'06)*, Orlando, FL, USA, May 15–19 2006, pp. 3128–3133.

[124] N. Ota and P. Wright, "Trends in wireless sensor networks for manufacturing," *International Journal of Manufacturing Research*, vol. 1, no. 1, pp. 3–17, 2006.

[125] G. Pei and C. Chien, "Low power TDMA in large wireless sensor networks," in *Proc. IEEE Military Communications Conf. (MILCOM'01)*, October 2001, pp. 347–351.

[126] C. Perkins, *Ad Hoc Networks*. Addison-Wesley, Reading, MA, 2000, vol. 1.

[127] D. Pescovitz, "The power of small tech," *Smalltimes*, vol. 2, no. 1, January 2002.

[128] C. Piguet, J.-M. Masgonty, C. Arm, S. Durand, T. Schneider, F. Rampogna, C. Scarnera, C. Iseli, J.-P. Bardyn, R. Pache, and E. Dijkstra, "Low-power design of 8-b embedded coolrisc microcontroller cores," *IEEE Journal of Solid-State Circuits*, vol. 32, no. 7, pp. 1067–1078, July 1997.

[129] J. Polastre, J. Hill, and D. Culler, "Versatile low power media access for wireless sensor networks," in *Proc. 2nd Internation Conf. on Embedded Networked Sensor Systems (Sensys'04)*, Baltimore, MD, USA, November 2004, pp. 95–107.

[130] J. Polastre, R. Szewczyk, and D. Culler, "Telos: enabling ultra-low power wireless research," in *Proc. 4th International Symposium on Information Processing in Sensor Networks (IPSN'05)*, Los Angeles, CA, USA, April 2005, pp. 364–369.

[131] I. Poole, "What exactly is...zigbee," *IEE Review*, vol. 2, no. 4, pp. 44–45, August-September 2004.

[132] G. Pottie and W. Kaiser, "Wireless integrated network sensors," *Communications of the ACM*, vol. 43, no. 5, pp. 51–58, May 2000.

[133] J. Rabaey, J. Ammer, J. da Silva Jr., D. Patel, and S. Roundy, "Picoradio supports ad hoc ultra-low power wireless networking," *IEEE Computer Magazine*, vol. 33, no. 7, pp. 42–48, July 2000.

[134] V. Raghunathan, C. Schurgers, S. Park, and M. Srivastava, "Energy-aware wireless microsensor networks," *IEEE Signal Processing Magazine*, vol. 19, no. 2, pp. 40–50, March 2002.

[135] V. Rajendran, K. Obraczka, and J. Garcia-Luna-Aceves, "Energy-efficient, collision-free medium access control for wireless sensor networks," in *Proc. 1st Int'l Conf. on Embedded Networked Sensor Systems (SenSys'03)*, Los Angeles, CA, USA, November 2003, pp. 181–192.

[136] T. Rappaport, "Indoor radio communications for factories of the future," *IEEE Communications Magazine*, vol. 27, no. 5, pp. 15–24, May 1989.

[137] ——, *Wireless Communications - Principles and Practice*, 2nd ed. Prentice Hall, 1996, ch. 1.

[138] T. Rappaport and C. McGillem, "Uhf fading in factories," *IEEE Journal on Selected Areas in Communication*, vol. 7, no. 1, pp. 40–48, January 1989.

[139] J. M. Reason and J. M. Rabaey, "A study of energy consumption and reliability in a multi-hop sensor network," *ACM SIGMOBILE Mobile Computing and Communications Review*, vol. 8, no. 1, pp. 84–97, January 2004.

[140] N. Reijers, G. Halkes, and K. Langendoen, "Link layer measurements in sensor networks," in *Proc. 1st IEEE Int'l Conf. on Mobile Ad-hoc and Sensor Systems (MASS'04)*, FL, USA, October 2004, pp. 224–234.

[141] RF Monolithics, Inc., "TR1001 868.35 MHz hybrid transceiver," Available: http://www.rfm.com/products/data/tr1001.pdf, 1999.

[142] ——, "TR3100 433.92 MHz hybrid transceiver," Available: http://www.rfm.com/products/data/tr3100.pdf, 1999.

[143] I. Rhee, A. Warrier, M. Aia, and J. Min, "Z-MAC: A hybrid MAC for wireless sensor networks," in *Proc. 3rd ACM Conf. on Embedded Networked Sensor Systems (Sensys '05)*, New York, NY, USA, November 2005, pp. 90–101.

[144] O. Riva and C. Borcea, "The urbanet revolution: Sensor power to the people!" *IEEE Pervasive Computing*, vol. 6, no. 2, pp. 41–49, April-June 2007.

[145] K. Römer, "Tracking real-world phenomena with smart dust," in *Proc. 1st European Workshop on Wireless Sensor Networks (EWSN'04)*, ser. LNCS, no. 2920. Berlin, Germany: Springer-Verlag, January 19–21 2004, pp. 28–43.

[146] K. Römer and F. Mattern, "The design space of wireless sensor networks," *IEEE Wireless Communications*, vol. 11, no. 6, pp. 54–61, December 2004.

[147] L. Roberts, "ALOHA packet system with and without slots and capture," *ACM SIGCOMM Computer Communication Review*, vol. 5, no. 2, pp. 28–42, April 1975.

[148] Round Solutions GmbH & Co KG, "CAM-VGA100 user manual," Available: http://www.roundsolutions.com/techdocs/docs/CAM-VGA100-User\%20Manual-v2-2.pdf, 2006.

[149] S. Roundy, D. Steingart, L. Frechette, P. Wright, and J. Rabaey, "Power sources for wireless sensor networks," in *Proc. 1st Eur. Workshop on Wireless Sensor Network (EWSN'04)*, Berlin, Germany, January 2004, pp. 1–17.

[150] S. Roundy, P. K. Wright, and J. Rabaey, "A study of low level vibrations as a power source for wireless sensor nodes," *Computer Communications*, vol. 26, no. 11, pp. 1131–1144, July 2003.

[151] R. Sachs, "Z-Wave, the standard in wireless home control," Available: http://www.zen-sys.com/, 2006.

[152] B. M. Sadler, "Fundamentals of energy-constrained sensor network systems," *IEEE A&E Systems Magazine*, vol. 20, no. 1, pp. 17–35, August 2005.

[153] A. Sakata, T. Yamazato, H. Okada, and M. Katayamat, "Throughput comparison of CSMA and CDMA slotted ALOHA in inter-vehicle communication," in *Proc. 7th International Conference on ITS Telecommunications (ITST'07)*, Sophia Antipolis, France, June 6–8 2007, pp. 1–6.

[154] Y. Sankarasubramaniam, I. Akyildiz, and S. McLaughlin, "Energy efficiency based packet size optimization in wireless sensor networks," in *Proc. 1st IEEE Int. Workshop on Sensor Network Platforms and Applications (SNPA'03)*, Anchorage, Alaska, May 11 2003, pp. 1–8.

[155] N. Sastry and D. Wagner, "Security considerations for IEEE 802.15.4 networks," in *Proc. 2004 ACM Workshop on Wireless Security (WiSE'04)*, Philadelphia, PA, USA, October 1 2004, pp. 32–42.

[156] A. Savvides and M. B. Srivastava, "A distributed computation platform for wireless embedded sensing," in *Proc. IEEE Int'l Conf. on Computer Design: VLSI in Computers and Processors (ICCD'02)*, Freiburg, Germany, September 16–18 2002, pp. 220–225.

[157] J. Schiller, A. Liers, and H. Ritter, "ScatterWeb: A wireless sensornet platform for research and teaching," *Elsevier Computer Communications*, vol. 28, no. 13, pp. 1545–1551, August 2005.

[158] T. Schmid, H. Dubois-Ferriere, and M. Vetterli, "Sensorscope: Experiences with a wireless building monitoring sensor network," in *Proc. Workshop on Real-World Wireless Sensor Networks (REALWSN'05)*, Stockholm, Sweden, June 20–21 2005.

[159] C. Schurgers, V. Tsiatsis, S. Ganeriwal, and M. Srivastava, "Optimizing sensor networks in the energy-latency-density design space," *IEEE Transactions on Mobile Computing*, vol. 1, no. 1, pp. 70–80, January-March 2002.

[160] L. Schwiebert, S. Gupta, and J. Weinmann, "Research challenges in wireless networks of biomedical sensors," in *Proc. 7th annual ACM/IEEE International Conference on Mobile Computing and Networking (MobiCom'01)*, Rome, Italy, July 16–21 2001, pp. 151–165.

[161] S. Seidel and T. Rappaport, "914 MHz path loss prediction models for indoor wireless communications in multifloored buildings," *IEEE Trans. Antennas and Propagation*, vol. 40, no. 2, pp. 207–217, February 1992.

[162] Seiko Instruments, Inc., "S-1206 series ultra low current consumption and low dropout CMOS voltage regulator," Available: http://dl.sii-ic.com.edgesuite.net/spd_dtst/dt_sht_e/vol_regu/S1206_E.pdf, 2008.

[163] Semtech, Corp., "XE1201A 300-500 MHz low-power UHF transceiver," Available: http://www.semtech.com/, 2005.

[164] ——, "XE8802 sensing machine," Available: http://www.semtech.com/, 2006.

[165] ——, "XE1203F 433 MHz/868 MHz/915 MHz low-power, integrated UHF transceiver," Available: http://www.semtech.com/, 2007.

[166] Sensicast, Inc., "SensiNet - the wireless sensor network from sensicast," Available: http://www.sensicast.com/, 2008.

[167] Sensorion AG, "SHT1x/SHT7x humidity & temperature sensor," Available: http://www.sensirion.com/images/getFile?id=25, 2004.

[168] C. Sharp, S. Schaffert, A. Woo, N. Sastry, C. Karlof, S. Sastry, and D. Culler, "Design and implementation of a sensor network system for vehicle tracking and autonomous interception," in *Proc. 2nd European Workshop on Wireless Sensor Networks (EWSN'05)*, Istanbul, Turkey, January 31–February 2 2005, pp. 93–107.

[169] M. Sichitiu, V. Ramadurai, and P. Peddabachagari, "Simple algorithm for outdoor localization of wireless sensor networks with in-accurate range measurements," in *Proc. Int'l Conf. on Wireless Networks (ICWN'03)*, Las Vegas, Nevada, USA, June 23-26 2003, pp. 300–305.

[170] A. Sikora, "Design challenges for short-range wireless networks," *IEE Proc. Communications*, vol. 151, no. 5, pp. 473–479, October 2002.

[171] M. Sikora, J. Laneman, M. Haenggi, J. D.J. Costello, and T. Fuja, "On the optimum number of hops in linear wireless networks," in *Proc. IEEE Information Theory Workshop (ITW'04)*, Texas, USA, October 24-29 2004, pp. 165–169.

[172] G. Simon, , M. Maróti, Ákos Lédeczi, G. Balogh, B. Kusy, A. Nádas, G. Pap, J. Sallai, and K. Frampton, "Sensor network-based countersniper system," in

Proc. 2nd Int'l Conf. on Embedded Networked Sensor Systems (SenSys'04), Baltimore, MD, USA, November 3–5 2004, pp. 1–12.

[173] S. Singh and C. S. Raghavendra, "PAMAS: Power-aware multi-access protocol with signaling for ad hoc networks," *ACM Computer Communication Review*, vol. 28, no. 3, pp. 5–26, July 1998.

[174] Smart-its, "Smart-its home page," Available: http://www.smart-its.org/, 2007.

[175] K. Sohrabi, J. Gao, V. Ailawadhi, and G. J. Pottie, "Protocols for self-organization of a wireless sensor network," *IEEE Personal Communications*, vol. 7, no. 5, pp. 16–27, October 2000.

[176] J. Song, S. Han, A. Mok, D. Chen, M. Lucas, and M. Nixon, "WirelessHART: Applying wireless technology in real-time industrial process control," in *Proc. 14th IEEE Real-Time and Embedded Technology and Applications Symposium (RTAS'08)*, St. Louis, MO, USA, April 22-24 2008, pp. 377–386.

[177] W. Stallings, *Data and Computer Communications*, 7th ed. Prentice-Hall, 2004.

[178] J. A. Stankovic, T. F. Abdelzaher, C. Lu, L. Sha, and J. C. Hou, "Real-time communication and coordination in embedded sensor networks," *Proceedings of the IEEE*, vol. 91, no. 7, pp. 1002–1022, July 2003.

[179] D. C. Steere, A. Baptista, D. McNamee, C. Pu, and J. Walpole, "Research challenges in environmental observation and forecasting systems," in *Proc. 6th Annual ACM/IEEE Int'l Conf. on Mobile Computing and Networking (MobiCom'00)*, Boston, MA, USA, August 6–11 2000, pp. 292–299.

[180] M. Stordeur and I. Stark, "Low power thermoelectric generator - self-sufficient energy supply for micro systems," in *Proc. 16th Int. Conf. Thermoelectrics (ICT'97)*, Dresden, Germany, August 26–29 1997, pp. 575–577.

[181] J. Suhonen, M. Kohvakka, M. Hännikäinen, and T. Hämäläinen, "Design, implementation, and outdoor deployment for wireless sensor network for environmental monitoring," in *Proc. Embedded Computer Systems: Architectures, Modeling, and Simulation (SAMOS VI)*, Samos, Greece, July 2006, pp. 109–121.

[182] ——, "Embedded software architecture for diagnosing network and node failures in wireless sensor networks," in *Proc. Embedded Computer Systems: Ar-*

chitectures, Modeling, and Simulation (SAMOS VIII), Samos, Greece, July 2008, pp. 1–10.

[183] J. Suhonen, M. Kohvakka, M. Kuorilehto, M. Hännikäinen, and T. D. Hämäläinen, "Cost-aware capacity optimization in dynamic multi-hop wsns," in *Proc. Design, Automation and Test in Europe (DATE'07)*, Nice, France, April 2007, pp. 666–671.

[184] J. Suhonen, M. Kuorilehto, M. Hännikäinen, and T. D. Hämäläinen, "Cost-aware dynamic routing protocol for wireless sensor networks - design and prototype experiments," in *Proc. 17th Annual IEEE Int'l Symposium on Personal, Indoor and Mobile Radio Communications (PIMRC'06)*, Helsinki, Finland, September 2006, pp. 1–5.

[185] R. Szewczyk, A. Mainwaring, J. Polastre, J. Anderson, and D. Culler, "An analysis of a large scale habitat monitoring application," in *Proc. 2nd Int'l Conf. on Embedded Networked Sensor Systems (SenSys'04)*, Baltimore, MD, USA, November 3–5 2004, pp. 214–226.

[186] Z. Tang and J. Garcia-Luna-Aceves, "A protocol for topology-dependent transmission scheduling in wireless networks," in *Proc. IEEE Wireless Communications and Networking Conference (WCNC'99)*, vol. 3, New Orleans, LA, USA, September 1999, pp. 1333–1337.

[187] Texas Instruments, Inc., "CC1020 single chip low power RF transceiver for narrowband systems," Available: http://www.ti.com/lit/gpn/cc1020, 2006.

[188] ——, "CC1100 single chip low cost low power RF transceiver," Available: http://www.ti.com/lit/gpn/cc1100, 2006.

[189] ——, "CC2500 single chip low cost low power RF transceiver," Available: http://www.ti.com/lit/gpn/cc2500, 2006.

[190] ——, "MSP430x15x, MSP430x16x, MSP430x161x mixed signal microcontroller," Available: http://focus.ti.com/lit/ds/symlink/msp430f169.pdf, 2006.

[191] ——, "TPS62000 high-efficiency step-down low power DC-DC converter," Available: http://focus.ti.com/lit/ds/symlink/tps62000.pdf, 2006.

[192] ——, "CC1000 single chip very low power RF transceiver," Available: http://www.ti.com/lit/gpn/cc1000, 2007.

[193] ——, "CC2400 2.4 GHz low-power RF transceiver," Available: http://www.ti.com/lit/gpn/cc2400, 2007.

[194] ——, "CC2420 2.4 GHz IEEE 802.15.4 / ZigBee-ready RF transceiver," Available: http://www.ti.com/lit/gpn/cc2420, 2007.

[195] ——, "TPS715x 50 mA, 24V, 3.2 μA supply current low-dropout linear regulator in SC70 package," Available: http://focus.ti.com/lit/ds/symlink/tps71530.pdf, 2007.

[196] J.-P. Thomesse, "Fieldbus technology in industrial automation," *Proceedings of the IEEE*, vol. 93, no. 6, pp. 1073–1101, June 2005.

[197] P. Thubert, "6LoWPAN backbone router, internet-draft," Available: http://tools.ietf.org/html/draft-thubert-6lowpan-backbone-router-01, 2008.

[198] F. A. Tobagi and L. Kleinrock, "Packet switching in radio channels: Part II - the hidden terminal problem in carrier sense multiple-access modes and the busy-tone solution," *IEEE Trans. Communications*, vol. 23, no. 12, pp. 1417–1433, December 1975.

[199] G. Tolle, J. Polastre, R. Szewczyk, D. Culler, N. Turner, K. Tu, S. Burgess, T. Dawson, P. Buonadonna, D. Gay, and W. Hong, "A macroscope in the redwoods," in *Proc. 3rd Int'l Conf. on Embedded Networked Sensor Systems (SenSys'05)*, San Diego, CA, USA, November 2–4 2005, pp. 51–63.

[200] V. Turau, M. Witt, and C. Weyer, "Analysis of a real multi-hop sensor network deployment: The heathland experiment," in *Proc. 3rd Int'l Conf. on Networked Sensing Systems (INSS'06)*, Chicago, IL, USA, May 31–June 2 2006.

[201] T. van Dam and K. Langendoen, "An adaptive energy-efficient MAC protocol for wireless sensor networks," in *Proc. 1st Int'l Conf. on Embedded Networked Sensor Systems (Sensys'03)*, Los Angeles, CA, USA, November 2003, pp. 171–180.

[202] E. Verriest, B. Friedlander, and M. Morf, "Distributed processing in estimation and detection," in *Proc. 18th IEEE Conference on Decision and Control including the Symposium on Adaptive Processes (CDC'79)*, Ft. Lauderdale, FL, USA, December 12–14 1979, pp. part 1: 153–158.

[203] N. Vlajic and D. Xia, "Wireless sensor networks: to cluster or not to cluster?" in *Proc. International Symposium on World of Wireless, Mobile and Multi-*

media Networks (WoWMoM '06), Buffalo, NY, USA, June 26–29 2006, pp. 11–9.

[204] VTI Technologies Oy, "SCA3000-E01 3-axis ultra low power accelerometer with digital spi interface," Available: http://www.vti.fi, 2002.

[205] ——, "SCP1000 series (120 kPa) absolute pressure sensor," Available: http://www.vti.fi, 2007.

[206] N. Wang, N. Zhang, and M. Wang, "Wireless sensors in agriculture and food industry - recent development and future perspective," *Computers and Electronics in Agriculture*, vol. 50, no. 1, pp. 1–14, January 2006.

[207] B. Warneke, M. Last, B. Leibowitz, , and K. S. J. Pister, "Smart dust: Communicating with a cubic-millimeter computer," *Computer*, vol. 34, no. 1, pp. 43–51, January 2001.

[208] B. Week, "21 ideas for the 21st century," Business Week, August 30th, 1999, pp. 78 - 167, 1999.

[209] M. Weiser, "Hot topics: ubiquitous computing," *IEEE Computer*, vol. 26, no. 10, pp. 71–72, October 1993.

[210] ——, "The computer for the 21st century," *ACM SIGMOBILE Mobile Computing and Communications Review*, vol. 3, no. 3, pp. 3–11, July 1999.

[211] A. Wheeler, "Commercial applications of wireless sensor networks using zigbee," *IEEE Communications Magazine*, vol. 45, no. 4, pp. 70–77, April 2007.

[212] Wibree, "Ultra-low power radio technology for small devices," Available: http://www.wibree.com/technology/Wibree_2Pager.pdf, 2007.

[213] A. Willig, "Recent and emerging topics in wireless industrial communications: A selection," *IEEE Transactions on Industrial Informatics*, vol. 4, no. 2, pp. 102–124, May 2008.

[214] A. Willig, K. Matheus, and a. Wolisz, "Wireless technology in industrial networks," *Proceedings of the IEEE*, vol. 93, no. 6, pp. 1130–1151, June 2005.

[215] WiMAX, "WiMAX forum website," Available: http://www.wimaxforum.org, 2007.

[216] M. Wolf and D. Kress, "Short-range wireless infrared transmission: the link budget compared to RF," *IEEE Wireless Communications Magazine*, vol. 10, no. 2, pp. 8–14, April 2003.

[217] K.-J. Wong and D. Arvind, "SpeckMAC: Low-power decentralized MAC protocols for low data rate transmissions in specknets," in *Proc. 2nd Int'l Workshop on Multi-hop Ad Hoc Networks: from Theory to Reality (REALMAN'06)*, Florenze, Italy, May 2006, pp. 71–78.

[218] T. Wu and S. Biswas, "A self-reorganizing slot allocation protocol for multi-cluster sensor networks," in *Proc. 4th International Symposium on Information Processing in Sensor Networks (IPSN'05)*, Los Angeles, CA, USA, April 2005, pp. 309–316.

[219] N. Xu, S. Rangwala, K. K. Chintalapudi, D. Ganesan, A. Broad, R. Govindan, and D. Estrin, "A wireless sensor network for structural monitoring," in *Proc. 2nd Int'l Conf. on Embedded Networked Sensor Systems (SenSys'04)*, Baltimore, MD, USA, November 3–5 2004, pp. 13–24.

[220] W. Ye, J. Heidemann, and D. Estrin, "An energy-efficient MAC protocol for wireless sensor networks," in *Proc. 21st Annual Joint Conf. of the IEEE Computer and Communications Societies (INFOCOM'02)*, vol. 3, New York, NY, USA, June 23–27 2002, pp. 1567–1576.

[221] W. Ye, F. Silva, and J. Heideman, "Ultra-low duty cycle MAC with scheduled channel polling," in *Proc. 4th ACM Conf. Embedded networked sensor systems (SenSys'06)*, Boulder, Colorado, USA, October 31 – November 3 2003, pp. 329–334.

[222] J. Yinghui and L. Qingchong, "Throughput analysis of spread slotted aloha systems using multiuser receivers," in *Proc. Military Communications Conference (MILCOM'02)*, Anaheim, CA, USA, October 7–10 2002, pp. 237–242.

[223] S. Yoon, "Power management in wireless sensor networks," North Carolina State University, PhD Thesis, Raleigh, NC, USA, January 2007.

[224] M. Yousef and N. El-Sheimy, "Wireless sensor network: research vs. reality design and deployment issues," in *Proc. 5th IEEE Annual Conference on Communication Networks and Services Research (CNSR'07)*, New Brunswick, Canada, May 14–17 2007, pp. 8–9.

[225] P. Zhang, C. M. Sadler, S. A. Lyon, and M. Martonosi, "Hardware design experiences in zebranet," in *Proc. 2nd Int'l Conf. on Embedded networked sensor systems (SenSys'04)*, Baltimore, MD, USA, November 3–5 2004, pp. 227–238.

[226] R. Zhang and J.-M. Gorce, "Optimal transmission range for minimum energy consumption in wireless sensor networks," in *Proc. IEEE Wireless Communications and Networking Conference (WCNC'08)*, Budapest, Hungary, March 31 – April 3 2008, pp. 757–762.

[227] J. Zheng, M. Lee, and M. Anshel, "Toward secure low rate wireless personal area networks," *IEEE Trans. Mobile Computing*, vol. 5, no. 10, pp. 1361–1373, October 2006.

[228] C. Zhu and M. Corson, "A five-phase reservation protocol (fprp) for mobile ad hoc networks," in *Proc. 17th Annual Joint Conference of the IEEE Computer and Communications Societies (INFOCOM'98)*, vol. 1, San Fransisco, CA, USA, March 29 - April 2 1998, pp. 322–331.

[229] *ZigBee Specification Version 1.0*, ZigBee Alliance, 2004.

PUBLICATIONS

PUBLICATION 1

M. Kohvakka, "TUTWSN MAC Protocol," book chapter in *Ultra-low energy wireless sensor networks in practice: theory, realization and deployment*, M. Kuorilehto, M. Kohvakka, J. Suhonen, P. Hämäläinen, M. Hännikäinen, and T.D. Hämäläinen, Chichester: John Wiley, 2007, pp. 145–182.

The publication is intentionally excluded from the electronic version due to copyright reasons.

PUBLICATION 2

M. Kohvakka, J. Suhonen, M. Hännikäinen, and T. D. Hämäläinen, "Transmission Power Based Path Loss Metering for Wireless Sensor Networks," in *Proceedings of the 17th Annual IEEE International Symposium on Personal, Indoor and Mobile Radio Communications (PIMRC 2006)*, Helsinki, Finland, Sep. 11–14, 2006, pp. 1–5.

The 17th Annual IEEE International Symposium on Personal, Indoor and Mobile Radio Communications (PIMRC'06)

TRANSMISSION POWER BASED PATH LOSS METERING FOR WIRELESS SENSOR NETWORKS

Mikko Kohvakka, Jukka Suhonen, Marko Hännikäinen and Timo D. Hämäläinen
Tampere University of Technology, Institute of Digital and Computer Systems
Tampere, Finland

ABSTRACT

The metering of path loss to neighbouring nodes is vital in multi-hop Wireless Sensor Networks (WSN) for managing network self-configuration, robust data routing, and node localization. Conventionally, path loss is measured by a Received Signal Strength Indicator (RSSI) mechanism of a transceiver. Yet, the lowest hardware complexity, energy consumption and cost are reached by transceivers without RSSI. We present a new simple transmission power based path loss metering method for WSNs without RSSI mechanism. The method determines path loss from frames transmitted at different power levels. Performance measurements with physical WSN prototypes indicate sufficient accuracy for network management. According to performance analysis, the power consumption of the proposed method is below 10 μW. An energy analysis in a large IEEE 802.15.4 network indicates 51% to 69% energy saving compared to RSSI-equipped transceivers by using the path loss metering method together with a simple and low power transceiver.

I. INTRODUCTION

Self-configuring Wireless Sensor Networks (WSN) are a relatively new family of wireless ad hoc networks developed for low data rate monitoring and actuating in home, office, industrial and outdoor environments [1]. WSN consist of even thousands of battery-powered WSN nodes, which combine sensing, processing and wireless communication with ultra-low energy consumption, size and cost. As the number of nodes is large, battery or node replacements are difficult, and nodes should operate for months to years without maintenance of any kind. The energy consumption in WSN nodes is typically dominated by transceiver circuitry [2]. To minimize transmission energy consumption, data is routed in the network by multiple low-energy hops instead of a single high-energy transmission. Communication links are formed dynamically with any node in a range creating a mesh network topology.

An energy efficient and robust WSN operation requires that nodes are capable to measure radio wave attenuation (path loss) to neighbouring nodes. This information is crucial for efficient network self-configuration and routing; nodes can form and maintain robust routing paths with sufficient radio link quality and energy efficient hop lengths [3]. A weakened radio link can be recognized and route changed before an actual link failure. In addition, transmission power levels are dynamically minimized for reducing network energy consumption and interferences with other nodes. As radio wave attenuates with the transmission distance [4], measured path loss can be used for estimating distances between nodes (ranging), and further for node localization [5]. Location information improves the applicability of gathered data in a dynamic network, and allows even random node deployments.

In practice, a path loss is estimated by measured signal strengths of received frames and their known transmission power levels [5]. Conventionally, signal strength is measured by a Received Signal Strength Indicator (RSSI) mechanism implemented on a transceiver PHY layer. A transceiver calculates the RSSI based on the gain in the receiver chain in conjunction with the energy of the signal after channel filtering, and stores the value in a register. Yet, the simplest and lowest power commercial off-the-shelf radio transceivers lack the quite complex RSSI mechanism. To be able to achieve the lowest energy and cost WSN realizations, a transceiver without RSSI may be the only option, and the implementation of a path loss metering otherwise is required.

In this paper we present a new type of a path loss metering mechanism for minimum power WSNs. The method utilizes receiver sensitivity as a simple signal strength meter, and estimates path loss according to succeed and failed receptions of beacon frames transmitted at different transmission power levels. This is possible since almost every transceiver has an adjustable transmission power. The accuracy of the path loss metering method is measured with low power WSN prototypes in indoor and outdoor environments. Achieved energy efficiency is demonstrated in an IEEE 802.15.4 Low-Rate Wireless Personal Area Network (LR-WPAN) [6] by analyzing coordinator power consumption with different low power transceivers.

The rest of this paper is organized as follows. A detailed description of the method is presented in Section 2. Section 3 presents performance measurements and power consumption analysis. Section 4 concludes the paper.

II. PATH LOSS METERING DESCRIPTION

The presented path loss metering method is designed for low duty cycle Medium Access Control (MAC) protocols with a periodic wakeup scheme. In a periodic wakeup scheme, data transmissions and reception are performed in short data exchange periods, while the rest of time nodes are in inactive mode conserving energy, as presented in Figure 1. Beacon transmissions at the beginning of data exchange periods are used for synchronizing data exchanges and signalling network

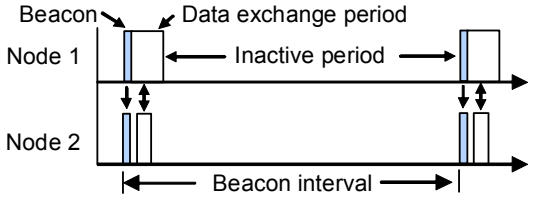

Figure 1: Periodic wakeup scheme.

management information. Most well-known low duty cycle MAC protocols are S-MAC [7] and its variants, and a beacon-enabled mode of LR-WPAN [6].

In this paper, a path loss A means the signal attenuation between a transmitter output and receiver input ports including antenna gain, and the losses in impedance matching network. Thus, A is determined as the ratio of transmission power level P_T to received signal strength P_R that is measured according to succeed and failed frame receptions and receiver sensitivity S_{min}. Receiver sensitivity is defined as the minimum mean power received at the input port at which the Bit Error Rate (BER) does not exceed a specified value (typically 0.1%). This yields that a frame of l bits can be received successfully exactly at the probability of $(1 - BER)^l$, when $P_R = S_{min}$. For simplification we approximate that $P_R \geq S_{min}$, when a frame is received successfully. The upper and lower limits for the path loss are estimated by retransmitting a frame with different transmission power levels, and detecting the lowest transmission power resulting a successful reception $P_{T(succeed)}$ and the highest power resulting a failed reception $P_{T(failed)}$ as

$$\frac{\max\left(P_{T(failed)}\right)}{P_R} < A \leq \frac{\min\left(P_{T(succeed)}\right)}{P_R}. \qquad (1)$$

As an example, calculated path loss values for a transceiver having S_{min} = -85 dBm and beacon transmission powers from -20 dBm to 0 dBm are presented in Table 1. Since path loss is typically quite equal for both directions [8], the same path loss is assumed to apply for transmissions to neighbours.

The path loss metering is implemented on MAC protocol beacons due to the following reasons. First, the interval of beacon transmissions of low duty cycle MAC protocols is very suitable for path loss measurements. In addition, beacon transmissions are synchronized, which allows the minimization of reception time. Beacons are also quite short, which provides energy efficient implementation without the need for a new frame type. Moreover, path loss information is typically needed together with the node status information transmitted in beacons for network management.

The operational principle of the path loss metering method is presented in Figure 2, where Node 3 measures the path losses between Node 3 and two other nodes (Node 1 and Node 2) by receiving their periodic beacons. Achieved ranges of beacon transmissions with four power levels are marked by circles. As Node 1 is quite close to Node 3, a beacon transmitted at the second lowest transmission power level can be received resulting low path loss. As a distance from Node 2 is much longer, only the highest power beacon is successfully received. This indicates a high path loss.

Table 1: Path loss according to succeed (1) and failed (0) receptions.

	transmission power level			
Resulted path loss	-20 dBm	-10 dBm	-5 dBm	0 dBm
≤ 65 dB	1	1	1	1
65 – 75 dB	0	1	1	1
75 – 80 dB	0	0	1	1
80 – 85 dB	0	0	0	1

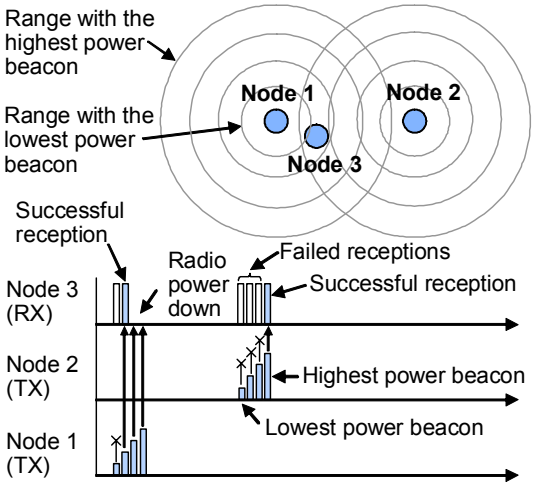

Figure 2: Path loss metering operational principle.

For reducing energy consumption, beacons are transmitted in the increased order of transmission power. This enables that beacon frames are received until one reception succeeds, after which the receiver may be switched to a power down mode. As the contents of the beacons are similar, the reception of higher power beacons does not bring any additional information, and they may be ignored.

III. Performance Analysis

The performance analysis of the path loss metering method consists of accuracy measurements in indoor and outdoor environment, and power consumption analysis in a large LR-WPAN network.

A. Accuracy Measurements

The accuracy of the path loss metering method is measured experimentally by two TUTWSN prototype platforms, presented in Figure 3. The platform utilizes 2.4 GHz low power Nordic Semiconductor nRF2401A transceiver, and a Microchip PIC18LF4620 microcontroller. The transceiver has adjustable transmit power level from -20 dBm to 0 dBm with four steps. Receiver sensitivity is -85 dBm at 1 Mbps data rate. A full-wave loop antenna provides a dipole-type radiation pattern, and around 4 dBi directivity (simulated). Since the transceiver lacks the RSSI mechanism, the platform is suitable for testing the performance of the path loss metering.

The transmission ranges of beacons with four different transmission power levels (-20 dBm, -10 dBm, -5 dBm and 0 dBm) are measured outdoors in a park in a fairly open space, and in a roadside mostly line-of-sight conditions. One plat-

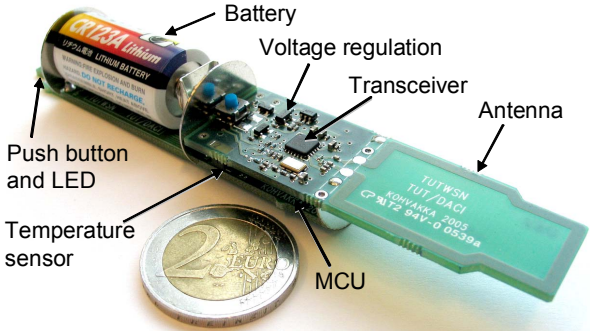

Figure 3: TUTWSN prototype platform.

form is placed 1.5 m above a snowy ground and configured to periodically transmitting beacons. Another node is moved away from the transmitter around 2 m above the ground, and is receiving beacons. The beams of loop antennas are directed towards each other. The minimum transmission power levels of succeed beacon receptions ($min(P_{T(succeed)})$) are recorded as a function of the distance between the transmitting and receiving node, as presented in Figure 4. In an open space, a path loss increases quite proportionally to the distance. Beacons transmitted at -20 dBm, -10 dBm, -5 dBm, and 0 dBm power levels are received until around 25m, 190 m, 350 m and 370 m distances, respectively. In a roadside, a significant radio wave fading and gaining is caused by reflections from ground and surrounding snowy trees and rocks. Beacons transmitted at -20 dBm, -10 dBm, -5 dBm, and 0 dBm power levels are received until around 60 m, 130 m, 340 m and 440 m distances, respectively. The results are reasonable and well comparable to RSSI measurements, such as presented in [8].

The accuracy of the path loss metering method should be sufficient for simple outdoor localization algorithms, such as presented in [5]. According to the measurements, antenna directivity and radio wave reflections have higher effect on the ranging accuracy than the path loss measurements mechanism itself. Localization accuracy would be highly improved by a more omni-directional antenna, such as a monopole.

Indoor measurements are conducted in office environment, presented in Figure 5. A beacon transmitting node is marked with *TX* and placed on a corridor around 2 m above a floor such that antenna beam is directed along the long corridor. The measuring points are marked with the numbers 1 to 4, according to the minimum power level the successfully received beacons are transmitted with. The measurement results are very reasonable. With the smallest -20 dBm transmission power around 40 m distance is achieved. A glass door and a wall attenuate a radio wave 5 to 10 dB.

The accuracy of the path loss metering is sufficient for managing robust network operation. The accuracy for indoor node localization depends on antenna directivity and radiation power, and node density. Since walls and doors cause very significant signal attenuation and reflections, high node density, omni-directional antennas and very low radiation power provide the highest localization accuracy.

B. Power Consumption Analysis

First, the average power consumed by the beacon transmissions and receptions (beacon exchange) caused by the path loss metering mechanism is analyzed. Only the transceiver power consumption is analyzed ignoring all other hardware components. For the analysis, a Nordic Semiconductor nRF24L01 transceiver is selected. The transceiver operates at 2.4 GHz frequency band and has 2 Mbps data rate. To the best of our knowledge, this is the most energy efficient commercial off-the-shelf transceiver available today having 6.25 nJ/bit energy consumption in RX mode and 3.5 nJ/bit energy consumption in TX mode with -18 dBm power level. The transceiver has a carrier detect functionality, but lacks RSSI. In the analysis, a beacon transmission power level is adjusted between -18 dBm and 0 dBm. A beacon length is 24 B to comply with the LR-WPAN standard [6].

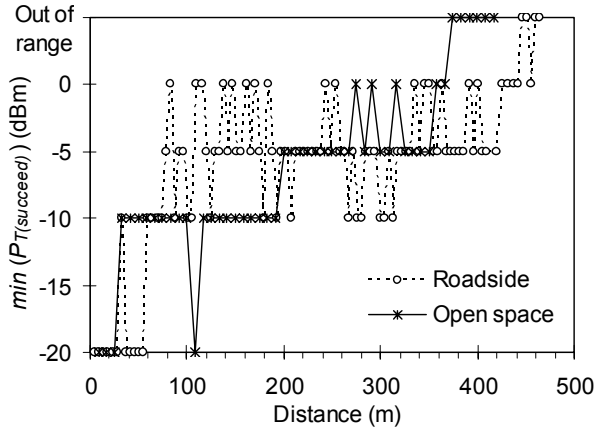

Figure 4: The minimum beacon transmission powers as a function of transmission distance in outdoor environment.

During a beacon interval, one set of one to four beacons are transmitted and received. This corresponds to the operation of a routing node in WSN. Transceiver start-up transients, crystal inaccuracy (20 ppm), and sleep mode power consumption are included in the analysis. For comparison, the same analysis is performed for a LR-WPAN compliant Chipcon CC2420 transceiver. Since the transceiver has an RSSI mechanism, only one beacon transmission and one reception during a beacon interval are required for a basic MAC operation.

The power consumption results are presented in Figure 6. The beacon exchange power consumption is typically far below 10 µW. With 4 s beacon interval (*BI*) a basic MAC operation with single beacon transmissions and receptions consumes 3.51 µW with the nRF24L01 transceiver. If two bea-

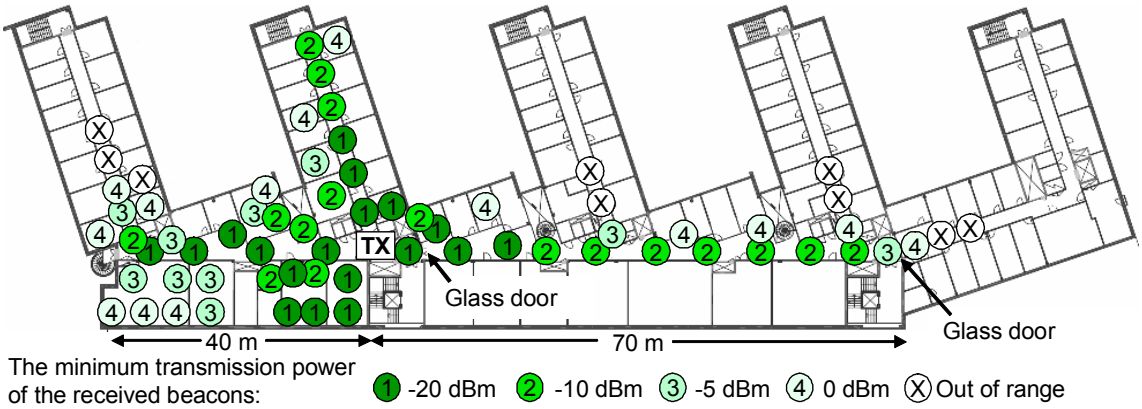

Figure 5: Test points and the minimum transmission powers of received beacons in office environment.

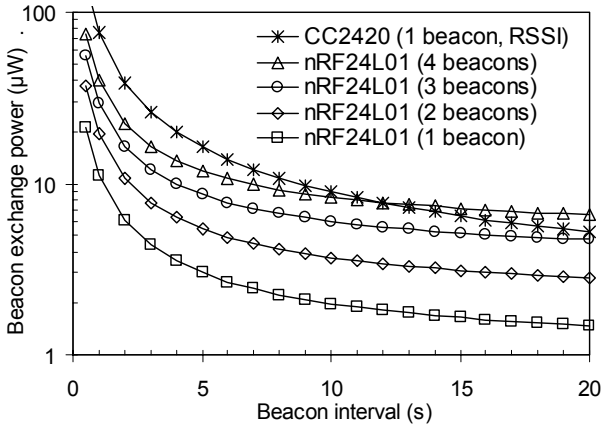

Figure 6: Beacon exchange power consumption as a function of a beacon interval with one to four beacons.

cons are sufficient for the path loss metering method, the increase for power consumption is 2.78 µW resulting 6.29 µW beacon exchange power. With four beacons, beacon exchange power is 13.6 µW. For comparison, the CC2420 transceiver beacon exchange power consumption with single beacons and RSSI measurements is 20.08 µW. Clearly, the increase of transmitted beacons increase measurement accuracy, but raise beacon exchange energy consumption. Energy can be saved by transmitting two beacons, but randomizing the transmission power of the lower power beacon. For maintaining network connectivity, the range of beacon transmissions must not vary, and the higher power beacon is always transmitted with the highest power. Thus, a node can accurately measure path loss during the time of few beacon intervals.

For demonstrating the energy efficiency of an entire WSN node utilizing the path loss metering method, the power consumption of a routing LR-WPAN coordinator is mathematically analyzed in a large-scale WSN application. Network energy consumption is minimized by selecting a cluster-tree network topology with a beacon-enabled mode. The analyzed coordinator routes data from ten associated devices (n_D) and one child coordinator (n_C), which forwards data from 200 child and grandchild nodes (n_{DL}). A low data rate sensing application is executed, where each node transmits a sensor value to uplink direction at 30 s intervals (I_U). Each sensing item (L_S) is 8 B long containing a sensor value, a node ID, and a time stamp. In addition, control and configuration data is broadcasted to downlink direction at 120 s intervals (I_D). This results totally 460 bits/s throughput requirement through the coordinator. A MAC superframe order is fixed to 2 resulting 57.6 ms Contention Access Period (CAP) length. Network dynamics and link failures are included in the analysis by averagely 1 hour network scan interval (I_{NS}), where each scan consumes energy E_{NS}. A probabilistic number of beacon reception attempts (p_B) is 75% of transmitted beacons (n_B), as more than one beacons are transmitted.

The performance of LR-WPAN is analyzed in a star network in [9]. We complement the performance analysis with contention models in a cluster-tree network. LR-WPAN MAC is prone to two types of collisions; collisions caused by the hidden node problem, and the selection of a same backoff slot with another node. The probability of a hidden node collision (p_h) between two nodes associated with a same coordinator, but outside the range of each other is modelled with the durations of a data (t_{DATA}) frame, an acknowledgement (t_{ACK}) frame and CAP (t_{CAP}) as

$$p_h = 2\frac{t_{DATA} + t_{ACK}}{t_{CAP}}. \tag{2}$$

Nodes randomize backoff delays using a backoff exponent (BE) initialized with *macMinBE* (default is 3). The probability (p_d) that two nodes select the same backoff delay is

$$p_d = \frac{1}{2^{BE} - 1}. \tag{3}$$

For modelling the probability of a successful transmission (p_s), models for the average number of data transmissions (d) and contenting nodes (C) in CAP are defined as

$$d = BI\left[\left(\frac{1}{I_U} + \frac{2}{I_D}\right)n_D + \frac{n_{DL}}{I_U N} + \frac{2n_C}{I_D}\right]u, \tag{4}$$

$$C = \min\left[\left(\frac{1}{I_U} + \frac{2}{I_D}\right)BIu, 1\right]n_D + \min\left[\left(\frac{n_{DL}}{I_U N} + \frac{2n_C}{I_D}\right)BIu, 1\right], \tag{5}$$

where u is the expected number of retransmissions. I_D is divided by 2 for approximating the effect of indirect communication. Coordinator aggregates data from n_{DL} nodes by transmitting N (defined as 12) sensing items in a frame. Thus, p_s can be modelled as

$$p_s = s(1 - p_h)^{hd}(1 - p_d)^C, \tag{6}$$

where h is the probability that two nodes in the range of a coordinator have a hidden node relationship (41% according to [10]), and s [9] is the probability of a successful clear channel assessment after *macMaxCSMABackoffs* attempts.

A frame is transmitted $a = aMaxFrameRetries+1$ times before declaring a transmission failure. The probability of a successful transmission (v) and the average number of transmission attempts per frame (u) are

$$v = \sum_{k=1}^{k=a} p_s(1 - p_s)^{k-1}, \tag{7}$$

$$u = (1 - v)a + \sum_{k=1}^{k=a} k p_s(1 - p_s)^{k-1}. \tag{8}$$

Finally, coordinator power consumption can be modelled as

$$\begin{aligned} P = {} & \frac{E_{TXB}n_B + E_{RXB} + \max(n_B p_B - 1, 0)E_{RXBU}}{BI} \\ & + t_{CAP}P_{RX} + \frac{(E_{TXD} + E_{RXA})(n_D + n_{DL})u}{I_U N} \\ & + \frac{(E_{TXD} + E_{RXA} + E_{RXDD} + E_{TXA})u}{I_D} + \frac{E_{NS}}{I_{NS}}, \end{aligned} \tag{9}$$

where E_{TXB}, E_{RXB}, E_{RXBU}, E_{TXD}, E_{TXA}, E_{RXA}, *and* E_{RXDD} are the energy consumptions of a beacon transmission and reception, an unsuccessful beacon reception, a data transmission, an

Table 2: Comparison of analyzed transceivers.

Radio	data rate [kbps]	RSSI	sleep [µA]	RX [mA]	TX (0dBm) [mA]	TX (-10dBm) [mA]
CC2400	1000	Yes	1.5	24	19	13
CC2420	250	Yes	0.02	18.8	17.4	11
nRF24L01	2000	No	0.9	12.3	11.3	7.5

acknowledge transmission and reception, and a data reception after a data request, respectively. P_{RX} is the coordinator power consumption in reception mode. Moreover, the achieved goodput (G) through a coordinator can be modeled with a requested throughput and v as

$$G = \left(\frac{n_D + n_{DL}}{I_U} + \frac{2(n_D + n_C)}{I_D} \right) L_S v. \quad (10)$$

Power consumptions and goodputs are separately analyzed for three low power 2.4 GHz transceivers, presented in Table 2. Chipcon CC2400 and CC2420 transceivers have RSSI mechanism, while Nordic Semiconductor nRF24L01 utilizes the implemented path loss metering method. Since the CC2400 transceiver has RSSI and high 1 Mbps data rate, high energy efficiency is expected. All the transceivers have on-chip data buffers for transmitted and received data, which allows interfacing with low-speed microcontrollers. Data buffer sizes are 32 B for nRF24L01 and CC2400 transceivers, and 128 B for the CC2420 transceiver. The rest of the analyzed hardware is similar to the TUTWSN prototype platform, presented in Figure 3.

Resulted coordinator power consumption as a function of achieved goodput is plotted in Figure 7. Results are calculated with 2.0 V supply voltage. According to the analysis, CC2420, CC2400 and nRF24L01 transceivers can achieve over 435 bits/s goodput with 2.25 mW, 1.45 mW, and 0.703 mW power consumptions, respectively. The beacon intervals in these points are 1.97 s, 3.93 s and 3.93 s, respectively (not shown in the figure). By increasing the number of beacons to four, the nRF24L01 achieves the same goodput with 0.711 mW power. The results indicate that energy saving using the lowest complexity transceiver is very considerable, and the energy consumption of the path loss metering method is insignificant. According to the analysis, the minimum power consumption with the nRF24L01 transceiver is 0.316 mW, which is achieved with 333 bits/s goodput and 15.7 s beacon interval. At longer beacon intervals the loading of CAP increases significantly, which increases collisions and retransmissions. This further increases CAP loading reducing achieved goodput and increasing power consumption, as seen with the nRF24L01 results. Also, the energy for network scan is very significant at long beacon intervals.

IV. CONCLUSIONS

The implementation of a simple transmission power based path loss metering method is presented. According to performance measurements, the method can provide the functionality of RSSI for the lowest complexity and power transceivers with very low power consumption. In the analyzed large-scale LR-WPAN application, the path loss metering consumes less than 0.5% of the entire node power consumption. In addition, achieved power saving by using the nRF24L01 transceiver and the path loss metering method is 69% compared to the CC2420 LR-WPAN compliant transceiver with RSSI. Compared to the CC2400 low power RSSI equipped transceiver, the power saving is still over 51%.

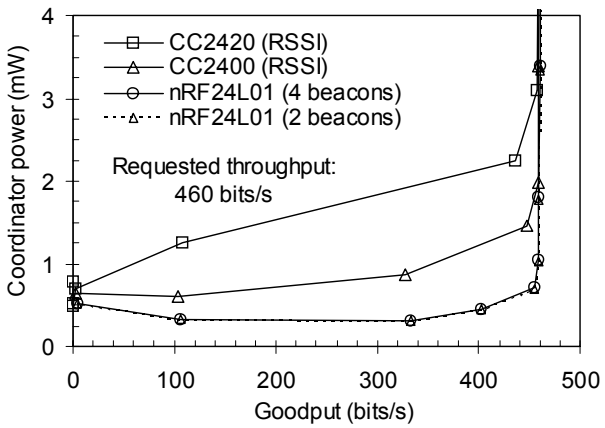

Figure 7: LR-WPAN coordinator power consumption as a function of achieved goodput.

REFERENCES

[1] H. Karl and A. Willig. *Protocols and Architectures for Wireless Sensor Networks*, John Wiley & Sons Ltd., Chichester, pages 1-13. 2005.

[2] F. Jin, H.-A. Choi and S. Subramaniam. Hardware-aware communication protocols in low energy wireless sensor networks. In *Proceeding of the IEEE Military Communications Conference*, volume 22, no. 1, Boston, USA, pages 676-681, 2003.

[3] M. Sikora, J.N. Laneman, M. Haenggi, D.J. Costello, Jr. and T. Fuja. On the Optimum Number of Hops in Linear Wireless Networks. In *Proceedings of the IEEE Information Theory Workshop*, Texas, USA, pages 165-169, 2004.

[4] T.S. Rappaport, Wireless Communications – Principles and Practice, Prentice Hall, 1996.

[5] M.L. Sichitiu, V. Ramadurai and P. Peddabachagari. Simple Algorithm for Outdoor Localization of Wireless Sensor Networks with Inaccurate Range Measurements. In *Proceedings of the International Conference on Wireless Networks*, Nevada, USA, pages 300-305, 2003.

[6] IEEE Std 802.15.4-2003, wireless medium access control (MAC) and physical layer (PHY) specifications for low-rate wireless personal area networks (WPANs).

[7] Y. Wei, J. Heidemann and D. Estrin. Medium access control with coordinated adaptive sleeping for wireless sensor networks. *IEEE/ACM Transactions on Networking*, 12(3): 493-506, June 2004.

[8] N. Reijers, G. Halkes and K. Langendoen. Link Layer Measurements in Sensor Networks. In *Proceedings of the 1st IEEE International Conference on Mobile Ad-hoc and Sensor Systems*, Florida, USA, pages 224-233, 2004.

[9] N.F. Timmons and W.G. Scanlon. Analysis of the performance of IEEE 802.15.4 for medical sensor body area networking. In *Proceedings of the 1st Annual IEEE Communications Society Conference on Sensor and Ad Hoc Communications and Networks,* California, USA, pages 16-24, 2004.

[10] Y.-C. Tseng, S.Y. Ni and E.Y. Shih. Adaptive approaches to relieving broadcast storms in a wireless multihop mobile ad hoc network. *IEEE Transactions on Computers*, 52(5): 545-557, May 2003.

PUBLICATION 3

M. Kohvakka, M. Kuorilehto, M. Hännikäinen, and T. D. Hämäläinen, "Network Signaling Channel for Improving ZigBee Performance in Dynamic Cluster-Tree Networks," *EURASIP Journal on Wireless Communications and Networking*, vol. 8, no. 3, pp. 1–15, January 2008.

Hindawi Publishing Corporation
EURASIP Journal on Wireless Communications and Networking
Volume 2008, Article ID 456535, 15 pages
doi:10.1155/2008/456535

Research Article

Network Signaling Channel for Improving ZigBee Performance in Dynamic Cluster-Tree Networks

Mikko Kohvakka, Jukka Suhonen, Mauri Kuorilehto, Marko Hännikäinen, and D. Hämäläinen

Institute of Digital and Computer Systems, Tampere University of Technology, P.O. Box 553, Tampere 33101, Finland

Correspondence should be addressed to Mikko Kohvakka, mikko.kohvakka@tut.fi

Received 30 April 2007; Revised 26 October 2007; Accepted 19 January 2008

Recommended by Biao Chen

ZigBee is one of the most potential standardized technologies for wireless sensor networks (WSNs). Yet, sufficient energy-efficiency for the lowest power WSNs is achieved only in rather static networks. This severely limits the applicability of ZigBee in outdoor and mobile applications, where operation environment is harsh and link failures are common. This paper proposes a network channel beaconing (NCB) algorithm for improving ZigBee performance in dynamic cluster-tree networks. NCB reduces the energy consumption of passive scans by dedicating one frequency channel for network beacon transmissions and by energy optimizing their transmission rate. According to an energy analysis, the power consumption of network maintenance operations reduces by 70%–76% in dynamic networks. In static networks, energy overhead is negligible. Moreover, the service time for data routing increases up to 37%. The performance of NCB is validated by ns-2 simulations. NCB can be implemented as an extension on MAC and NWK layers and it is fully compatible with ZigBee.

1. INTRODUCTION

Wireless sensor network (WSN) is an emerging technology enabling fully autonomous self-configuring ad-hoc networks [1]. WSN may consist of thousands of small nodes, which sense their environment, communicate wirelessly with each other, and share collaborative tasks. Nodes route sensed data and events to a sink node, which forms a gateway to other networks. WSN nodes may be embedded deeply in our living environment or operate under harsh conditions in outdoors or a machinery hall. Thus, a high tolerance against unreliable radio links, variable network size, and mobile nodes is required [2, 3]. Due to the large number of nodes, battery replacements are difficult. Hence, nodes may have to scavenge supply energy solely from their operation environment [4], or operate up to several years with small batteries. This necessitates very high energy-efficiency in communication protocols, algorithms, and hardware platforms. WSNs have a vast number of potential applications [5], for example monitoring and controlling in home, office, and industrial environments, monitoring of remote or hostile geographical regions, tracking of animals and objects, and surveillance.

The wireless personal area networks (WPANs) working group was initially focused on creating the IEEE 802.15.1 standard for physical (PHY) and medium access control (MAC) layers based on Bluetooth technology [6]. The working group soon formed two other subgroups, firstly IEEE 802.15.3 focusing on high-speed WPAN [7] for multimedia applications. In December 2000, IEEE 802.15.4 [8] low-rate WPAN was initiated for providing low-complexity, low-cost, and low-power wireless connectivity among inexpensive devices, such as WSN nodes [9]. ZigBee [10] is an open specification for low-power wireless networking, which complements IEEE 802.15.4 with a network layer, security modes, and application profiles. The first version of the ZigBee specification was announced in December 2004.

IEEE 802.15.4 together with ZigBee is one of the most potential standardized technologies for enabling WSNs. As available energy is scarce, the beacon-enabled network is essential, since time synchronized sleep and wakeup mechanism can be adopted [11]. Moreover, large network size with widely located nodes is enabled by a cluster-tree network topology. By these settings, ZigBee can achieve very high energy-efficiency in static networks [12]. However, even an immobile WSN has a dynamic behavior caused by

low-transmission power levels combined with dynamic operating environment, such as opened and closed doors, moving objects, and interferences from other networks that all affect radio frequency (RF) propagation. In addition, many envisioned WSN applications, such as asset tracking and interactive games, require mobility support for nodes. In these conditions, ZigBee performance is unsatisfactory due to energy-hungry passive scan operations. Hence, techniques for reducing passive scan energy are one of the key challenges.

In this paper, we propose a network channel beaconing (NCB) algorithm for improving the performance and reducing the energy consumption of ZigBee in dynamic networks. NCB utilizes frequent beacon transmissions on a dedicated network signaling channel. A passive scan is performed by receiving these beacons resulting in dramatically reduced passive scan duration and energy consumption in low-data-rate applications. NCB can be implemented as a manufacturer specific extension on MAC and NWK layers and it is fully compatible with standard ZigBee devices.

The rest of this paper is organized as follows. The related work is discussed in Section 2. An introduction to ZigBee and IEEE 802.15.4 standard is presented in Section 3. Section 4 presents the design of NCB. The performance of NCB equipped ZigBee is analyzed and compared against standard ZigBee in Section 5. In Section 6, the beacon transmission rate of NCB is energy optimized for further energy saving. Simulations for validating the results are presented in Section 7. Finally, this paper is concluded in Section 8.

2. RELATED WORK

Most of researches about the IEEE 802.15.4 beacon-enable network have been restricted to a star topology. The performance of a star network with 10 nodes has been analyzed in [13]. The analysis focused on the effect of crystal tolerance, a frame size, and the usage of guaranteed time slots (GTSs) on a node lifetime. Bougard et al. [14] have presented a mathematical analysis of a large-scale star network. A special contribution is bit error rate measurements with two evaluation boards connected through a set of calibrated attenuators. The operational analysis considers mainly the effect of path loss and packet size on energy consumption. The performance simulations of IEEE 802.15.4 in a star network have been presented in [15]. It has been found that a significant energy saving is achieved by a low-duty-cycle operation.

An analysis and experimental measurements of IEEE 802.15.4 in a cluster-tree network has been presented in [11]. It has been found that beacon-enabled cluster-tree networks are prone to beacon collisions, which will lead to synchronization failures. The beacon collisions can be reduced by utilizing a rather long beacon interval. Clearly, another option is to use more frequency channels for the network. Yet, both of these options increase the energy consumption of passive scans proprotionally.

Beacon collisions can also be reduced by scheduling. A wakeup scheduling scheme presented in [16] utilizes synchronized superframe timing such that coordinators begin beaconing at the same time, and active periods are fully overlapping. Since entire inactive period can be used for sleeping, energy consumption is reduced. To reduce collisions, beacon transmission period is extended to contain a number of subslots during which beacons can be sent. Yet, the selection of a noninterfering subslot has not been specified. Another scheduling scheme presented in [17] organizes the entire active periods of different coordinators in a nonoverlapping manner. This minimizes the changes to the current IEEE 802.15.4 specification. Scheduling has also been proposed for reducing hidden node collisions that are typical for the carrier sense multiple access with collision avoidance (CSMA-CA) mechanism of IEEE 802.15.4 [18].

While the above scheduling schemes utilize software-based time synchronization; also hardware-based synchronization mechanisms exist. RT-Link [19] is a time division multiple access (TDMA) MAC protocol for multihop WSNs. The protocol employs two out-of-band synchronization sources: atomic clock broadcasts for outdoors and amplitude modulation (AM) transmissions for in indoor conditions. The latter utilizes building's power grid as an antenna to radiate time sync pulses. According to experimental measurements, the hardware-based synchronization is robust, scalable, and energy-efficient option to software-based techniques. Yet, the hardware cost and complexity are increased.

In our previous work [12], we have analyzed the performance of IEEE 802.15.4 and ZigBee in large-scale WSN applications. An energy analysis on a cluster-tree multihop network indicated that the highest energy-efficiency in a low-data-rate WSN application is achieved by moderate (30.7 milliseconds) superframe duration and by scaling beacon interval according to requested throughput. According to simulations, random error situations are energy-hungry, since they usually cause the reconstruction of a complete subtree. During the reconstruction, leaf nodes may need to perform several passive scans until the above network hierarchy is initialized. Simulations also depicted that the probability that two coordinators randomize the same slot for their superframes is significant. For better scalability, it would be advantageous to divide clusters into several frequency channels.

Furthermore, our previous work [20] has proposed the use of frequent beacon transmissions to improve the performance of synchronized low-duty-cycle MAC protocols in dynamic networks. The work focused on flat networks, for which energy optimized beacon rate was determined. It has been found that optimized beacon rate results in a very significant energy saving.

In this paper, we will extend our idea of frequent beacon transmissions to ZigBee. In contrast to [20], we will utilize a cluster-tree network topology and a dedicated network signaling channel for frequent network beacons. Network beacons allow energy-efficient passive scans on the network channel, independently from the utilized IEEE 802.15.4 beacon interval and the amount of frequency channels for superframes. This enables the optimization of energy-consumption and scalability in dynamic networks. As the network beacons are transmitted on the network channel only; collisions with data and control frames are eliminated. We will also present performance analysis of the network

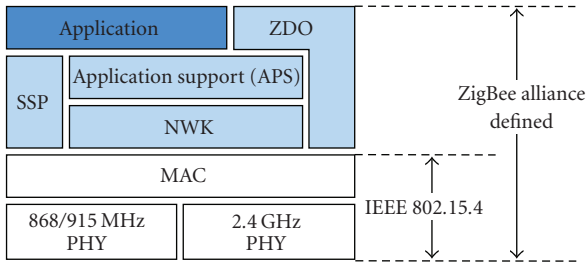

Figure 1: IEEE 802.15.4 and ZigBee.

channel approach. Performance models are validated by simulations.

3. ZigBee AND IEEE 802.15.4 OVERVIEWS

3.1. ZigBee protocol stack

A ZigBee protocol stack is presented in Figure 1 [21]. An application layer at the top of the stack determines node relationships, and supervises network initiation and association functions. Overall node management is performed by a ZigBee device object (ZDO). Application endpoints may call ZDO in order to discover other ZigBee nodes on the network and the services they offer, and to define security and network settings. A security service provider (SSP) offers security functions including encryption, key generation, key distribution, authentication, and access control lists.

A network (NWK) layer provides network self-organization and multihop routing capability. NWK performs route discovery and maintenance, and message relaying functions. NWK can initiate a new network and assign network addresses to new nodes associating with the network for the first time.

An application support (APS) sublayer connects NWK, SSP, and endpoints, and routes messages to different endpoints.

MAC and PHY layers are defined by IEEE 802.15.4. MAC is responsible for the channel access mechanism, acknowledged frame delivery, network association, and disassociation.

IEEE 802.15.4 supports two direct sequence spread spectrum (DSSS) PHY layers operating in industrial, scientific, and medical(ISM) frequency bands. A low-band PHY operates in the 868 MHz or 915 MHz frequency band and has a raw data-rate of 20 Kbps or 40 Kbps, respectively. A high-band PHY operating in the 2.4 GHz band specifies a data-rate of 250 kbps and has nearly worldwide availability. The 2.4 GHz frequency band is the most potential for large-scale WSN applications, since the high-radio data-rate reduces frame transmission time and usually also the energy per transmitted and received bit.

3.2. Node types

IEEE 802.15.4 defines three types of logical devices, a personal area network (PAN) coordinator, a coordinator, and a device. ZigBee denotes them as ZigBee coordinator, ZigBee router, and ZigBee end-device, respectively. For clearness, we utilize the naming of IEEE 802.15.4 from now on.

PAN coordinator is the primary controller of PAN, which initiates the network and operates often as a gateway to other networks. Each PAN must have exactly one PAN coordinator. Coordinators collaborate with each other for executing data routing and network self-organization operations. Devices do not have data routing capability and can communicate only with coordinators.

Due to the low-performance requirements of devices, they may be implemented with very simple and low-cost hardware. The standard designates these low-complexity nodes as reduced function devices (RFD). Nodes with the complete set of MAC services are called as full function devices (FFDs).

3.3. Network topologies

The standard supports two network topologies, star, and peer-to-peer, presented in Figure 2. In the star topology, all data exchanges are controlled by a PAN coordinator that operates as a network master, while devices operate as slaves and communicate only with the PAN coordinator. This single-hop network is most suitable for delay critical applications, where large network coverage is not required.

A peer-to-peer topology allows "mesh" type of networks, where any coordinator may communicate with any other coordinator within its range, and have messages multihop routed to coordinators outside its range. This enables the formation of complex self-organizing network topologies. The network may contain also RFDs as devices. Peer-to-peer topologies are suitable for industrial and commercial applications, where efficient self-configurability and large coverage are important. A disadvantage is the increased network latency due to message relaying.

One special type of peer-to-peer topology is a cluster-tree network, defined by ZigBee. The network consists of clusters, each having a coordinator as a cluster head and multiple devices as leaf nodes. A PAN coordinator initiates the network and serves as the root. The network is formed by parent-child relationships, where new nodes associate as children with the existing coordinators. This well-defined structure simplifies multihop routing and allows effective energy saving; each node maintains synchronization of data exchanges with its parent coordinator only. The rest of time, nodes may save energy in a sleep mode. This is not possible in the peer-to-peer networks, where coordinators need to receive continuously to be able to receive data from any node in the range. A disadvantage is that a coordinator failure may cause a large amount of orphaned child and grandchild nodes causing energy wasting during network reassociations [12].

3.4. MAC layer

The MAC layer can operate on both beacon-enabled and nonbeacon modes. In the nonbeacon mode, a protocol is a simple CSMA-CA. This requires a constant reception of possible incoming data. The power saving features that are critical in WSN applications are provided by the beacon-enabled

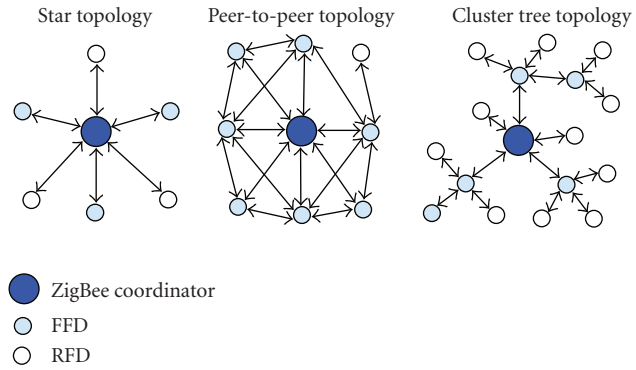

Figure 2: Star, peer-to-peer, and cluster-tree topology examples.

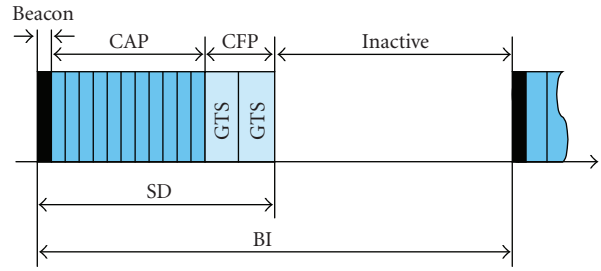

Figure 3: Superframe structure in beacon-enabled mode.

mode. Hence, we concentrate on the beacon-enabled mode from now on.

In the beacon-enabled mode, all communications are performed in a superframe structure presented in Figure 3. A superframe is bounded by periodically transmitted beacon frames, which allows network nodes to synchronize themselves to the network. An active part of a superframe is divided into three parts: the beacon, contention access period (CAP), and contention-free period (CFP). At the end of the superframe is an inactive period, when nodes may enter to a power saving mode.

CAP is a mandatory part of a superframe during which channel is accessed using a slotted CSMA-CA scheme. Coordinators are required to listen to the channel the whole CAP to detect and receive any data from their child nodes. The child nodes may only transmit data and receive an optional acknowledgement (ACK) on demand, which increases their energy-efficiency.

CFP is an optional part of a superframe. Nodes requiring dedicated bandwidth and low-latency transmissions [22] may request GTS from a PAN coordinator. CFP does not utilize any collision avoidance mechanism. Due to inter-cluster collisions, the applicability and benefits of GTS are very limited in large peer-to-peer or cluster-tree networks. In addition, CFP can be utilized only for a direct communication with a PAN coordinator.

The beacon interval (BI) and the active superframe duration (SD) are adjustable by IEEE 802.15.4 parameters beacon order (BO) and superframe order (SO) as

$$\begin{aligned} \text{BI} &= \text{aBaseSuperframeDuration} \times 2^{\text{BO}}, \\ \text{SD} &= \text{aBaseSuperframeDuration} \times 2^{\text{SO}}, \end{aligned} \tag{1}$$

where $0 \le \text{SO} \le \text{BO} \le 14$, and aBaseSuperframeDuration equals 960 radio symbols or 15.36 milliseconds in the 2.4 GHz band. Hence, BI and SD range between 15.36 milliseconds and 251.7 seconds. The superframe structure is maintained by a PAN coordinator. In cluster-tree networks, all coordinators transmit beacons for assisting other nodes to maintain synchronization with them.

For minimizing inter-cluster interferences, it is desirable to concatenate superframes of neighboring clusters. ZigBee specifies that BI is divided into BI/SD slots. During a start-up, each coordinator randomizes a free slot for its superframe.

4. THE DESIGN OF NETWORK CHANNEL BEACONING

The designed algorithm should improve ZigBee energy-efficiency, throughput, and scalability in dynamic low-duty-cycle cluster-tree networks, while the energy overhead in static networks should be insignificant.

A starting point for the design is IEEE 802.15.4 configured to a beacon-enabled mode with inactive period. These settings provide the highest energy-efficiency in static networks. For maintaining the energy-efficiency also in dynamic networks, we focus on minimizing the energy consumption caused by link failures.

4.1. Network scan in IEEE 802.15.4

A network scan over a given list of channels is initiated by a *MLME-SCAN.request* primitive. The most important parameters are *ScanType, ScanChannels,* and *ScanDuration*. *ScanType* is used to select a suitable scan type among energy detection (ED) scan, active scan, passive scan, or orphan scan. *ScanChannels* is a bitmap indicating which channels are to be scanned. *ScanDuration* is used to calculate the length of time to spend scanning each channel. ED scan is used to determine channel usage, active or passive scan to locate beacon frames containing any PAN identifier, or an orphan scan to locate a PAN to which the device is currently associated. Passive and orphan scans are mandatory requirements for all devices. ED and active scans are optional for an RFD.

The ED scan is used by a prospective PAN coordinator to select a suitable channel for a new PAN. The ED scan estimates the received signal power within the bandwidth of a channel, while no attempt is made to identify or decode signal on the channels. Based on the detected energy, the channel with the lowest energy can be selected.

The active and passive scans allow a device to locating any coordinator transmitting beacon frames within its personal operating space (POS). These scan types are used by a prospective PAN coordinator to select a PAN identifier prior to starting a new PAN, or they could be used by a device for selecting a suitable coordinator prior to association.

The active scan is performed by sending a beacon request command and then by receiving for possible beacon frames in return. Upon receiving the beacon request, each node in

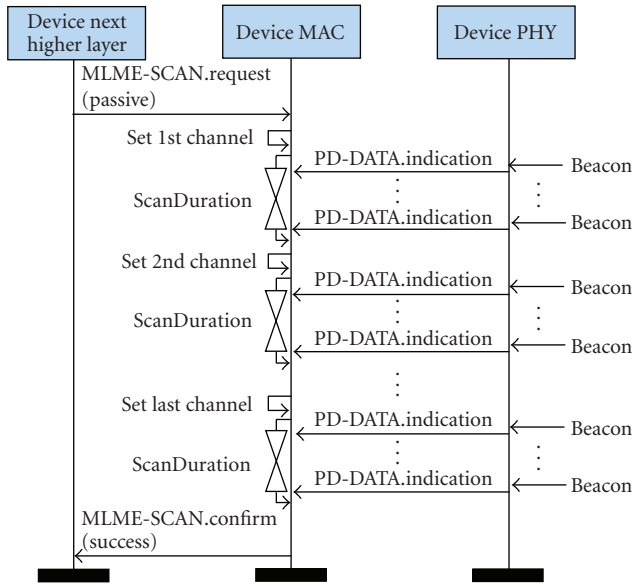

Figure 4: Passive scan message sequence chart of ZigBee.

a range transmits a beacon. This necessitates that each coordinator is continuously in reception mode.

The passive scan is performed by receiving beacons without transmitting any requests. This necessitates that all coordinators transmit beacons at predetermined intervals in some of the specified frequency channels. However, coordinators are not required to be constantly in reception mode allowing the inactive time, which is crucial for energy-efficiency. The message sequence chart of the IEEE 802.15.4 passive scan is presented in Figure 4. For detecting all coordinators in POS, passive scan should be conducted on each selectable channel at least a beacon transmission interval. In ZigBee, passive scan duration equals BI + aBaseSuperframDuration.

The orphan scan allows a device to attempt to relocate its coordinator following a loss of synchronization. The scan is performed in each of specified set of channels by sending an orphan notification command and then by receiving for a possible coordinator realignment command until a *macResponseWaitTime* (491.2 milliseconds at 2.4 GHz band) expires. The scan is terminated, if the realignment command is received, or all the specified channels have been scanned.

The orphan scan is suitable for networks, where coordinators are constantly in reception mode. In energy-efficient networks utilizing the inactive period, coordinators are typically most of time in sleep mode, and the reception of the orphan notification command cannot be guaranteed. Thus, the orphan scan should be replaced by a MAC sublayer reset followed by a passive scan, and a network reassociation, as specified by IEEE 802.15.4.

As the focus of this paper is on networks where all nodes utilize the inactive period, only ED scan and passive scan are applicable. Since ED scan is utilized only at the startup of a PAN coordinator, we can focus purely on the minimization of passive scan energy consumption.

4.2. Minimization of passive scan energy

Passive scan energy consumption is a product of transceiver power consumption in reception mode and passive scan duration. Since it is difficult to affect the transceiver power characteristics, we focus on minimizing the scanning time.

As found in [19], the energy consumption of a one second long network (passive) scan equals the energy of nearly 3000 beacon transmissions by a typical low-power transceiver. One can easily conclude that it is worthwhile to increase beacon transmissions rate by reducing BI. Yet, the cost of a shorter BI is increased beacon reception energy due to beacon synchronization. Due to time drift, the synchronized reception of beacons is also more energy hungry than the transmission of them.

For eliminating this drawback, the designed NCB algorithm utilizes additional beacon transmissions on a dedicated network signaling channel. These *network beacons* are transmitted without collision avoidance independently from the IEEE 802.15.4 specified beacons (*standard beacons*) and received during passive scans only. Since the dedicated network channel eliminates collisions with data transmissions, the transmission rate of network beacons can be significantly higher than the rate of standard beacons. This effectively minimizes the required passive scan duration reducing both energy consumption and data routing breaks. Moreover, the passive scan duration is independent from BI and the number of utilized channels for superframes, which is a major improvement for the standard passive scan. Thus, the scalability can be improved by increasing BI length and the number of utilized frequency channels, while maintaining rapid and low-energy passive scans. As the 2.4 GHz and 915 MHz, frequency bands have 16 and 10 selectable channels, respectively, the use of a separate network signaling channel is feasible.

In principle, the network beacons are used for searching a suitable coordinator with which to associate. Then, the association is performed on the *cluster channel* of a desired coordinator, where standard beacon, data, and control frames are exchanged. In practice, occasional collisions between beacons are possible. However, they do not interfere with data and control frame exchanges, or the standard beacon synchronization. Assuming that the transmission interval of network beacons is around two orders of magnitude longer than a beacon length, the probability of collisions is very low in sparse networks. In dense networks, we can assume that adequate number of beacons can be received correctly even though some collisions occur.

Due to frequency selective channel fading, the link quality of the network and cluster channels may differ [23]. This causes two consequences: all coordinators in the range of the cluster channel are not detected, or the signal strength of a selected coordinator is too low for communication, when operation is switched to the cluster channel. However, we can assume that an adequate number of network beacons can be received during the passive scan for ensuring network connectivity. According to the schedule and frequency channel information of received network beacons, a node attempts to receive the standard beacons, one after another, until

a suitable coordinator with adequate signal strength is found. Standard beacons are received accurately at the specified moments minimizing the energy consumption of idle listening.

If the network beacons of two coordinators collide, collisions are also probable with beacons transmitted later on, because beacons are sent periodically at constant intervals. To prevent beacon collisions without the need of network beacon scheduling, we propose delaying network beacon transmission by a random jitter (J), defined as

$$J = \varphi[0 \cdots J_{\mathrm{MAX}}] \cdot t_{\mathrm{TXB}}, \tag{2}$$

where $\varphi[a, b]$ is a random function on the interval $[a, b]$, J_{MAX} is the maximum jitter, and t_{TXB} is the time required to send a network beacon.

As presented in Figure 5, network beacons are broadcasted by all coordinators during inactive periods. This is easily managed by a single radio transceiver. Normally, network beacons are transmitted at rate f_N. However, assuming one radio per station, a coordinator may not send a network beacon, while maintaining an active period or communicating with another coordinator. Then, the transmission of a beacon must be delayed until the end of the active period, causing at most $1/f_N$ + SD interval between network beacons. While it is possible to avoid delaying the transmission by selecting suitable network beacon interval and active period boundaries, the presented interval is considered as a practical network scan time with NCB.

The algorithm operates similarly on PANs operating on a single channel and PANs, where coordinators are divided into several frequency channels. Additional information carried in network beacons in respect to IEEE 802.15.4 beacons are an exact time to the beginning of the next superframe, and the frequency channel of the coordinator. The presented design does not have any effect on the standard beacons transmitted at the beginning of superframes.

The message sequence chart of a passive scan utilizing NCB is presented in Figure 6. As network beacons are transmitted at rate f_N, passive scan is performed by the MLME-SCAN.request primitive by setting: *ScanType* = passive, *ScanChannels* = network channel, and *ScanDuration* = $1/f_N$ + SD.

If the network will be deployed in an environment having high-RF interferences, some frequency channels may be locally jammed [23]. The robustness of network channel can be improved by defining two network channels, where network beacons are transmitted consecutively. Correspondingly, a passive scan is conducted on the both channels. The network channels should be selected before deployment according to RF spectrum measurements. It should also be noted that it is always possible to fall back into the standard passive scan. However, in the rest of this paper we assume rather low-RF interferences and utilize one network channel.

4.3. Implementation guidelines

The management functions of NCB algorithm should be implemented on the NWK layer. In addition, IEEE 802.15.4 MAC should be modified by adding functionality for network beacon transmissions. The format of network beacons is a slight variation of an IEEE 802.15.4 beacon frame. We suggest replacing the fields *GTS fields* and *pending addresses* of the IEEE 802.15.4 beacon frame with *time to next superframe* and *coordinator channel*, as illustrated in Figure 7. For adequate resolution, the space allocated for these fields are 4 B and 1 B, respectively. The initialization and transmissions of network beacons are very similar to standard beacons.

For maintaining all the benefits of standardized technology, interoperability with standards is essential. In principle, a ZigBee node should be able to find a NCB equipped coordinator by a passive scan and to associate with it and vice versa.

We suggest adding a NCB specification field in the payload of standard beacons specifying the utilized network channel, and the transmission rate of network beacons. The NCB field that can be utilized for determining is NCB supported in the PAN.

At a startup, a new PAN coordinator should perform active/passive and an ED scans, as specified by IEEE 802.15.4. According to the scans, free channels for the PAN and network beacons are selected, and beacon transmissions are initiated.

At a startup, other nodes perform a passive scan and select a suitable PAN to associate with, as specified in IEEE 802.15.4. According to the NCB specification field, nodes determine the usage of network channel in PAN. If NCB is supported, network beacon transmissions are initiated. For allowing compatibility with nodes lacking the NCB functionality, the standard specified passive scan should be performed each time the NCB passive scan cannot find suitable parents. Since the NCB algorithm does not affect standard beacon transmissions, the ordinary passive scan easily finds all nodes resulting in cross-compatibility with ZigBee.

For the highest energy-efficiency, it is important to energy to optimize network beacon rate according to the level of network dynamics [19]. A successful operation of NCB necessitates that the network beacon rate is uniform and globally known in entire network. It is possible to predetermine the network beacon rate according to presumable network dynamics in a given application. However, a more efficient option is to adjust the network beacon rate dynamically. We suggest that each node observes and maintains a record of an average link lifetime. The maintained values are transmitted to a PAN coordinator in data frames upon a request. It is suggested that the PAN coordinator broadcasts the request at regular intervals, for example once per hour. According to the gathered link lifetimes, the PAN coordinator determines an energy optimal network beacon rate for the PAN. The network beacon rate is flooded through the network by utilizing the NCB specification field of standard beacons minimizing a control frame overhead.

5. PERFORMANCE ANALYSIS

To be able to analyze purely the effect of NCB on the energy of network maintenance operations, we first divide the energy consumed by the wireless communication into three classes [19]: *node startup*, *network maintenance*, and *data exchange* energies, as illustrated in Figure 8. Node startup

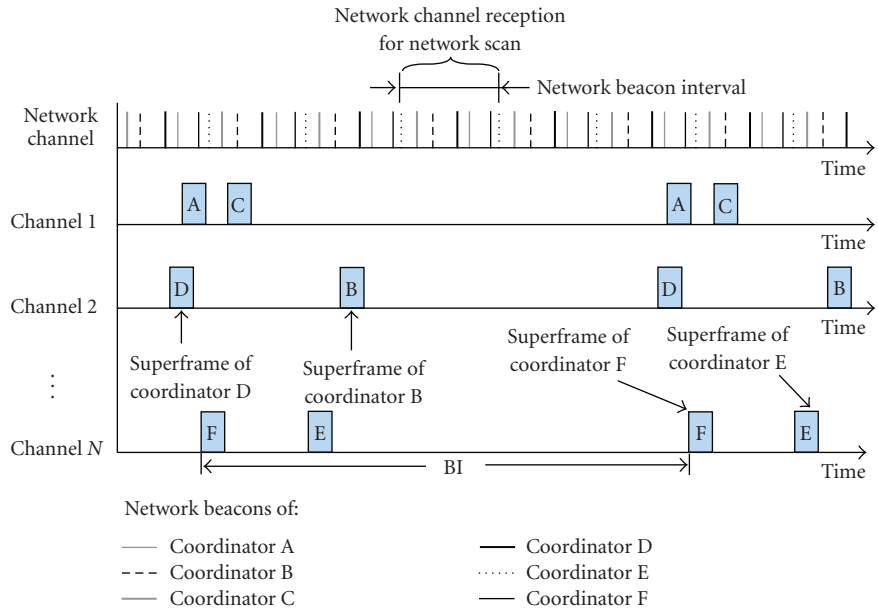

Figure 5: Principle of frequent network beacons.

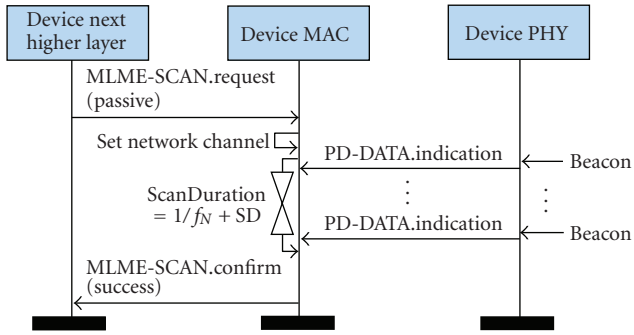

Figure 6: Passive scan message sequence chart of NCB equipped ZigBee.

energy is composed of a passive scan for detecting coordinators in a range, and a network association for connecting the node to the network. The network association consists of control packet exchange according to the IEEE 802.15.4 specification. Network maintenance and data exchange operations are executed after the startup period. Network maintenance energy consists of beacon transmissions and reception, passive scans, and network reassociations according to occurred link failures. Data exchange energy is consumed by upper-layer payload data and acknowledgement transmissions and receptions. We define that network beacon transmissions have lower priority than data exchanges. Hence, network beacon broadcasts do not affect data exchange energy. From now on, we can focus on the minimization of network maintenance energy.

Next, the performance analysis of NCB algorithm in a WSN application will be presented. The analysis begins by an energy analysis of a reference hardware platform, and proceeds to network maintenance power analysis through MAC operation models.

5.1. Hardware platform

To obtain realistic results, steady-state power consumptions of a commercial IEEE 802.15.4 compliant Chipcon CC2420EM/EB [24] transceiver evaluation board are measured. In addition, the power consumption of a PIC18LF8722 [25] microcontroller is measured to estimate the energy consumption of a low-power MAC protocol processor. The measured power consumptions of the platform in different operation modes are presented in Table 1. Highest power of 56.5 mW is consumed in reception mode (P_{RX}). In transmission mode, power consumption varies from 26.6 mW to 48.0 mW. We define that frames are always transmitted with the highest transmission power level resulting in 48.0 mW transmission power (P_{TX}). Sleep more power consumption is 30 μW. Table 2 presents the measured transient times as the transceiver switches from sleep to idle mode and from idle to active (RX or TX) mode. The transient times from active to idle and from idle to sleep mode are negligible.

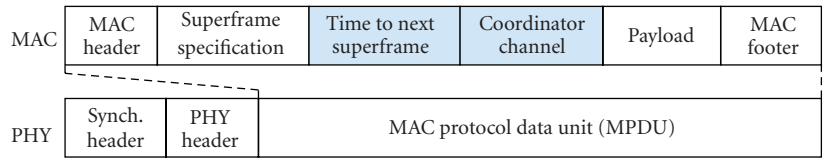

Figure 7: Suggested format of an NCB network beacon frame.

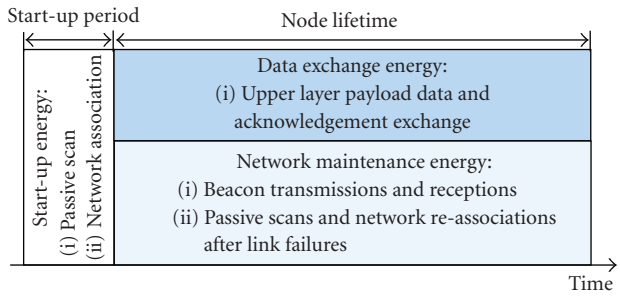

Figure 8: Node energy consumption classification.

Table 1: Measured static platform power consumptions at 3 V supply voltage.

Symbol	MCU mode	Radio mode	Power consumption
P_{TX}	Active	TX (0 dBm)	48.0 mW
	Active	TX (−1 dBm)	45.0 mW
	Active	TX (−3 dBm)	42.1 mW
	Active	TX (−5 dBm)	39.1 mW
	Active	TX (−7 dBm)	36.0 mW
	Active	TX (−10 dBm)	32.9 mW
	Active	TX (−15 dBm)	29.8 mW
	Active	TX (−25 dBm)	26.6 mW
P_{RX}	Active	RX	56.5 mW
P_I	Active	Idle	2.79 mW
P_S	Sleep	Sleep	30 μW

Table 2: Measured chipcon CC2420 transient times.

Symbol	Description	Time (μs)
t_{ST}	Sleep to idle	970
t_{IA}	Idle to active	192

5.2. Network configuration

We analyze the energy-efficiency of NCB in a cluster-tree network, where each cluster contains n_D (11) devices and n_C (2) child coordinators. Network depth (d) is 4 levels of hierarchy. Coordinators broadcast standard beacons once per BI resulting a standard beacon rate $f_C = 1/\text{BI}$, where BI gets values between 0.246 second and 15.7 seconds. Network beacon rate f_N is varied from 0.1 Hz to 100 Hz. The network operates on n_{CH} channels. The utilized parameters and their values are presented in Table 3.

5.3. MAC operation models

To be able to analyze the network maintenance energy, MAC operation models are defined for a beacon transmission, a beacon reception, and a passive scan.

A beacon frame transmission consists of a sleep-to-idle (t_{SI}) transient, idle-to-active (t_{IA}) transient, and actual data transmission defined as the ratio of beacon frame length (L_B) and radio data-rate (R). No CCA analysis is needed for a beacon frame. During the sleep-to-idle transient, radio power consumption equals P_I, after which power consumption rises to P_{TX}. The beacon transmission energy (E_{TXB}) is

$$E_{TXB} = t_{SI}P_I + (t_{IA} + L_B/R)P_{TX}. \quad (3)$$

The resulting energy consumption per transmitted frame is $E_{TXB} = 39.6\,\mu$J, which equals 190 nJ per a PHY layer data bit.

A beacon reception begins with radio startup transients. The radio is in reception mode until a beacon frame has been received including a time margin required due to synchronization inaccuracy (t_I), and the time drift between a transmitting and a receiving node. As synchronization is obtained by standard beacon receptions; the time drift caused by crystal tolerance (ε) is directly proportional to BI. The beacon reception energy (E_{RXB}) is

$$E_{RXB} = t_{SI}P_I + (t_{IA} + 2\varepsilon\text{BI} + t_I + L_B/R)P_{RX}. \quad (4)$$

The resulting energy consumption per received frame is $E_{RXB} = 70.2\,\mu$J (BI = 0.96 second). This equals 338 nJ per a PHY layer data bit.

A passive scan begins with the startup transients. Then, a radio is in RX mode during passive scan duration (t_{NS}). The energy required for message exchanges during a reassociation is negligible compared to the energy of the passive scan, and thus it is ignored in the following analysis. Thus, the passive scan energy (E_{NS}) is

$$E_{NS} = t_{SI}P_I + (t_{IA} + t_{NS})P_{RX}. \quad (5)$$

The passive scan duration depends on the utilization of NCB. For ZigBee, the durationis a function of the number of scanned cluster channels and a beacon order as

$$t_{NS} = n_{CH} \cdot \text{aBaseSuperframeDuration}\,(2^{BO} + 1). \quad (6)$$

As defined above, practical network scan duration for NCB equipped ZigBee is

$$t_{NS} = 1/f_N + \text{SD}. \quad (7)$$

Table 3: Utilized parameters and their values.

Symbol	Parameter	Value
f_C	Standard beacon rate	63.8 mHz–16.4 Hz
f_N	Network beacon rate	0.1 Hz–100 Hz
L_B	Beacon frame length	26 B
n_{D}	Number of devices associated with each coordinator	12
n_C	Number of child-coordinators associated with each coordinator	3
n_{CH}	Number of cluster channels	1 or 10
R	Radio data-rate	250 Kbps
r	Radio range	20 m
t_I	Synchronization inaccuracy	0.10 ms
v	Node mobility	0.01–10 m/s
ε	The crystal tolerance	20 ppm

5.4. Network maintenance power analysis

Network maintenance operations are performed continuously during entire network lifetime. Hence, it is most convenient to consider a long-time energy consumption divided by the elapsed time resulting in average power consumption. Average network maintenance power P_M is defined as a sum of passive scan power P_{NS} and beacon exchange power P_B.

The interval of passive scans depends on the average link lifetime (t_{LF}). In should be noted that a link failure somewhere along the routing path between a given node and a sink may cause a passive scan and network reassociation. For simplicity, we omit these link failures in this analysis, and the interval between passive scans equals a link lifetime. We also omit occasional frame errors, and determine link lifetime according to node mobility. Assuming a random mobility for all nodes, average link lifetime can be approximated by a radio range (r) and node mobility (v) as

$$t_{\mathrm{LF}} = r/v. \tag{8}$$

The resulted link lifetime as a function of node mobility is plotted in Figure 9. As mobility increases, node quickly moves out of the communication range of its coordinator, and the lifetime of a link drops rapidly. According to the link lifetime, the average power consumption of network scans (P_{NS}) is obtained as

$$P_{\mathrm{NS}} = E_{\mathrm{NS}}/t_{\mathrm{LF}}. \tag{9}$$

We determine average beacon exchange power according to beacon transmission and reception energies. All nodes receive beacons, but they are transmitted by coordinators only. In standard ZigBee, beacons are transmitted and received from a parent at rate f_C. As beacon exchange power is averaged over all the nodes of a cluster; beacon exchange power consumption (P_B) for ZigBee is

$$P_B = \frac{f_C}{n_D + 1} E_{\mathrm{TXB}} + f_C E_{\mathrm{RXB}}. \tag{10}$$

When NCB is utilized, beacon transmissions are increased. Besides the standard beacons, each coordinator transmits network beacons on the network channel at rate f_N. For NCB equipped ZigBee, average beacon exchange power consumption is

$$P_B = \frac{f_N + f_C}{n_D + 1} E_{\mathrm{TXB}} + f_C E_{\mathrm{RXB}}. \tag{11}$$

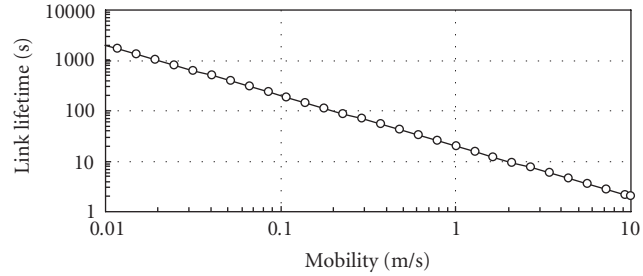

Figure 9: The effect of mobility to link lifetime in the simulated scenario.

5.5. Energy analysis results

The network maintenance powers are compared between standard ZigBee and NCB equipped ZigBee. BI and v are fixed to 3.96 seconds and 0.01 m/s, respectively. As the network operation is divided into 1 and 10 channels, the maintenance power of the standard ZigBee equals 132 μW, and 1.13 mW, respectively, as presented in Figure 10. When NCB is used, the network maintenance power P_M (the sum of P_{B} and P_{N}) has a minimum of 42 μW at 2.6 Hz network beacon rate. At low-beacon rates below 1 Hz, P_M typically doubles as the beacon rate halves and the power consumption are dominated by the passive scan power. The effect is reversed at high-beacon rates above 10 Hz, when the beacon transmissions dominate the power consumption. At the energy optimum 2.6 Hz network beacon rate, NCB algorithm reduces the network maintenance power up to 96%. Yet, the BI may also be energy optimized reducing the network maintenance power of standard ZigBee.

For finding an energy optimal value for BI, the network maintenance power of ZigBee is analyzed as the function of BI. From now on, the number of channels is fixed to 1.

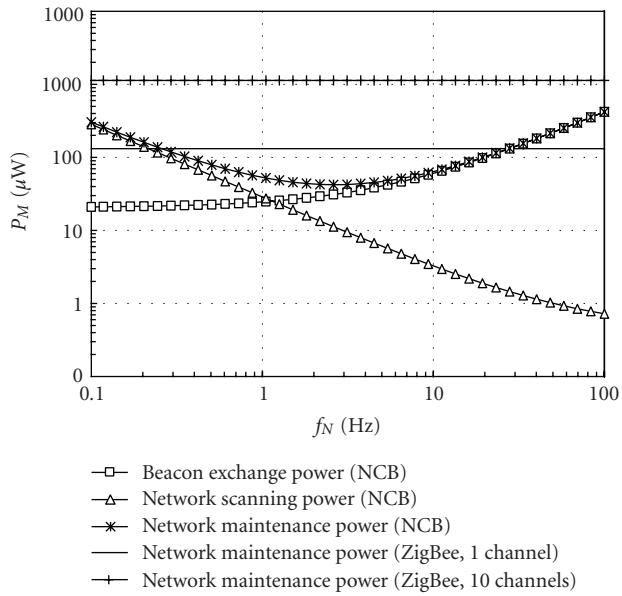

Figure 10: Average beacon exchange, passive scan, and network maintenance power consumptions as the function of network beacon transmission rate.

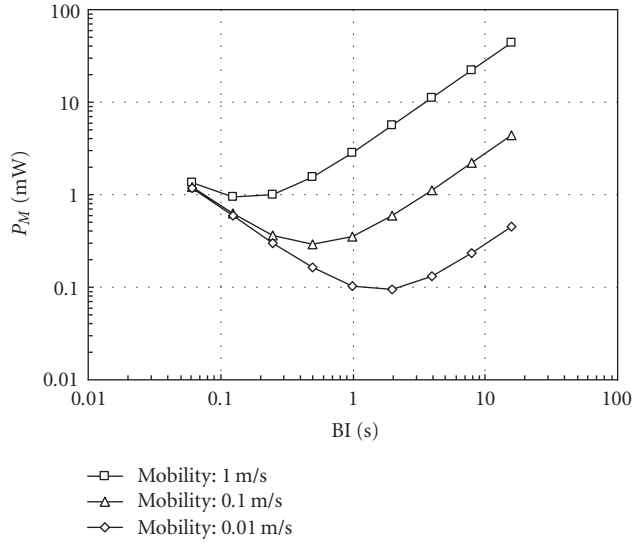

Figure 11: Average network maintenance power of ZigBee as the function of BI, while node mobility varies.

Average node mobility gets values 0.01 m/s, 0.1 m/s, and 1 m/s, ranging from a nearly static network to a quite dynamic network, respectively. The results are presented in Figure 11. At shorter values of BI, network maintenance power is dominated by beacon exchange power consumption. At longer BI values, passive scans dominate the power consumption. An energy optimal BI depends on the node mobility. The energy optimal values of BI at 0.01 m/s, 0.1 m/s, and 1 m/s mobility levels are 1.97 second, 0.49 second, and 0.12 second, respectively. The resulted minimum network maintenance power consumptions at these points are 94 μW, 288 μW, and 936 μW, respectively.

Next, the network maintenance power of NCB equipped ZigBee is analyzed as the function of network beacon transmission rate. Node mobility gets values 0.01 m/s and 1 m/s, and BI is varied from 0.246 second to 15.7 seconds. The results are presented in Figure 12. In contrast to ZigBee, the network maintenance power is minimized by maximizing BI. This is logical, since passive scans are performed by receiving network beacons independently of the transmission rate of standard beacons. Hence, the increase of BI reduces beacon transmission and reception power consumption. The minimum network maintenance power is achieved by optimizing network beacon transmission rate. At 0.01 m/s and 1 m/s node mobility levels, energy optimal network beacon rates are 2.6 Hz and 28 Hz, respectively. Achieved network maintenance power consumptions at these points are 28.1 μW and 220 μW, respectively, as BI = 15.7 seconds. Compared to ZigBee at these link lifetimes, NCB equipped ZigBee achieves 70%–76% lower-network maintenance power. The results also indicate that NCB algorithm operates most efficiently in dynamic networks, and an energy optimal network beacon rate depends significantly on a link lifetime. A shorter link

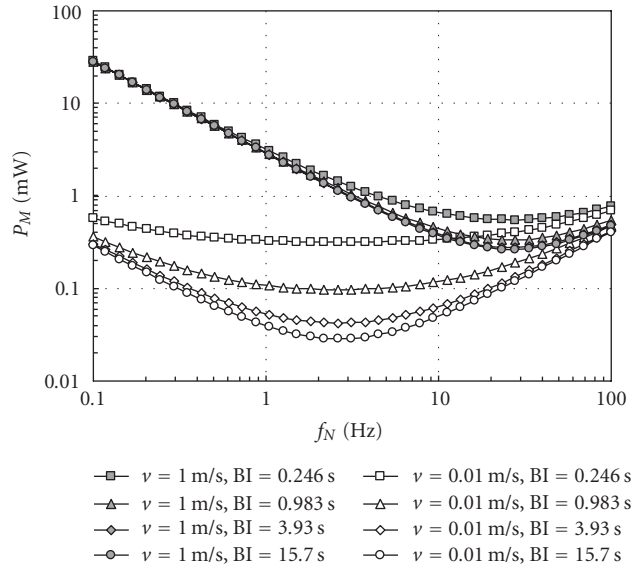

Figure 12: Average network maintenance power of NCB equipped ZigBee as the function of network beacon rate, as BI, and node mobility varies.

lifetime increases passive scan power consumption and thus, shifts the P_M minimum to higher-network beacon rates. According to [12], the typical power consumption of a ZigBee node in a static low-data-rate network is below 1 mW. Hence, network maintenance power has a very significant effect on entire network lifetime and the optimization of network beacon rate is very important.

6. NETWORK BEACON RATE OPTIMIZATION

An optimal network beacon rate (f_N^*) is determined by minimizing the network maintenance power with respect to the

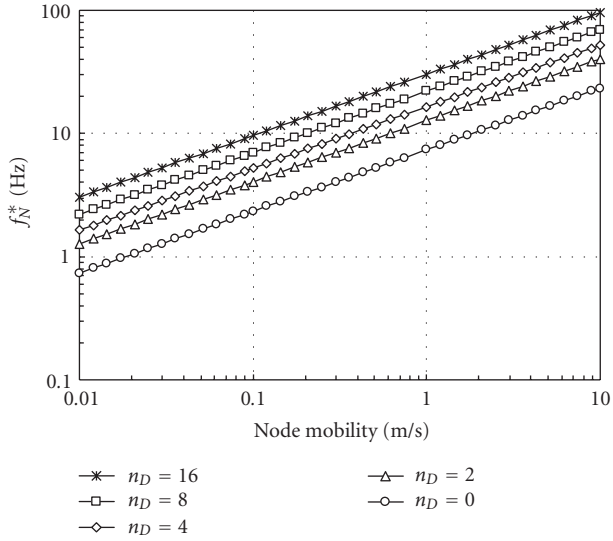

Figure 13: Network maintenance power of NCB equipped ZigBee at f_N^* as the function of node mobility, and comparison with standard ZigBee.

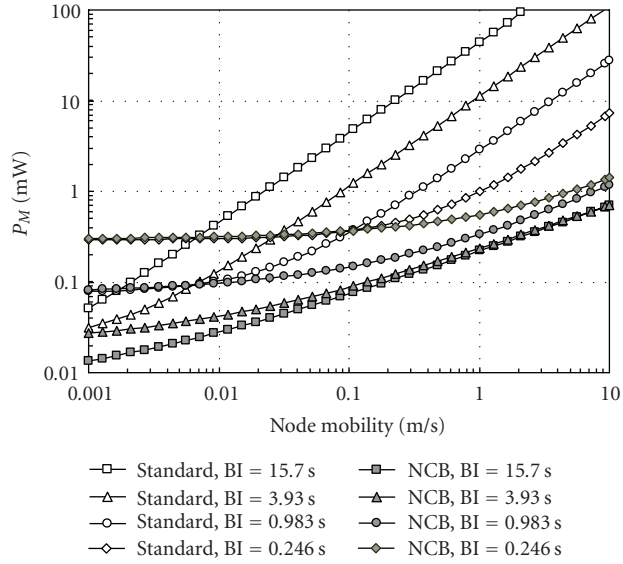

Figure 14: Energy optimal network beacon rate as the function of node mobility, and as the number of devices per a cluster varies.

network beacon rate. An optimization function can be written as

$$P_m = \frac{f_N + f_C}{n_D + 1} E_{\mathrm{TXB}} + f_C E_{\mathrm{RXB}} + \frac{t_{\mathrm{SI}} P_I + (t_{\mathrm{IA}} + 1/f_N + \mathrm{SD}) P_{\mathrm{RX}}}{r} \nu. \tag{12}$$

It can be shown that there exists a unique minimum at f_N^* that is obtained by setting $dP_m/df_N = 0$ in (12). This yields

$$f_N^* = \sqrt{\frac{P_{\mathrm{RX}} \nu (n_D + 1)}{E_{\mathrm{TXB}} r}}. \tag{13}$$

The optimal network beacon rate is determined by radio parameters E_{TXB}, P_{RX}, and r, and network parameters n_D and ν.

The effect of a link lifetime and a cluster size on the optimal network beacon rate is presented in Figure 13. The optimal rate is nearly directly proportional to node mobility. As the number of devices per cluster (n_D) increases from 0 to 16, the energy optimal network beacon rate increases 312%. Although, a higher-network beacon rate increases P_B in coordinators, overall network maintenance power consumption is reduced due to shorter passive scans.

The network maintenance powers of ZigBee and NCB equipped ZigBee are compared as the function of node mobility. In the comparison, BI varies from 0.246 second to 15.7 seconds, and NCB is operating at the energy optimal network beacon rate. The results are presented in Figure 14. In static networks with very low mobility, obtained network maintenance powers are nearly the same. Hence, the energy overhead of NCB is small. The energy saving of NCB compared to standard ZigBee increases rapidly with higher-node mobility. At 1 m/s node mobility, achieved energy saving using NCB is from 44% to 99.5%.

Finally, we analyze the effect of NCB on a service time, during which a node is connected to a network and capable for routing data. We consider a time period equaling to t_{LF}. The active operation time between passive scans equals t_{LF} reduced by the durations of a passive scan (t_{NS}) and network association (t_A) operations. After a passive scan, a node selects a suitable parent and waits for the beginning of parent's next superframe requiring on average a half BI. Then, the node transmits an association request and waits for a response to the next superframe. Hence, on average $t_A = 1.5\mathrm{BI}$. The service time (S) is determined as the percentual duration of active operation time in proportion to the entire period as

$$S = \frac{I_{\mathrm{NS}} - t_{\mathrm{NS}} - t_A}{t_{\mathrm{LF}}}. \tag{14}$$

The resulted service time as the function of a link lifetime is plotted in Figure 15. Due to the time required for association, the service time depends significantly on BI. However, NCB algorithm improves the service time of ZigBee up to 37%. The improvement is the most significant at node mobility levels above 0.1 m/s.

7. SIMULATIONS

The performance of the network channel beaconing was compared against standard ZigBee using ns-2 simulation tool (version 2.31) [26]. Next, the NCB implementation for ns-2 and obtained performance results are discussed.

7.1. Implementation

For enabling simulations in ZigBee network, few modifications for the IEEE 802.15.4 implementation provided by ns-2 were made. First, the code was modified to support a cluster-tree topology with inactive time and to perform synchronization to the coordinator prior to each association attempt.

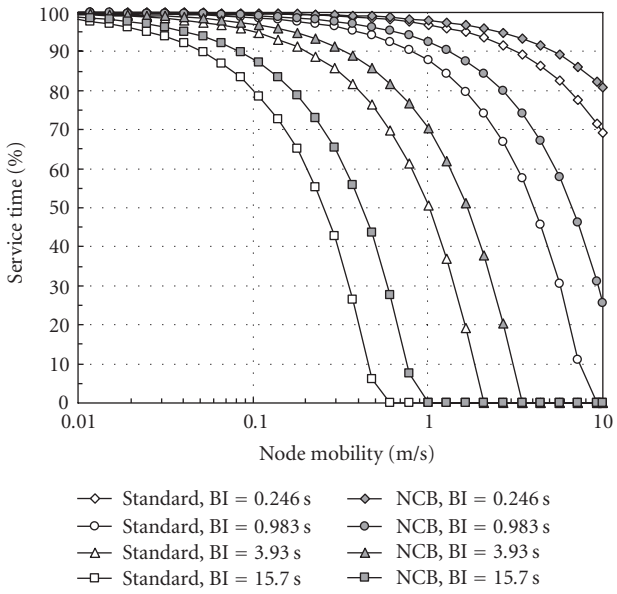

Figure 15: Service time versus node mobility at f_N^* and comparison with ZigBee.

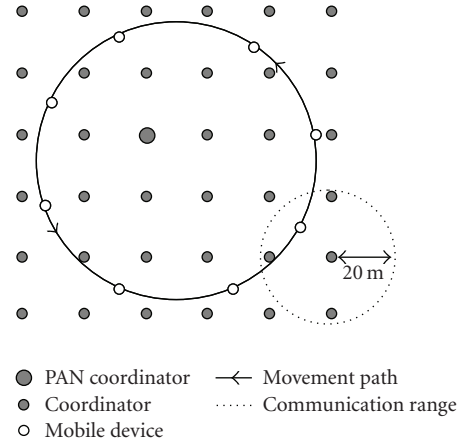

Figure 16: Simulated network topology. Coordinators are located on a grid around a PAN coordinator, while devices move around the grid.

Otherwise, the synchronization procedure would have included a long-term idle listening. Second, a beacon scheduling was implemented, as required by the ZigBee. Because the standard does not specify the exact method to determine the beacon schedules, a custom algorithm was used. The algorithm utilizes precalculated beacon transmission times to ensure unique time slots for each coordinator within an interference range. It should be noted that while end-to-end delay varies in different schedules, the energy, throughput, and reliability results are the same, assuming that a nonconflicting schedule is found.

Moreover, the simplest version of ZigBee routing was implemented by omitting the optional routing tables and route discovery procedure. Instead, the packets were routed along the formed cluster tree. While the route discovery procedure allows communication between two arbitrary nodes in the network, it causes high-initial delay, since a node must communicate with its destination. Therefore, the route discovery is impractical for networks having high degree of mobility.

For NCB, the NWK layer was modified to issue the passive scan command with the network channel instead of the usual channel range. The received network beacon frames were distinguished from other frames by a unique frame type value. The received beacons were handled similarly to the standard beacons, expect for the time of next superframe which was calculated with *time to next superframe* field. Each station was preconfigured with network channel and network beacon interval, thus the beacon interval was the same during a simulation run. Coordinator transmitted network beacons periodically by briefly switching to the network channel. For these simulations, network beacon transmission jitter J_{MAX} was set to the value of eight, which was found to reduce collisions adequately.

The simulated scenario consisted of 36 stationary coordinators and 8 mobile devices. The coordinators were formed on a grid around a PAN coordinator, while mobile devices moved along a circle having a radius of 45 m, as illustrated in Figure 16. Each coordinator was within the communication range of its adjacent nodes. That is, the coordinators in the center had four neighbors. Maximum hop count (network depth) to the PAN coordinator was six. The simulation utilized a two-ray ground propagation model allowing communication range of 20 m. This was enough for reliable communication between immediate neighbors, but prevented interference from other nodes. To simulate normal network operation, each mobile device transmitted 40 B packets periodically to the PAN coordinator with 30 s as a period. Simulation time was one hour.

IEEE 802.15.4 was simulated without CFP and battery life extension options. During CAP, channel access mode was slotted CSMA-CA. For evaluating power consumption, the measured power consumption and transient times of Chipcon CC2420 were used, as presented in Tables 2 and 3. Frames were always sent with the highest transmission power level (0 dBm).

7.2. Simulation results

The simulations produced power consumption and service time results for each node in the network. The obtained results are averaged among all nodes of the same type resulting in average node behavior. It should be noted that the power consumption results include also the power consumptions of a startup and all data exchanges. Thus, the presented power consumptions are higher than that in the analysis.

We present first the simulated service time as the function of node mobility. The results are presented in Figure 17. In the results, the maximum relative error with 95% confidence is 7%. The service time depends heavily on the beacon interval, as long interval increases association delays. Because shorter network scan time allows faster neighbor discovery and thus, minimizes the time in which a node is not

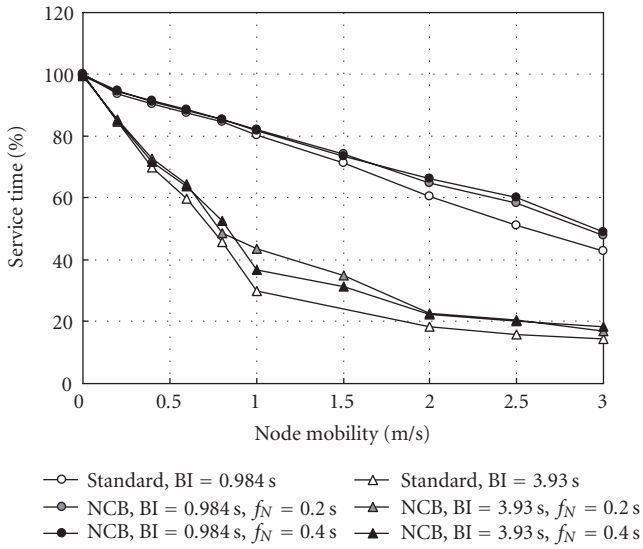

Figure 17: Simulated service time of a mobile device (SO = 1).

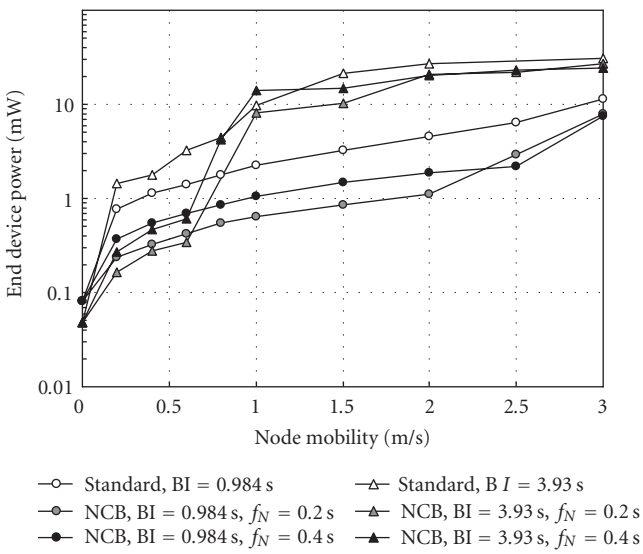

Figure 18: Simulated power consumption of mobile devices (SO = 1).

connected to the network, NCB increases service time up to 14%. The simulations results slightly lower service time than the analysis. This is mostly caused by occasional unsuccessful associations.

Power usage of a mobile device is presented in Figure 18. In the results, the maximum relative error with 95% confidence is 12%. When a device is stationary, only an initial network scan is performed. As the normal operation is identical between standard ZigBee and NCB, the difference on energy usage is minimal. When mobility increases, links break often and more network scans are required. Then, NCB performs significantly better than standard due to its short network scan time.

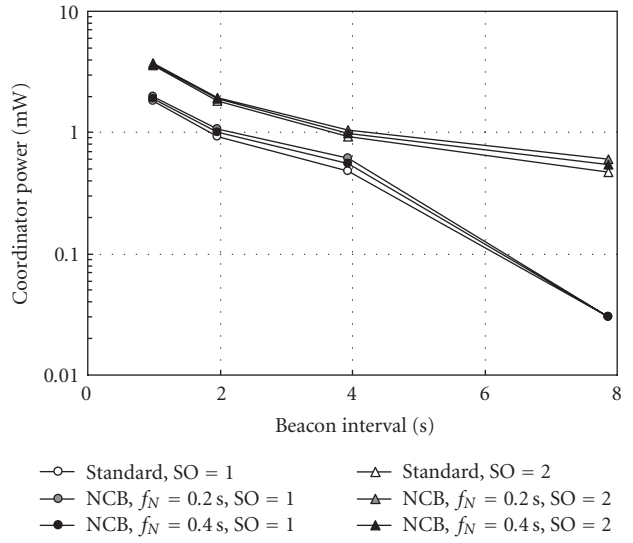

Figure 19: Simulated coordinator power consumption.

On low mobility and at 3.93 seconds beacon interval, NCB has order of magnitude lower power consumption than the standard. Yet, the power consumption increases significantly between 0.6 m/s and 0.8 m/s due to increased failures during synchronization. As beacon interval is long, a device may try to synchronize to a neighbor that has already moved outside its communication range. The device tries to track beacons and enables its radio for several beacon intervals before failing. Thus, after 0.6 m/s, NCB results are nearly the same with the standard. At shorter, at 0.98 second beacon interval, the same effect occurs after 2.5 m/s mobility.

Figure 19 shows the average power usage on a stationary ZigBee coordinator. The increased power requirement of NCB is only 2%–4% higher. This is expected, as network beacons are short and do not require CSMA-CA mechanism. Thus, the transceiver receptions dominate the power consumption. This is evident in Figure 19, as the superframe length (beacon order) has the most profound effect on power.

Generally, the simulations show higher-power consumption than the analysis. The reason is that simulations included also power consumption due to data exchange, while analysis focused on the network maintenance power only. However, the results and findings are comparable and prove the energy-efficiency of proposed network channel beacons.

8. CONCLUSIONS

The design and performance analyses of the NCB algorithm for ZigBee are presented. A dedicated frequency channel for frequent network beacons reduces the energy consumption of IEEE 802.15.4 passive scans. Energy-efficiency is further improved by optimizing the network beacon transmission rate according to observed link lifetimes.

According to the energy analysis, NCB algorithm reduces the network maintenance power of ZigBee in dynamic networks 70%–76%. This equals even milliwatts absolute power

saving using low-power hardware platforms. As coordinator power consumption in a static network and a low- data-rate application is typically below 1 mW [12], achieved power saving is dramatic. In addition, the NCB algorithm improves network performance by increasing the service time for data routing up to 37%. Simulations validate the energy-efficiency of NCB, although the energy saving is slightly lower than in the analysis.

As the NCB algorithm minimizes passive scan energy regardless the number of utilized PAN channels, the division of clusters into several frequency channels becomes feasible and energy-efficient. This would improve ZigBee scalability and performance especially in dense and large WSNs by even eliminating inter-cluster interferences. It should be also noted that the network beacons provide an efficient way to signal network maintenance, neighborhood, and routing information for additional algorithms and protocols. NCB can be implemented as an extension on MAC and NWK layers, and it is fully compatible with ZigBee.

REFERENCES

[1] I. F. Akyildiz, W. Su, Y. Sankarasubramaniam, and E. Cayirci, "Wireless sensor networks: a survey," *Computer Networks*, vol. 38, no. 4, pp. 393–422, 2002.

[2] J. Polastre, R. Szewczyk, A. Mainwaring, D. Culler, and J. Anderson, "Analysis of wireless sensor networks for habitat monitoring," in *Wireless Sensor Networks*, C. S. Raghavendra, K. M. Sivalingam, and T. Znati, Eds., pp. 399–425, Springer, New York, NY, USA, 2004.

[3] J. Suhonen, M. Kohvakka, M. Hännikäinen, and T. D. Hämäläinen, "Design, implementation, and experiments on outdoor deployment of wireless sensor network for environmental monitoring," in *Proceedings of the 6th International Workshop on Embedded Computer Systems: Architectures, Modeling, and Simulation (SAMOS '06)*, pp. 109–121, Samos, Greece, July 2006.

[4] S. Roundy, P. K. Wright, and J. Rabaey, "A study of low-level vibrations as a power source for wireless sensor networks," *Computer Communications*, vol. 26, no. 11, pp. 1131–1144, 2003.

[5] M. Haenggi, "Opportunities and challenges in wireless sensor networks," in *Handbook of Sensor Networks: Compact Wireless and Wired Sensing Systems*, M. Ilyas and I. Mahgoub, Eds., pp. 1.1–1.14, CRC Press, Boca Raton, Fla, USA, 2004.

[6] IEEE Std 802.15.1-2002, wireless medium access control (MAC) and physical layer (PHY) specifications for wireless personal area networks (WPANs).

[7] IEEE Std 802.15.3-2003, wireless medium access control (MAC) and physical layer (PHY) specifications for high rate wireless personal area networks (WPANs).

[8] IEEE Std 802.15.4-2006, wireless medium access control (MAC) and physical layer (PHY) specifications for low-rate wireless personal area networks (WPANs).

[9] J. A. Gutierrez, E. H. Callaway Jr., and R. L. Barrett Jr., *Low-Rate Wireless Personal Area Networks—Enabling Wireless Sensors with IEEE 802.15.4*, IEEE Press, New York, NY, USA, 2003.

[10] "ZigBee Alliance Document 053474r06; ZigBee Specification, Version 1.0," December 2004.

[11] J. Ha, W. H. Kwon, J. J. Kim, Y. H. Kim, and Y. H. Shin, "Feasibility analysis and implementation of the IEEE 802.15.4 multihop beacon enabled network," in *Proceedings of the 15th Joint Conference on Communications & Information (JCCI '05)*, pp. 1–5, Korea, April 2005.

[12] M. Kohvakka, M. Kuorilehto, M. Hännikäinen, and T. D. Hämäläinen, "Performance analysis of IEEE 802.15.4 and ZigBee for large-scale wireless sensor network applications," in *Proceedings of the 3rd ACM International Workshop on Performance Evaluation of Wireless Ad Hoc, Sensor and Ubiquitous Networks (PE-WASUN '06)*, pp. 48–57, Terromolinos, Spain, August 2006.

[13] N. F. Timmons and W. G. Scanlon, "Analysis of the performance of IEEE 802.15.4 for medical sensor body area networking," in *Proceedings of the 1st Annual IEEE ICommunications Society Conference on Sensor and Ad Hoc Communications and Networks (SECON '04)*, pp. 16–24, Santa Clara, Calif, USA, October 2004.

[14] B. Bougard, F. Catthoor, D. C. Daly, A. Chandrakasan, and W. Dehaene, "Energy-efficiency of IEEE 802.15.4 standard in dense wireless microsensor networks: modeling and improvement perspectives," in *Proceedings of Design, Automation and Test in Europe (DATE '05)*, vol. 1, pp. 196–201, Munich, Germany, March 2005.

[15] G. Lu, B. Krishnamachari, and C. S. Raghavendra, "Performance evaluation of the IEEE 802.15.4 MAC for low-rate low-power wireless networks," in *Proceedings of the 23rd IEEE International Performance Computing and Communications Conference (IPCCC '04)*, pp. 701–706, Phoenix, Ariz, USA, April 2004.

[16] D. Mirza, M. Owrang, and C. Schurgers, "Energy-efficient wakeup scheduling for maximizing lifetime of IEEE 802.15.4 networks," in *Proceedings of the 1st International Conference on Wireless Internet (WICON '05)*, pp. 130–137, Budapest, Hungary, July 2005.

[17] A. Koubâa, A. Cunha, and M. Alves, "A time division beacon scheduling mechanism for IEEE 802.15.4/Zigbee cluster-tree wireless sensor networks," in *Proceedings of the 19th Euromicro Conference on Real-Time Systems (ECRTS '07)*, pp. 125–135, Pisa, Italy, July 2007.

[18] L.-J. Hwang, S.-T. Sheu, Y.-Y. Shih, and Y.-C. Cheng, "Grouping strategy for solving hidden node problem in IEEE 802.15.4 LR-WPAN," in *Proceedings of the 1st IEEE International Conference on Wireless Internet (WICON '05)*, pp. 26–32, Budapest, Hungary, July 2005.

[19] A. Rowe, R. Mangharam, and R. Rajkumar, "Rt-link: a time synchronized link protocol for energy constrained multi-hop wireless networks," in *Proceedings of the 3rd Annual IEEE Communications Society Conference on Sensor, Mesh and Ad Hoc Communications and Networks (SECON '06)*, vol. 2, pp. 402–411, Reston, Va, USA, September 2006.

[20] M. Kohvakka, M. Hännikäinen, and T. D. Hämäläinen, "Energy optimized beacon transmission rate in a wireless sensor network," in *Proceedings of the 16th IEEE International Symposium on Personal, Indoor and Mobile Radio Communications (PIMRC '05)*, vol. 2, pp. 1269–1273, Berlin, Germany, September 2005.

[21] B. Heile, "Wireless sensors and control networks: enabling new opportunities with ZigBee," ZigBee Alliance Tutorial, December 2006, http://www.zigbee.org.

[22] A. Koubaa, M. Alves, and E. Tovar, "GTS allocation analysis in IEEE 802.15.4 for real-time wireless sensor networks," in *Proceedings of the 14th International Workshop on Parallel and Distributed Real-Time Systems (WPDRTS '06)*, pp. 1–8, Rhodes, Greece, April 2006.

[23] D. Sexton, M. Mahony, M. Lapinski, and J. Werb, "Radio channel quality in industrial wireless sensor networks," in *Proceedings of the Sensors for Industry Conference (SIcon '05)*, pp. 88–94, Houston, Tex, USA, February 2005.

[24] Data Sheet for CC2420 2.4 GHz IEEE 802.15.4/ZigBee RF Transceiver, http://focus.ti.com/lit/ds/symlink/cc2420.pdf.

[25] Data Sheet for PIC18LF8722 Microcontroller, http://focus.ti.com/lit/ds/symlink/cc2420.pdf.

[26] The Network Simulator - ns-2, version 2.31, http://www.isi.edu/nsnam/ns.

PUBLICATION 4

M. Kohvakka, J. Suhonen, M. Kuorilehto, V. Kaseva, M. Hännikäinen, and T. D. Hämäläinen, "Energy-Efficient Neighbor Discovery Protocol for Mobile Wireless Sensor Networks," *Ad Hoc Networks*, vol. 7, no. 1, pp. 24–41, January 2009.

PUBLICATION 5

M. Kohvakka, M. Hännikäinen, and T. D. Hämäläinen, "Energy Optimized Beacon Transmission Rate in a Wireless Sensor Network," in *Proceedings of the 16th International Symposium on Personal Indoor and Mobile Radio Communications (PIMRC 2005)*, Berlin, Germany, Sep. 11–14, 2005, pp. 1269–1273.

Energy Optimized Beacon Transmission Rate in a Wireless Sensor Network

Mikko Kohvakka, Marko Hännikäinen, and Timo D. Hämäläinen
Tampere University of Technology
Institute of Digital and Computer Systems
P.O.Box 553, FI-33101 Tampere, Finland
mikko.kohvakka@tut.fi, marko.hannikainen@tut.fi, timo.d.hamalainen@tut.fi

***Abstract*—Resource constrained Wireless Sensor Networks (WSN) require an energy efficient Medium Access Control (MAC) protocol that minimizes the radio active time (duty cycle). Time slotted MAC schemes provide lowest duty cycles by dividing time into consecutive data exchange and sleep periods. Synchronization for data exchange and network maintenance is achieved by exchanging beacons. For detecting changes in network topology, nodes periodically perform scanning during which beacons are received from neighbors. This is energy consuming, and the energy required equals to the transmission of thousands of packets. This paper shows that the energy consumption is mainly depending on the beacon transmission rate, and that an optimal rate is a function of three parameters: a network scanning interval, beacon transmission energy, and radio reception power. The optimal beacon transmission rate is derived for a TUTWSN prototype by power analysis and energy models. According to the analysis, the optimization decreases the average network energy consumption up to an order of magnitude. For the prototype, the optimal beacon transmission rate is 3.7 Hz, when network scanning is performed with 2 minutes intervals.**

I. Introduction

Wireless Sensor Networks (WSN) are a relatively new family of ad hoc networks [1]. They are developed for low data rate monitoring in home, outdoor and industrial environments [2]. WSN nodes combine wireless communication, sensor elements and application computing with ultra-low energy consumption, size and cost. Nodes are autonomous and they operate without any kind of maintenance. Nodes are powered by tiny batteries for months to years, or they scavenge energy from environment [3].

The energy consumption in WSN nodes is typically dominated by transceiver circuitry [4]. Thus, energy conservation requires the minimizing of the radio transmitting and receiving times (*duty cycle*) while meeting the delay and throughput requirements [5]. Radio transmissions and receptions on the shared wireless channel are controlled by a Medium Access Control (MAC) protocol. Time slotted MAC protocols are the most energy efficient due to small idle listening time [6], [7]. Data is exchanged periodically using either contention based or dedicated assignment channel access, while the rest of time radios are in a sleep mode.

Dynamic WSN with multi-hop data routing needs network maintenance information exchange between nodes. In this paper, this maintenance traffic is generally denoted as beacons. Especially, time slotted protocols utilize beacon transmissions at the beginning of a data exchange period for scheduling transmissions, obtaining time synchronization, and informing node status. Beacons are also employed when associating or leaving a network. In network scanning, nodes actively search new neighbors by listening beacons on the wireless channel.

At best, time slotted protocols can reduce the duty cycle significantly, reaching far below 1%. In practice, the duty cycle is higher because of network scanning and for reducing data transfer delays. In very low data rate WSNs, the duty cycle is reduced by extending the sleep times between data exchange periods. This usually reduces the beacon transmission rate, but increases the required network scanning time and energy proportionally. The network scanning may consume energy equal to the transmission of thousands of data packets. Hence, techniques for controlling the network scanning energy are very important.

This paper proves that a significant energy reduction is obtained by optimizing the beacon transmission rate. Furthermore, the transmission of additional beacons during node sleep time for reducing the network scanning time is proposed.

This paper is focused on ad-hoc networks with homogeneous nodes. The analysis employs TUTWSN prototype power measurements and energy models. Yet, results are general and applicable for different time slotted WSNs, such as Sensor-MAC (S-MAC) [5], the Timeout-MAC (T-MAC) [8], and IEEE 802.15.4 Low Rate Wireless Personal Area Network (LR-WPAN) standard [9].

To the best of our knowledge, there is no previous work that considers the effect of beacon transmission rate on time slotted WSN energy consumption.

The rest of this paper is organized as follows. Section 2 presents the classification of energy consumptions in the MAC layer. The TUTWSN prototype platform with power consumption analysis and radio energy models is presented in Section 3. The network maintenance power consumption is analyzed in Section 4. The optimization model for beacon transmission rate is presented in Section 5. Section 6 concludes the paper.

II. WSN Energy Classification

For reasoning the effect of the beacon transmission rate on node energy consumption, we first divide the energy consumed by wireless communication into three energy classes:

- node start-up,
- network maintenance, and
- data exchange.

These are presented in Fig. 1. The node start-up energy consists of *network scanning* for detecting nodes in a range, and network association for connecting a node to a network. The network maintenance and data exchange operations are executed after the start-up period during the node lifetime. The network maintenance energy consists of beacon transmissions and receptions (*beacon exchange*), network scanning, and possible re-associations. This periodic scanning is needed in dynamic WSNs with node failures, mobility, and radio environment changes. The data exchange energy is consumed by payload data transmissions and receptions, and MAC signaling, such as acknowledgement.

As node lifetimes are expected to be from months to years, the start-up energy is negligible small compared to the total node energy consumption. Furthermore, we assume that data exchange operations have a higher priority than beacon transmissions. Thus, data exchange energy is not affected by the beacon transmission rate. Hence, we can focus on analyzing the network maintenance energy.

A. Network Maintenance Power

Network maintenance operations are performed continuously during the entire network lifetime. Hence, we consider the energy consumption over 1 s period of operation, which equals to the average power consumption. The evaluation of power instead of energy is more convenient due to the independence of time.

The average network maintenance power P_m is defined as the sum of the network scanning power P_{ns} and the beacon exchange power P_b. The network scanning power P_{ns} depends on the energy of a single scanning procedure E_{ns}, and the network scanning interval T_s. T_s determines the maximum delay for detecting changes in a network neighborhood. Shorter T_s improves network robustness, but also increases the average network scanning power consumption. A long time average network scanning power is obtained by

$$P_{ns} = \frac{E_{ns}}{T_s}. \tag{1}$$

Beacons are transmitted at rate f_{btx} and received at f_{brx}. Beacons may be received from multiple neighbors, which increases f_{brx} proportionally. The average power consumed by the beacon exchange is

$$P_b = E_{tx} f_{btx} + E_{rx} f_{brx}. \tag{2}$$

The network maintenance power in a practical case is estimated by combining this theoretical analysis with the measurements and energy models of a real TUTWSN prototype platform.

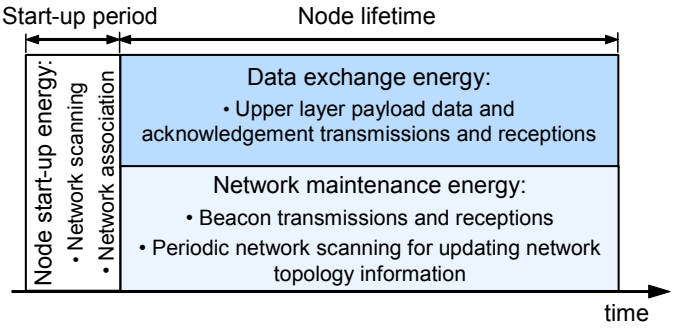

Fig. 1. The classification of the WSN node energy consumption.

III. TUTWSN Prototype Platform

TUTWSN is a low energy WSN developed at Tampere University of Technology. TUTWSN design goal has been minimized radio duty cycle, while maintaining the data transfer requirements of applications. Despite of low duty cycle operation, TUTWSN achieves rapid and low energy network start-up and maintenance operations.

The TUTWSN prototype platform is an improved version of the first version presented in [10]. The platform is controlled by Xemics XE88LC02 MicroController Unit (MCU), which integrates a CoolRisc 816 processor core with a 16-bit Analog-to-Digital Converter (ADC), 22 KB program memory and 1 KB data memory. An external 8 KB EEPROM provides a non-volatile data storage. In the prototype, ADC samples data from a temperature sensor, but nearly any type of sensor may be used.

For wireless communication, the platform utilizes a NordicVLSI nRF2401 2.4 GHz radio with selectable 250 kbps or 1 Mbps transmission data rate. The radio has integrated pattern recognition and CRC functions, which simplify communication protocol processing in MCU. In addition, the radio has an interface for low speed MCU, which consists of data buffers for transmission and reception. Radio is used with 256-bit fixed length packets, which enables the use of the higher 1 Mbps transmission data rate improving overall energy efficiency.

The prototype is powered by a 0.22 F super-capacitor and a linear voltage regulator. An interface for an ambient energy scavenging circuit is also available.

The prototype platform is implemented on a 31 mm x 23 mm x 5 mm sized printed circuit board presented in Fig. 2. The top side of the board contains the radio, antenna, EEPROM, sensor, and connectors. MCU and regulator are mounted on the bottom side.

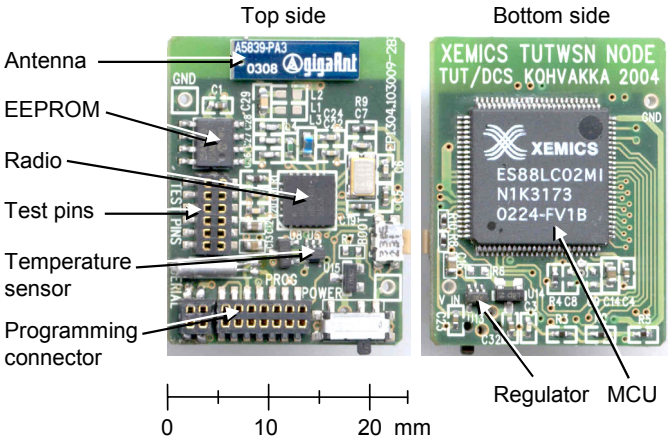

Fig. 2. TUTWSN prototype platform.

A. TUTWSN Prototype Power Analysis

The static power consumptions of the main TUTWSN platform components are measured at different operation modes. The supply voltage used in the measurements was 2.4 V. The results are presented in Table I. The minimum power consumption is 17 µW, when all components are in the sleep mode. The maximum power consumption is 46.08 mW, when the radio is in the receive mode (RX). The MCU power consumption is 1.33 mW at 1.8 MIPS processing speed. Clearly, the radio is the most power consuming component, taking nearly 33 times the power of MCU.

B. TUTWSN Radio Energy Models

Energy consumption in TUTWSN prototype is modeled according to the MAC protocol procedures (reception, transmission, and scanning) and the frame formats. While the frame formats for the procedures vary, the radio frame in TUTWSN has a fixed length of 256 bits. The symbols with defined or measured values are presented in Table II. Also, the symbols defined in the equations are summarized in Table III.

A frame transmission consists of data loading from MCU to the radio data buffer, a radio start-up transient and a data transmission. During the start-up transient, the radio power consumption is approximated to be equal to the transmission mode (TX) power consumption. Thus, the frame transmission energy E_{tx} is modeled as

$$E_{tx} = L_f E_l + \left(T_{st} + \frac{L_f}{R} \right) P_{tx} . \quad (3)$$

TABLE I
MEASURED TUTWSN PROTOTYPE POWER CONSUMPTION.

MCU	ADC	Sensor	Radio	Power (mW)
active	active	active	RX	46.08
active	active	active	TX (0 dBm)	31.78
active	active	active	TX (-20 dBm)	21.17
active	active	active	data loading	3.76
active	active	active	sleep	2.45
active	active	off	sleep	2.41
active	off	off	sleep	1.35
sleep	off	off	sleep	0.017

TABLE II
SYMBOL DESCRIPTIONS AND MEASURED OR DEFINED VALUES FOR TUTWSN PROTOTYPE PLATFORM.

Symbol	Description	Defined value
L_f	frame length	256 bits
R	radio data rate	1 Mbps
T_i	idle listening time	100 µs
T_{st}	transmitter and receiver start-up time	250 µs

Symbol	Description	Measured value
P_{tx}	power consumption in TX mode, MCU in active mode	0 dBm: 30.68 mW -20 dBm: 20.07 mW
P_{rx}	power consumption in RX mode, MCU in active mode	44.98 mW
E_l	energy for exchanging 1 bit data between transceiver and MCU	2.3 nJ/bit

The resulting energy consumptions are $E_{tx(high)}$ = 16.11 µJ at the higher transmission power (0 dBm) and $E_{tx(low)}$ = 10.74 µJ at the lower transmission power (-20 dBm). This equals to 63 nJ and 42 nJ per transmitted physical layer data bit at the higher and lower transmission power, respectively.

The frame reception begins with the radio start-up transient. The radio remains in the RX mode until a frame has been received including the idle listening time due to TDMA synchronization inaccuracy. Then, a received frame is loaded from the radio to MCU. The frame reception energy E_{rx} is modeled as

$$E_{rx} = \left(T_{st} + T_i + \frac{L_f}{R} \right) P_{rx} + L_f E_l . \quad (4)$$

The resulting energy consumption per received packet is E_{rx} = 27.85 µJ. This yields 109 nJ per received physical layer data bit.

The network scanning begins with the radio start-up transient. To be able to receive beacons from all neighboring nodes, the radio is in the RX mode for the whole beacon interval, which is an inverse of the beacon transmission rate f_{btx}. Each received beacon is loaded from the radio to MCU,

TABLE III
SYMBOL DESCRIPTIONS FOR ENERGY CONSUMPTION MODELS.

Symbol	Description
E_{tx}	packet transmission energy (256-bit packet)
E_{rx}	packet reception energy (256-bit packet)
E_{ns}	network scanning energy
E_s	node start-up energy
f_{btx}	beacon transmission energy
f_{brx}	beacon reception energy
P_m	average network maintenance power consumption
P_{ns}	average power consumption for network scanning
P_b	average power consumption for beacon transmissions
T_s	average network scanning interval

and an association request may be transmitted. These energies are difficult to estimate, but they are negligibly small compared to the channel reception energy and therefore ignored in the model. Thus, the network scanning energy E_{ns} can be modeled as

$$E_{ns} = \left(T_{st} + \frac{1}{f_{btx}} \right) P_{rx} . \quad (5)$$

When f_{btx} is set to 1 Hz, the resulting network scanning energy is E_{ns} = 44.99 mJ. This equals to the energy of 2793 beacon transmissions at the higher transmission power. Clearly, the effect of scanning on the whole energy consumption of a node is very significant, and becomes more critical at slower beacon transmission rates.

IV. Effect of the Beacon Transmission Rate on Power Consumption

The network maintenance power consumption is estimated for the TUTWSN prototype platform by combining the energy models with the real measurements. In this way, we are able to separate the network maintenance power from other power classes and obtain results that are independent on the TUTWSN MAC protocol.

The network scanning, beacon transmission and network maintenance powers in the function of the beacon transmission rate f_{btx} are presented in Fig. 3. T_s and f_{brx} are fixed to 500 s and 0.25 Hz. The figure clearly shows how the network scanning power P_{ns} decreases rapidly as f_{btx} increases. A decrease from 900 µW to 90 µW is obtained as the beacon transmission rate increases from 0.1 Hz to 1 Hz.

In contrast to P_{ns}, the beacon transmission power P_b can be minimized by minimizing f_{btx}. P_b decreases from 269 µW to 26.9 µW as f_{btx} decreases from 10 Hz to 1 Hz. As shown in the figure, the network maintenance power P_m has the minimum (98 µW) at the 1.9 Hz beacon transmission rate. At low beacon transmission rates below 1 Hz, P_m typically doubles as the beacon transmission rate halves. The effect is reversed at high beacon transmission rates above 10 Hz.

Next, we consider the effect of the network scanning interval on network maintenance power consumption. Clearly, the increase of network scanning interval reduces the power for network scanning and shifts the P_m minimum to lower beacon transmission rates. This is plotted in Fig. 4, where P_m varies with f_b, while T_s equals to 20 s, 100 s, and 500 s. The network scanning interval affects the maintenance power most significantly at lower beacon transmission rates. When f_b is 1 Hz, P_m increases from 137 µW to 2.3 mW as T_s decreases from 500 s to 20 s. Next, we will determine optimal beacon transmission rate in respect of the network scanning interval.

V. Beacon Transmission Rate Optimization

An optimal beacon transmission rate (f_{btx}^*) is determined by minimizing the network maintenance power with respect to the beacon transmission rate. The whole network maintenance power can be summarized as

$$P_m = \frac{P_{rx}}{T_s} \left(T_{st} + \frac{1}{f_{btx}} \right) + E_{tx} f_{btx} + E_{rx} f_{brx} . \quad (6)$$

It can be shown that there exists a unique minimum at f_{btx}^* that is obtained by setting $\partial P_m / \partial f_{btx} = 0$ in (6). This yields

$$f_{btx}^* = \sqrt{\frac{P_{rx}}{E_{tx} T_s}} . \quad (7)$$

An optimal beacon transmission rate is determined by a network parameter (scanning interval) T_s, and the radio parameters E_{tx} and P_{rx}. Fig. 5 presents the variation of f_{btx}^* with T_s. For the TUTWSN prototype platform, the optimal

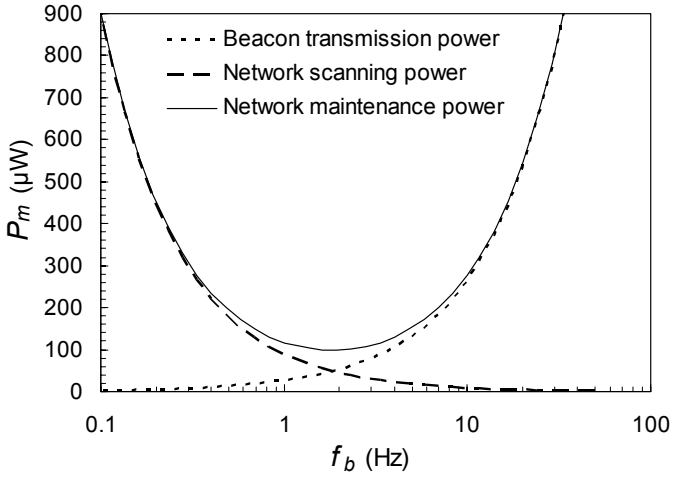

Fig. 3. Beacon exchange, network scanning and network maintenance power consumptions as a function of beacon transmission rate (T_s = 500 s, f_{brx} = 0.25 Hz).

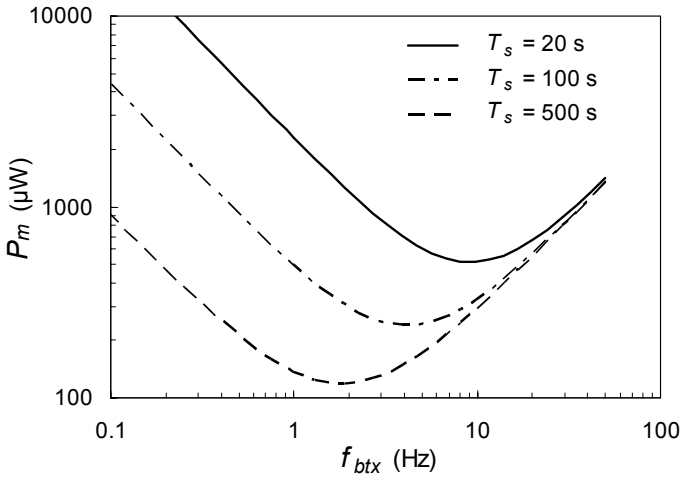

Fig. 4. Network maintenance power in function of beacon transmission rate with different network scanning intervals (f_{brx} = 0.25 Hz).

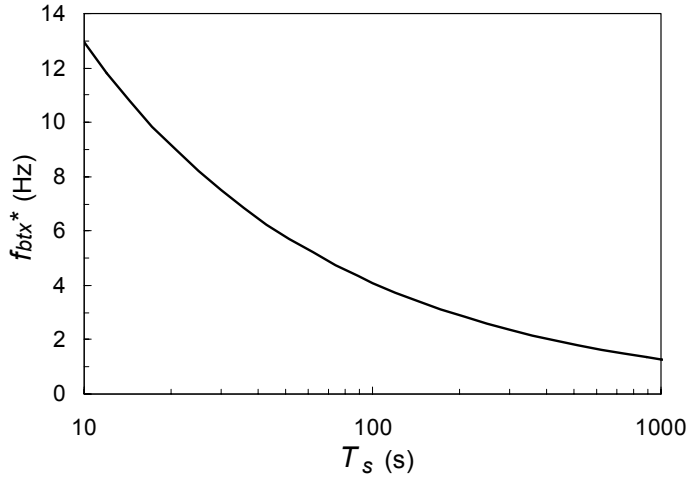

Fig. 5. Energy optimal beacon transmission rate in function of network scanning interval.

beacon transmission rate increases from 1.3 Hz to 12.9 Hz, as T_s decreases from 1000 s to 10 s.

VI. Conclusions

The estimations and measurements with the TUTWSN prototype platform depict that the network maintenance power ranges from below 100 µW to several milliwatts, for which the beacon transmission rate has the most significant effect. To enable WSN operation solely from ambient energy, a node power consumption should be in the order of 200 µW [11]. Hence, the optimization of the beacon transmission rate is critical.

The optimal beacon transmission rate is a function of three parameters: the network scanning interval, beacon frame transmission energy and radio power consumption in a RX mode. For the TUTWSN prototype, the optimal beacon transmission rate with a typical temperature sensing application and quite stable network with 120 s network scanning interval is 3.7 Hz. For a highly dynamic network with 20 s network scanning interval, the optimal beacon transmission rate is about 10 Hz.

The beacon rate optimisation results of this paper are not dependent on the data exchange interval. Therefore, we propose the use of additional beacons in the middle of the data exchange interval during idle periods. This lowers the energy consumption at new nodes scanning for a network and at existing nodes that detect changes in the network neighborhood. The utilized optimization function does not consider collisions on the RF channel, which become noteworthy at higher beacon transmission rates and dense networks. Hence, we propose using a separate network signalling channel for beacon transmissions.

The findings of this paper are generic and can be applied on at least LR-WPAN standard, and S-MAC and T-MAC protocols. Especially for LR-WPAN, the proposed additional beacons transmitted during the coordinator inactive period would effectively reduce the network scanning time when over 1 s beacon intervals are used.

References

[1] K. Sohrabi, J. Gao, V. Ailawadhi, and G. J. Pottie, "Protocols for self-organization of a wireless sensor network," *IEEE Personal Communications*, vol. 7, no. 5, pp. 16-27, Oct. 2000.

[2] E. H. Jr. Callaway, and E. H. Callaway, *Wireless sensor networks: architectures and protocols*, Auerbach Publications, 2003.

[3] S. Roundy, P. K. Wright, and J. Rabaey, "A study of low level vibrations as a power source for wireless sensor nodes," *Computer Communications*, vol. 26, no. 11, pp 1131-1144, Jul. 2003.

[4] F. Jin, H.-A. Choi, S. Subramaniam, "Hardware-aware communication protocols in low energy wireless sensor networks," in *Proc. IEEE Military Communications Conf.*, vol. 22, no. 1, Boston, MA, Oct 2003, pp. 676-681.

[5] W. Ye, J. Heidemann, and D. Estrin, "Medium access control with coordinated, adaptive sleeping for wireless sensor networks," *ACM/IEEE Trans. Networking*, vol. 12, no. 3, pp. 493-506, Jun. 2004.

[6] I. F. Akyildiz, W. Su, Y. Sankasubramaniam, and E. Cayirci, "Wireless sensor networks: a survey," *Computer Networks*, vol. 4, no. 38, pp. 393-422, Mar. 2002.

[7] W. R. Heinzelman, A. P. Chandrakasan, and H. Balakrishnan, "An Application-Specific Protocol Architecture for Wireless Microsensor Networks," *IEEE Trans. Wireless Communications*, Vol. 1, No. 4, pp. 660-670, Oct. 2002.

[8] T. van Dam, and K. Langendoen, "An adaptive energy-efficient MAC protocol for wireless sensor networks," in *Proc. 1st ACM Conf. on Embedded Networked Sensor Systems*, Los Angeles, CA, Nov. 2003, pp. 171-180.

[9] *Wireless Medium Access Control (MAC) and Physical Layer (PHY) Specifications for Low-Rate Wireless Personal Area Networks (LR-WPANS)*, IEEE Std 802.15.4-2003 edition.

[10] M. Kohvakka, M. Hännikäinen and T. Hämäläinen, "Wireless sensor prototype platform," in *Proc. IEEE Int. Conf. Industrial Electronics, Control and Instrumentation*, Roanoke, VA, Nov. 2003, pp. 1499-1504.

[11] S. Roundy, P. K. Wright, and J. Rabaey, "A study of low level vibrations as a power source for wireless sensor nodes," *Computer Communications*, vol. 26, no. 11, pp 1131-1144, Jul. 2003.

PUBLICATION 6

M. Kohvakka, M. Kuorilehto, M. Hännikäinen, and T. D. Hämäläinen, "Performance Analysis of IEEE 802.15.4 and ZigBee for Large-Scale Wireless Sensor Network Applications," in *Proceedings of the 3rd ACM International Workshop on Performance Evaluation of Wireless Ad Hoc, Sensor, and Ubiquitous Networks (PE-WASUN 2006)*, Torremolinos, Spain, Oct. 6, 2006, pp. 48–57.

PUBLICATION 7

M. Kohvakka, M. Hännikäinen, and T. D. Hämäläinen, "Wireless Sensor Prototype Platform," in *Proceedings of the 29th Annual Conference of the IEEE Industrial Electronics Society (IECON 2003)*, Virginia, USA, Nov. 2–6, 2003, pp. 1499–1504.

Wireless Sensor Prototype Platform

Mikko Kohvakka, Marko Hännikäinen, and Timo D. Hämäläinen
Tampere University of Technology
Institute of Digital and Computer Systems
Korkeakoulunkatu 1, FIN-33720 Tampere, Finland
Tel. +358 3 3115 2111, Fax +358 3 3115 4786
mikko.kohvakka@tut.fi, marko.hannikainen@tut.fi, timo.d.hamalainen@tut.fi

***Abstract* – This paper presents the design and performance measurements of a wireless sensor prototype platform (UbiSensor). UbiSensor combines techniques used in wireless microsensors and radio frequency identification (RFID) resulting a wireless sensor having sensing, data processing, network protocol execution, and energy scavenging capabilities. The platform design is driven by energy consumption minimization of given tasks. A commercially available microcontroller, low power RF transceiver, and power generator circuits are used. The measurements indicate 430 µW power consumption in typical operating conditions, using 1 Hz sample and transmit rate, which can be scavenged by a 29 mm^2 sized solar cell or using a transponder interface circuit in a near proximity to a RFID reader. UbiSensor performance results are promising, but further research is required.**

I. INTRODUCTION

The rapid development of low power radio frequency circuits and microcontrollers has enabled new wireless applications in industrial and home automation. One class of applications is wireless microsensor networks, where numerous wireless low power sensors enable robust and powerful sensing even for automated control applications.

Several research projects, e.g. WINS [1] and SmartDust [2], are aiming to integrate sensing, computing, and wireless communication in small size and low-cost production. This paper presents design of a new type of wireless sensor called UbiSensor that has been developed at Tampere University of Technology. UbiSensor combines low power radio and microcontroller of wireless microsensors and power management of radio frequency identification (RFID). This results a prototype, which is able to scavenge and store energy from operating environment. Supported sensor types are e.g. light, temperature, acceleration, pressure, and gas sensors.

This paper is organized as follows. The design requirements for the UbiSensor network and platform are presented in Section 2. Section 3 gives a detailed description of the UbiSensor hardware platform design. Power performance measurements are presented in Section 4. Finally, conclusions are given and future work projected.

II. UBISENSOR DESIGN REQUIREMENTS

The aim of this research is to improve the quality of industrial manufacturing processes by utilizing wireless sensor networks. As one of the results, the UbiSensor has been developed.

The design of UbiSensor platform is driven by the requirements of sensing applications and operational environments. Wireless sensors can be embedded and distributed into the environment. Thus, battery replacement is a difficult option and sensors may have to generate their supply energy from environment. The small physical size and light weight of a sensor are central limitations. Also, due to the large number of sensors required, the production cost should be low.

While wireless sensors have scarce power budged, the performance requirements are considerable. Our UbiSensors are required to measure 16-bit samples with 1-10 Hz sample rates, perform different type of processing tasks on data, and transfer processed samples through the sensor network by executing network protocols.

The energy awareness should be incorporated into every stage on the network design and operation. In platform design, component selection is important and compromises have to be made between obtained performance and power consumption to minimize overall energy consumption of given tasks. Dynamic power consumption is reduced by minimizing supply voltage and operating frequency. In software design it is important to minimize the number of executed instructions in the given tasks. In network protocols, energy consumption is reduced by minimizing the number and duration of receive and transmit operations, while using effectively power save modes. Furthermore, the entire system must be able to dynamically adjust system performance and make tradeoffs between energy consumption and operational fidelity [2 - 5].

UbiSensor network is controlled by a developed ubiquitous network protocol. The protocol design is driven by the required support for dynamic ad-hoc routing. The protocol also defines a gateway node, which bridges the sensor network to outside resources. The network should be flexible to manage, which means that no manual configuration is needed for changes of network contents. Sensors are mobile and can join or leave the network in ad-hoc manner. The protocol should contain power saving support. Furthermore, the network should provide place and time information associated with the measurement data. The network protocol design is outside of the scope of this paper, and we are concentrating on the UbiSensor platform design.

III. UBISENSOR PLATFORM DESIGN

General platform architecture for a wireless microsensor can be divided into four subsystems [4]:

- Computing subsystem consisting of a Micro Controller Unit (MCU)
- Communication subsystem consisting of a short range radio transceiver
- Sensing subsystem consisting of a set of sensors and actuators, which link the microsensor to the outside world, and
- Power subsystem consisting of a battery and a voltage converter, which provides the system supply voltage.

The general architecture is used as a base for the UbiSensor design. The developed UbiSensor platform architecture is presented in Fig. 1. The central component of the platform is MCU that includes the computing subsystem. In addition, part of the communication and sensing subsystems are executed on MCU. For communication, MCU includes the network protocol and drivers for accessing the radio. MCU also controls the Analog-to-Digital Converter (ADC) that gathers data from sensors. The power subsystem consists of power generators, a set of voltage converters and a capacitor. The power subsystem provides system supply energy, which is scavenged from operating environment.

A. Communication Subsystem

The communication subsystem consists of a radio transceiver, which enables wireless communication with neighbouring UbiSensors. In general, radio has four operation modes: transmit, receive, idle and sleep. In transmit and receive mode, radio requires minimum power levels on the order of multiple milliwatts due to analog mixers, filters and oscillators. Thus, it is important to minimize the communication time and maximize the low power time in idle and sleep modes. Furthermore, the operating mode change transients may dissipate a lot of energy, e.g. from sleep mode to transmit mode, which should be considered in the network protocol [2][4].

Frequency band affects significantly to the radio properties. The operating frequency determines radio operating range and interferences from the surrounding machinery. For industrial environment the interferences emitted from the machinery are significant below few hundred megahertz and drops rapidly above 1 GHz frequency [6]. Most commercial short-range radio transceivers in European region operate in the 433, 868 and 2400 MHz license-free Industrial Scientific Medicine (ISM) frequency bands. The characteristics of some of the most potential low power transceivers currently available are summarized in Table 1 [7 - 16].

The power efficiency of the radio can be determined by

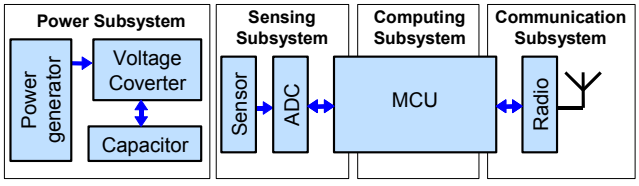

Fig. 1. UbiSensor architecture.

TABLE I
TRANSCEIVER FEATURES

Manufacturer	Model	Data Rate (kbps)	Band (MHz)	Sleep (uA)	Idle (mA)	RX (mA)	TX (mA)
NordicVLSI	nRF2401	1000	2400	1	0.03	19	8.8
Skyworks	CX72303	1000	2400	1	0.02	24	11
Conexant	RF109	1200	2400	5	25	89	31
Infineon	PBA31305	1000	2400	70	35	50	60
RFM	TR1001	115.2	868	0.75	-	3.8	12
Xemics	XE1201A	64	433	0.2	0.06	6	5.5
Infineon	TDA 5250	64	868	9	0.75	8.6	4.9
NordicVLSI	nRF903	76.8	433-950	1	0.6	18.5	12.5
Xemics	XE1202	76.8	868/433	0.2	0.85	14	33
NordicVLSI	nRF401	20	433	-	0.01	11	8

dividing radio power consumption by radio bit rate in transmit or receive mode, which yields energy per bit ratio (E/bit). The E/bit is computed to the radios above and results are presented in Fig. 2. The supply voltage is fixed to 3.0 V for comparability. As seen in the figure, radios operating at the 2.4 GHz frequency band are the most energy efficient due to high data rates. Yet, these high data rates require also a high performance microcontroller with a high-speed serial bus.

This problem is solved in the NordicVLSI nRF2401 [9] transceiver by an on-chip buffer, which adapts a low data rate microcontroller interface with a high data rate (250 kbps or 1 Mbps) radio. The output power is adjustable between -20 and 0 dBm. The nRF2401 is utilized and analyzed in the UbiSensor prototype.

B. Computation Subsystem

The choice of MCU affects significantly the power consumption of a wireless sensor. Microcontroller power efficiency can be analyzed by dividing processor performance, using million instructions per second (MIPS), by the power consumption. Thus, MIPS/W ratio can be computed as

$$\frac{MIPS}{W} = \frac{f \cdot 10^{-6}}{CPI \cdot f \cdot C_{SW} \cdot V_{dd}^2} = \frac{10^{-6}}{CPI \cdot C_{SW} \cdot V_{dd}^2}, \qquad (1)$$

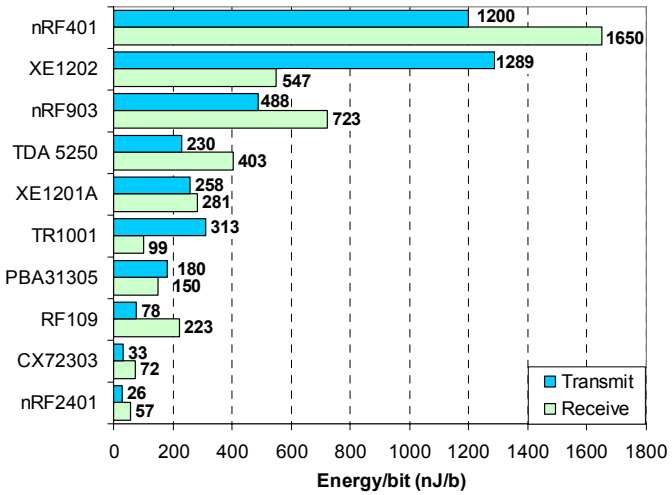

Fig. 2. Transceiver energy consumption comparison.

where C_{SW} is switch capacitance, V_{dd} system supply voltage, f operating frequency and CPI clock per instruction ratio [17]. The MIPS/W ratio is not dependent on the operating frequency. Power efficiency of some low power microcontrollers is compared in Fig. 3. The supply voltage is fixed to 3.0 V for fairness. We should note that the instruction set affects the performance to some extend. Thus, only orders of magnitude are important. As seen in the figure, CoolRisc processors are the most power efficient. The differences between 81, 88 and 816 models are basically in the amount of registers and memory [17].

The UbiSensor computation subsystem uses Xemics XE88LC01 [18] microcontroller, which integrates CoolRisc 816 processor core with ADC. The microcontroller has 8 k instructions program memory and 512 B data memory. Maximum clock frequency is 2 MHz and CPI ratio is 1. According to measurements, power consumption of the XE88LC01 is 1.8 mW at 1.8 MHz clock frequency and 3.0 V supply voltage yielding power efficiency of 1000 MIPS/W. Result is worse than in Fig. 3 due to the integrated peripheral components, i.e. ADC, UART, USRT, counters, timers and I/O ports.

C. Sensing Subsystem

The selection of ADC is driven by current consumption and sample resolution. Sample rate is typically not critical and is in the order of 10 Hz. UbiSensor sensing subsystem uses a simple low power temperature sensor, and a 16-bit ADC, which is integrated in the MCU. The ADC includes three pre-amplification stages for signal pre-processing and a switch for selecting input from four differential sources [18].

D. Power Subsystem

The UbiSensor power subsystem design is presented in Fig. 4. The power subsystem consists of two power generators, which scavenge system supply energy. Panasonic BP-376634 solar panel is 37 mm x 66 mm sized having 5.5 V open circuit voltage and 33 mA short circuit current. Atmel U3280 [19] transponder interface circuit is designed for RFID applications and is able to generate energy and communicate using 125 kHz magnetic field. Yet, only energy generator is used and communication is implemented using

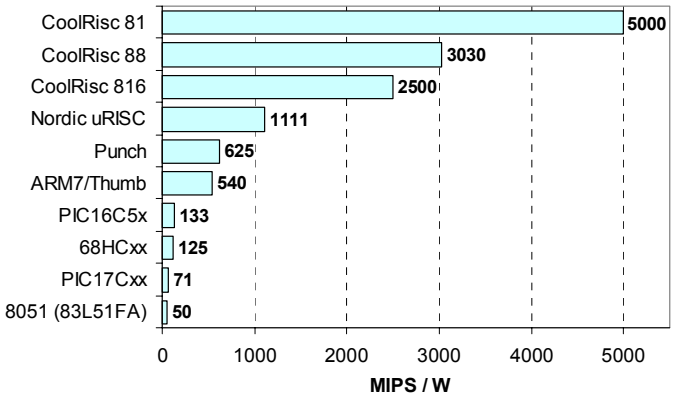

Fig. 3. MIPS/W comparison [17].

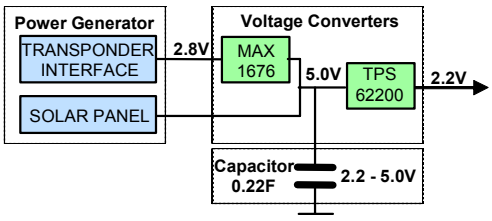

Fig. 4. Power subsystem architecture.

higher performance radio transceiver. Output voltage of the generator is limited to 2.8 V and current to 8 mA. However, magnetic field of the operation environment is not sufficient for energy scavenging and extra field is generated by the Atmel TMEB8704 RFID reader application kit [20].

The voltage converters provide voltage conversions and regulation. An important issue is efficiency. Thus, switch-mode regulators are used. The UbiSensor power subsystem consists of Maxim MAX1676 [21] step-up and Texas Instruments TPS62200 [22] step-down regulators, which are selected due to small quiescent current and good efficiency at the required current range. The step-down regulator output voltage is minimized to 2.2 V to reduce system power consumption. This is below the specified supply voltage range of MCU, but the system reliability is verified.

A capacitor ensures the UbiSensor supply energy and applicability when energy cannot be generated from the operating environment. The UbiSensor uses Panasonic EECS0HD224H [23] capacitor rated to 0.22 F and 5.5 V. The capacitor voltage depends on the energy of the capacitor and varies between 2.2 V and 5.0 V. The lower 2.2 V limit is determined by the output voltage of the step-down regulator.

E. Implementation

Implemented UbiSensor prototype is presented in Fig. 5.

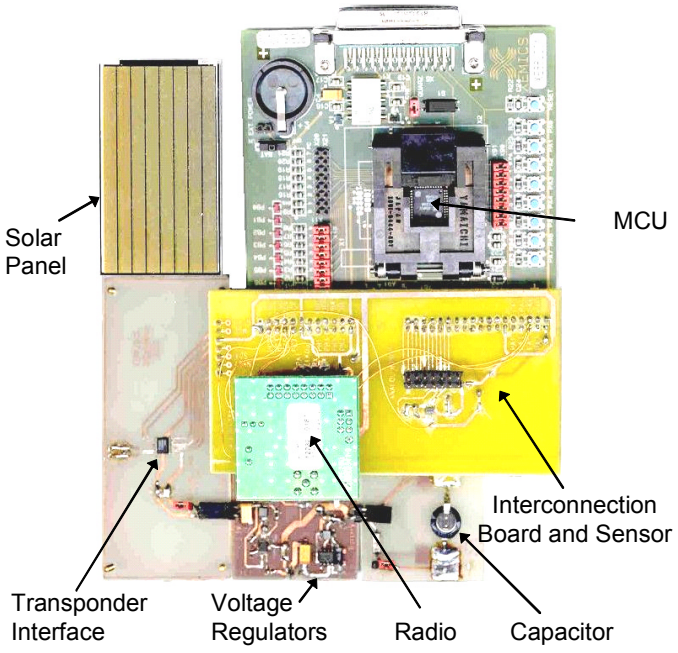

Fig. 5. Photograph of the UbiSensor prototype.

Computation and communication subsystems are implemented using the evaluation boards of component manufacturers. Power subsystem is implemented using separate circuit boards for each functional block, which are then optimized and measured separately. An interconnection board is used to connect the circuit boards together, and is also equipped with the temperature sensor.

IV. PROTOTYPE POWER PERFORMANCE

UbiSensor prototype power consumption is first calculated using data sheets of the selected components. Best case and lowest power operating conditions are used to find the lower limit of the consumption. Then, power consumption and power generator performance are measured in typical operating configuration. In both cases the following operation sequence is used.

MCU is powered up from idle mode and the temperature sensor is sampled. Then, the transceiver is powered up and measured data is transmitted in a packet of 96 bits. Finally, the system returns to idle mode. System wake up frequency is 1 or 10 Hz.

A. Calculated Minimum Power Consumption

Minimum power consumption is calculated using 2.2 V supply voltage and the following system configuration.

Radio – Transceiver power consumption is estimated according to the NordicVLSI nRF2401data sheet [9]. The packet is loaded into the radio transmit buffer using 50 kbps data rate and transmitted using 1 Mbps data rate and -20 dBm output power. Transceiver current consumptions in transmit and idle mode are 8.8 mA and 32 µA. The transmitter power up time is 195 µs.

MCU and ADC – The power consumption of CPU and ADC is estimated according to the Xemics XE88LC01 data sheet [18]. ADC current consumption is approximated using 16-bit conversion and 512 kHz input sampling frequency with 256 times oversampling. Thus, the conversion time is 500 µs. The MCU and ADC use 2 MHz clock frequency. Idle mode power consumption is 1.7 µA.

Voltage converter – The efficiency of the voltage converter (DC-DC) is estimated to be 80%.

The results of the calculation are presented in Fig. 6a. As seen in the figure, calculated minimum power consumptions using 1 Hz and 10 Hz sample rates are 117 µW and 314 µW.

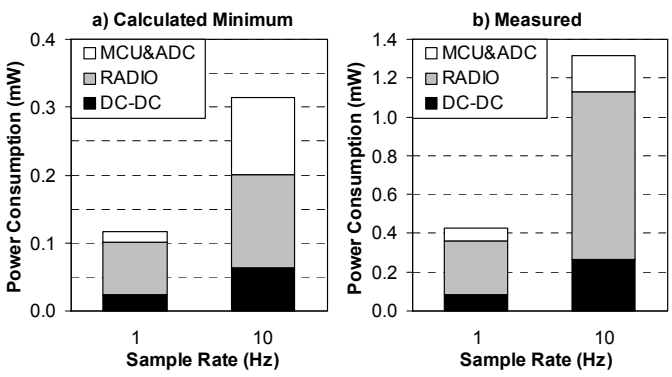

Fig. 6. Calculated and measured power consumption.

B. Measured Power Consumption

UbiSensor power consumption is measured in typical operating conditions. Operating frequency is set to 1.8 MHz due to correct timing of UART, which is used for diagnostics reasons. The measured power consumptions for each subsystem are presented in Fig. 6b. The system power consumptions using 1 Hz and 10 Hz sample rates are 430 µW and 1.32 mW. Results are significantly higher than the calculated minimum. This is probably due to the higher actual power consumption on the idle mode than estimated. As seen in the figure, the transceiver power consumption is remarkably high at 10 Hz transmit frequency. One reason for that is the energy consumption at the transmitter power down transient, which is unspecified and ignored in the calculations.

The current waveforms of microcontroller and transceiver are measured and presented in Fig. 7. and Fig. 8. Due to

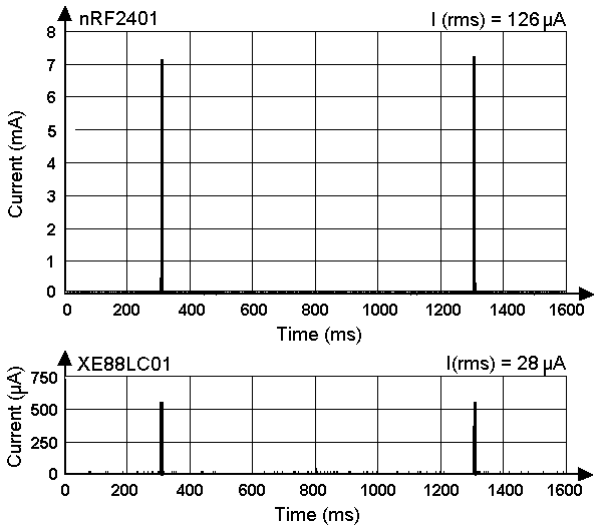

Fig. 7. Measured current consumption waveforms.

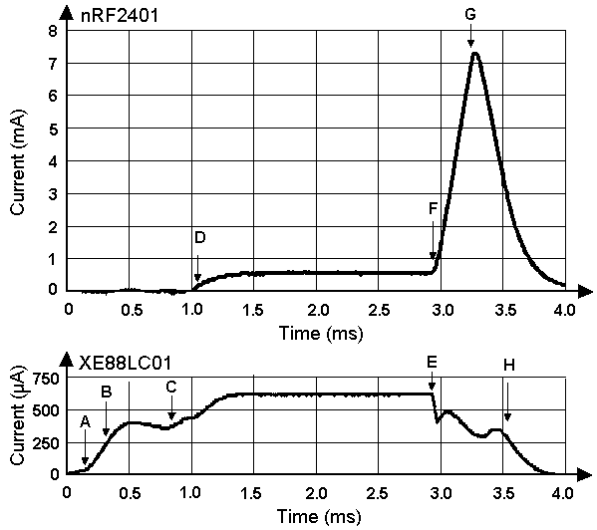

Fig. 8. Zoomed current consumption waveforms.

decoupling capacitors on the device boards, the waveforms are slightly smoothed. As seen in the figure, system is powered up at 1000 ms intervals. Average current consumption of transceiver and microcontroller are 126 µA and 28 µA. Detailed current consumption waveforms are presented in Fig. 8. System wake up event is marked in the figure as A. During the first 150 µs after the wake up MCU and ADC are initialized (A - B), which is followed by 500 µs long ADC measurement. During this, MCU is in the idle mode and the current consumption is low. When conversion is ready (C), MCU is powered up and the radio is initialized. That lasts around 230 µs (C - D). The transmitted data is loaded into the radio transmit buffer using 55 kbps data rate, which lasts 1.8 ms (D - E). Then, the radio is powered up to transmit mode (F - G) and the packet is transmitted using 1 Mbps data rate (G). Finally, the system returns to idle mode (H).

UbiSensor power consumption is analyzed in typical operating conditions and supply voltages. The results are presented in Table 2. The analysis excludes the power consumption of the voltage converter. The highest power consumption of 61.98 mW is reached when the radio is receiving and MCU, ADC and the sensor are active. Reducing the supply voltage from 3.0 V to 2.4 V decreases system power consumption 24% - 77%, depending on the operation mode. Reducing the transmit power from the maximum (0 dBm) to the minimum (-20 dBm) decreases power consumption 33%. Furthermore, the system power consumption is 54% higher in the receive mode than in the transmit mode using the lowest (-20dBm) RF transmission power. That should be considered when designing network protocols.

TABLE II
POWER ANALYSIS OF THE UBISENSOR

MCU Mode	ADC Mode	Sensor Mode	Radio Mode	Vcc (V)	Power (mW)
Active	Active	Active	Receive Data	3.0	**61.98**
				2.4	**46.28**
			Transmit Data (Power: 0 dBm)	3.0	**43.41**
				2.4	**31.98**
			Transmit Data (Power: -20 dBm)	3.0	**29.82**
				2.4	**21.37**
			Configuration and data loading	3.0	**5.25**
				2.4	**3.95**
			Idle	3.0	**3.70**
				2.4	**2.70**
			Sleep	3.0	**3.63**
				2.4	**2.65**
		Idle		3.0	**3.39**
				2.4	**2.35**
	Off			3.0	**2.10**
				2.4	**1.29**
Idle				3.0	**0.44**
				2.4	**0.10**
			Not installed	3.0	**0.44**
				2.4	**0.10**
		Not installed		3.0	**0.14**
				2.4	**0.02**

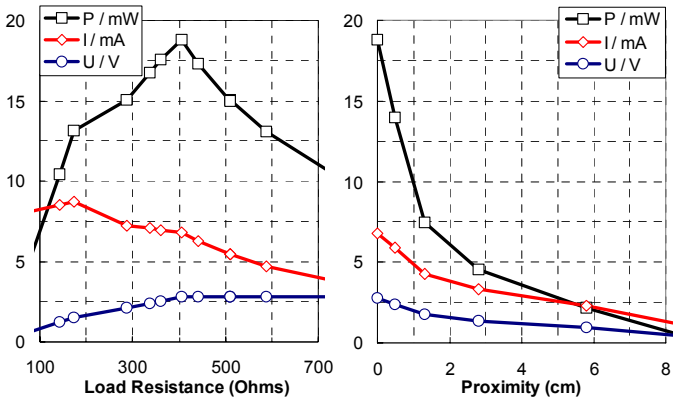

Fig. 9. Transponder interface performance.

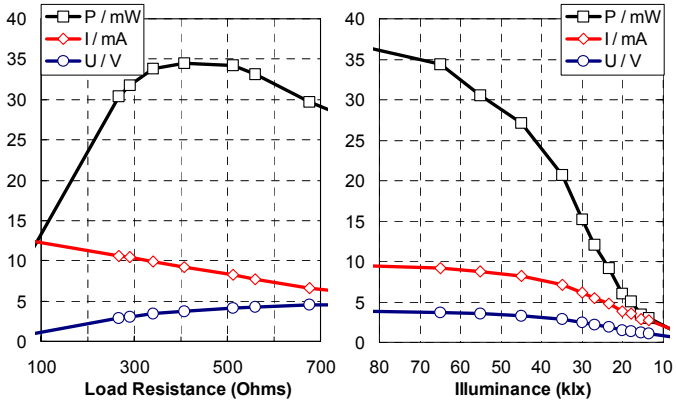

Fig. 10. Solar panel performance.

C. Measured Power Generator Performance

The energy scavenging performance of the solar panel and transponder interface circuit are analyzed. The transponder interface circuit is implemented using the Atmel U3280 transponder interface chip. The circuit uses LC-resonance circuit tuned to 125 kHz using 2.2 nF capacitor and 737 µH coil. The coil area is 31 cm^2.The Atmel TMEB8704 reader application kit is used to generate magnetic field and the output power of the U3280 is measured with various load resistances and distances between reader coil and transponder coil. The results are presented in Fig. 9. The maximum power is around 19 mW at 410 ohms load resistance. The chip has internal voltage and current limiters, which make a distinct peak to the output power plot and should be considered when designing voltage converter circuit. As seen in the right figure, the U3280 chip requires fairly strength magnetic field and practically an external field generator is required. When using TMEB8704 application kit, useful operating range is on the order of few centimeters. For longer operating range, a higher power field generator is required.

The Panasonic BP-376634 solar panel consists of small and serial connected solar cells gaining totally 5.5V output voltage. The output power of the solar panel is measured with various loading impedances at the same time as the light intensity is varied. The results are presented in Fig. 10. As seen in the figure, optimal loading impedance is 400 ohms and measured maximum output power is 36 mW at 80 klx

light intensity, which correspond approximately a bright sun light. Generated energy corresponds to the power of 1.5 mW/cm^2. The characteristics of the solar panel are promising. The selected solar panel is optimal for outdoor use, where sunlight enables adequate power generation.

V. CONCLUSIONS

A prototype for a wireless ubiquitous sensor network is designed and implemented. The design process includes specification of system requirements, analysis and selection of system components, and performance calculations. The prototype is implemented and its applicability according to power consumption verified by measurements. The power consumption measurements indicate promising results.

The prototype average power consumption using 1 Hz sample and transmit rate is 430 µW, which can be scavenged by the both power generator methods, e.g. using a 29 mm^2 sized solar cell in a bright sunlight or using the transponder interface circuit in a near proximity to the RFID reader. The average power consumption depends significantly on the executed network protocol and the sample rate requirements of the sensor application. The measure-and-transmit type of operation presented in this paper requires a continuously receiving destination node. When power consumption should be minimized in the entire network, this type of communication is usually not practical.

UbiSensor is passive most of time and the power consumption depends strongly on the utilization of low power operating modes. Important issues in the UbiSensor development are the research of efficient energy scavenging methods and the design of an intelligent network protocol combined with a power management algorithm.

REFERENCES

[1] G. Asada, M. Dong, T. Lin, F. Newberg, G. Pottie, W. Kaiser, and H. Marcy, "Wireless Integrated Network Sensors: Low Power Systems on a Chip*", European Solid State Circuits Conference,* (ESSCIRC'98), Sep 1998.

[2] B. Warneke, M. Last, B. Leibowitz, and K. S. J. Pister, "Smart Dust: Communicating with a Cubic-Millimeter Computer", *Computer*, vol. 34 no. 1, pp. 43-51, Jan 2001.

[3] R. Min, M. Bhardwaj, Seong-Hwan Cho, E. Shih, A. Sinha, A. Wang, and A. Chandrakasan, "Low-Power Wireless Sensor Networks", *Fourteenth International Conference on VLSI Design*, Jan 2001, pp. 205 – 210.

[4] V. Raghunathan, C. Schurgers, S. Park, M. B. Srivastava, "Energy-aware wireless microsensor networks", *IEEE Signal Processing Magazine*, vol. 19 no. 2, pp. 40-50, Mar 2002.

[5] A. Bellaouar, M. Elmasry, *Low-Power Digital VLSI design Circuits & Systems*, Kluwer Academic Publishers: 1995.

[6] T.S. Rappaport, "Indoor radio communications for factories of the future", *IEEE Communications Magazine*, vol. 27, no. 5, May 1989, pp. 15 –24.

[7] Xemics SA, "*XE1201A 300-500MHz Low-Power UHF Transceiver*" Data Sheet, 2002. Available: http://www.xemics.com/

[8] Xemics SA, "*XE1202 433MHz/868MHz/915MHz Low-power, integrated UHF transceiver*", Data Sheet, 2003. Available: http://www.xemics.com/

[9] NordicVLSI ASA, "*Single Chip 2.4 GHz Transceiver nRF2401*", Product Specification, Rev. 1.0, 2003. Available: http://www.nvlsi.no/

[10] NordicVLSI ASA, "*433MHz-950MHz Single Chip RF Transceiver nRF903*", Product Specification, Rev. 3.1, 2002. Available: http://www.nvlsi.no/

[11] NordicVLSI ASA, "*433 MHz Single Chip RF Transceiver nRF401*", Product Specification, Rev. 1.6, 2002. Available: http://www.nvlsi.no/

[12] Infineon Technologies AG, "*PBA 313 05 Bluetooth Radio Transceiver*", Product Brief, 2003. Available: http://www.infineon.com/

[13] Infineon Technologies AG, "*ASK/FSK 868MHz Wireless Transceiver TDA 5250 D2*", Data Sheet, Rev 1.6, 2002. Available: http://www.infineon.com/

[14] Skyworks Solutions, Inc, "*CX72303: 1.8 V Ultra-Low Power Bluetooth RF Transceiver*", Product Summary, 2003. Available: http://www.skyworksinc.com/

[15] RF Monolithics, Inc., "*TR1001 868.35 MHz Hybrid Transceiver*", Data Sheet, Rev. 2003.07.17, 2003. Available: http://www.rfm.com/

[16] Conexant Systems, Inc, "*RF109 2400 MHz Digital Spread Spectrum Transceiver*", Data Sheet, 2000. Available: http://www.conexant.com/

[17] C. Piguet et al., "Low-Power Design of 8-b Embedded CoolRisc Microcontroller Cores", *IEEE Journal of Solid-State Circuits*, vol. 32, no. 7, Jul 1997, pp. 1067-1078.

[18] Xemics SA, "*XE88LC01 Sensing Machine Data Acquisition with 16+10 bit ZoomingADC*", Data Sheet, 2002. Available: http://www.xemics.com/

[19] Atmel Corp., "*U3280M Transponder Interface for Microcontroller*", Data Sheet, Rev. A4, 2001. Available: http://www.atmel.com/

[20] Atmel Corp., "*RFID Application Kit TMEB8704*", Application Note, 2001. Available: http://www.atmel.com/

[21] Maxim Integrated Products, Inc., "*MAX1674 – MAX1676 High-Efficiency, Low-Supply-Current, Compact, Step-Up DC-DC Converters*", Data sheet, Rev. 3, 2000. Available: http://www.maxim-ic.com/

[22] Texas Instruments Inc., "*TPS62200 – TPS62205 High-Efficiency, SOT23 Step-Down, DC-DC Converter*", Data sheet, Mar 2002. Available: http://www.ti.com/

[23] Matsushita Electric Corporation of America, "*Electric Double Layer Capacitors (Gold Capacitor)/SD*", Data Sheet. Available: http://www.panasonic.com/

PUBLICATION 8

M. Kohvakka, M. Hännikäinen, and T. D. Hämäläinen, "Ultra Low Energy Wireless Temperature Sensor Network Implementation," in *Proceedings of the 16th International Symposium on Personal Indoor and Mobile Radio Communications (PIMRC 2005)*, Berlin, Germany, Sep. 11–14, 2005, pp. 801–805.

Ultra Low Energy Wireless Temperature Sensor Network Implementation

Mikko Kohvakka, Marko Hännikäinen, and Timo D. Hämäläinen
Tampere University of Technology
Institute of Digital and Computer Systems
P.O.Box 553, FI-33101 Tampere, Finland
mikko.kohvakka@tut.fi, marko.hannikainen@tut.fi, timo.d.hamalainen@tut.fi

***Abstract*—Condition monitoring in buildings is one of the most potential and foreseen applications for Wireless Sensor Networks (WSN). This paper presents the design and full scale prototype implementation of WSN for temperature monitoring. The prototypes are implemented using low power commercial of-the-shelf components including a 2.4 GHz radio, microcontrollers, and a custom TUTWSN communication protocol. A user application provides a graphical data analysis. Measurements indicate 183 μW to 390 μW average node power consumptions, as temperature is measured at 5 s intervals and data is multi-hop routed to a gateway. Predicted lifetime with two AA batteries is up to 4.9 years. In addition, experiments indicate that time accuracy is extremely important in hardware prototypes.**

I. Introduction

Wireless Sensor Networks (WSN) will soon enable various intelligent applications in home, office, industrial and outdoor environments [1]. WSNs consist of thousands of fully autonomous nodes, which communicate wirelessly with each other, sense their environment and share collaborative tasks. Data is routed using multiple hops for robust and scalable operations [2]. Although the network management is complex, available energy and radio bandwidth are very scarce.

Conditional monitoring in buildings, including temperature, humidity, and gas measurements is a straightforward and one of the most potential applications for WSNs [1]. The data rate and latency requirements are quite low, but the required node lifetime should be years without maintenance [3].

Only few experimental evaluations of conditional monitoring multi-hop WSNs have been published. One WSN implementation presented in [4] employs totally 65 Berkeley Mica II Commercial Off-The-Shelf (COTS) motes, which monitor temperature in a vineyard. Temperature values are gathered at 5 minutes intervals, and the data is routed to a base station node with at maximum 8 hops. The motes are implemented with low power microcontrollers and 916 MHz radios. For the application, the motes are supplied by large 42 Ah battery packs. The reported lifetimes of the routing nodes are about 3 months.

Another WSN implementation consisting of 25 COTS type PicoNodes is implemented and measured in [5]. The nodes employ StrongARM SA-1100 microprocessors and Bluetooth physical layers with custom data link layer and higher layer protocols. In a performance evaluation, the nodes measure temperature values at 5 s intervals, and multi-hop route data to a base station node. Measured average power consumption per node is about 6 mW resulting approximately 50 days lifetime with two AA-batteries.

In this paper we present the implementation of a full featured WSN for temperature sensing. Compared to current proposals, significantly longer WSN node lifetimes with smaller node size are pursued to achieve. The system consists of sensor nodes and a gateway to connect the network to a PC for data analysis. The network is based on our TUTWSN wireless sensor network design that provides very high energy efficiency.

The case application is a home temperature monitor network, where the nodes are mounted on the ceilings and walls as depicted in Fig. 1. The nodes acquire temperature values at 5 s intervals with at least 1°C accuracy. The number of nodes is 100, but this is not limited by TUTWSN. The network is ranging up to 100 meters, where the proximity between the nodes is at most ten meters. There are no strict delay requirements for the data collection, but the latency per hop should be below 5 s.

The paper is organized as follows. Section 2 gives an overview of the TUTWSN topology and its MAC protocol. The design of the WSN prototypes and the user application are presented in Section 3. Section 4 presents the performance evaluation, including component power analysis and prototype performance measurements. Section 5 concludes the paper.

II. TUTWSN Overview

The TUTWSN protocol stack is targeted at low data rate applications with unlimited scalability and extremely low energy consumption. An important TUTWSN design goal has been minimized communication duty cycle, while providing rapid and low energy network configuration and maintenance operations. TUTWSN utilizes a clustered network topology, where each cluster consists of a cluster head (headnode) and several subnodes. The headnodes form a flat topology with multi-hop data routing as depicted in Fig. 1. All nodes can move freely and the network is created and reconfigured autonomously.

978-3-8007-2909-8/05/$20.00

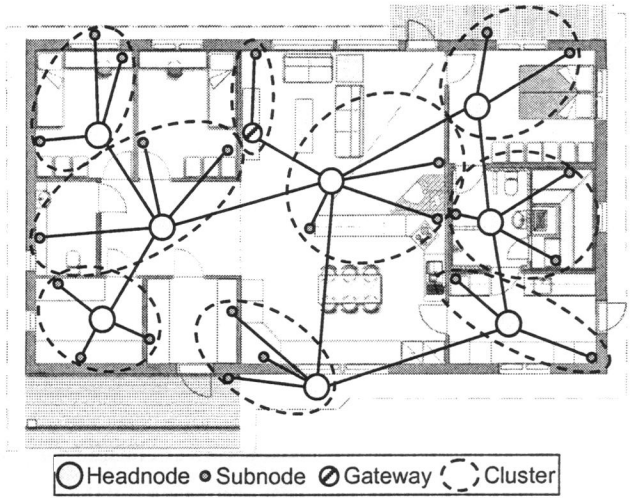

Fig. 1. TUTWSN topology in temperature monitoring application.

A. TUTWSN MAC

TUTWSN is based on our previous QoS capable TUTWLAN MAC protocol [6]. It is a time slotted protocol, which divides each access cycle into an active period (superframe) and idle time as depicted in Fig. 2. Data is exchanged in superframes, while on idle time the nodes are in a power save mode. The access cycle length is an adjustable MAC protocol parameter, which allows a trade off between energy, data rate and latency.

For enabling scalability, each headnode controls its superframe structure asynchronously to each other. Inter-cluster interferences are eliminated by allocating different RF channels for neighboring clusters. The applied local synchronization within a cluster reduces headnode duty cycle and is much easier to control than maintaining a global synchronization [7].

Each superframe begins with a beacon, which specifies slot reservations and synchronizes data exchanges. The beacon is succeeded by four ALOHA and at most eight reservable time slots. The ALOHA slots are used for association and slot reservation requests, and for low priority data. The reservable slots provide reliable data transfer with a fixed throughput, but they require a slot reservation procedure. The combination of ALOHA and TDMA slots is applicable for different traffic types and operating conditions, such as radio interference. In addition, all headnodes broadcast network beacons on a common network signaling channel at 500 ms intervals. The network beacon contains a cluster channel and an exact time to a following superframe, which effectively reduces the required radio receiving time and energy for neighbor discovery operations and inter-cluster synchronization.

Inter-cluster communication is performed during a source cluster idle time and a destination cluster superframe. A source headnode acts similarly as a subnode and synchronizes itself to the schedule of a destination headnode. In addition, a source headnode has to keep track of time offsets to all utilized destination headnodes.

III. Wireless Temperature Sensor Prototypes

Two prototype nodes have been implemented for the temperature network. The *TUTWSN node prototype* is designed for very high energy efficiency and adequate performance for operating both as a subnode and headnode. A simpler *TUTWSN subnode prototype* targets to lower cost and even smaller size.

A. TUTWSN Node Prototype

The node prototype hardware architecture is presented in Fig. 3. The prototype has Xemics XE88LC02 MicroController Unit (MCU) including a 16-bit ADC, 22 KB program memory and 1 KB data memory. An external 8 KB Microchip 25AA320 EEPROM is included for non-volatile data memory. MCU is selected due to adequate 2 MIPS performance and high 1344 MIPS/W energy efficiency.

Nordic Semiconductor 2.4 GHz nRF2401A radio transceiver provides wireless communication. The high frequency allows physically small antennas and enough channels for frequency spreading between clusters. The radio has 1 Mbps data rate, which enables very high energy efficiency. The consumed energy per a physical layer bit is about 109 nJ at RX mode and 63 nJ at TX mode with 0 dBm power level [8]. Transmission power is selectable between -20 dBm and 0 dBm. The radio has 84 selectable RF channels, which enables good network scalability. Furthermore, the radio has an internal Cyclic Redundancy Check (CRC) error detection and a data buffer, which reduces MCU performance requirements. The prototype uses a quarter-wave GigaAnt Rufa SMD antenna due to small size, omni-directional radiation and good 68% efficiency. Measured radio range is about 15 m.

A temperature sensing is implemented with a Maxim MAX6607 temperature sensor, a Maxim MAX6018 voltage reference, and the integrated ADC. ADC has pre-amplification and offset compensation stages, which improve

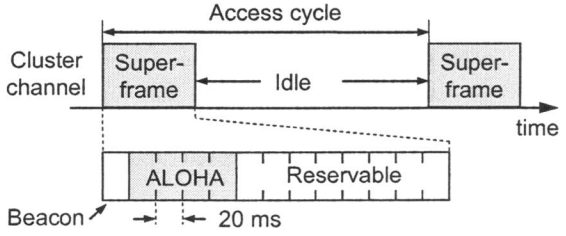

Fig. 2. TUTWSN access cycle and superframe.

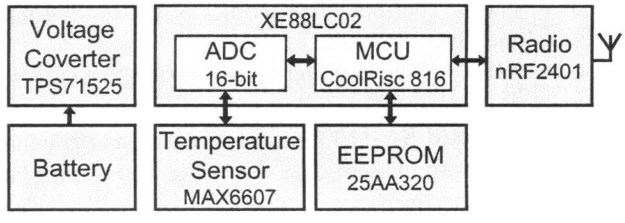

Fig. 3. TUTWSN node prototype hardware architecture.

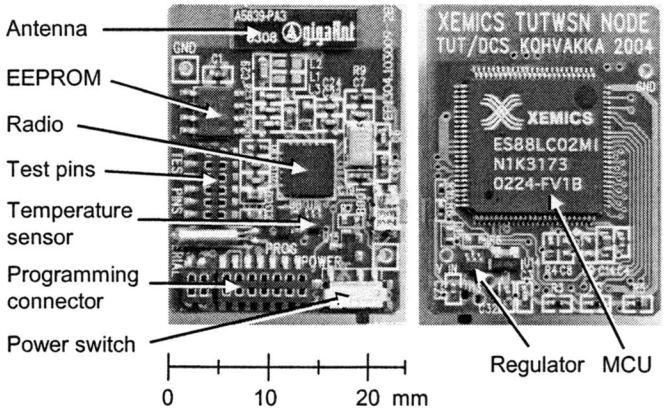

Fig. 4. The TUTWSN node prototype.

accuracy. The maximum sample rate using 16-bit resolution is 2 kHz.

The supply voltage is stabilized to 2.5 V by a Texas Instruments TPS71525 linear voltage regulator. The regulator is selected due to very low electromagnetic interferences and quiescent current. The prototype has a connector for a battery that is selected according to measured power consumption and the required lifetime.

The TUTWSN node prototype is implemented in a PCB presented in Fig. 4. The top side of the prototype contains the radio, antenna, EEPROM, temperature sensor, some test pins and a programming connector. The bottom side contains MCU and the voltage regulator. The size of the prototype is 31 mm x 23 mm x 5 mm.

B. TUTWSN Subnode Prototype

The TUTWSN subnode prototype is based on a Nordic Semiconductor nRF24E1 chip, which integrates a radio transceiver, MCU and ADC on a single package. The radio PHY layer is similar to the nRF2401A providing good compatibility with the TUTWSN node prototype.

The hardware architecture of the subnode prototype is presented in Fig. 5. The chip includes a 8051 compatible MCU core running at 16 MHz. The processor performance is about 2 MIPS and has 4 KB RAM for a program and 256 B RAM for data. In addition, there is a low power RC oscillator for a wake-up timer. An external EEPROM is used for program memory.

The RC oscillator provides low, 2 µA sleep mode current consumption, but is very inaccurate. The oscillator frequency is typically between 1 kHz and 5 kHz, depending on processing, temperature and supply voltage. The prototype utilizes a Maxim MAX6607 temperature sensor and the ADC

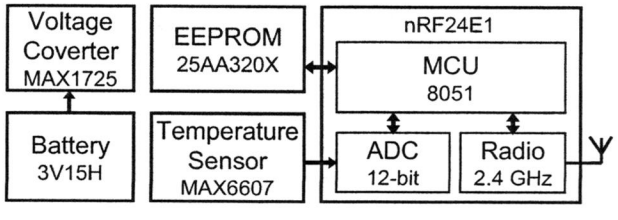

Fig. 5. TUTWSN subnode prototype hardware architecture.

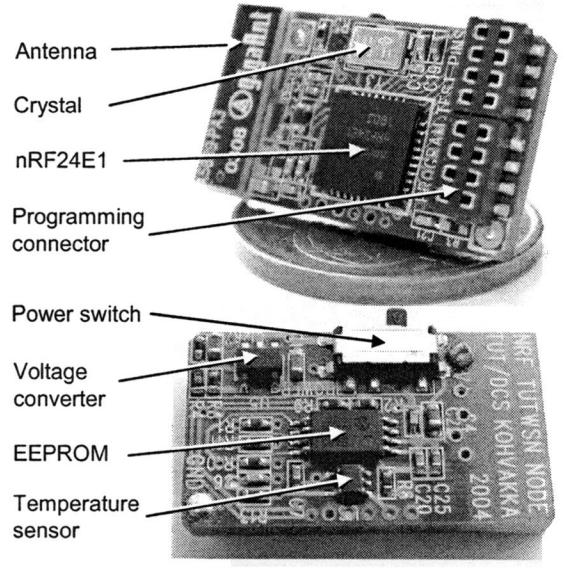

Fig. 6. The TUTWSN subnode prototype on a 5 cent coin.

embedded in the nRF24E1 chip. For simplicity, the prototype uses an internal bandgab voltage reference. ADC has at maximum 100 kHz sample rate and 12-bit resolution.

The TUTWSN subnode prototype is presented in Fig. 6. The top side of the prototype contains the nRF24E1 chip with crystal, antenna and a programming connector. The bottom side contains voltage converter, EEPROM, temperature sensor and a power switch. The size of the prototype is 23 mm x 13 mm x 5 mm.

C. TUTWSN Gateway Prototype

The TUTWSN gateway bridges TUTWSN to a RS-232 serial bus. The gateway utilizes the same MCU and radio than the TUTWSN node prototype. The RS-232 bus is accessed by a Maxim MAX3381 RS-232 transceiver and the UART of MCU. The implementation of the WSN gateway prototype is presented in [9].

D. User Application

The user application is executed in a PC for presenting measured data graphically and for configuring the measurements. The user application is implemented in Java enabling independence of underlying PC platform. The application uses the Java Communication Application Programming Interface (API) that supports RS-232 serial ports, and provides software porting for Windows and Linux. Above the API, the Swing technology provides Graphical User Interface (GUI) components [10].

A screenshot of the user application is presented in Fig. 7. The application presents the current cluster topologies on TUTWSN, and the data routing paths. These are updated constantly as the topology changes. Nodes are presented as information boxes, which contain a node ID, a logical node type (subnode or headnode), a sensor type, and the last measured value. Sensor data can be displayed as graphical charts, as presented in the figure.

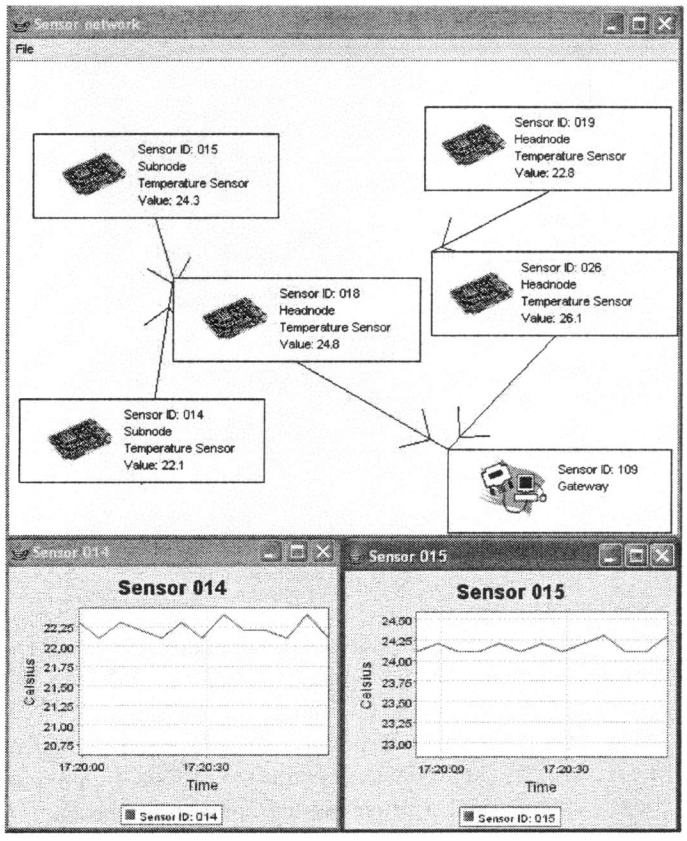

Fig. 7. A screenshot of the user application.

IV. Prototype Performance

The energy performance is measured from the implemented prototypes. The measurements contain the static power consumptions of the main components of prototypes, and the average consumption while executing the wireless temperature sensing application.

A. Power Analysis

The measurements are carried out in states where the radio, MCU, ADC and sensor are programmed to enter different operation modes. The MCU power consumption is measured in an active mode, when the MCU core is executing the sensor application, and in a sleep mode, when only a wake up timer is active. The ADC and sensor power consumptions are measured in active and shut down (off) modes. The radio power consumption is measured in sleep, reception and transmission modes with a minimum and maximum transmission power level.

TABLE I
THE POWER ANALYSIS OF THE TUTWSN SUBNODE AND TUTWSN NODE PROTOTYPES.

MCU	ADC	Sensor	Radio	TUTWSN subnode power	TUTWSN node power
active	active	active	RX	66.03 mW	59.55 mW
active	active	active	TX (0 dBm)	44.10 mW	37.70 mW
active	active	active	TX (-20 dBm)	32.90 mW	26.60 mW
active	active	active	sleep	11.64 mW	3.04 mW
active	active	off	sleep	11.60 mW	3.01 mW
active	off	off	sleep	10.56 mW	1.69 mW
sleep	off	off	sleep	15 µW	24 µW

The results are presented in Table I and include the power dissipation in the voltage converter, while the prototypes are supplied with 3 V supply voltage. The minimum power consumptions for the prototypes are 15 µW and 24 µW, when all components are inactive. A higher power in the node prototype is mostly caused by an external 32 kHz crystal that drives the MCU wake up timer.

The maximum power consumptions are achieved when all components are in active mode and the radio is in receive mode. Then, the subnode prototype and the node prototype power consumptions are 66.03 mW and 59.55 mW, respectively. The analysis shows the Xemics core has a very high energy efficiency compared to the 8051 core. Moreover, the radio clearly dominates the momentary power consumption in both prototypes. Particularly, radio receiving time is costly. The node power consumption over doubles during the reception compared to transmission with the lowest -20 dBm transmission power.

B. Measurements

The average power consumptions are measured from implemented prototypes, which execute the TUTWSN stack and the sensor application. For the measurements, the routing protocol employs a strategy where routing is dynamic, but the lowest cost route towards the TUTWSN gateway is selected according to the physical positions of the nodes. All prototypes sample their temperature sensors at 5 s intervals and route data to a WSN gateway using reservable data slots.

TUTWSN node prototypes utilize a power saving strategy, where data frames are transmitted and received only at the beginning of TUTWSN MAC slots. During the remaining time, nodes are in a sleep mode. However, the TUTWSN subnode prototype lacks the required timing accuracy and resolution of the wake-up timer. Also, the low memory resources limit the accuracy of the wake-up timer calibration algorithm. Hence, the subnode prototypes do not enter the lowest power sleep mode during the measurements. Thus, the subnode prototype power consumption with the full power saving features is estimated.

For the measurements, prototypes are supplied by 1 F capacitors and the average current consumptions are determined by the slopes of the capacitor terminal voltages. From the obtained currents, power consumptions are determined using the 3.0 V supply voltage.

First, the power consumptions of both prototypes are measured operating as subnodes. The power results with 5 s

TABLE II
MEASURED SUBNODE POWER CONSUMPTIONS AND ESTIMATED LIFETIMES WITH A CR2540 AND TWO AA BATTERIES (5 S ACCESS CYCLE LENGTH).

	Average power	Lifetime with a CR2450 battery	Lifetime with 2 AA batteries
TUTWSN node as a subnode	88.2 µW	879 days	10.1 years
TUTWSN subnode	10.6 mW	6.6 days	30.5 days
TUTWSN subnode with power saving (estimated)	80.7 µW	960 days	11.0 years

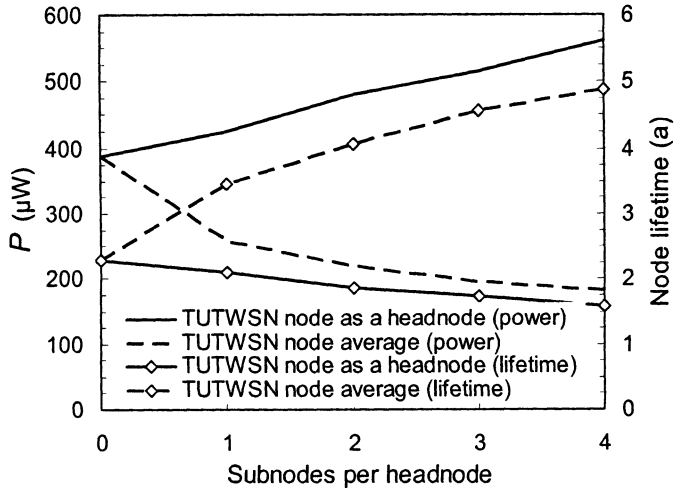

Fig. 8. Measured headnode power consumptions and estimated lifetimes with two AA batteries (5 s access cycle length).

MAC access cycle length are presented in Table II. According to the measurements, the node prototype and the subnode prototype consume 88.2 μW and 10.6 mW, respectively. In addition, the estimated TUTWSN subnode prototype power consumption with full power saving would reduce to 80.7 μW.

In the basis of the power consumption results, node lifetimes are estimated with two battery types: a CR2450 lithium coin battery and two serially connected AA alkaline batteries. With the full power saving, the lifetimes of both prototypes with the CR2450 are about 900 days, and with the two AA batteries over 10 years.

In practice, the lifetimes are limited by the battery self-discharging. The subnode prototype lifetime with the limited power saving is below a month. This clearly shows the importance for the MAC layer power save functionality with compatible hardware.

Next, the power consumption of the TUTWSN node prototype is measured in the headnode mode. The MAC access cycle length is fixed to 5 s, and the number of associated subnodes increases from 0 to 4, which is typical in the case application.

The resulted headnode power consumption increases from 390 μW to 560 μW, as presented in Fig. 8. To distribute power consumption more equally between nodes, the headnode operation is to be rotated between TUTWSN node prototypes. In this case, the average power consumption of the TUTWSN node prototypes reduces from 390 μW to 183 μW. This is also presented in the figure. The average latency per hop is about 2.5 s.

The lifetime of the TUTWSN node prototype with two AA batteries is estimated for a headnode, and averagely for a headnode and 0 to 4 subnodes. The results are presented in the right axis of Fig. 8. Without the rotation of the headnode functionality, the headnode lifetime reduces from 2.3 years to 1.6 years as subnodes are added. If the headnode rotation is applied, average node prototype lifetime increases from 2.3 years to 4.9 years.

Practically, the upper limit for associated subnodes is set by the radio range and the headnode loading. The proximity between headnodes should not be more than ten meters. Also, in practice the network scanning caused by node failures, interferences and mobility would increase power consumption around 100 μW.

V. Conclusions

Physical implementations for a temperature sensing WSN has been presented. Network energy consumption is minimized by the time slotted MAC protocol and very low power COTS hardware components. The measurements show the importance of accurate timing and proper power saving modes in time slotted MAC protocols. The power consumption with the rotation of headnodes and a stable network is as low as 183 μW resulting nearly 5 years lifetime with two AA batteries. Compared to the Mica II type backbone nodes in [4], a headnode lifetime is 100 to 300 times longer depending on the rotation of the headnodes. Compared to the PicoNodes in [5], TUTWSN node average lifetime is over 30 times longer.

A reasonable usability is achieved by the long node lifetimes and the fully autonomous network operation. The power consumption is low enough for scavenging the supply energy purely from ambient energy, including low level vibrations, ambient light and temperature gradients.

References

[1] E. H. Jr. Callaway, and E. H. Callaway, *Wireless sensor networks: architectures and protocols*, Auerbach Publications, 2003.

[2] J. N. Al-Karaki, and A. E. Kamal, "Routing techniques in wireless sensor networks: a survey," *IEEE Wireless Communications*, vol. 11, no. 6, pp. 6-28, Dec. 2004.

[3] J. Weatherall and A. Jones, "Ubiquitous networks and their applications," *IEEE Wireless Communications*, vol. 9, no. 1, pp. 18-29, Feb. 2002.

[4] R. Beckwith, D. Teibel, and P. Bowen, "Report from the field: results from an agricultural wireless sensor network," In *Proc. IEEE Conf. on Local Computer Networks*, Nov. 2004, Tampa, FA, pp. 471-478.

[5] J. M. Reason, and J. M. Rabaey, "A study of energy consumption and reliability in a multi-hop sensor network," *Mobile Computing and Communications Review*, vol. 8, no. 1, pp. 84-97, Jan. 2004.

[6] M. Hännikäinen, T. Lavikko, P. Kukkala, and T. Hämäläinen, "TUTWLAN - QoS supporting wireless network," *Telecommunication Systems - Modelling, Analysis, Design and Management*, vol. 23, no. 3-4, Kluwer Academic Publishers, 2003, pp. 297-333.

[7] C. R. Lin, and M. Gerla, "Adaptive clustering for mobile wireless networks," *IEEE Journal on Selected Areas in Communications*, vol. 15, no. 7, pp. 1265-1275, Sep. 1997.

[8] [14] M. Kohvakka, M. Hännikäinen, T. D. Hämäläinen, "Energy optimized beacon transmission rate in a wireless sensor network," in *Proc. IEEE Int. Symp. on Personal Indoor and Mobile Radio Communications*, Germany, Sep. 2005, accepted.

[9] M. Kohvakka, M. Hännikäinen, T. D. Hämäläinen, "Wireless sensor network implementation for industrial linear position metering," In *Proc. IEEE Euromicro Conf. on Digital Systems Design*, Aug. 2005, Portugal, accepted.

[10] Java Foundation Classes (JFC/Swing), http://java.sun.com/products/jfc/

PUBLICATION 9

M. Kohvakka, M. Hännikäinen, and T. D. Hämäläinen, "Wireless Sensor Network Implementation for Industrial Linear Position Metering," in *Proceedings of the 8th Euromicro Conference on Digital System Design – Architectures, Methods, and Tools (DSD 2005)*, Porto, Portugal, Aug. 30–Sept. 3, 2005, pp. 267–273.

Wireless Sensor Network Implementation for Industrial Linear Position Metering

Mikko Kohvakka, Marko Hännikäinen, and Timo D. Hämäläinen
Tampere University of Technology
Institute of Digital and Computer Systems
P.O.Box 553, FI-33101 Tampere, Finland
mikko.kohvakka@tut.fi

Abstract

This paper presents the design and performance measurements of a prototype Wireless Sensor Network (WSN) for industrial linear position metering. Design includes two different prototype platforms and a user application. Prototypes combine energy efficient commercial off-the-shelf components including a 2.4 GHz radio, and the custom TUTWSN communication protocols resulting high robustness, autonomous operation and very low power consumption. The user application displays sensor data graphically and enables further data analysis. Measurements contain component power analysis and prototype performance measurements. The measurements indicate 200 µW to 400 µW average node power consumption, as 16-bit sample is measured with 1 Hz sample rate, and routed to a WSN gateway with 1 s latency per hop and 512 bps throughput between nodes. Predicted lifetime of implemented WSN is 2 months with a small rechargeable battery or over 2 years with two AA batteries.

1. Introduction

Wireless Sensor Networks (WSN) nodes are characterized as very small, low energy and cheap platforms that are able to sense, process data and communicate wirelessly. Suitable applications are found from home, outdoor and industrial environments [1].

A fundamental WSN research challenge has been the combination of a complex network management with very scarce energy resources. Wireless communication protocols and algorithms are usually very complex, allowing fully autonomous ad-hoc operation in large scale networks. Network control is distributed to the whole network, which enables high robustness against local radio path interferences and node failures. WSN nodes are deployed in the area of interest as a sensor field, where data is routed using multiple low energy hops [2], [3].

For practical reasons, nodes should operate by small batteries for years, or they have to scavenge all supply energy from their operating environment [4]. This requires very high energy efficiency in both communication protocols and hardware implementation, which both have to be tailored according to application requirements.

WSN nodes have been designed by several research groups over the last decade. Most often they are implemented by commercial off-the-shelf (COTS) components, which provide sufficient performance with low development and production costs.

BTnode [5] is a demonstration platform for ad-hoc networks. BTnode combines an Ericsson ROK 101 007 Bluetooth module with an Atmel ATmega128L microcontroller. BTnode supports only a star network topology with one master and at maximum seven slave nodes. However, a multi-hop WSN can be implemented by dual-radio BTnodes [6]. Reported power consumption of a connected dual-radio BTnode is 445 mW. Due to the high energy consumption, BTnodes are most suitable for applications that are active over a limited time period, while requiring high network throughput.

PicoNode combines a Bluetooth physical layer with custom data link layer and higher layer protocols, which are executed on a StrongARM SA-1100 microprocessor. The performance of a temperature sensing WSN with 25 PicoNodes is evaluated in [7]. Temperature is measured at 5 s intervals and data is multi-hop routed to a base station node. Reported average power consumption per node is about 6 mW resulting approximately 50 days lifetime with two AA-batteries.

Berkeley Mica II mote [8] is a commercial platform, which consists of an Atmel ATmega128L microcontroller and a 916 MHz radio. A WSN implementation with 65 Mica II motes deployed in a vineyard is presented in [9]. The motes gather temperature values at 5 minutes intervals and multi-hop route data to a base station node. The

reported lifetimes of routing nodes are about 3 months with large 42 Ah battery packs.

In this paper we present the implementation of a full featured WSN for industrial linear position metering. The work includes two different prototype platforms and a user application. Linear position sensors are widely used in industry for measuring the displacements of moving parts. WSN eliminates the need of extensive cabling, thus reducing both material and installation costs. A new WSN design has been selected, as current proposals do not fulfill the performance and lifetime requirements of the metering application. The physical WSN prototypes are implemented using low power COTS components and custom TUTWSN communication protocols.

The rest of this paper is organized as follows. The design requirements for the new WSN are presented in Section 2. Section 3 gives an overview of the TUTWSN topology and its MAC protocol. The design of WSN prototype platforms is presented in Section 4. Section 5 presents the performance evaluation, including component power analysis and prototype performance measurements. The paper is concluded in Section 6.

2. Application Design Requirements

The WSN application design contains a complete linear position metering system from a sensor to data analysis on a workstation. The design utilizes TUTWSN as a base technology, including its protocol stack and network architecture. Two different prototypes are needed, one for the linear position sensor, and one for a WSN gateway that connect the WSN to other networks and terminals.

The linear position metering system measures low frequency movements, where data is gathered from sensors at 1 Hz sample rate and 16-bit resolution. All samples are time stamped. The expected number of sensors is 50, but this should not be limited. The network range is one hundred meters, where sensors are at most ten meters apart from each other. WSN data is multi-hop routed in the network while the targeted latency per hop is 1 s. The required network throughput is 512 bits/s. There are no strict delay requirements for the data collection, but the reliability of the WSN is critical. Therefore, the node must be able to buffer and retransmit samples.

A wireless linear position sensor is assembled by two parts, as a WSN node is attached on the physical connector of a linear position sensor. Thus, the WSN nodes should not increase the size or weight of the existing physical sensor significantly. The sensors will operate in harsh physical environment containing fluids, dust, vibration and electromagnetic interferences. Hence, WSN nodes should be sealed on waterproof metal containers. The sensors should be powered by rechargeable batteries having at least 1 month lifetime.

3. TUTWSN Overview

TUTWSN protocol stack has been developed for low data rate applications, where good scalability and low energy consumption are required. An important TUTWSN design goal has been minimized communication duty cycle, while providing rapid and low energy network configuration and maintenance operations. TUTWSN is based on our previous experience on QoS supporting, proprietary WLAN MAC implementation [10].

TUTWSN utilizes clustered network topology, presented in Figure 1. Each cluster consists of two logical types of nodes: a single cluster head (headnode) and several members (subnode). Headnodes maintain cluster synchronization and participate in multi-hop data routing in network. Subnodes can communicate only with headnodes, thus having significantly lower performance and energy requirements than headnodes. Network contains also one or more WSN gateways, which request data from WSN nodes and form bridges to other networks.

The implemented linear sensing application employs homogenous nodes, which select their logical type (headnode or subnode) dynamically during operation. The selection is made according to heard neighboring clusters and their loading. The portion of subnodes is higher in densely deployed parts of the network for achieving energy saving. Network lifetime is extended by actively rotating the headnode functionality among nodes.

3.1 TUTWSN MAC

TUTWSN utilizes a time slotted MAC protocol, which divides each access cycle into an active period for data exchanging (superframe) and an idle time, when nodes are in a power saving mode. These are presented in Figure 2. The slotted structure allows a trade off between energy and data rate. The duty cycle is further reduced by applying slotted-ALOHA and Time Division Multiple Access (TDMA) mechanisms in superframes. For

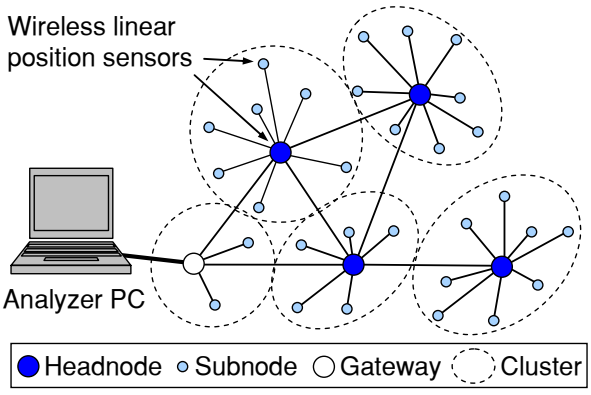

Figure 1. TUTWSN clustered ad-hoc topology.

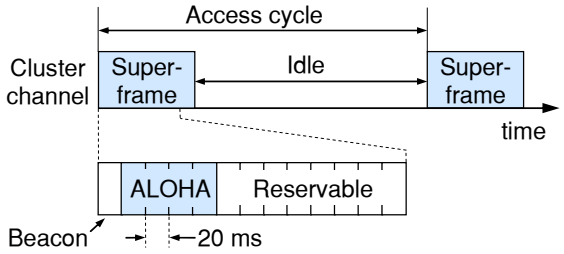

Figure 2. TUTWSN access cycle and superframe.

enabling scalability, each headnode controls its superframe structure asynchronously to each other. Inter-cluster interferences are eliminated by allocating different RF channels for neighboring clusters. Applied local synchronization in clusters reduces headnode duty cycle and is much easier to control than a global synchronization [11].

Each superframe begins with a beacon, which is succeeded by four ALOHA and at most eight reservable time slots, each 20 ms long. These are presented in Figure 2. The beacon synchronizes a cluster, specifies time slot assignments and provides cluster status information. ALOHA slots are used for association and slot reservation requests, and for low priority data. Reservable slots provide reliable data transfer with fixed throughput, but require a slot reservation procedure. In addition, all headnodes broadcast network beacons on a network signaling channel at 500 ms intervals. The network beacon contains an exact time to a following superframe, which effectively reduces the required radio receiving time and energy for network maintenance operations.

Inter-cluster communication is performed during source cluster idle time and destination cluster superframe. A source headnode acts similarly as a subnode and synchronizes itself to the schedule of a destination headnode. Source headnode has to keep track of time offsets to utilized destination headnodes.

4. Prototype WSN Design

Prototype WSN design includes hardware prototype implementations for a WSN node and a WSN gateway, and software implementations for a WSN application in nodes and a user application in the analyzer PC.

4.1 WSN Node

A WSN node prototype is an improved version of the WSN prototype platform presented in [12]. The hardware architecture for the WSN node is presented in Figure 3. The architecture is divided into four subsystems: communication, computing, sensing and power subsystems.

The communication subsystem provides wireless communication links to neighboring nodes. The subsystem consists of a Nordic Semiconductor nRF2401A radio transceiver operating at 2.4 GHz license free Industrial Scientific Medicine (ISM) frequency band. The 2.4 GHz frequency band is high enough for avoiding interferences from machinery [13] and for allowing physically small and efficient antennas. The radio has 1 Mbps data rate, which enables very high energy efficiency. The consumed energy per a physical layer bit is about 109 nJ at RX mode and 63 nJ at TX mode with 0 dBm power level [14]. The transmission power level is selectable between -20 dBm and 0 dBm. The radio has 84 selectable RF channels, which allows very good network scalability. Radio has an internal Cyclic Redundancy Check (CRC) error detection logic and a data buffer, which reduces microcontroller speed and time accuracy requirements. Antenna is implemented with a quarter-wave external monopole antenna due to good efficiency and omni-directional radiation. Measured radio range is about 30 m.

The computing subsystem manages node operations and executes sensor application. The subsystem consists of a Xemics XE88LC02 MicroController Unit (MCU), which integrates CoolRisc 816 processor core with a 16-bit Analog-to-Digital Converter (ADC), 22 KB program memory and 1 KB data memory. Maximum instruction execution speed is 2 MIPS. MCU is connected to an 8 KB Microchip 25AA320 EEPROM for non-volatile data memory. MCU is selected due to low 2.4 V supply voltage, high 1344 MIPS/W energy efficiency, and accurate ADC. Moreover, low 5 µW sleep mode power consumption, versatile timers and good availability are the advances of the MCU.

The sensing subsystem gathers requested data from node environment. The subsystem consists of a linear position sensor and the ADC integrated with MCU. The sensor utilizes a 5 kΩ linear potentiometer. During measurement, a constant voltage is applied over the potentiometer and the deviation is determined by the wiper voltage. ADC has pre-amplification and offset compensation stages, which increase sampling accuracy. The maximum sample rate using 16-bit resolution is 2 kHz.

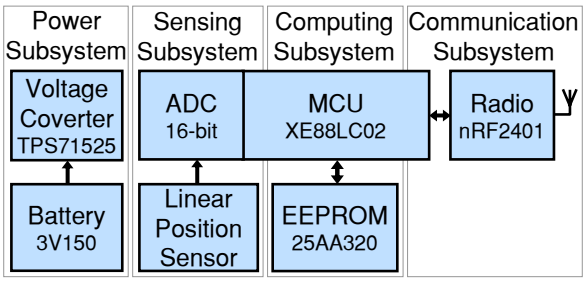

Figure 3. WSN node prototype architecture.

The power subsystem utilizes three serially connected 150 mAh Varta V150H NiMH batteries achieving a 3.6 V nominal voltage. The NiMH chemistry is selected due to good energy density, cheap price and better robustness against high temperatures and currents than lithium chemistries. The battery voltage is converted down to 2.5 V supply voltage by a Texas Instruments TPS71525 linear voltage regulator. The converter is selected due to low electromagnetic interferences and quiescent current. These are important, since proximity to other components is short and the average current consumption is low. Moreover, the converter is small and cheap. For the required one month WSN node lifetime, the power subsystem can deliver 208 µA average current drain.

The WSN node prototype is implemented in a four-layer FR-4 Printed Circuit Board (PCB), presented in Figure 4. The top side of the prototype contains radio, battery, programming connector, antenna and two diagnostics LEDs. The bottom side contains MCU, voltage regulator and a connector for the linear position sensor. The prototype is enclosed in an aluminum casing presented in Figure 5. The size of the prototype is 120 mm x 25 mm x 25 mm. The connector for the linear position sensor is also used for battery recharging.

4.2. WSN Gateway

A WSN gateway forms a bridge between WSN and an analyzer PC using a RS-232 serial port.

The WSN gateway prototype architecture is presented in Figure 6. The gateway utilizes the same MCU, radio and antenna than the WSN node. These are selected due to the high energy efficiency and radio compatibility with the WSN node prototypes. RS-232 bus is accessed by a Maxim MAX3381 RS-232 transceiver and a Universal Asynchronous Receiver Transmitter (UART) of MCU.

The required supply power is obtained directly from the

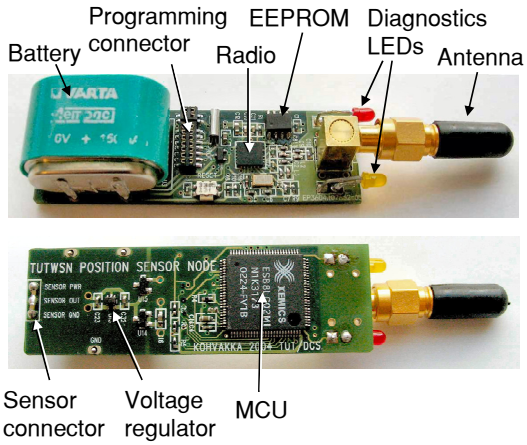

Figure 4. WSN node prototype.

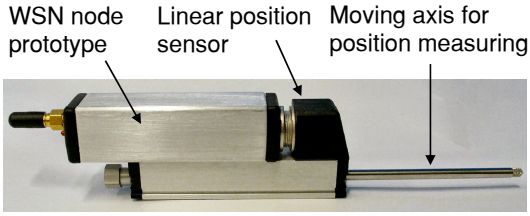

Figure 5. Complete wireless linear position sensor prototype consisting of a WSN node attached to a position sensor.

serial port; the power is rectified and filtered from Data Terminal Ready (DTR) and Request to Send (RTS) signals of RS-232. According to measurements, the these signals deliver 12 V open circuit voltage and 5 mA to 10 mA short circuit current, depending on PC hardware. The obtained voltage is converted down to 2.7 V supply voltage by a Texas Instruments TPS71501 linear voltage regulator.

The WSN gateway prototype is implemented in a four-layer RF-4 PCB, presented in Figure 7. The upper side of the prototype contains antenna, MCU, RS-232 transceiver, RS-232 connector, filter capacitors and two diagnostics LEDs. The bottom side contains radio, voltage rectifier diodes, voltage regulator and programming connector. The size of the prototype is 67 mm x 31 mm x 37 mm including antenna.

4.3. User Application

The user application is executed in the analyzer PC for presenting measured data graphically and for configuring the measurements. There are no power switches available on the prototypes itself, but the network is activated by the user applications.

The user application is implemented in JAVA enabling independence of underlying PC platform. The user application is based on a Java Communication API. The API supports RS-232 serial ports, and provides software porting for Windows and Linux. Above the Java Communications API, Swing provides User Interface (UI) components, which are utilized for implementing a Sensor UI.

A screenshot of the user application is presented in

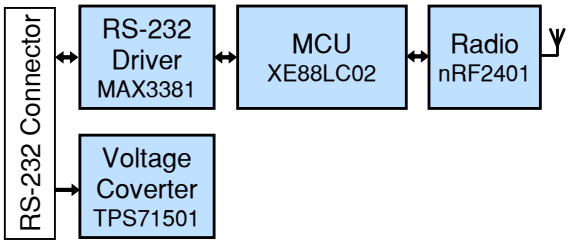

Figure 6. WSN gateway prototype architecture.

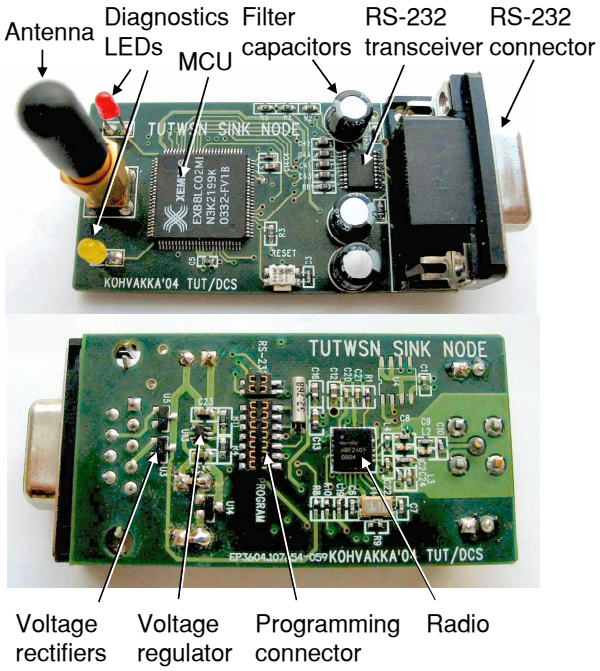

Figure 7. WSN gateway prototype.

Figure 8. The application shows the current cluster topologies on WSN, and the data routing paths. These are updated constantly as the topology changes. Nodes are presented as information boxes, which contain a node ID, a logical node type (subnode or headnode), a sensor type and a current sensor value. Sensor data can be presented graphically for individual sensors or as jointed graph, as presented in the figure.

5. Prototype Performance

Power performance is measured from the implemented WSN node prototype. The measurements include static power consumptions of the main components and an average consumption while executing the wireless linear position metering.

5.1. Power Analysis

The static power consumptions of the radio, MCU, ADC and the linear position sensor are measured at different operating modes. The MCU power consumption is measured in an active mode, when the core is running on 1.8 MIPS speed, and in a sleep mode, when only wake up timer is active. The ADC and sensor power consumptions are measured in active and shut down (off) modes. The radio power consumption is measured in various operation modes, including data loading between MCU and the radio buffer.

Measurement were done at 3 V supply voltage

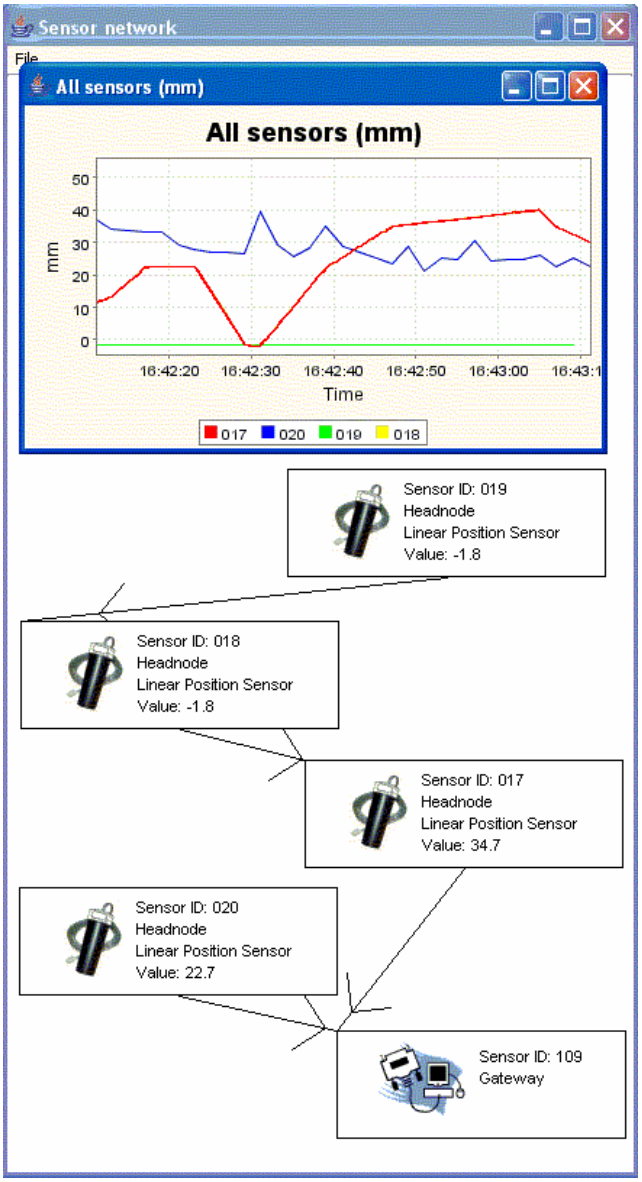

Figure 8. A screenshot of the user application.

including power dissipation in the power subsystem. The analysis results are presented in Table 1. The minimum power consumption is 21 µW, which is achieved when all components are inactive. The maximum required power is 57.60 mW, when all components are active and radio is in receive mode. In the implemented prototype, the radio clearly dominates the momentary power consumption. Particularly, radio receiving time is costly. The node power consumption over doubles during reception compared to transmission with the lowest -20 dBm transmission power. The linear position sensor power consumption is 960 µW.

Table 1. WSN node prototype power analysis.

MCU mode	ADC mode	Sensor mode	Radio mode	Power (mW)
Active	Active	Active	Receive data	**57.60**
			Transmit data (Power: 0 dBm)	**39.73**
			Transmit data (Power: -20 dBm)	**26.46**
			Data loading	**4.70**
		Off	Sleep	**3.06**
	Off			**3.01**
				1.69
Sleep				**0.021**

5.2. Measurements

The average power consumptions are measured from a set of implemented WSN node prototypes, which execute the TUTWSN stack and the sensor application. For the measurements, the logical types of nodes are fixed. The routing protocol employs a strategy where routing is dynamic, but the lowest cost route towards the WSN gateway is established according to the physical positions of the nodes. All WSN node prototypes sample their linear position sensors at 1 Hz rate and route data to the WSN gateway prototype using reservable data slots. For achieving accurate time stamps, nodes execute a time synchronization algorithm. The synchronization algorithm loads the MCU notably, especially in headnodes. An oscilloscope screenshot of the headnode and subnode current waveforms are presented in Figure 10. The waveforms present a 20 ms time period, which contains ADC sampling, and TUTWSN data transmission and acknowledgement reception. A peak current during reception is about 20 mA.

For the measurements, a headnode and a subnode are supplied by 1 F and 0.22 F super capacitors. The average current consumptions are determined by measuring the slopes of the capacitor terminal voltages. From the obtained currents, power consumptions are calculated using the 3.0 V supply voltage.

First, the average subnode and headnode power consumptions were measured, while MAC access cycle length is increased from 1 s to 10 s. Only one subnode is associated on each headnode. The power consumption results with maximum throughputs between headnodes are presented in Figure 9. The minimum power is obtained with 10 s access cycle, when subnode and headnode power consumptions are 59.6 µW and 302 µW, respectively. The available throughput is 102 bits/s. The throughput is inversely proportional to the TDMA access cycle length. With 1 s access cycle, throughput is increased to 1024 bits/s, but the power consumptions of a subnode and a headnode are raised to 249 µW and 968 µW, respectively. The average latency per hop is about a half of the access cycle length.

Then, the average headnode power consumption was measured, while the number of subnodes per each headnode was increased from 1 to 5. The TUTWSN MAC access cycle length is fixed to 2 s, which fulfills application requirements in data rate and latency. As the number of subnodes increase, the subnode power remains in 162 µW, but the headnode power consumption increases. The resulted headnode and network average power consumptions, and predicted WSN node lifetimes are presented in Figure 11. The increase of subnodes per headnode from 0 to 5 reduces the average node power consumption from 400 µW to 299 µW and increase node

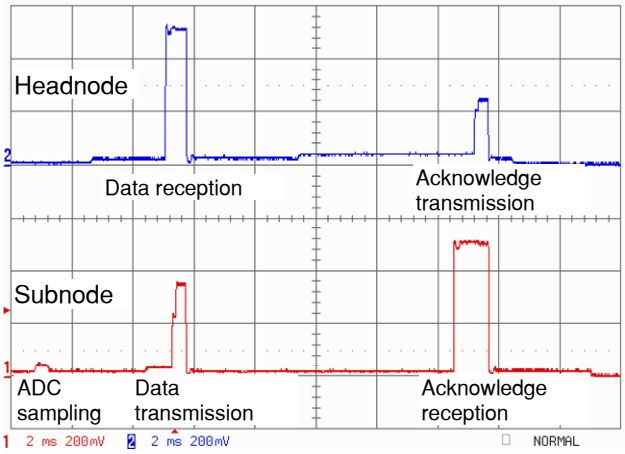

Figure 10. Oscilloscope screenshot of the headnode and subnode current waveforms during ADC sampling, data transmission and reception.

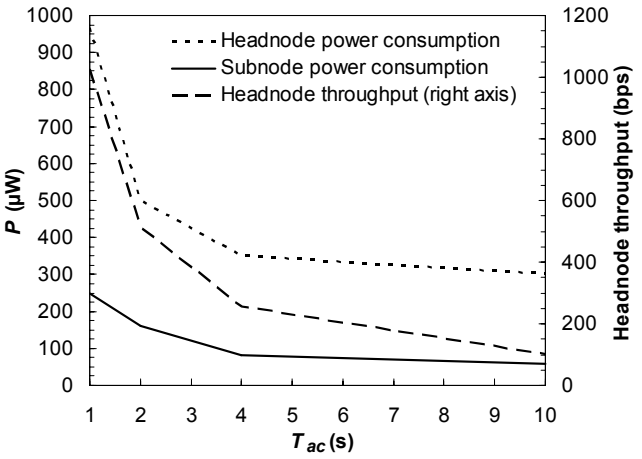

Figure 9. Power consumption and throughput in function of TUTWSN MAC access cycle length (1 subnode per headnode).

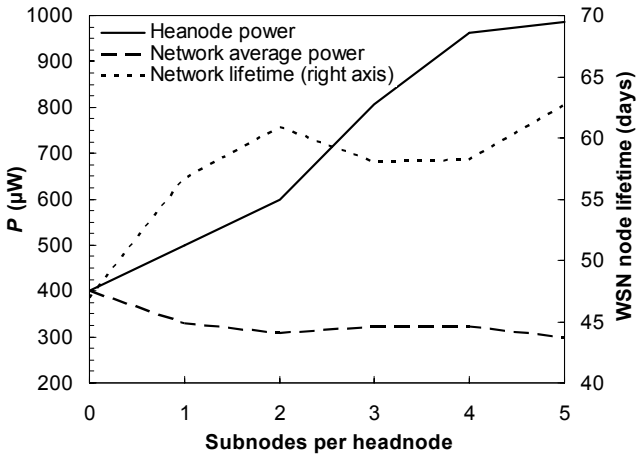

Figure 11. Headnode, subnode and network average power consumptions in the function of the number of subnodes per headnode (TUTWSN access cycle length = 2 s).

lifetime from 47 days to 63 days. The required 31 days battery recharging interval is clearly exceeded regardless the number of subnodes per headnode.

Practically, the number of subnodes per each headnode is determined dynamically. To minimize energy consumption and improve scalability, the number of subnodes per headnode is maximized. The upper limit is set by radio range and headnode loading. The proximity between headnodes should be no more than ten meters.

6. Conclusions

A prototype WSN is implemented for industrial linear position metering including two different hardware prototypes and a user application. For reducing energy consumption and improving scalability, a clustered network topology is used. Yet, the rotation of the headnode operation among nodes is needed to distribute energy consumption more equally and increase network lifetime. The measurements are carried out on a stable network without network discovery operations. In practice, interferences and node failures require occasional network scanning operations, which increase headnode power consumption around 100 µW [14]. However, required 31 days lifetime is clearly exceeded. Significantly longer lifetime would be obtained using primary batteries. For instance, two AA-type alkaline batteries would extend node lifetime to 27 months.

Results indicate that WSN technology is matured enough for real applications with high reliability requirements. The design and tailoring of WSN protocols according to the application is required for adequate energy efficiency and performance. Also, careful platform design and component selection for supporting protocol operation is required.

References

[1] E.H.Jr. Callaway, and E.H. Callaway, *Wireless sensor networks: architectures and protocols*, Auerbach Publications, 2003.

[2] J.M. Rabaey, J. Ammer, J.L.Jr. da Silva, D.Patel, and S.Roundy, "PicoRadio supports ad hoc ultra-low power wireless networking", *IEEE Computer Magazine*, vol. 33, no. 7, Jul. 2000, pp. 42-48.

[3] J. Weatherall and A. Jones, "Ubiquitous networks and their applications", *IEEE Wireless Communications*, vol. 9, no. 1, Feb. 2002, pp. 18-29.

[4] S. Roundy, P.K. Wright, and J. Rabaey, "A study of low level vibrations as a power source for wireless sensor nodes", *Computer Communications*, vol. 26, no. 11, Jul. 2003, pp 1131-1144.

[5] BTnodes homepage. http://www.btnode.ethz.ch/

[6] M. Leopold, M.B. Dydensborg, and P. Bonnet. "Bluetooth and Sensor Networks: A Reality Check", in *Proc. 1st ACM Conf. Embedded Networked Sensor Systems,* Los Angeles, Nov. 2003, pp. 103-113.

[7] J.M. Reason, and J.M. Rabaey, "A study of energy consumption and reliability in a multi-hop sensor network", *Mobile Computing and Communications Review*, vol. 8, no. 1, Jan. 2004, pp. 84-97.

[8] Crossbow Technology homepage. http://www.xbow.com/

[9] R. Beckwith, D. Teibel, and P. Bowen, "Report from the field: results from an agricultural wireless sensor network", In *Proc. IEEE Conf. on Local Computer Networks*, Tampa, Florida, Nov. 2004, pp. 471-478.

[10] M. Hännikäinen, T. Lavikko, P. Kukkala, and T. Hämäläinen, "TUTWLAN - QoS supporting wireless network", *Telecommunication Systems - Modelling, Analysis, Design and Management*, vol. 23, no. 3-4, 2003, pp. 297-333.

[11] C.R. Lin, and M. Gerla, "Adaptive clustering for mobile wireless networks", *IEEE Journal on Selected Areas in Communications*, vol. 15, no. 7, Sep. 1997, pp. 1265-1275.

[12] M. Kohvakka, M. Hännikäinen and T. Hämäläinen, "Wireless sensor prototype platform", in *Proc. IEEE Int. Conf. Industrial Electronics, Control and Instrumentation*, Virginia, Nov. 2003, pp. 1499-1504.

[13] T.S. Rappaport, "Indoor radio communications for factories of the future", *IEEE Communications Magazine*, vol. 27, no. 5, May 1989, pp. 15-24.

[14] M. Kohvakka, M. Hännikäinen, T. D. Hämäläinen, "Energy optimized beacon transmission rate in a wireless sensor network", in *Proc. IEEE Int. Symp. on Personal Indoor and Mobile Radio Communications*, Germany, Sep. 2005, accepted.

PUBLICATION 10

M. Kohvakka, T. Arpinen, M. Hännikäinen, and T. D. Hämäläinen, "High-Performance Multi-Radio WSN Platform," in *Proceedings of the 2nd International Workshop on Multi-hop Ad Hoc Networks: from theory to reality (REALMAN 2006)*, Florence, Italy, May 26, 2006, Italy, pp. 95–97.